CONFERENCE NOTES

OPEN CHANNEL FLOW

Dave Cozakos, COE

L.A. Corps makes allowance for 2' of debris on bridge piers

Inlet and Outlet Control in Culvert Analysis

Types of inlet and outlet control are shown on figures 8 and 9. Solutions for each type of flow are given.

Outlet Control

Type A - Outlet and Inlet Submerged

$$Q = A\sqrt{2g\,H/K}$$

where:

A = cross sectional area of culvert

H = difference in tailwater elevation and upstream energy grade line

K = sum of loss coefficients

$K = k_e + k_o + k_f$

k_e = entrance losses given in Table 1

k_o = outlet losses = 1.0

k_f = friction losses = $\frac{29.1\,n^2 L}{R^{4/3}}$

n = .015 for concrete

.022 for corrugated metal

R = A/p

P = inside wetted perimeter

L = LENGTH OF PIPE

Ref. 1. Hydraulic Charts for the Selection of Highway Culverts U.S. D.O.T. F.H.A. Dec. 1965

Ref 2. Hydraulics of Bridge Waterways 1973

Type B & C - Culvert flowing full but not under tailwater condition

$$Q = A\sqrt{2g\,H/K}$$

where:

H = difference in the downstream water surface elevation, estimated by 1/2 (y_c + D), and the upstream energy grade line

y_c = critical depth at outlet

D = height of culvert

Type D - open channel flow

Use standard step backwater computation (HEC-2)

Special Case for Reduced Capacity at Inlet

For the special case where debris is assumed on the piers at the culvert entrance the velocity at the inlet will be different than the velocity thru the rest of the culvert. It is therefore necessary to apply a correction factor to the loss coefficient, K, used in the outlet control equation, because all the individual components of K (i.e. k_e, k_f, k_o) must be applied to the same velocity head.

The outlet control equation can be written:

$$H = K\left(\frac{Q}{A_N}\right)^2 \frac{1}{2g}$$

Expressing the equation in terms of the various components that contribute to the total head loss we can write:

$$h_e + h_f + h_o = (k_e + k_f + k_o)\left(\frac{Q}{A_N}\right)^2 \frac{1}{2g}$$

For the special case where debris is assumed at the inlet, the area at the inlet is less than the area thru the rest of the culvert. The outlet control equation then becomes:

$$h_e + h_f + h_o = k_e \left(\frac{Q}{A_e}\right)^2 \frac{1}{2g} + (k_o + k_f)\left(\frac{Q}{A_N}\right)^2 \frac{1}{2g}$$

where:

A_e = area at inlet reduced by assumed debris

Since only one value for area and K can be used in the HEC-2 program, the following adjustment is recommended.

$$H = k_e\left(\frac{Q}{A_e}\right)^2 \frac{1}{2g} + (k_o + k_f)\left(\frac{Q}{A_e}\right)^2\left(\frac{A_e}{A_N}\right)^2 \frac{1}{2g}$$

which reduces to:

$$H = \left[k_e + \left(\frac{A_e}{A_N}\right)^2 (k_o + k_f)\right]\left(\frac{Q}{A_e}\right)^2 \frac{1}{2g}$$

Thus the outlet control equation to be used in the HEC-2 program is:

$$Q = A_e \sqrt{2g\, H/K} \qquad A_e = \text{"BAREA"}$$

where:

CAN USE EITHER

A_e = area at the (entrance) inlet reduced by assumed debris

$K = k_e + \left(\frac{A_e}{A_N}\right)^2 (k_o + k_f)$

OR

A_N = NET AREA THRU REST OF CULVERT

$K = k_e\left(\frac{A_N}{A_e}\right)^2 + k_o + k_f$; USE WITH $Q = A_N \sqrt{2g\, H/K}$

Inlet Control

Inlet control means that the downstream water surface elevation and the culvert length have no effect on capacity of the culvert. Culvert capacity depends entirely on inlet conditions. There are no options in the HEC-2 model to handle inlet control problems.

Type A flow can be described as critical depth control. The upstream water surface can be determined by calculating critical depth at the inlet.

The Bureau of Public Roads has published several charts for use in determining upstream water surfaces for inlet control conditions. Three of the most useful are reproduced here as figures 10, 11, 12.

Henderson has recommended use of the following equation:

$$Q = C A_o \sqrt{2g (HW - Cd)}$$

where C = varies between .8 for rounded inlets and .6 for square inlets

HW = headwater depth above the invert (energy grade line)

d = the height of the culvert

The orifice equation can also be used to compute inlet control:

$$Q = C A_o \sqrt{2gH}$$

where H = the distance from the center of the culvert opening to the energy grade line

C = orifice coefficient from King's Handbook

It should be noted that if the value of $HW/_d$ varies between 0.8 and 1.2 then unstable flow conditions will exist at the inlet. Under these conditions inlet control will oscillate between critical and orifice control.

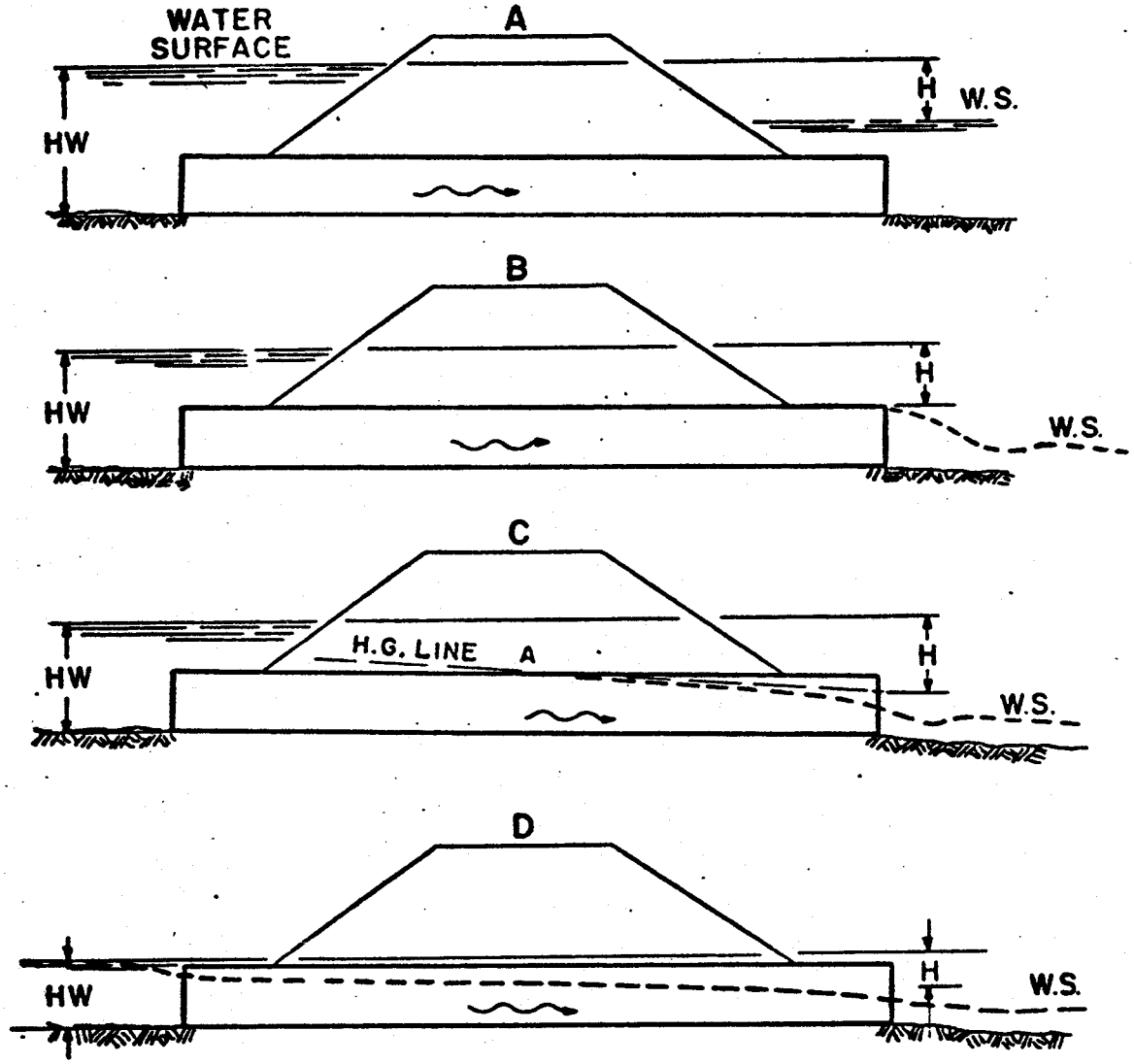

FIGURE 8: OUTLET CONTROL

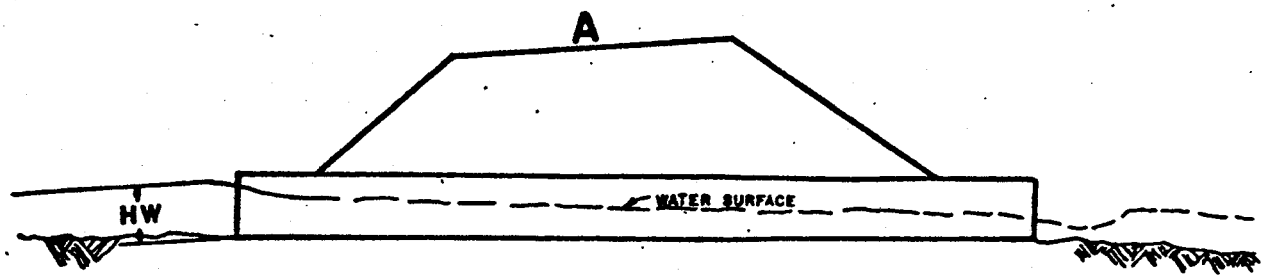

INLET UNSUBMERGED

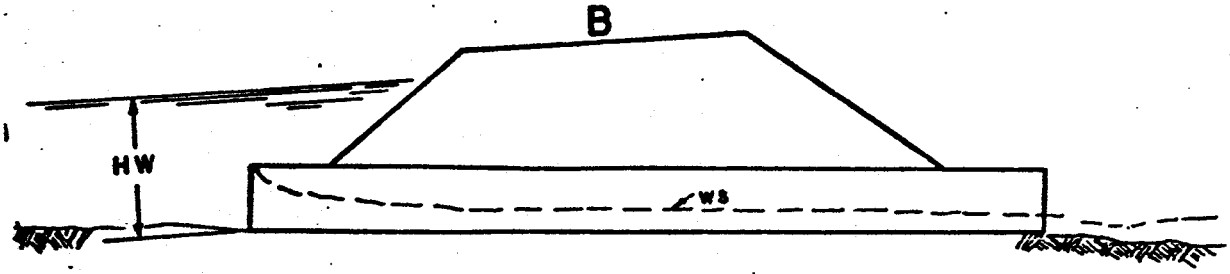

INLET SUBMERGED

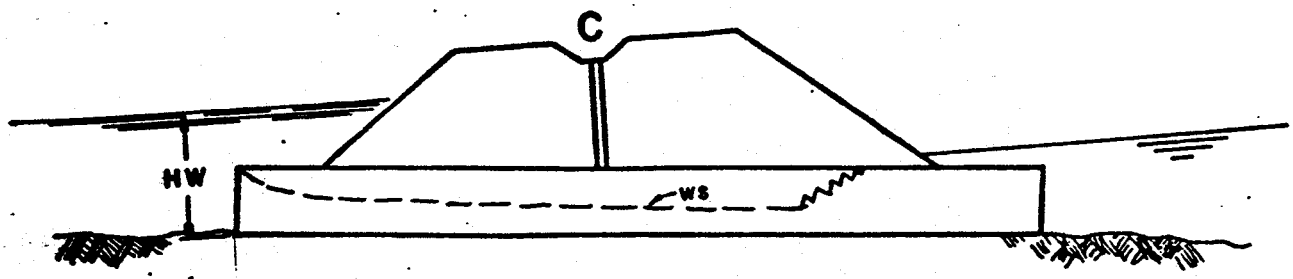

OUTLET SUBMERGED

FIGURE 9: INLET CONTROL

TABLE 1 - ENTRANCE LOSS COEFFICIENTS

Coefficient k_e to apply to velocity head $\frac{V^2}{2g}$ for determination of head loss at entrance to a structure, such as a culvert or conduit, operating full or partly full with control at the outlet.

$$\text{Entrance head loss } H_e = k_e \frac{V^2}{2g}$$

Type of Structure and Design of Entrance	Coefficient k_e
Pipe, Concrete	
Projecting from fill, socket end (groove-end)	0.2
Projecting from fill, sq. cut end	0.5
Headwall or headwall and wingwalls	
Socket end of pipe (groove-end)	0.2
Square-edge	0.5
Rounded (radius = 1/12D)	0.2
Mitered to conform to fill slope	0.7
*End-Section conforming to fill slope	0.5
Pipe, or Pipe-Arch, Corrugated Metal	
Projecting from fill (no headwall)	0.9
Headwall or headwall and wingwalls	
Square-edge	0.5
Mitered to conform to fill slope	0.7
*End-Section conforming to fill slope	0.5
Box, Reinforced Concrete	
Headwall parallel to embankment (no wingwalls)	
Square-edged on 3 edges	0.5
Rounded on 3 edges to radius of 1/12 barrel dimension	0.2
Wingwalls at 30° to 75° to barrel	
Square-edged at crown	0.4
Crown edge rounded to radius of 1/12 barrel dimension	0.2
Wingwalls at 10° to 25° to barrel	
Square-edged at crown	0.5
Wingwalls parallel (extension of sides)	
Square-edged at crown	0.7

*Note: "End Section conforming to fill slope," made of either metal or concrete, are the sections commonly available from manufacturers. From limited hydraulic tests they are equivalent in operation to a headwall in both inlet and outlet control. Some end sections, incorporating a closed taper in their design have a superior hydraulic performance. These latter sections can be designed using the information given for the beveled inlet, p. 5-13.

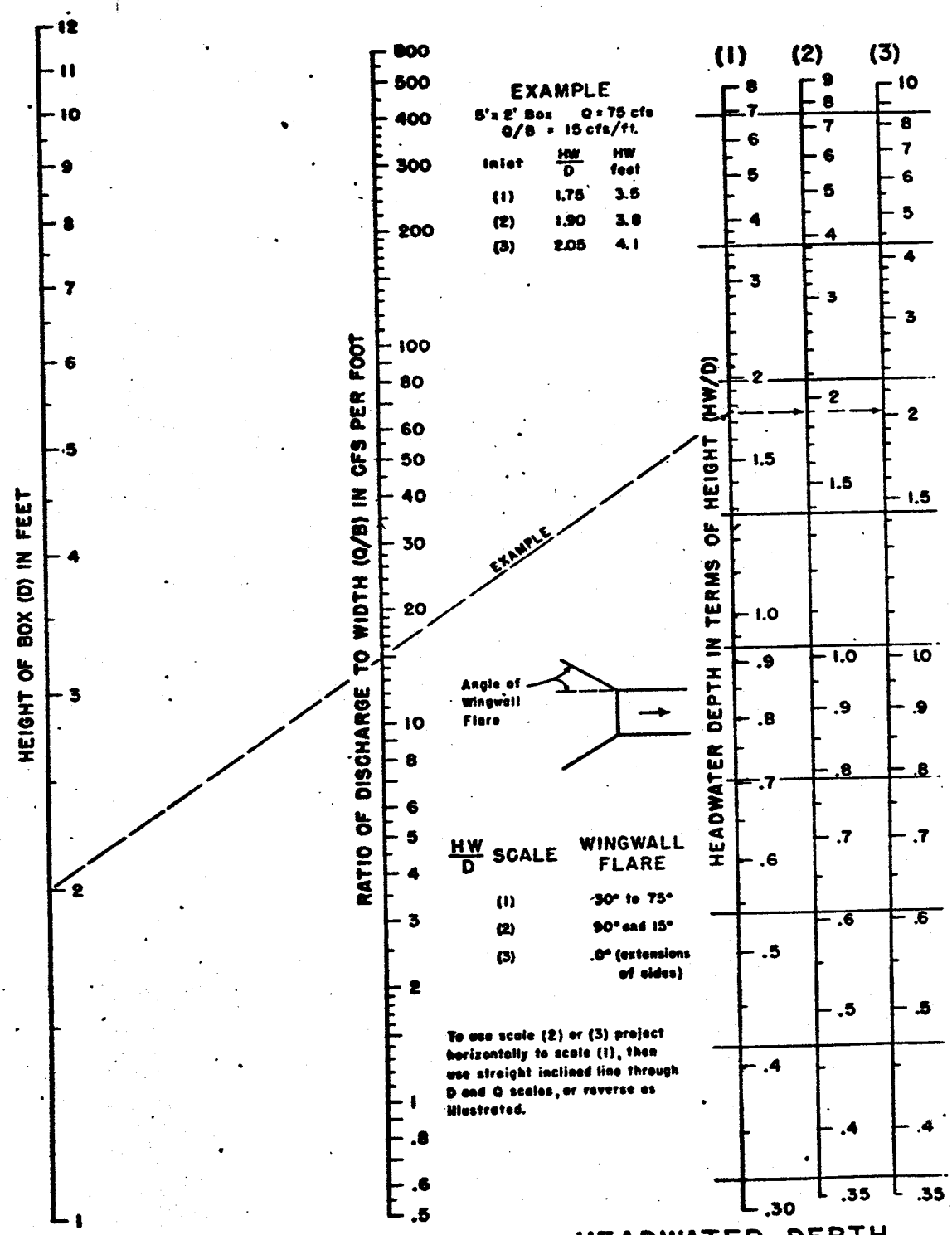

HEADWATER DEPTH FOR BOX CULVERTS WITH INLET CONTROL

FIGURE 10

BUREAU OF PUBLIC ROADS JAN 1963

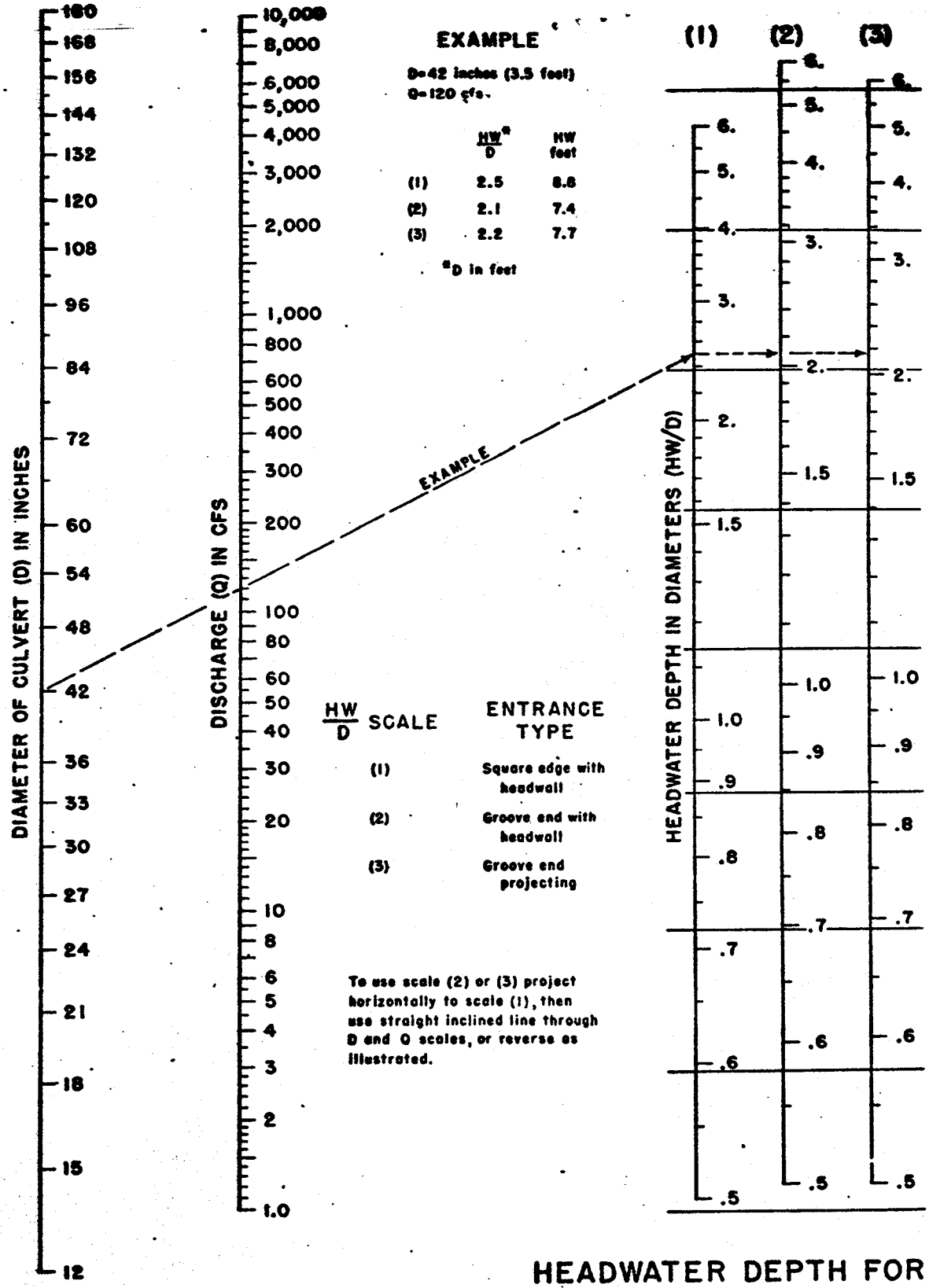

HEADWATER DEPTH FOR CONCRETE PIPE CULVERTS WITH INLET CONTROL

FIGURE 11

BUREAU OF PUBLIC ROADS JAN. 1963

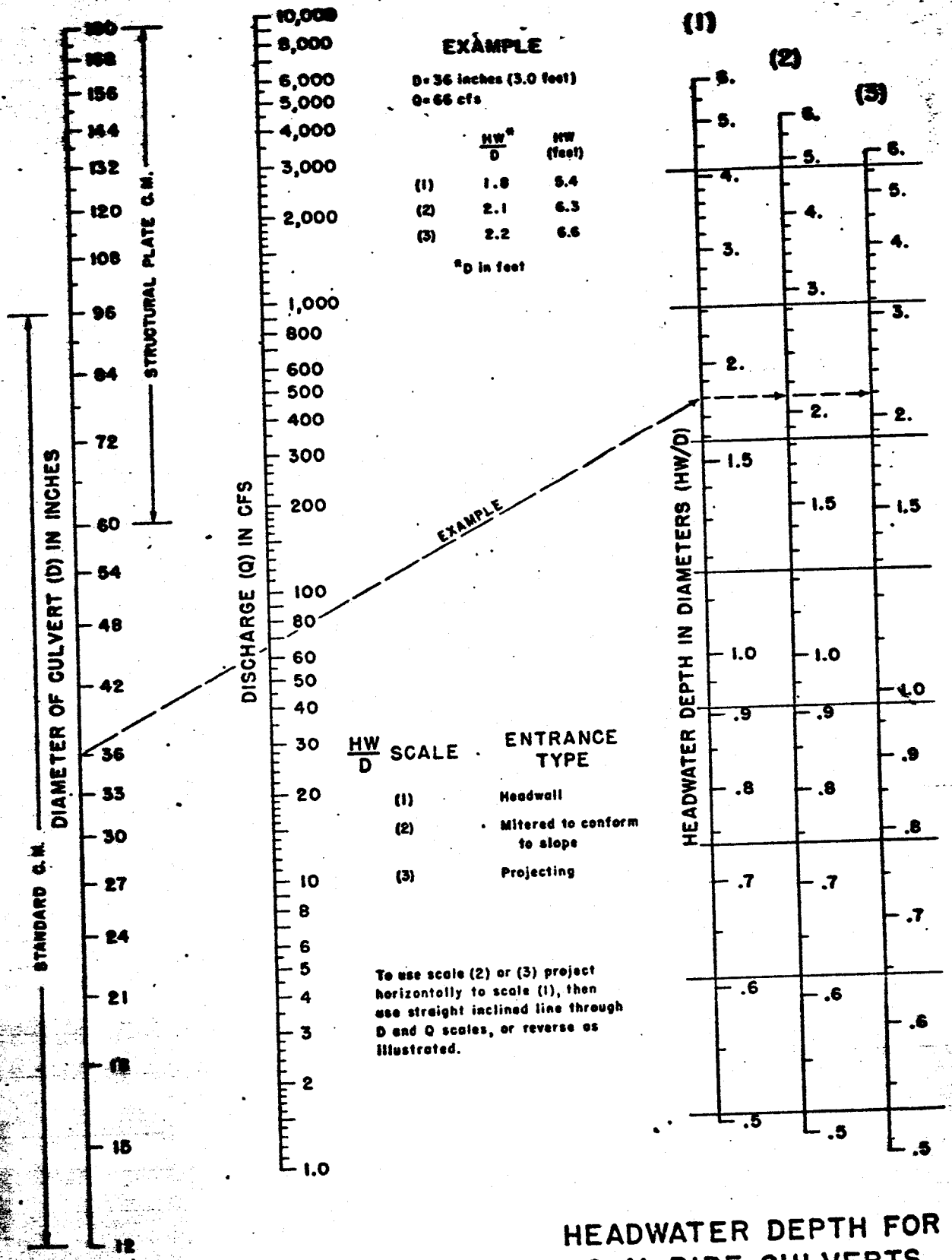

HEADWATER DEPTH FOR C. M. PIPE CULVERTS WITH INLET CONTROL

FIGURE 12

BUREAU OF PUBLIC ROADS JAN. 1963

INDEX

A. Table on Contents

B. References

C. Nomenclature

D. Class Notes

E. Uniform and critical flow tables for circular sections
Ref. - Design of Small Dams, Tables B-2 and B-3

F. Flow in natural channels
Ref. - Design of Small Dams, Appendix B

G. A simplified slope-area method for estimating flood discharges in natural channels
Ref. - H. C. Riggs, Jour. Research, USGS, Vol. 4, No. 3, May-June 1976, p. 285-291.

H. Critical flow in rivers with flood plains
Ref. - ASCE, Vol. 104, No. HY5, May 1978, p. 583-594

I. HEC-2 Water Surface Profiles, Users Manual
Ref. - U.S. Army Corps of Eng., Hyd. Eng. Center, Davis, CA, January 1981

J. HP - 41C computer programs and examples

K. Reservoir routing
Ref - Design of Urban Highway Drainage
FHWA - TS - 79 - 225, Federal Highway Admin.

L. Shallow wave propagation in open channel flow
Ref. - V. M. Ponce, and D. B. Simons
ASCE, Vol. 103, No. HY 12, Dec. 1977, p. 1461-1476

M. Applicability of Kinematic and diffusion models
Ref. - V. M. Ponce, R.M. Li, and D. B. Simons
ASCE, Vol. 104, No. HY3, March 1978, p. 353-360

N. Magnitude and timing of dam releases from El Vado Reservoir for white water rafting
Ref. - T. J. Ward
New Mexico State Park and Recreation Div.
Dept. Of Natural Resources
Santa Fe, NM, Nov. 1982

REFERENCES

Textbooks

1. Bakhmeteff, Boris A.
   Hydraulics of Open Channels
   McGraw-Hill Book Company, Inc. 1932

2. Chow, Ven Te
   Open-channel hydraulics
   McGraw-Hill Book Co., 1959

3. Henderson, F. M.
   Open Channel Flow
   The Macmillan Co., New York, 1966

4. Posey, Chesley J.
   Fundamentals of open channel hydraulics
   Rocky Mountain Hydraulic Laboratory
   Allenspark, Colorado, 1967.

5. Sellin, Robert H. J.
   Flow in channels
   Macmillan and Co. Ltd., 1969.

6. Woodward, Sherman M. and Posey, Chesley J.
   Hydraulics of steady flow in open channels
   John Wiley and Sons, Inc., 1941.

7. Simons, Daryl B. and Senturk, Fuat
   Sediment Transport Technology
   Water Resources Publications
   Ft. Collins, CO, 1976

U. S. Bureau of Reclamation

1. Canals and Related Structures
   Design Standard No. 3

2. Design of Small Canal Structures

3. Design of Small Dams

4. Hydraulic Design of Transitions for Small Canals

5. Linings for Irrigation Canals

USDA Soil Conservation Service

1. Hydraulics: Section 5, National Engineering Handbook

2. Planning and Design of Open-Channels
   Technical Release No. 25

3. Hydraulics of Broad-Crested Spillways
   Technical Release No. 39

4. Handbook of Channel Design for Soil and Water Conservation
   Technical Paper 61

5. UD Method of Reservoir Flood Routing
   Technical Release No. 35

Federal Highway Administration

1. Design of Stable Channels with Flexible Linings
   Hydraulic Engineering Circular No. 15

2. Hydraulics of Bridge Waterways
   Hydraulic Design Series No. 1

3. Design Charts for Open-Channel Flow
   Hydraulic Design Series No. 3

4. Design of Supercritical Flow Channel Junctions
   Highway Research Board, Highway Research Record No. 123, p. 17-35,
   Highway Drainage and Scour Studies.

U.S. Geological Survey

1. Roughness Characteristics of Natural Channels
   Water Supply Paper 1849

U.S. Army Corps of Engineers

1. HEC-2 Water Surface Profiles, January 1981

2. Hydraulic Design of Flood Control Structures,
   Engineer Manual EM 1110-2-1601

NOMENCLATURE

A	cross-sectional area
a_n	normal component of acceleration
a_t	tangential component of acceleration
D	hydraulic depth
d_c	critical depth
d_n	normal depth
ΔE	energy loss
F	force
F_o	specific force
$\mathbb{F}$	Froude No.
g	acceleration due to gravity
H	total energy head
H_e	specific energy
H_L	total energy loss
h	pressure head
h_f	frictional head loss
h_e	head loss
I	inflow rate
K	conveyance
k	roughness height
m	mass
n	Manning's coefficient
O	outflow rate
P	wetted perimeter of channel
p	pressure
Q	discharge
q	discharge per unit width
R	hydraulic radius

$\mathbb{R}$	Reynolds No.
r	radius
S	storage volume
S_f	energy gradient
S_o	channel bed slope
ΔS	change in storage volume
T	top width
t	time
Δt	incremental time
v	velocity
$\bar{v}$	discharge velocity
v_f	shear velocity
x	channel length
Δx	incremental channel length
Y	depth of section
$\bar{Y}$	depth from water surface to centroid of area
y	depth of flow
y_n	normal depth
Z	section factor for critical flow
z	elevation head
α	energy coefficient
β	momentum coefficient
γ	unit weight of water
θ	channel slope, in degrees
ν	Kinematic viscosity
ρ	mass density
τ	shear stress
τ_f	shear velocity

LECTURE NOTES

TABLE OF CONTENTS

Lecture Number	Subject	Page
2	Definitions	1
2	Section properties	2
2	Reynolds Number	3
2	Froude Number	4
3	Pressure distribution	7
3	Shear distribution	9
3	Velocity distribution	11
4	Continuity equation	13
4	Energy equation	14
4	Momentum equation	15
4	Energy coefficient	16
4	Momentum coefficient	16
5	Specific energy	18
5	Specific force	27
5	Hydraulic jump	29
5	Critical flow	31
6	Uniform flow	33
7	Resistance to flow	38
8	Slope-area and simplified slope-area	58
10	Gradually varied flow theory	61
11	Computation by direct step method	67
12	Direct step by computer	72
13	Standard step method	74
14	Computation by standard step method	75
15	Standard step method by computer	85
17	Unsteady flow theory	95
18	Method of characteristics	101
19	Reservoir routing	104
20	Channel routing	110
20	Muskingum method	112
20	Muskingum - Cunge method	115
20	Finite difference method	119

Definitions

steady flow – no change in flow with time at a point.

$$\frac{\partial(\,)}{\partial t} = 0 \,, \quad \text{for a given } x$$

unsteady flow – change in flow with time at a point.

$$\frac{\partial(\,)}{\partial t} \neq 0 \,, \quad \text{for a given } x$$

uniform flow – no change in flow for a reach of channel at an instant in time.

$$\frac{\partial(\,)}{\partial x} = 0 \,, \quad \text{for a given } t$$

varied flow – not uniform.

$$\frac{\partial(\,)}{\partial x} \neq 0 \,, \quad \text{for a given } t$$

Varied flow is further classified as gradually varied (gvf) or rapidly varied (rvf).

Hydraulic Depth, $D = A/T$

Section	Area a	Wetted Perimeter p	Hydraulic Radius r	Top Width T
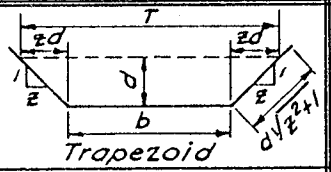 Trapezoid	$bd+zd^2$	$b+2d\sqrt{z^2+1}$	$\frac{bd+zd^2}{b+2d\sqrt{z^2+1}}$	$b+2zd$
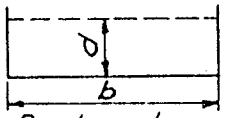 Rectangle	bd	$b+2d$	$\frac{bd}{b+2d}$	b
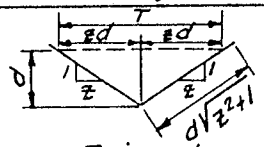 Triangle	zd^2	$2d\sqrt{z^2+1}$	$\frac{zd}{2\sqrt{z^2+1}}$	$2zd$
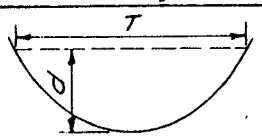 Parabola	$\frac{2}{3}dT$	$T+\frac{8d^2}{3T}$ [1]	$\frac{2dT^2}{3T^2+8d^2}$ [1]	$\frac{3a}{2d}$
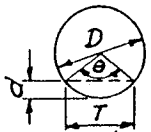 Circle - < 1/2 full [2]	$\frac{D^2}{8}\left(\frac{\pi\theta}{180}-\sin\theta\right)$	$\frac{\pi D\theta}{360}$	$\frac{45D}{\pi\theta}\left(\frac{\pi\theta}{180}-\sin\theta\right)$	$D\sin\frac{\theta}{2}$ or $2\sqrt{d(D-d)}$
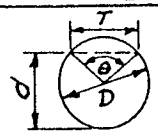 Circle - > 1/2 full [3]	$\frac{D^2}{8}\left(2\pi-\frac{\pi\theta}{180}+\sin\theta\right)$	$\frac{\pi D(360-\theta)}{360}$	$\frac{45D}{\pi(360-\theta)}\left(2\pi-\frac{\pi\theta}{180}+\sin\theta\right)$	$D\sin\frac{\theta}{2}$ or $2\sqrt{d(D-d)}$

[1] Satisfactory approximation for the interval $0 < \frac{d}{T} \leq 0.25$
When $d/T > 0.25$, use $p = \frac{1}{2}\sqrt{16d^2+T^2} + \frac{T^2}{8d}\sinh^{-1}\frac{4d}{T}$

[2] $\theta = 4\sin^{-1}\sqrt{d/D}$
[3] $\theta = 4\cos^{-1}\sqrt{d/D}$
} Insert θ in degrees in above equations

HYDRAULICS: ELEMENTS OF CHANNEL SECTIONS

REFERENCE

U. S. DEPARTMENT OF AGRICULTURE
SOIL CONSERVATION SERVICE
H. H. Bennett, Chief
ENGINEERING STANDARDS UNIT

STANDARD DWG. NO. ES-33
SHEET 1 OF 1
DATE 6-6-50

2

Reynolds Number

Ratio of inertial forces to viscous forces.

For open-channel hydraulics:

$$\mathcal{R} = \frac{\bar{v} R}{\nu}$$

where $\bar{v}$ is discharge velocity $\left(\frac{Q}{A}\right)$, ft/sec

R is hydraulic radius $\left(\frac{A}{P}\right)$, ft

ν is kinematic viscosity, ft^2/sec

Flow is laminar when $\mathcal{R} < 500$

Flow is turbulent when $\mathcal{R} > 2000$

Flow is transitional when $500 < \mathcal{R} < 2000$

Ref. - Chow, Figs 1-3 and 1-4.

For most engineering applications flow is turbulent.

Froude Number

Ratio of inertia forces to gravity forces.

For open-channel hydraulics:

$$\mathbb{F} = \frac{\bar{v}}{\sqrt{gD}}$$

where $\bar{v}$ is discharge velocity $\left(\frac{Q}{A}\right)$, ft/sec

D is hydraulic depth $\left(\frac{A}{T}\right)$, ft

g is 32.2 ft/sec^2

Flow is critical when $\mathbb{F} = 1.0$

Flow is subcritical when $\mathbb{F} < 1.0$

Flow is supercritical when $\mathbb{F} > 1.0$

Example:

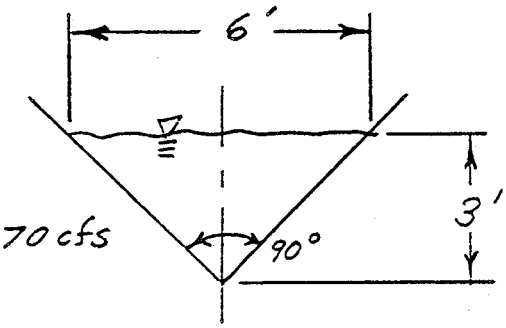

$Q = 70$ cfs

$A = 9$ ft^2

$\bar{v} = \frac{Q}{A} = \frac{70}{9} = 7.78$ ft/sec

$D = \frac{A}{T} = \frac{9}{6} = 1.5$ ft

correct: $\mathbb{F} = \frac{\bar{v}}{\sqrt{gD}} = \frac{7.78}{\sqrt{g\,1.5}} = 1.12$ (supercritical)

incorrect: $\mathbb{F} = \frac{\bar{v}}{\sqrt{gY}} = \frac{7.78}{\sqrt{g\,3.0}} = 0.79$ (subcritical)

Example using Tables B-2 and 3-3 from "Design of Small Dams"

Given: 10-ft diameter concrete conduit ($n = .012$) with a 0.002 ft/ft slope.

Discharge is 800 cfs.

1. Determine the critical depth, d_c.

$$\frac{Q_c}{D^{5/2}} = \frac{800}{10^{5/2}} = 2.53 \quad \text{(Col. 3, Table B-2)}$$

$$\frac{d}{D} = .68 \quad \text{(Col. 1, Table B-2)}$$

$$\therefore d_c = .68(10) = 6.8 \text{ ft}$$

2. Determine the normal depth, d_n.

$$\frac{Q\,n}{D^{8/3}\,S^{1/2}} = \frac{(800)(.012)}{10^{8/3}\,(.002)^{1/2}} = .463 \quad \text{(Col. 4, Table B-3)}$$

$$\frac{d}{D} = .82 \text{ (or) } 1.00 \quad \text{(Col. 1, Table B-3)}$$

flow is subcritical $\qquad d_n = 8.2$ ft (or) 10.0 ft

3. Determine velocity & velocity head @ $d = 8.2$ ft.

$$\frac{d}{D} = .82 \quad \text{(Col. 1, Table B-3)}$$

$$\frac{A}{D^2} = .6893 \quad \text{(Col. 2, Table B-3)}$$

$$A = 68.93 \text{ ft}^2$$

$$\bar{v} = Q/A = \frac{800}{68.93} = 11.6 \text{ fps}$$

$$\frac{\bar{v}^2}{2g} = \frac{11.6^2}{2g} = 2.1 \text{ ft}$$

4. Determine static pressure @ $d = 8.2$ ft

$$\frac{P}{D^3} = .2584 \quad \text{(Col. 4, Table B-2)}$$

$$P = 10^3(.2584)(62.4) = 16{,}124 \text{ lb}$$

Example - use of SECPROP

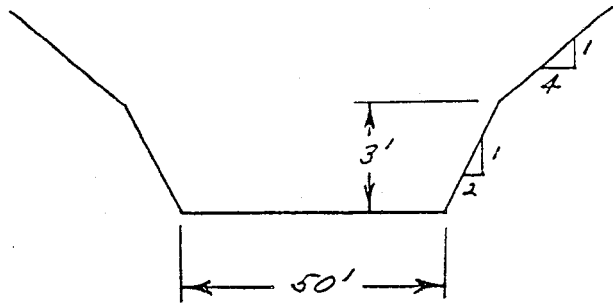

SECPROP

a = 3.0000
B = 50.0000
Z1 = 2.0000
Z2 = 4.0000

Y = 0.5000
A = 25.5000
T = 52.0000
D = 0.4904
ZG = 101.2492
P = 52.2361
RH = 0.4882
AR = 15.8096

Y = 1.0000
A = 52.0000
T = 54.0000
D = 0.9630
ZG = 289.3285
P = 54.4721
RH = 0.9546
AR = 50.4146

Y = 1.5000
A = 79.5000
T = 56.0000
D = 1.4196
ZG = 537.0009
P = 56.7082
RH = 1.4019
AR = 99.5821

Y = 2.0000
A = 108.0000
T = 58.0000
D = 1.8621
ZG = 835.6121
P = 58.9443
RH = 1.8322
AR = 161.7131

Y = 2.5000
A = 137.5000
T = 60.0000
D = 2.2917
ZG = 1,180.2160
P = 61.1803
RH = 2.2475
AR = 235.9192

Y = 3.00
A = 168.00
T = 62.00
D = 2.71
ZG = 1,568.02
P = 63.42
RH = 2.65
AR = 321.65

Y = 3.00
A = 168.00
T = 62.00
D = 2.71
ZG = 1,568.02
P = 63.42
RH = 2.65
AR = 321.65

Y = 3.50
A = 200.00
T = 66.00
D = 3.03
ZG = 1,974.04
P = 66.73
RH = 3.00
AR = 415.74

Y = 4.00
A = 234.00
T = 70.00
D = 3.34
ZG = 2,425.02
P = 70.05
RH = 3.34
AR = 522.90

Y = 4.50
A = 270.00
T = 74.00
D = 3.65
ZG = 2,924.24
P = 73.37
RH = 3.68
AR = 643.59

Y = 5.00
A = 308.00
T = 78.00
D = 3.95
ZG = 3,470.26
P = 76.68
RH = 4.02
AR = 778.25

Y = 6.00
A = 390.00
T = 86.00
D = 4.53
ZG = 4,709.02
P = 83.32
RH = 4.68
AR = 1,091.33

Y = 7.00
A = 480.00
T = 94.00
D = 5.11
ZG = 6,150.08
P = 89.95
RH = 5.34
AR = 1,465.78

Y = 8.00
A = 578.00
T = 102.00
D = 5.67
ZG = 7,801.44
P = 96.58
RH = 5.98
AR = 1,905.23

Pressure Distribution

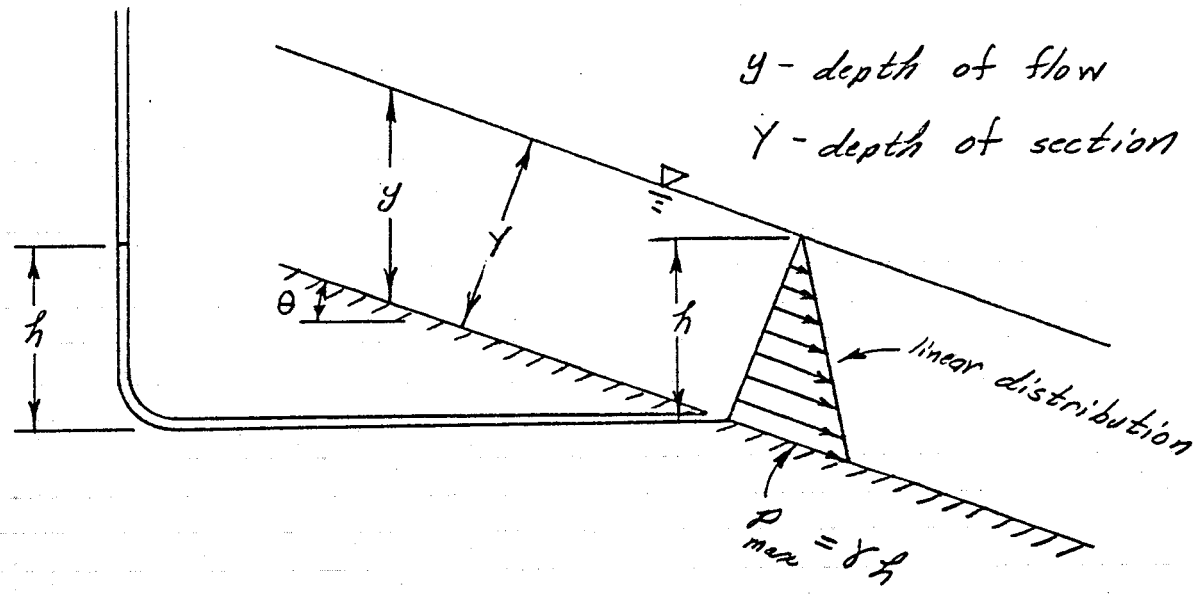

$$Y = y \cos\theta$$

$$h = Y \cos\theta$$

$$\therefore h = y \cos^2\theta$$

For open-channel flow where θ is small ($< 10°$):

$$p_{max} \approx \gamma Y$$

Pressure Distribution - Curvilinear flow

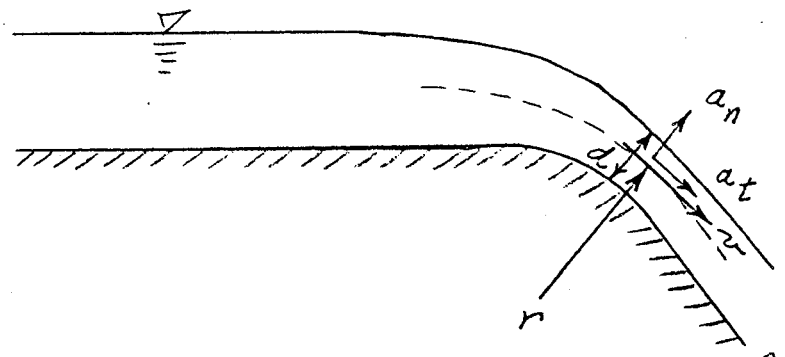

normal acceleration $a_n = \frac{v^2}{r}$

Force due to curvilinear flow:

$$F_c = m a_n$$

mass of a column of water, $m = d(1 ft^2)\rho$

ρ = mass density

For a constant radius of curvature and uniform velocity distribution:

$$F_c = d\rho \frac{v^2}{r}$$

In general, $F_c = \int \rho \frac{v^2}{r} dr$

The pressure distribution is not linear

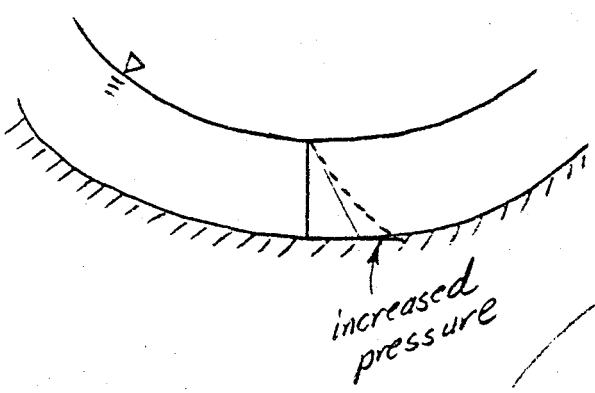

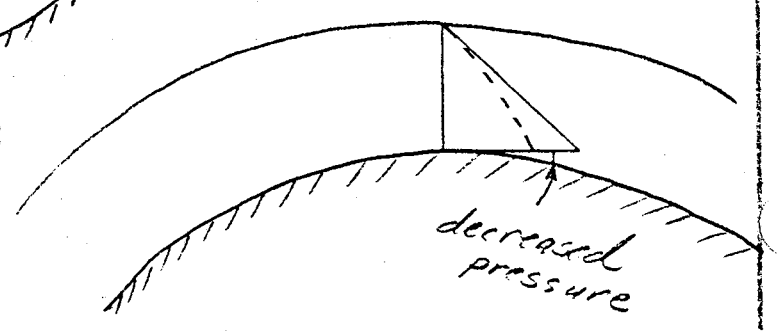

Tractive Force

When water flows in an open channel it creates a "pull" on the wetted perimeter.

For a constant discharge through a channel section of fixed cross section the tractive force can be related to the down slope component of the weight of water in the channel

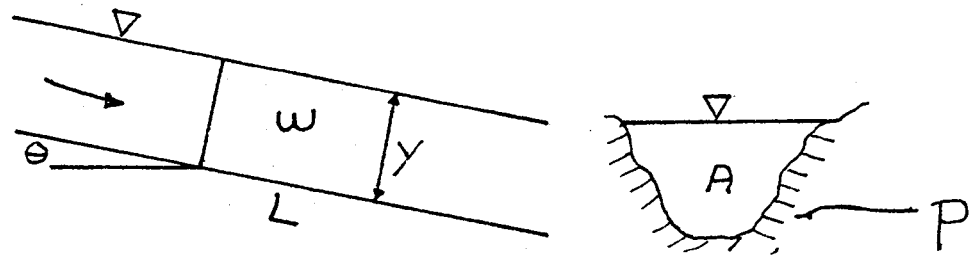

w = weight of water = $\gamma A L$

Weight in downslope direction = $\gamma A L \sin\theta$

τ = resisting shear (average) $= \frac{F}{A_F} = \frac{F}{pL} = \frac{\gamma A L \sin\theta}{pL}$

or $\boxed{\tau = \text{tractive force} = \gamma R \sin\theta}$

This is the total or effective shear stress ("force")

Simplifing assumptions

$R \rightarrow y$ for wide channels

$\sin\theta \approx \tan\theta = S$ for $\theta < 10°$

This yields:

$\tau = \gamma y S$ or $\gamma d S$ depending on symbols

The tractive force or shear stress is not constant in a cross section as the previous equation for "average" shear indicates.

Information from velocity distributions in channels indicates that shear can vary considerably from point to point along the wetted perimeter. This can be illustrated by the following figure.

Ref. Figs 7-6 and 7-7 of Chow

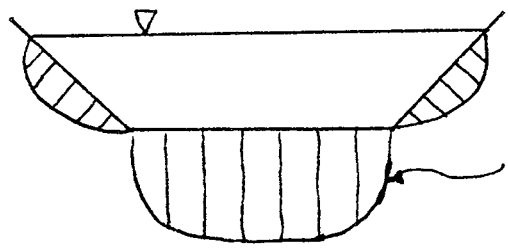

Variation is affected by channel shape, channel alignment (bends), and velocity distribution.

However, the concept and formulation for the average shear stress are important characteristics for describing open channel flow.

Velocity Distribution

Except for unusual cases, velocity is not constant horizontally or vertically in a channel cross section. The velocity distribution in the horizontal direction is controlled by many factors including shear stress, channel alignment, and the development of lateral velocity components.

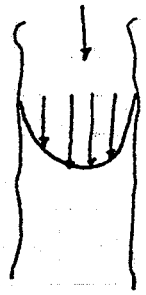

Horizontal velocity distribution

Plan view

The vertical velocity distribution has been shown (numerous times) to be related to shear stress and flow resistance (later section)

The Prandtl-von Karman vertical velocity distribution is of the form

$$v = 5.75\, v_f \log(y/k)$$

Where v_f = "shear velocity" = $\sqrt{\frac{\tau}{\rho}} = \sqrt{gRS}$

k = a parameter depending on type of channel boundary

For hydraulically "smooth" boundaries

$$k = (\nu / 9 v_f)$$

For hydraulically "rough" boundaries

$k = \frac{k}{30}$ with k = roughness height

These <u>logrithmic</u> velocity profiles indicate a zero (non existant) velocity at $y=0$ and a maximum velocity at $y=$ depth of flow. In reality, the maximum velocity is a bit below the surface because of the air-water interface drag.

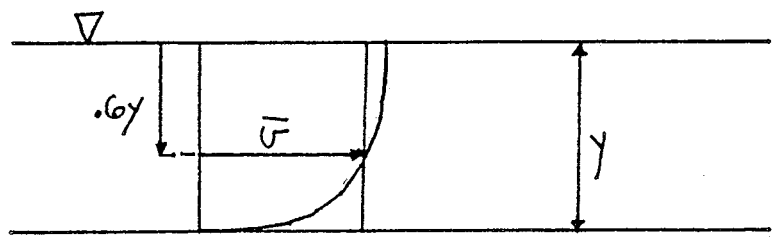

The vertical velocity equations can be integrated to yield the fact that the average velocity occurs at about

$0.6y$ down from the water surface

and that

$$\bar{v} \cong \frac{v \text{ at } 0.8 \text{ depth} + v \text{ at } 0.2 \text{ depth}}{2}$$

Continuity Equation

Conservation of mass

Steady flow :

$$Q_1 = Q_2 \equiv A_1 V_1 = A_2 V_2$$

or $Q_1 - Q_2 = 0$

Unsteady flow : $Q_1 \neq Q_2$

$$I - O = \frac{dS}{dt} \quad (Q_1 = I, Q_2 = O)$$

where I is inflow rate, L^3/T

O is outflow rate, L^3/T

S is storage volume, L^3

and t is time, T

Energy Equation

Conservation of energy

Total energy = Σ KE + Σ PE

$$KE = \alpha \frac{\bar{v}^2}{2g} \quad \text{(velocity "head")}$$

$$PE = z \text{ (elevation "head")} + \frac{p}{\gamma} \text{ (pressure "head")}$$

$$E = \alpha \frac{\bar{v}^2}{2g} + z + \frac{p}{\gamma}$$

E is energy in $\frac{\text{ft-lbs}}{\text{lb of water}}$. Total energy = $E \gamma Q (\Delta T)$

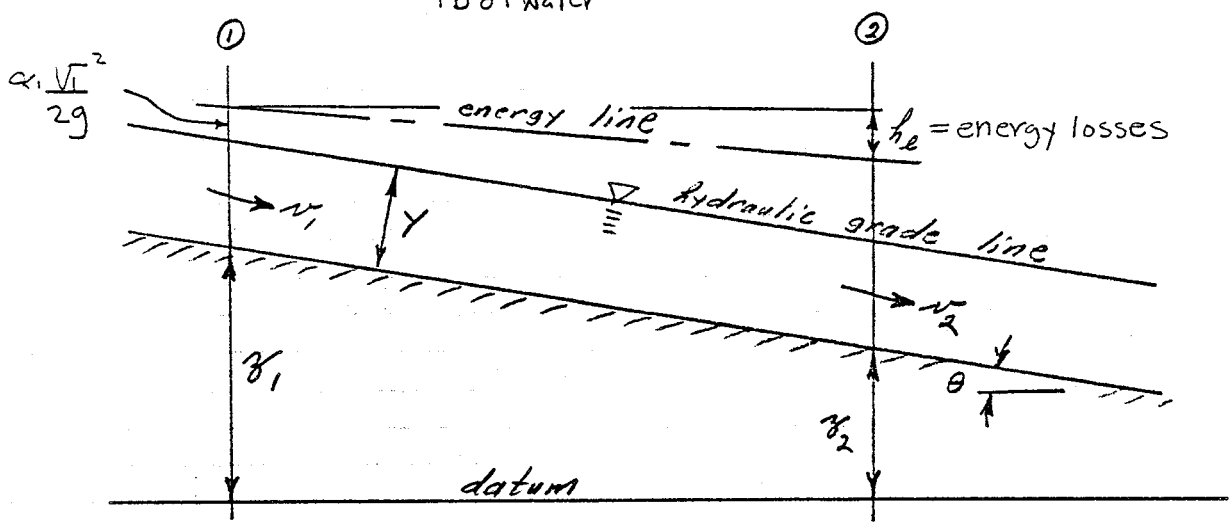

Energy at both sections must be equal

$$\alpha_1 \frac{\bar{v}_1^2}{2g} + Y_1 \cos\theta + z_1 = \alpha_2 \frac{\bar{v}_2^2}{2g} + Y_2 \cos\theta + z_2 + h_e$$

Simplifying assumptions:

$\alpha_1 = \alpha_2 = 1$
$\theta < 10°$

Restrictions:

One-dimensional
flow lines are straight and parallel

Power of the flow = P = $\gamma Q E$

Momentum Equation

Conservation of momentum

Sum of external forces = time rate of change of momentum

$$\Sigma \vec{F} = \frac{d(m\vec{v})}{dt}$$

$\vec{F}$ & $\vec{v}$ are vectors.

For open-channel <u>steady</u> flow :

In the x-direction

$$\Sigma F_x = Q\rho\left(\beta_2 \bar{v}_{x_2} - \beta_1 \bar{v}_{x_1}\right)$$

This is used to calculate forces.

Energy Coefficient, a

Kinetic energy (KE) is estimated by $\frac{\bar{v}^2}{2g}$.

For "nonuniform" velocity distributions, this may not be a good estimate of KE.

$$KE = a\frac{\bar{v}^2}{2g}, \quad a \geq 1.0$$

where

$$a = \frac{\int v^3 dA}{\bar{v}^3 A}$$

Computational form:

$$a = \frac{\Sigma v^3 \Delta A}{\bar{v}^3 A}$$

Momentum Coefficient, β

Momentum (M) is estimated by $m\bar{v}$.

For "nonuniform" velocity distributions, this should be corrected.

$$M = \beta m \bar{v}, \quad \beta \geq 1.0$$

where

$$\beta = \frac{\int v^2 dA}{\bar{v}^2 A}$$

Computational form:

$$\beta = \frac{\Sigma v^2 \Delta A}{\bar{v}^2 A}$$

Example: The flow in a river downstream of a bridge constriction is as shown. Calculate the energy & momentum coefficients.

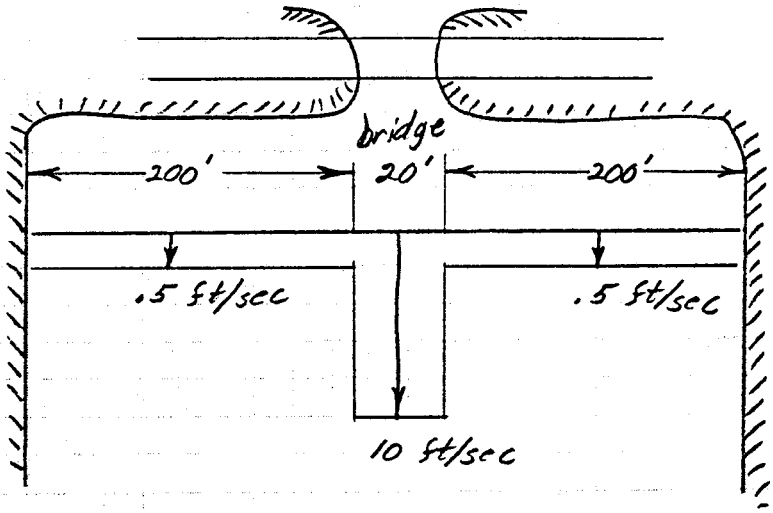

Plan View

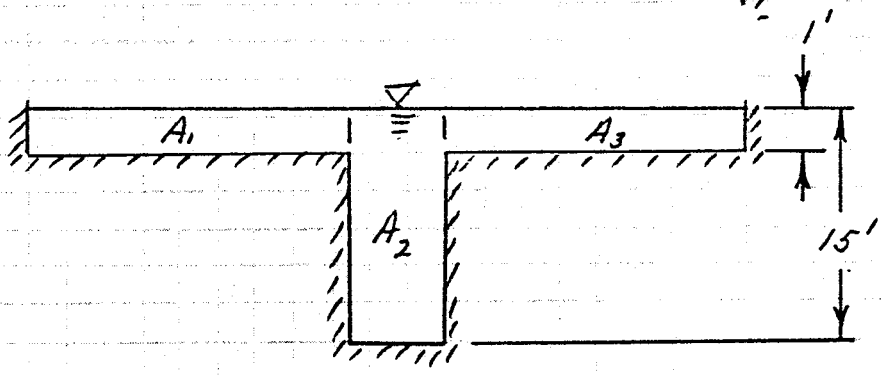

Cross-section

$$Q = (.5)(1)(200) + (10)(15)(20) + (.5)(1)(200) = 3200 \text{ cfs}$$

$$A = A_1 + A_2 + A_3 = 200 + 300 + 200 = 700 \text{ ft}^2$$

$$\bar{v} = \frac{Q}{A} = \frac{3200}{700} = 4.57 \text{ ft/sec}$$

$$\alpha = \frac{\sum v^3 \Delta A}{\bar{v}^3 A} = \frac{(.5)^3(200) + (10)^3(300) + (.5)^3(200)}{(4.57)^3(700)}$$

$$\alpha = 4.49$$

$$\beta = \frac{\sum v^2 \Delta A}{\bar{v}^2 A} = \frac{(.5)^2(200) + (10)^2(300) + (.5)^2(200)}{(4.57)^2(700)}$$

$$\beta = 2.06$$

Specific Energy

Specific energy - unit energy of water at any section measured with respect to the channel bottom.

$$H_e = \alpha \frac{\bar{v}^2}{2g} + Y \cos\theta$$

For small θ and $\alpha = 1.0$,

$$H_e = \frac{\bar{v}^2}{2g} + Y = \frac{Q^2}{2gA^2} + Y = \frac{q^2}{2gd^2} + Y$$

For a given specific energy there are (2) possible depths of flow.

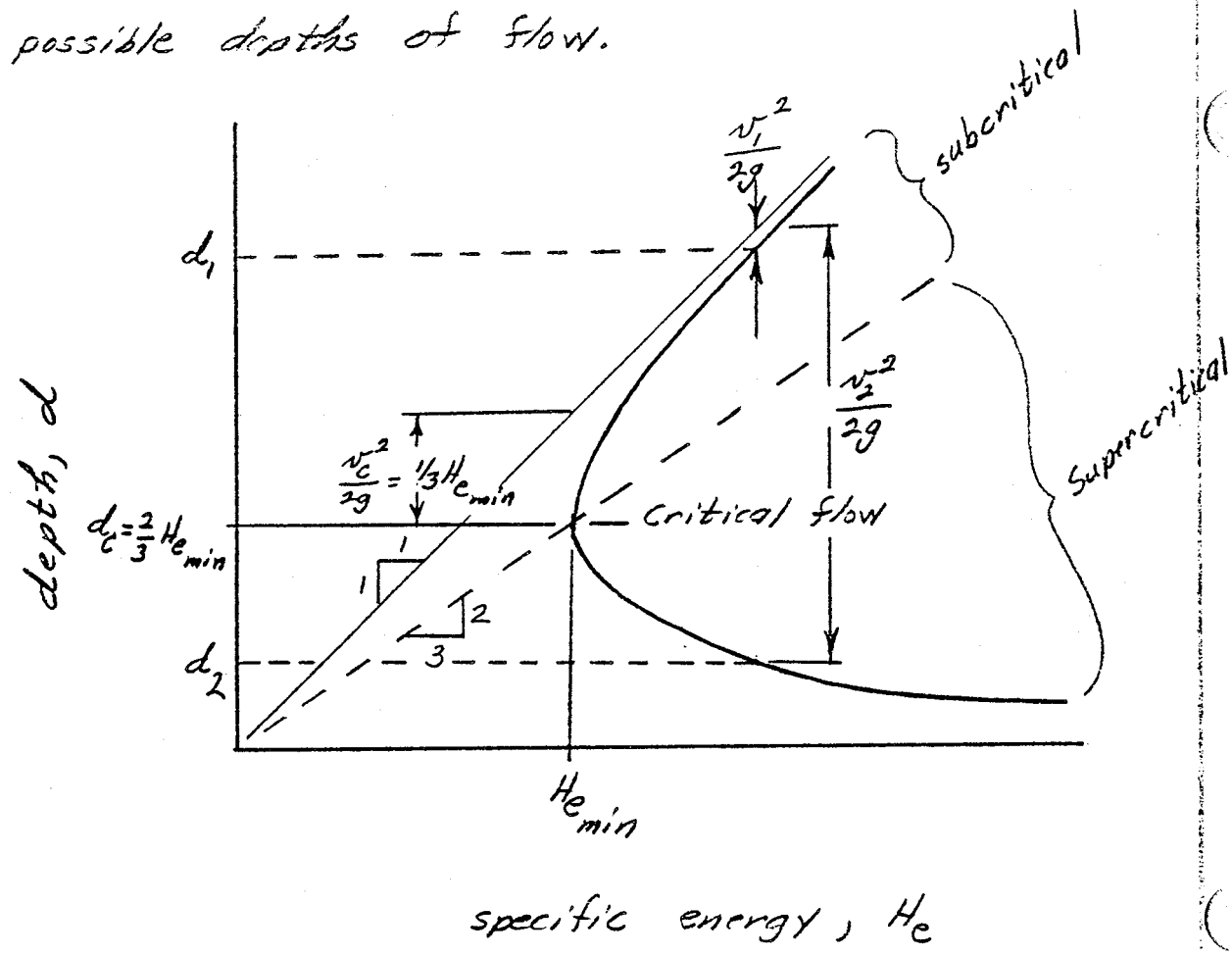

HYDRAULICS: RELATIONSHIP BETWEEN DEPTH OF FLOW AND SPECIFIC ENERGY FOR RECTANGULAR SECTION

Equations:

$$H_e = d + \frac{v^2}{2g} = d + \frac{q^2}{2gd^2}$$ where q = discharge per unit width.

$$d_c = \left(\frac{q_c}{\sqrt{g}}\right)^{\frac{2}{3}} = \frac{2}{3} H_{e\,min.}$$ where d_c = critical depth
q_c = critical discharge per unit width
$H_{e\,min.}$ = minimum energy content

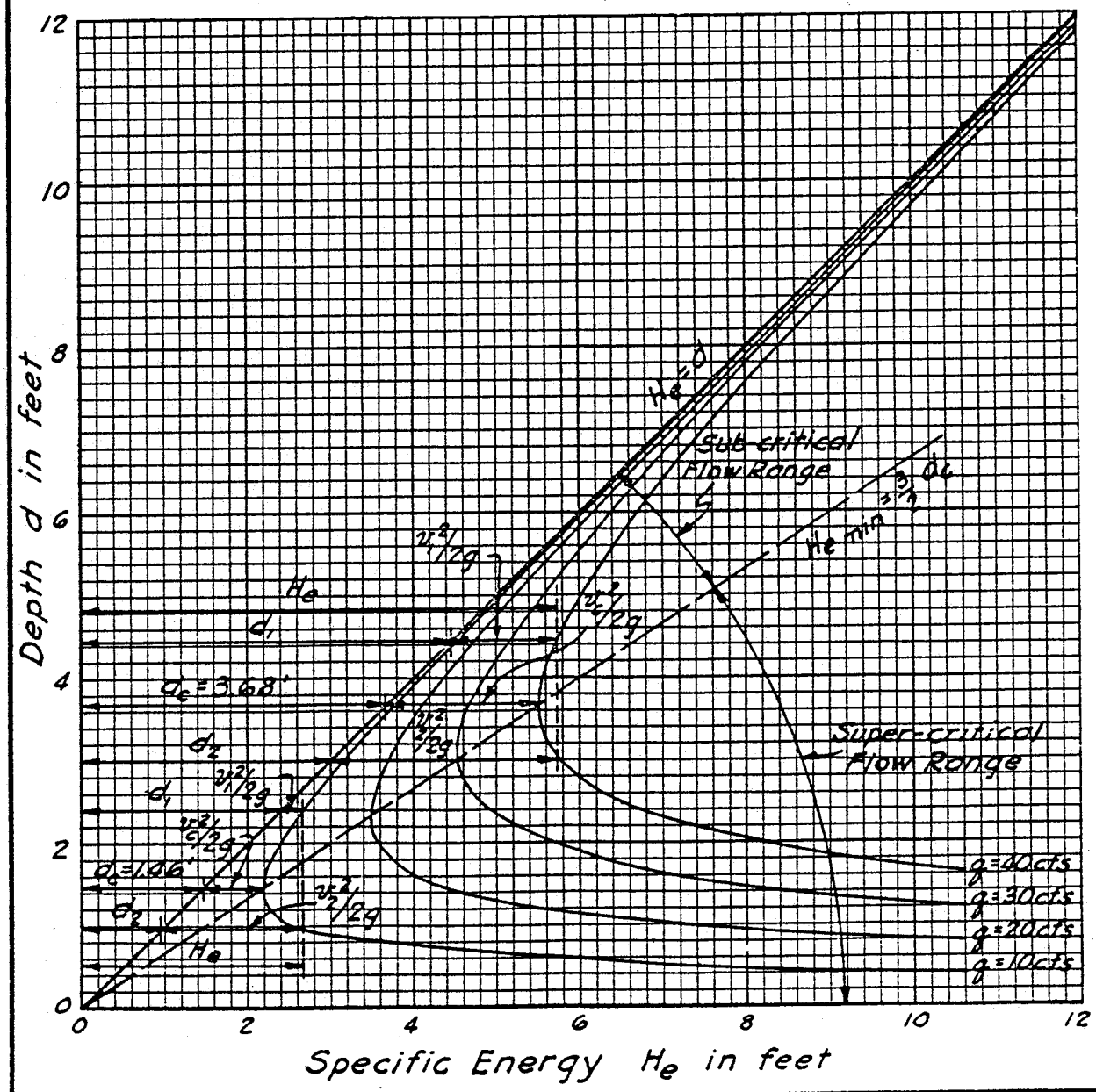

REFERENCE	U. S. DEPARTMENT OF AGRICULTURE SOIL CONSERVATION SERVICE H. H. Bennett, Chief ENGINEERING STANDARDS UNIT	STANDARD DWG. NO. ES-35 SHEET 1 OF 1 DATE 6-28-50

Ref. - SCS National Engineering Handbook
Section 5, Hydraulics

4.5.5 Significance of Critical Flow in Design. Critical, subcritical and supercritical flow affect design in the following manner:

(a) Critical flow. Uniform flow at or near critical depth is unstable. This results from the fact that the unique relationship between energy head and depth of flow which must exist in critical flow is readily disturbed by minor changes in energy. Examine the curve for q = 40 c.f.s. on drawing ES-35. The critical depth is 3.68 feet and the corresponding energy head is 5.52. If the energy head is increased to 5.60, the depth may be 3.2 or 4.2. Those who have seen uniform flow at or near critical depth have observed the unstable, wavy surface that is caused by appreciable changes in depth resulting from minor changes in energy. In channel design these conditions must be recognized. Variations in channel roughness, cross section, slope, or minor deposits of sediment or debris may cause fluctuations in depth of flow that are significant to channel operation. In many cases it is desirable to base design computations on two or more values of n in order to establish the probable range of operating conditions. Because of the unstable flow, channels carrying uniform flow at or near critical depth should not be used unless the situation allows no alternative.

The critical flow principle is the basis for the design of control sections at which a definite stage-discharge relation is desired or required.

(b) Subcritical flow. Two general characteristics of subcritical flow are important. First, at all stages in the subcritical range, except those in the immediate vicinity of the critical, the velocity head is small in comparison with the depth of flow. Study of the curves of constant discharge, drawing ES-35, will make this point clear. Second, the velocities are less than wave velocity for the depths involved and a backwater curve will result from retardation of velocity. Thus, in the subcritical range we are concerned with cases in which the depth of flow is of greater importance than kinetic energy as represented by velocity head. In practice, this means that changes in channel cross section, slope, roughness, and alignment may be made without the danger of developing seriously disturbed flow conditions so long as the design assures that flow in the supercritical range will not be created for some discharges in the operational range.

However, in many cases the latitude in design which may be possible as a result of dealing with subcritical flow will be offset by limited head requiring that friction losses be held to a minimum.

(c) Supercritical flow. The design of structures to carry supercritical flow requires consideration of some of the most complex problems in hydraulics. In supercritical flow the velocity head may range from a value approximately equal to depth of flow to many times the depth of flow. Note from the curves on drawing ES-35 that the velocity head increases very rapidly with decreases in depth throughout the supercritical range. Supercritical velocities exceed the velocities at which gravity waves may be propagated upstream. Any obstruction of flow will result in a standing wave, and there will be no effect upon flow upstream from the obstruction. The fact that kinetic energy predominates in supercritical flow and cannot be dissipated through the development of a water surface curve extending upstream is of primary importance in design.

Channels involving changes of direction, contraction or expansion of cross section, or the joining of two flows at a confluence at which either or both of the flows may be supercritical require careful consideration. Changes in direction or channel contractions develop disturbances at the walls of the channel which take the form of standing waves reflected diagonally from wall to wall downstream from the disturbance points. The height of these standing waves may be several times the depth of flow immediately upstream from the origin of the disturbance. Confluences at which either flow or both flows may be supercritical also develop disturbances resulting in standing waves. In expanding channels the discharge may be incapable of following the channel walls because of the high velocities involved. This results in nonuniform depth and the development of a hydraulic jump which is unstable as to both location and height.

A number of the factors that must be determined as a basis for design of these high velocity structures cannot be evaluated through theoretical analyses only. General experimental results as well as experimentation with individual structures are required. Basic requirements for projects and structures should first be determined and tentative designs to meet these requirements selected. The tentative designs should then be perfected through model tests.

Water surface profiles applying to cases of supercritical flow in straight channels of uniform width can normally be determined with sufficient accuracy for design by standard methods of analysis. Most structures must have outlet velocities in the subcritical range to prevent erosion damage. The creation of the hydraulic jump by the use of stilling basins is an efficient means of dissipating the excessive energy in supercritical flow. Design criteria, based on thorough model investigation, are available for some types of stilling basins. An example is the SAF stilling basin. Under unusual conditions or when exacting requirements must be met, stilling basin designs should also be perfected by model tests.

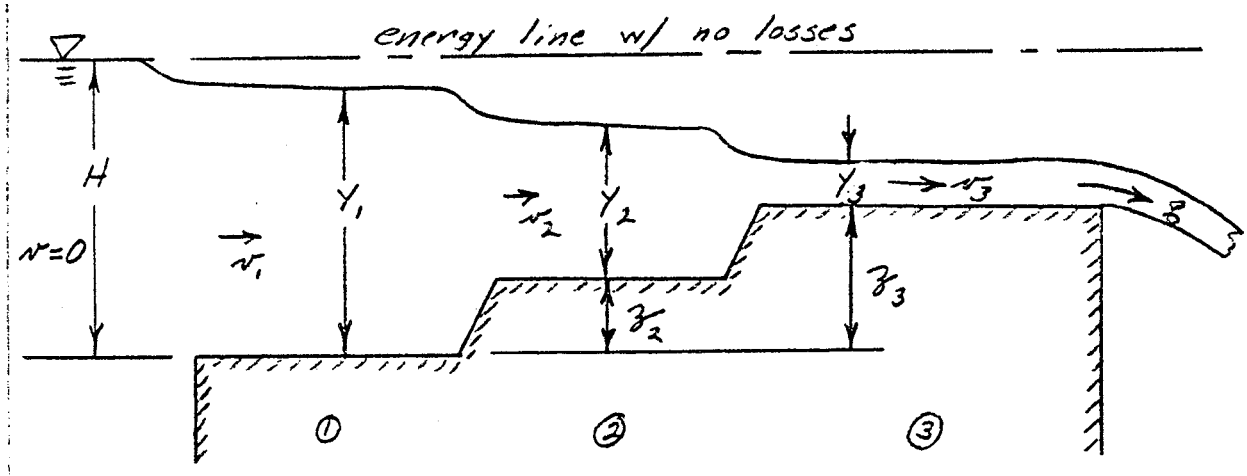

Total energy available = H

From the energy equation with no losses:

$$H = \underbrace{\frac{\bar{v}_1^{\,2}}{2g} + Y_1}_{He_1} = \underbrace{\frac{\bar{v}_2^{\,2}}{2g} + Y_2 + z_2}_{He_2} = \underbrace{\frac{\bar{v}_3^{\,2}}{2g} + Y_3 + z_3}_{He_3}$$

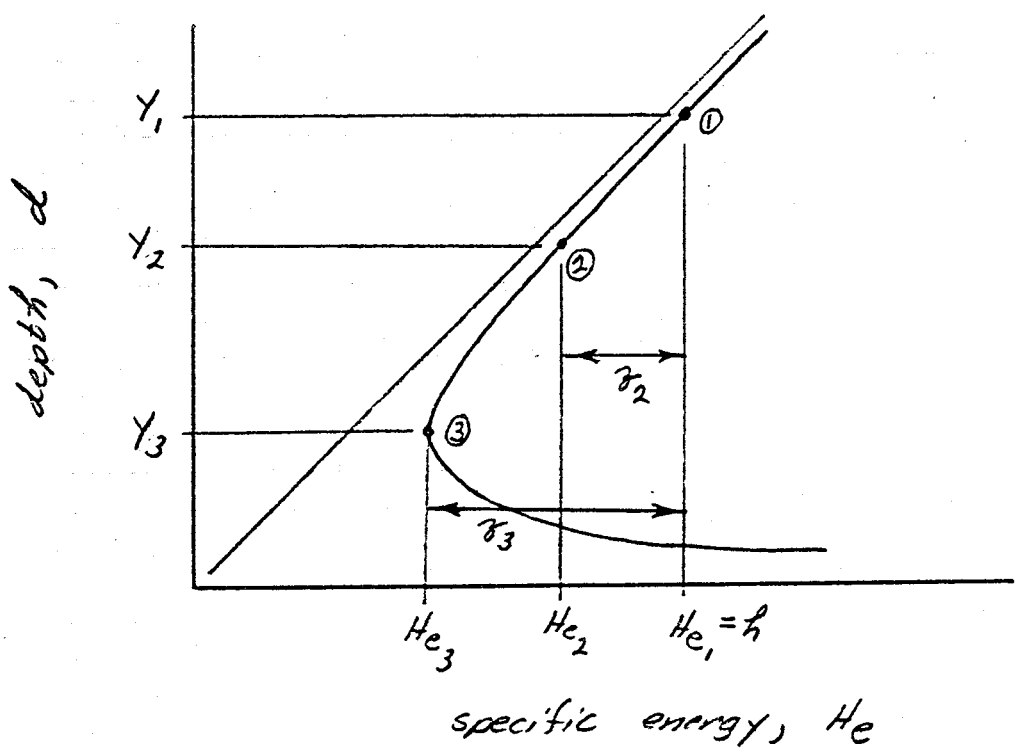

Example: Flow passes out of a detention basin into a rectangular channel, as shown. The channel ends with a vertical drop.

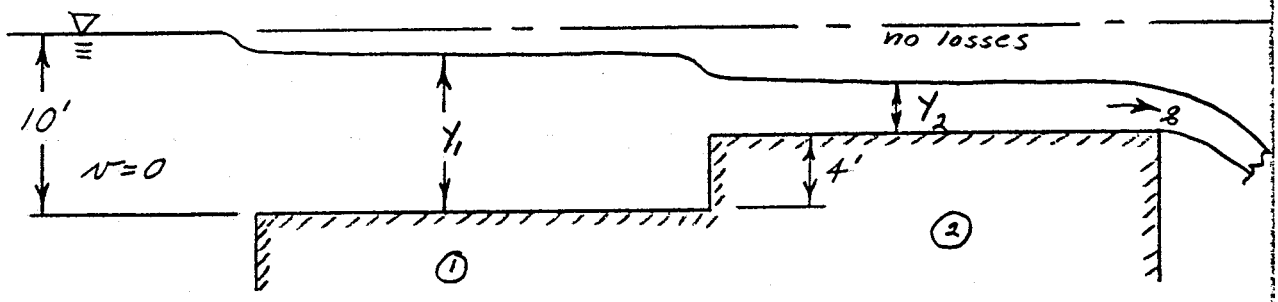

What is the discharge per unit width, q, and the depths, Y_1 and Y_2?

1. Flow at a free overfall is either critical or supercritical.
2. The He_{min} occurs at the highest elevation in the channel.
3. Flow is critical at ②.
4. $$Y_2 = d_c = \tfrac{2}{3} He_2$$

$$Y_2 = \tfrac{2}{3}(10-4) = 4 \text{ ft}$$

5. $$q = (g d_c^3)^{1/2} = (g\, 4^3)^{1/2} = 45.4 \text{ cfs}$$

6. $$He_1 = 10' = \frac{\bar{v}_1^2}{2g} + Y_1$$

$$\bar{v}_1 = \frac{q}{Y_1} = \frac{45.4}{Y_1}$$

$$10 = \frac{45.4^2}{2g\, Y_1^2} + Y_1$$

$$Y_1 = 9.7 \text{ ft.}$$

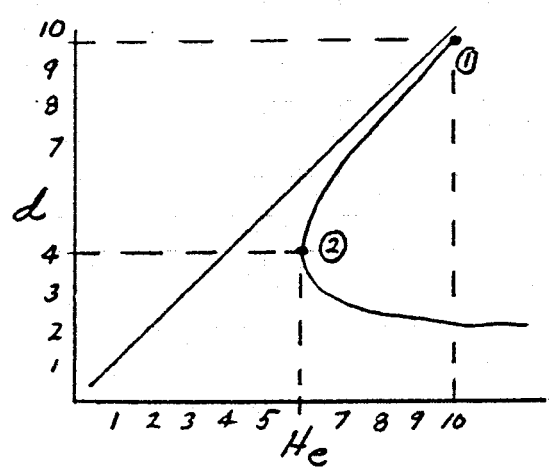

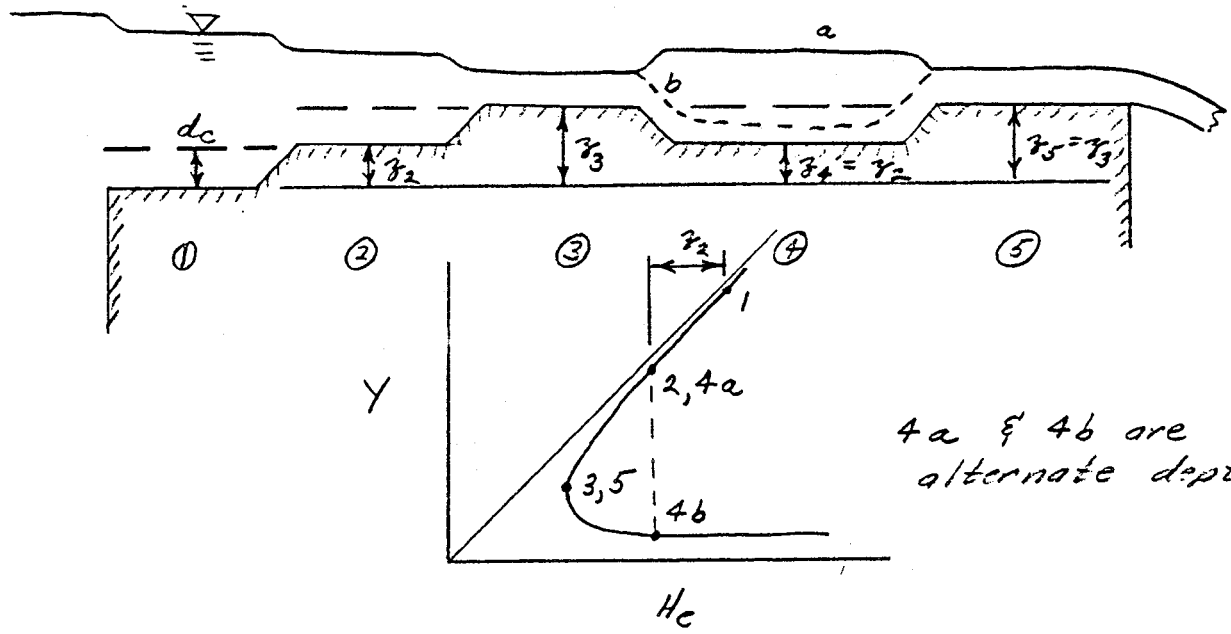

4a & 4b are alternate depths

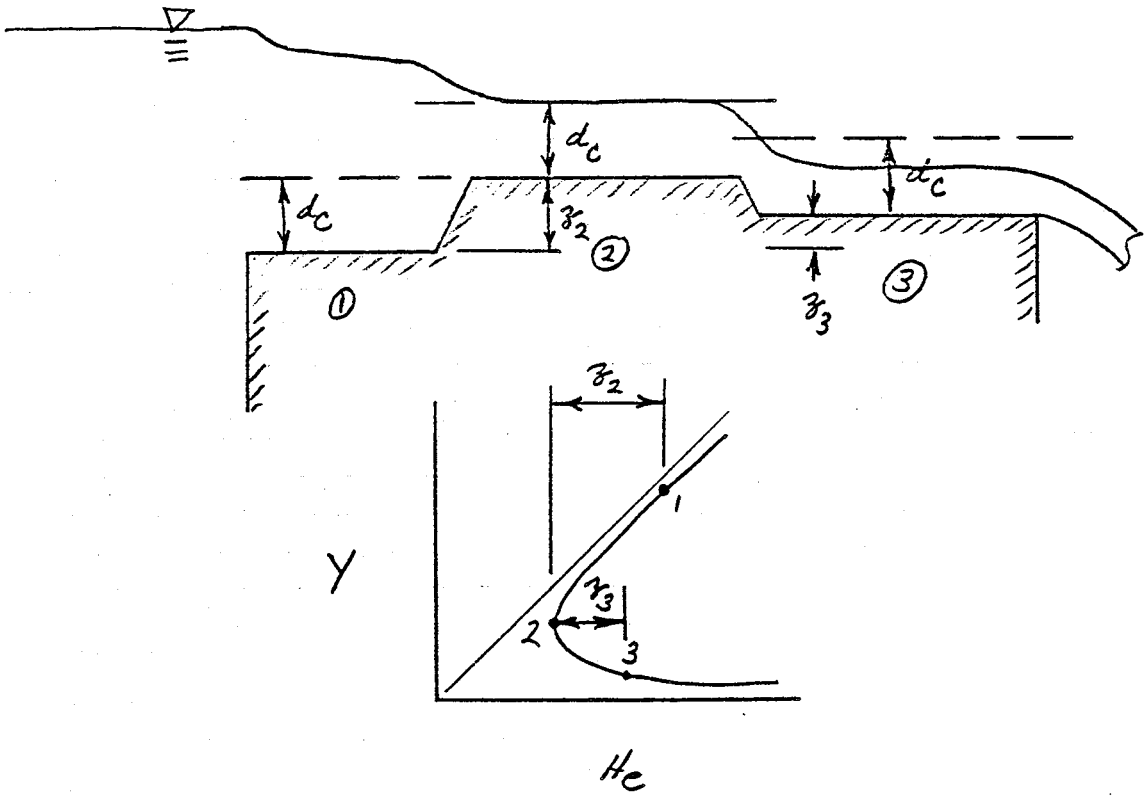

Specific Energy w/ varying width

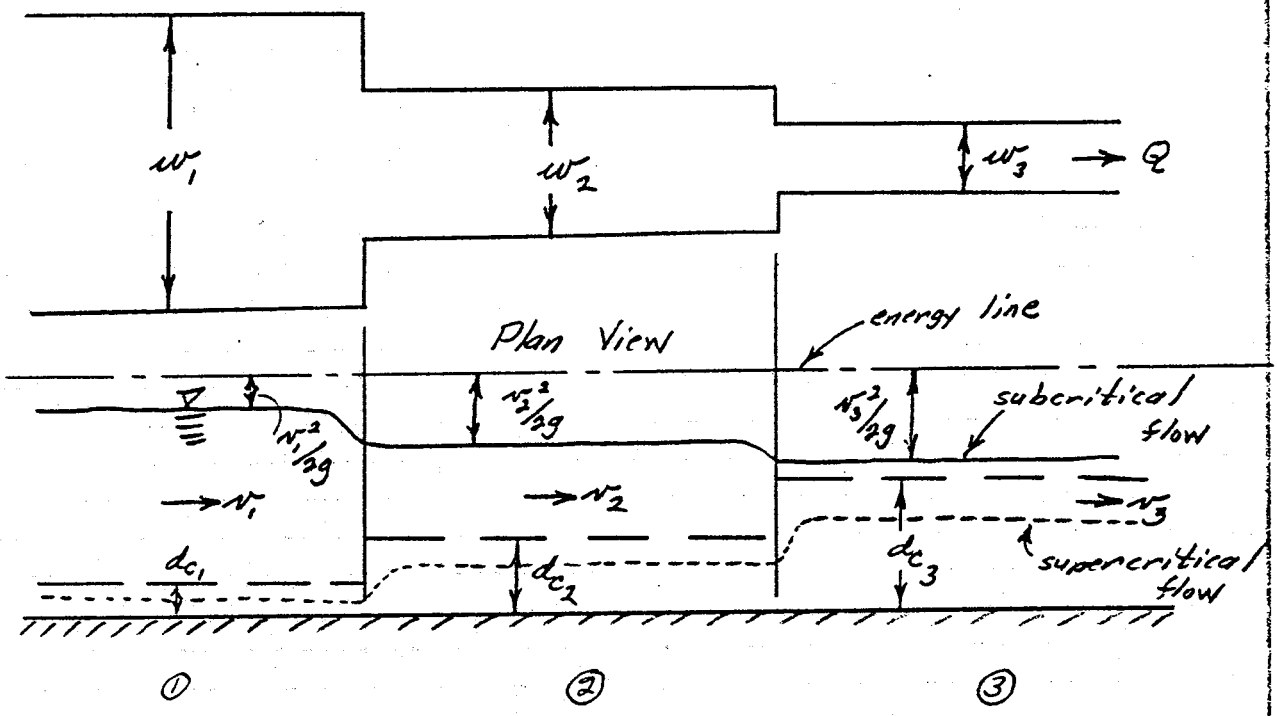

Profile

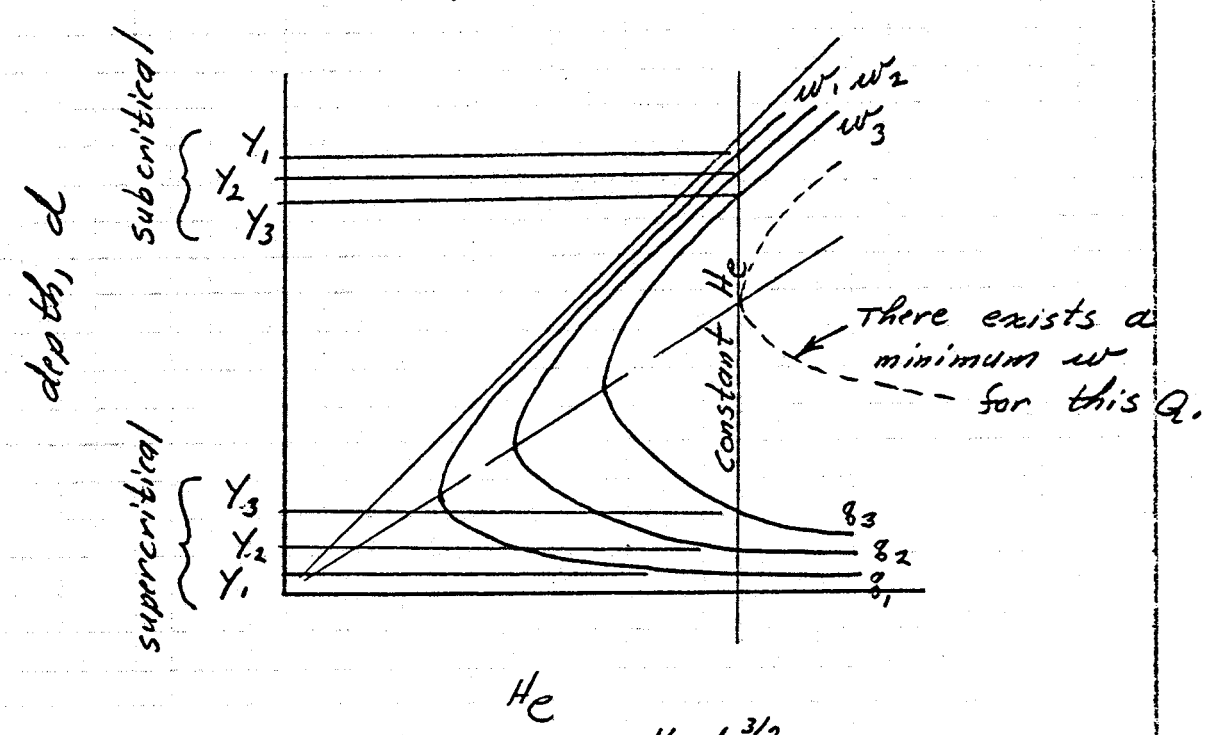

$$q_1 = \frac{Q}{w_1}$$

$$q_2 = \frac{Q}{w_2}$$

$$q_3 = \frac{Q}{w_3}$$

$$q = g^{1/2} d_c^{3/2}$$

$$q_1 < q_2 < q_3$$

Specific Energy w/ varying width & elevation

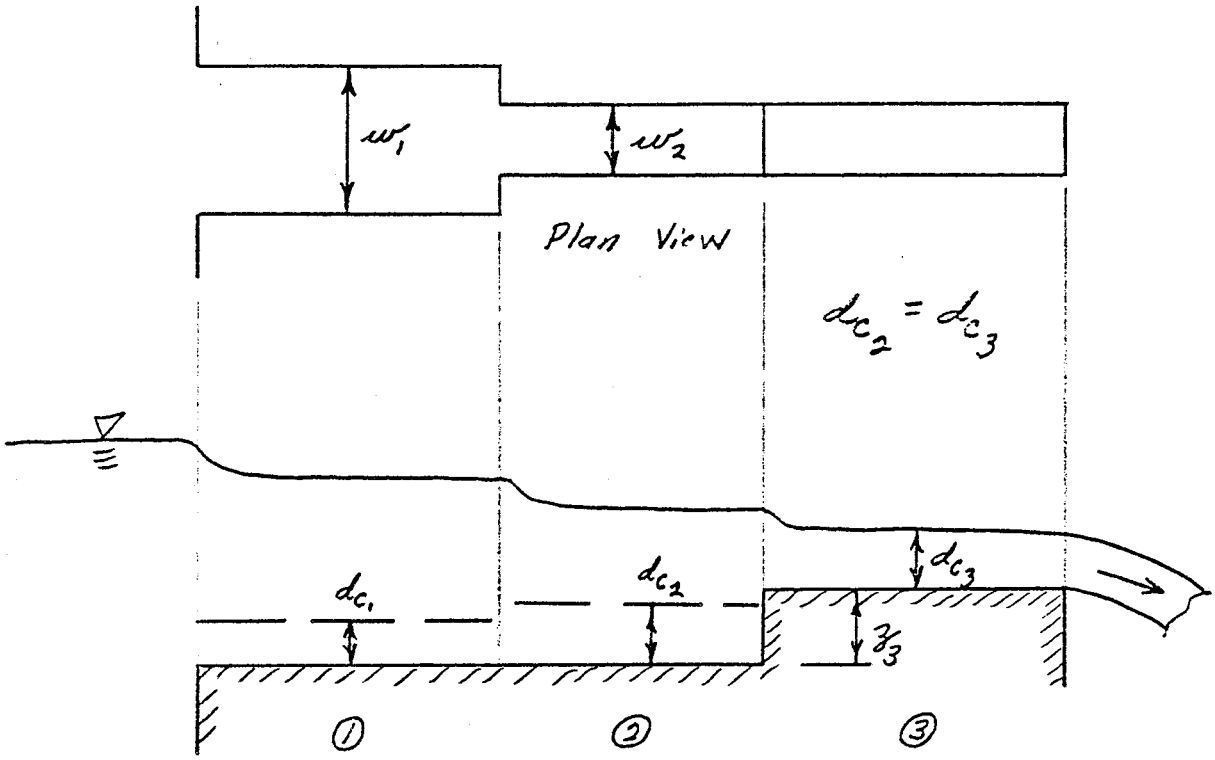

Profile

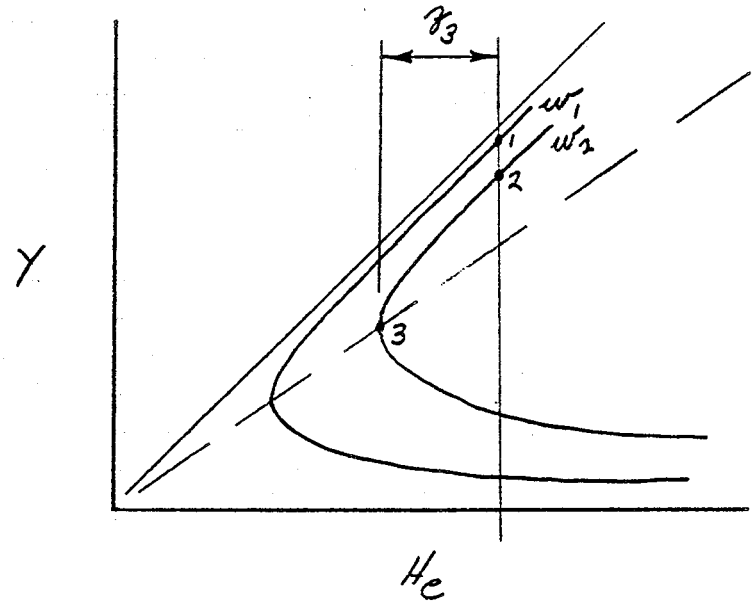

Specific Force

$$\Sigma \vec{F} = \frac{d(m\vec{v})}{dt}$$

External forces :

$$\Sigma \vec{F} = \underset{\rightarrow}{F_{pressure_1}} - \underset{\leftarrow}{F_{pressure_2}} - \underbrace{\underset{\leftarrow}{F_{friction}} - \underset{\leftarrow}{F_{obstructions}}}_{\text{These are difficult to determine explicitly.}} + \underset{\rightarrow}{F_{weight}} + \cdots$$

$$\frac{d(m\vec{v})}{dt} = \rho \beta_2 \frac{Q^2}{A_2} - \rho \beta_1 \frac{Q^2}{A_1}$$

Specific force (F_0) = momentum per unit weight + pressure force at a section.

$$F_0 = \rho \beta \frac{Q^2}{A} + \gamma \bar{Y} A \cos\theta$$

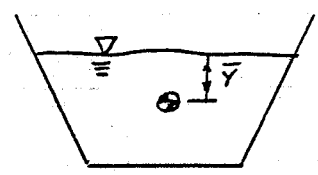

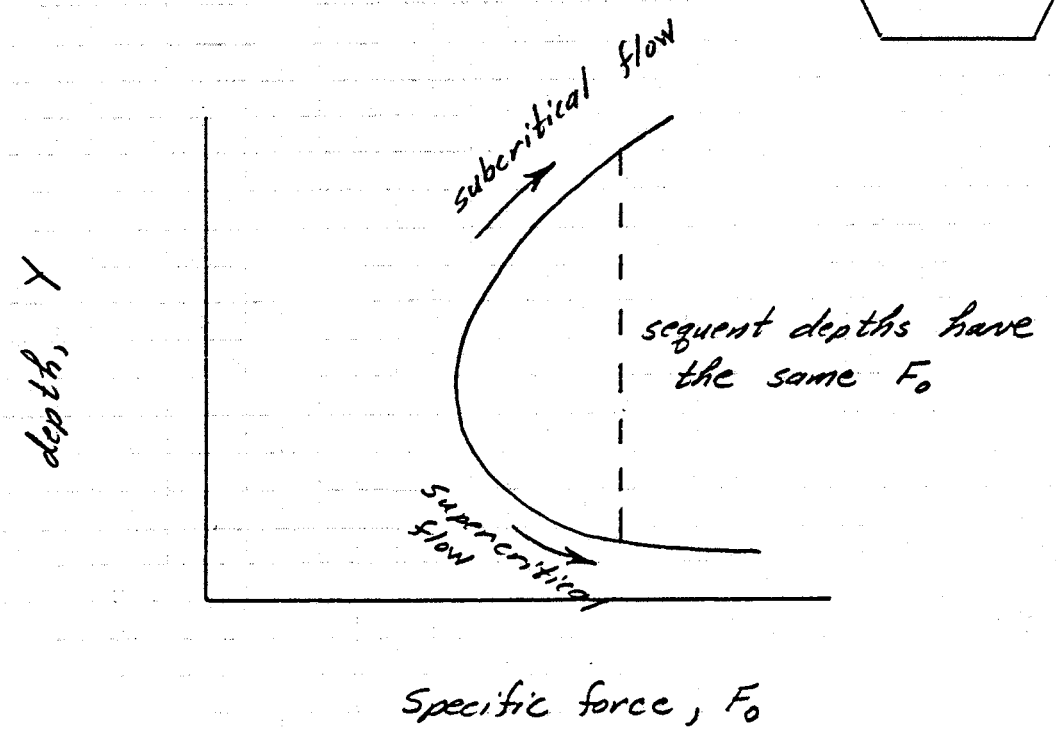

Examples:

Flow under a sluice gate

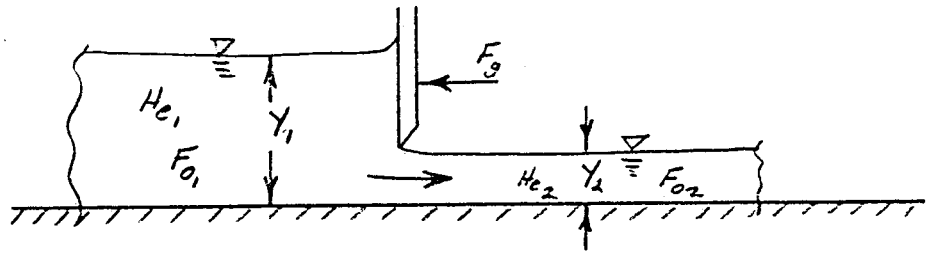

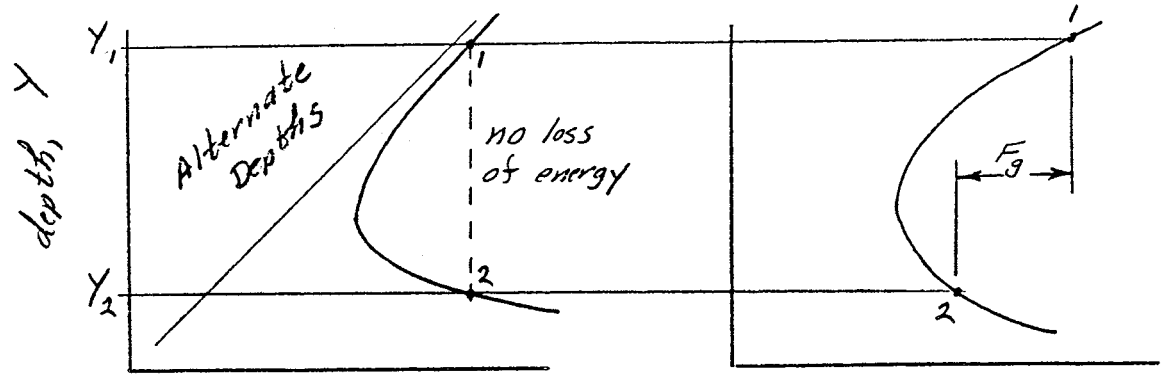

Specific Energy, H_e Specific Force, F_o

Hydraulic Jump

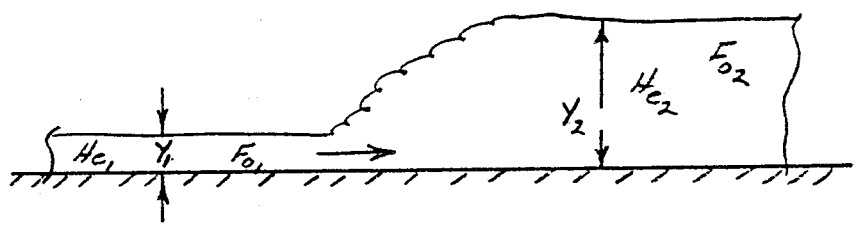

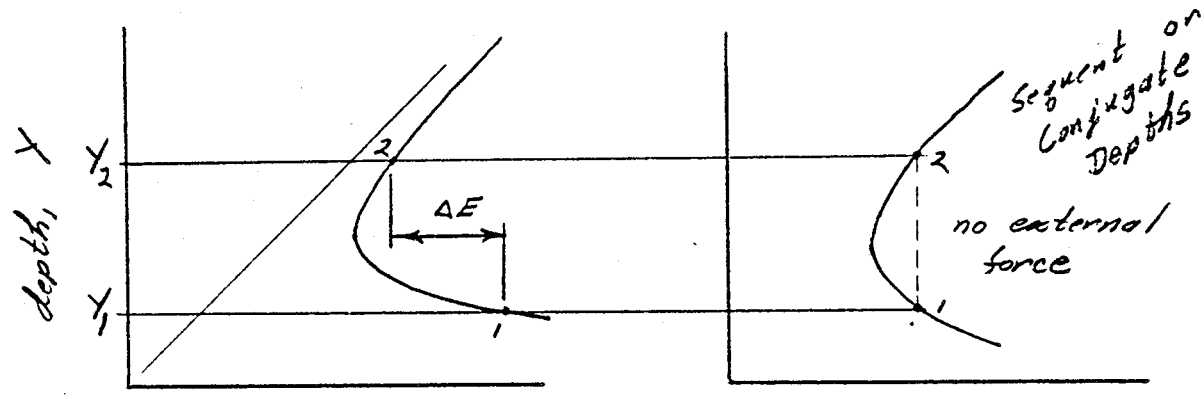

Specific Energy, H_e Specific Force, F_o

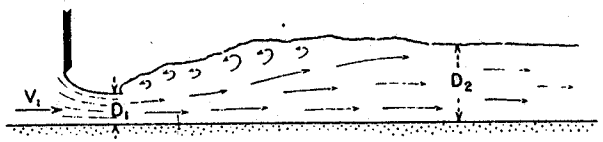

F_1=1.7 to 2.5
A—Pre-jump—very low energy loss

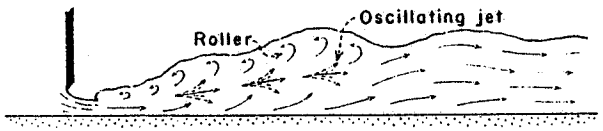

F_1=2.5 to 4.5
B—Transition—rough water surface

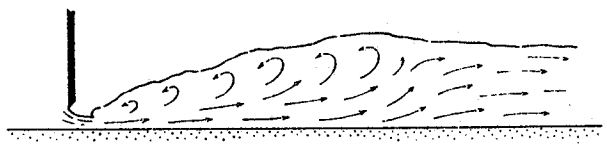

F_1=4.5 to 9.0—range of good jumps
C—Least affected by tail water variations

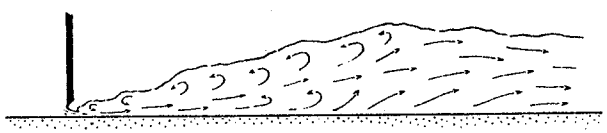

F_1=9.0 upward
D—effective but rough

Form of hydraulic jump

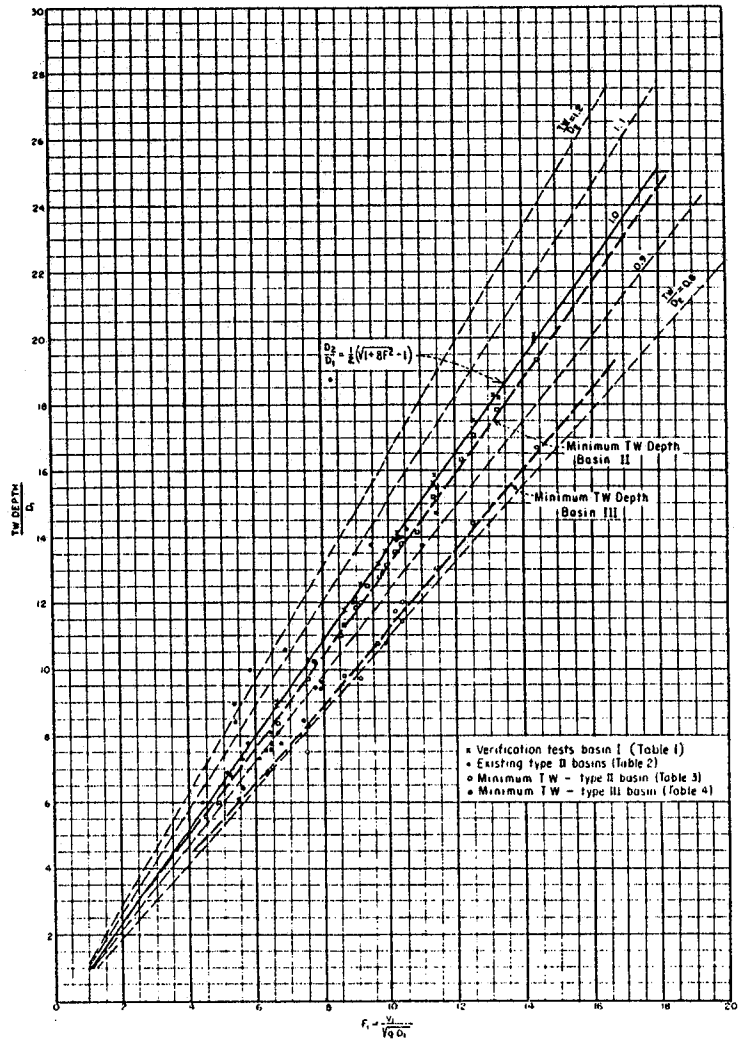

Conjugate depth

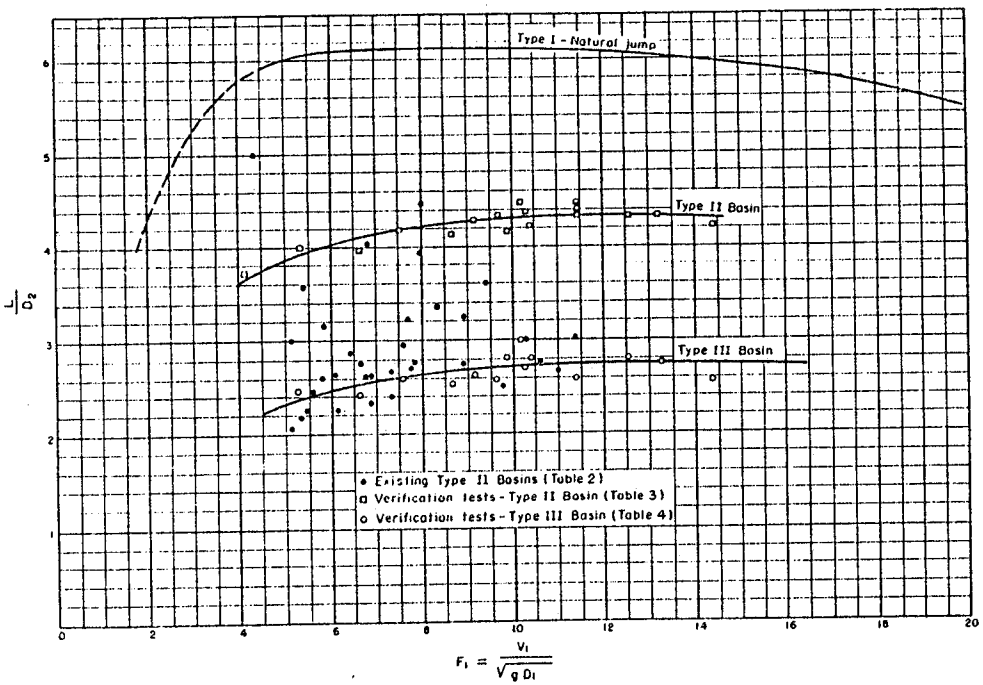

Length of jump

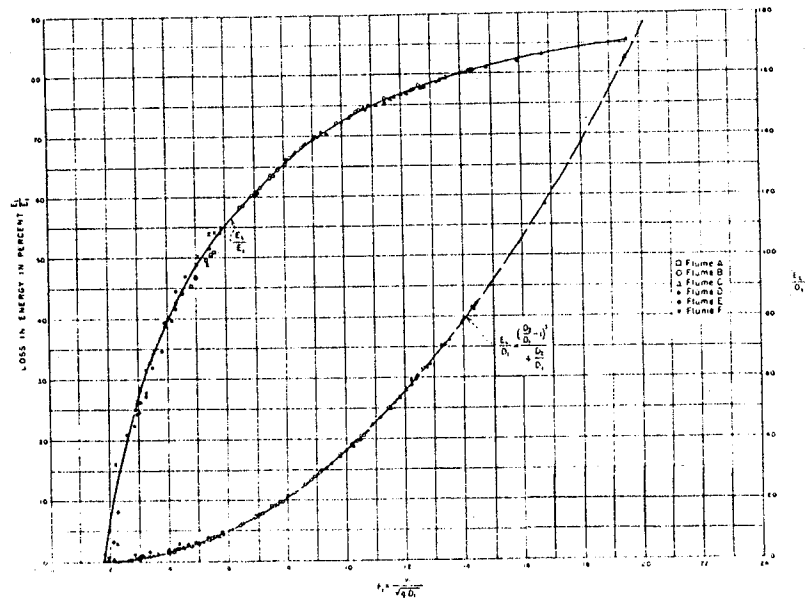

Energy loss in jump

Critical Flow

Characteristics of critical flow:

1. $F = 1.0$
2. $\alpha \frac{v^2}{2g} = \frac{1}{2} D_c \qquad \therefore \; q = (g d_c^3)^{1/2}$
3. H_e is a minimum for a given Q
4. Q is a maximum for a given H_e

For critical flow there is a unique relation between discharge and depth. Critical flow is a "control."

Section Factor for critical flow

$$\frac{\alpha \bar{v}^2}{2g} = \frac{D_c}{2}$$

$$\bar{v} = Q/A$$

$$\therefore \; \frac{Q}{\sqrt{g/\alpha}} = A\sqrt{D_c} = Z$$

Methods of solution for critical depth:

1. Solve $\frac{Q}{\sqrt{g/\alpha}} = A\sqrt{D_c}$ for d_c, (trial & error).

2. Prepare a design curve of d vs Z.

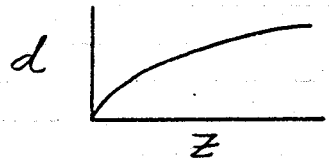

3. Use dimensionless charts & tables.
   a.) Chow, Fig. 4-1
   b.) Design of Small Dams, Tables B-2 & B-3

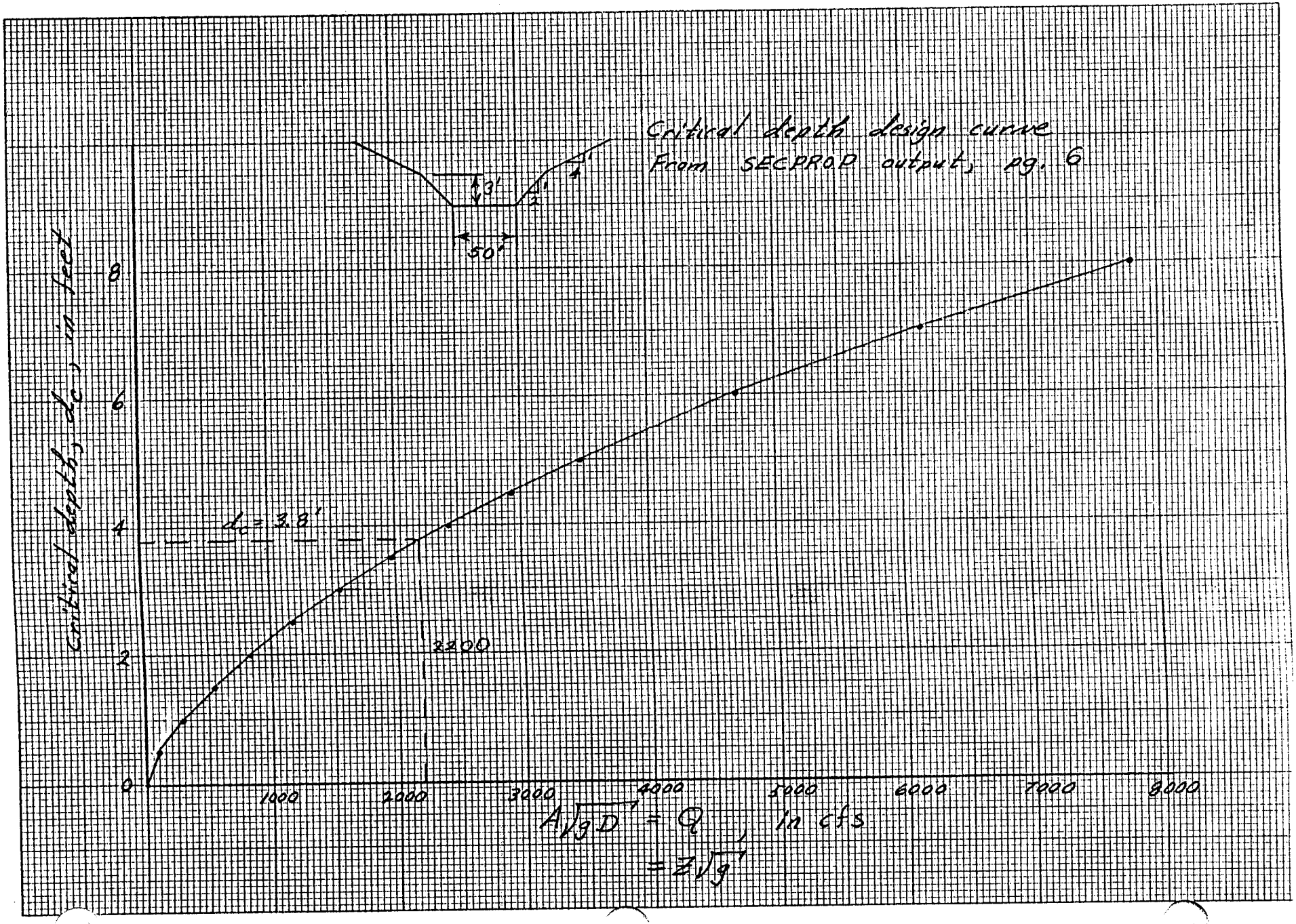

CITADEL® NO. 643 - CROSS SECTION - 20 SQUARES TO INCH

OPEN-CHANNEL HYDRAULICS

Uniform Flow -- Part I

A. Definitions

Uniform Flow has the following main features:

(1) the depth, water area, velocity, and discharge at every section of the channel reach are constant; and

(2) the energy line, water surface, and channel bottom are all parallel (that is $S_f = S_w = S_o = S$)

Basically

$$\frac{dy}{dx} = 0 \quad \text{and} \quad \frac{dy}{dt} = 0$$

(uniform) (steady)

Normal Depth - depth that exists during uniform flow.

B. Chezy Equation

General Equation for Uniform Flow:

$$\bar{v} = CR^x S^w \quad \text{(eq.1)}$$

where

$\bar{v}$ - mean velocity (length/time)
R - hydraulic radius (length)
S - energy slope (length/length)
x & w are exponents
C - factor of flow resistance that varies as ($\bar{v}$, R, n, μ, etc)

Chezy Formula (1769) describes the x & w = 1/2 or $\bar{v} = C\sqrt{RS}$

and Chezy's C can be determined to vary according to many different methods.

C. Manning Formula

$$\bar{v} = \frac{1.49}{n} R^{2/3} S^{1/2} \quad \text{English Units} \qquad \text{(eq. 2)}$$

$$\text{or } \bar{v} = \frac{1}{n} R^{2/3} S^{1/2} \quad \text{Metric Units}$$

where

$\bar{v}$ - mean velocity (length/time)
R - hydraulic radius (length)
S - slope of energy line (length/length)
n - coefficient of roughness or Manning's n

Comparing Chezy Formula vs Manning Formula, we can obtain

$$C = \frac{1.49}{n} R^{1/6} \qquad \text{(eq. 3)}$$

D. Normal Depth Determination

Looking at a trapezodial channel

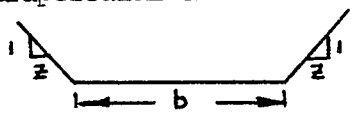

n = 0.025
Q = 400 cfs

where b = 20 ft, z = 2 and S_o = 0.0016

$$\text{then } R = \frac{A}{P} = \frac{y\,(b + zy)}{b + 2y\sqrt{1+z^2}}$$

$$R = \frac{y\,(20 + 2y)}{20 + 2y\sqrt{5}} = \frac{y\,(10 + y)}{10 + y\sqrt{5}}$$

$$\text{and } \bar{v} = \frac{Q}{A} = \frac{400}{y\,(20 + 2y)}$$

$$\text{and } \bar{v} = \frac{1.49}{n} R^{2/3} S^{1/2}$$

$$\text{then } \frac{400}{y(20 + 2y)} = \frac{1.49}{0.025} \left[\frac{y(10+y)}{10 + y\sqrt{5}}\right]^{2/3} (0.0016)^{1/2}$$

$$\text{or } 7680 + 1720y = \left[y\,(10 + y)\right]^{2.5}$$

Trial and error give y_n = 3.36 ft
and A_n = 89.8 ft^2 and $\bar{v}_n$=4.46 ft/sec.

E. Normal Slope Determination

The normal slope equation would become:

$$S_n = \left(\frac{Q\,n}{1.49\,A_n\,R_n^{2/3}} \right)^2 \qquad \text{(eq. 4)}$$

where R_n and A_n are a function of y_n, b, and z for a trapezoidal channel.

F. Conveyance

Conveyance (K) is a measure of the carrying capacity of a channel section or $Q = KS^Y$ or $K = Q/S^Y$

For Chezy's Equation:

$$K = Q/\sqrt{S} = CAR^{1/2} \qquad \text{(eq. 5)}$$

For Manning's Equation

$$K = Q/\sqrt{S} = \frac{1/49}{n} AR^{2/3} \qquad \text{(eq. 6)}$$

G. Section Factor

A factor used in computation of uniform flow is expressed as

$$AR^{2/3} = \frac{nK}{1.49} = \frac{nQ}{1.49\sqrt{S}} \qquad \text{(eq. 7)}$$

It can be used in calculation of the normal depth, y_n, when the conditions of n (roughness), flow (Q), and S (slope) are known. There is only one y_n that will satisfy the equation for section factor.

(Example of Design Chart Method)

H. Uniform Flow in Composite Channels

Must determine an equivalent roughness when channel section is made up of different roughness or when section is not regular.

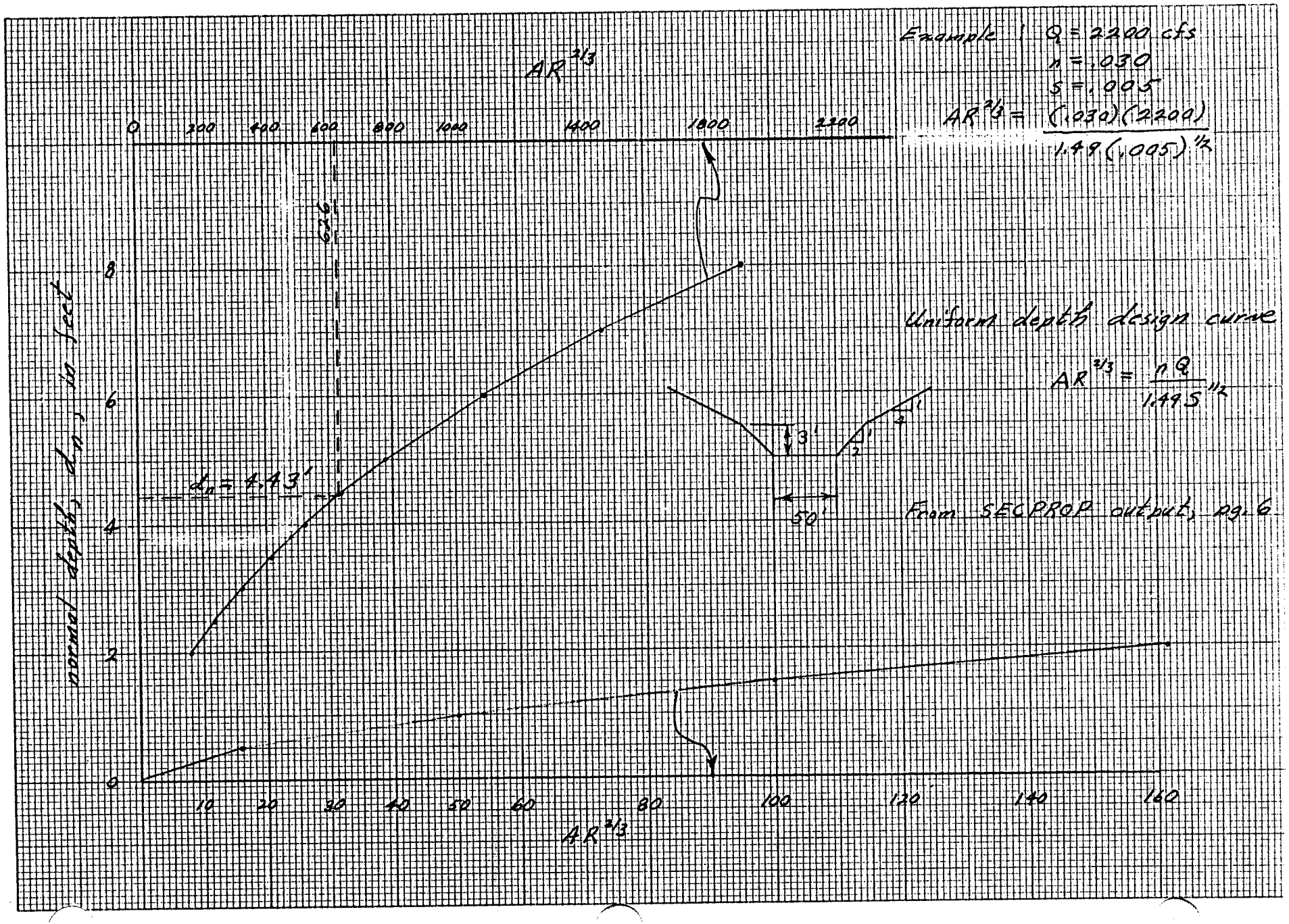

CITADEL® NO. 643 - CROSS SECTION - 20 SQUARES TO INCH

Design discharge = 2200 cfs

Riprap lined lower bank, earthen upper bank, and sand bed channel.

Practical range of n .02 → .04 ?

1. What is the critical depth for 2200 cfs ?

$\underline{\underline{d_c = 3.8 \text{ ft}}}$ from pg. 32

2. If the bed slope is .5%, what is the normal depth ?

$$AR^{2/3} = \frac{nQ}{1.49 S^{1/2}}$$

$$= n \frac{2200}{1.49 (.005^{1/2})}$$

$$= n (20,881)$$

n	$AR^{2/3}$	d_n	comment
.02	417	3.5	supercritical
.025	522	4.0	subcritical
.03	626	4.5	subcritical
.035	730	4.7	subcritical
.04	835	5.2	subcritical

This channel could easily fluctuate between subcritical and supercritical flow, with waves 2 ft high!

3. What is the critical slope ?

@ $d_c = d_n = 3.8$ ft, $AR^{2/3} = 480 = \frac{nQ}{1.49 S_c^{1/2}}$

$\hookrightarrow S_c = n^2(9.46)$

n	S_c
.02	.0038
.025	.0059
.03	.0085
.035	.0116
.04	.0151

channel slopes from .3% to 1.5% could be critical!

Resistance to Flow

Cause- energy continually being dissipated because fluid must work against resistance originating from fluid viscosity.

Momentum transfer-

$$\vec{F} = \rho Q (\vec{v_2} - \vec{v_1})$$

ρQ need not be in direction of $\vec{v}$ but may be transferring between faster and slower "layers" of water.

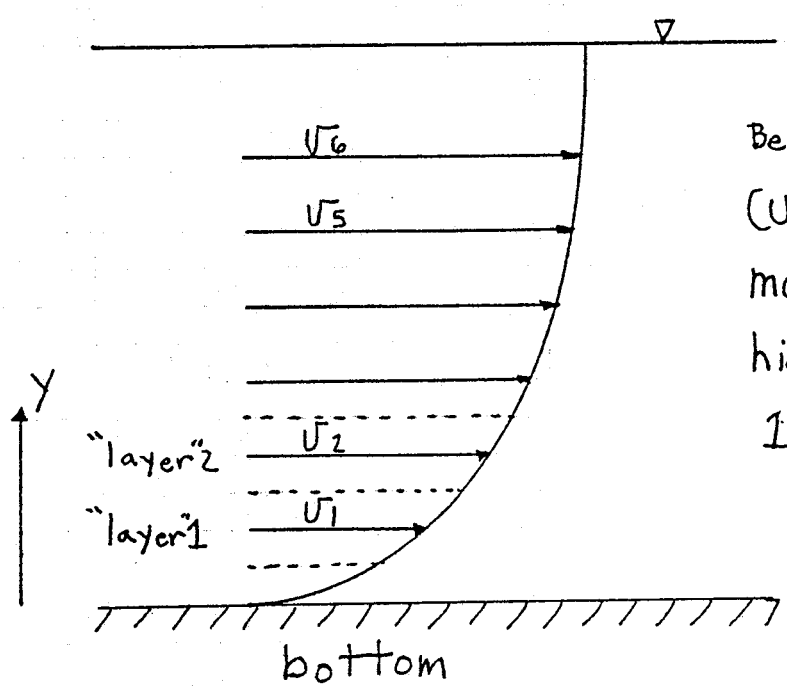

Because:

$(v_2 - v_1) > (v_6 - v_5)$

momentum transfer is higher between "layers" 1 and 2.

Laminar and turbulent flow boundary layers grow at different rates with down stream distance.

For turbulent flow an equation relating velocities and depths is

$$\frac{U}{U_o} = \left(\frac{y}{\delta}\right)^{1/7}$$

Where U = velocity at position y (vertical)

U_o = mean velocity outside of the boundary layer

δ = boundary layer thickness

This is the so called "one-seventh power law"

<u>Form drag</u> occurs when the flow is separated around (or over) an object. Boundary layer fluid does not have sufficient energy to cross from the layer to a higher pressure environment in the surrounding flow.

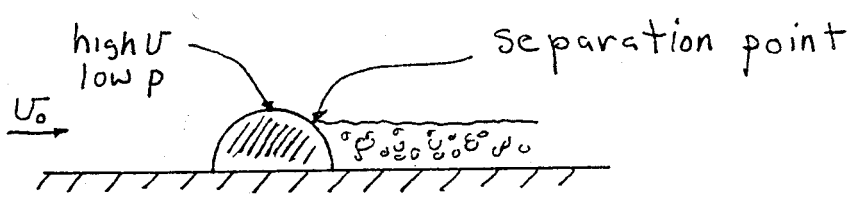

Laminar flow – exchange is on microscopic level
random movement of molecules

Turbulent flow – exchange is on macroscopic level
created by random fluctuations
of velocity.

"Shear" between layers is a means of transmitting force from an origin.

This origin is typically a solid surface, channel bottom and bank materials.

<u>Surface drag</u> creates a velocity profile or gradient between a "no slip" (zero) velocity at the solid water interface and the flowing water above.

In this layer, shear stress is being transmitted between "layers" and rotation of fluid elements occurs.

The "boundary layer" where all this is occurring grows in a downstream direction until it reaches the water surface.

Depending on size, type, and spacing of channel roughness, the importance of surface and form drag in creating resistance changes.

Boundary conditions can be classified on the basis of roughness element size, shear velocity, and kinematic viscosity.

Smooth $0 \leq \frac{k U_f}{\nu} \leq 3.8 \sim 5$

Transition $3.8 \sim 5 < \frac{k U_f}{\nu} \leq \sim 70$

Rough $\frac{k U_f}{\nu} > 70$

In a small zone near the boundary, a layer exists that behaves like laminar flow - the <u>laminar sublayer.</u> When roughness elements are larger than that layer, the boundary acts like a hydraulically rough surface.

Above this sublayer, the flow is usually in a fully developed turbulent boundary layer.

For "smooth" surfaces the logrithmic, vertical velocity distribution can be written as

$$\frac{U}{U_f} = 5.75 \log \frac{9 U_f y}{\nu}$$

For "rough" surfaces it is

$$\frac{U}{U_f} = 5.75 \log \frac{30 y}{k}$$

where k = roughness height

It is important to note that for the "rough" boundary situation the flow velocity is dependent on the relative roughness $= \left(\frac{y}{k}\right)$.

Resistance coefficients -

<u>Manning's n</u> -

most common, has units of $\left(\frac{T}{L^{1/3}}\right)$ but in practice it is often multiplied by $\sqrt{g}$ to give units of $(L)^{1/6}$.

Tabulated values need not be converted but used directly in the equation!

<u>Chezy C</u> -

has units of $\frac{L^{1/2}}{T}$. Dividing by $\sqrt{g}$ yields a non-dimensional value as

$$C' = \frac{C}{\sqrt{g}}$$

Darcy-Weisbach f -

from pipe flow analogy, for open channels the equation is

$$U = \left(\frac{8 g R S_f}{f}\right)^{1/2}$$

f is dimensionless

Inter relationships -

$$\frac{U}{U_f} = \sqrt{\frac{8}{f}}$$

$$\frac{C}{\sqrt{g}} = \sqrt{\frac{8}{f}}$$

$$\frac{R^{1/6}}{3.8n} = \sqrt{\frac{8}{f}}$$

The above indicate the dependence of resistance on relative roughness.

Selection of an appropriate resistance value -

Typically, n values are often selected because of the popularity of the Manning's equation

Factors affecting n include:

1) Surface roughness - from grains (sand - boulders)
2) Vegetative roughness - trees, brush, weeds, grass, etc
3) Changes in cross section - bars, holes
4) Channel alignment - straight or meandering
5) Fill and scour - changes shape, buries roughness
6) obstructions - bridge piers, debris
7) Size and shape of channel - influences A and P
8) Stage and discharge - relative roughness, overbank
9) Seasonal changes - plants, ice

"Typical" values of n have been tabulated by Chow (1959, pp 110–113) and pictures showing different channels with a wide variety of n values have been prepared by Barnes (1967; USGS Water Supply 1849, 213 pages)

Below is a list of "normal" values of n for common surfaces. Variations of 20% or more are common.

Surface		Normal n value
neat surface cement	–	0.011
trowel finished concrete	–	0.013
unfinished concrete	–	0.017
rip rap sides, gravel bottom	–	0.033
gravel, cobbles, boulders	–	0.040
brush and grass on floodplain	–	0.050

Equivalent n for a composite section

Motayed and Krishnamurthy (1980, ASCE, J. of Hyd. Div., Vol. 106, No. HY6, June, pp 1111–1116) tested four methods and found the Lotter method to be best or

$$n_c = \frac{P R^{5/3}}{\sum_{i=1}^{N} \left(\frac{P_i R_i^{5/3}}{n_i} \right)}$$

For compound geometry, divide the section with imaginary lines (commonly vertical) then compute flow for each section.

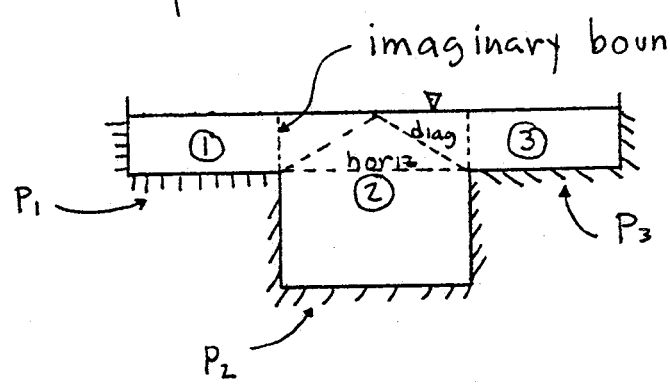

A_1, A_2, A_3
n_1, n_2, n_3
Q_1, Q_2, Q_3

$Q_1 + Q_2 + Q_3 = Q_{total}$

Practice is to exclude the perimeter from the imaginary boundaries, but count the flow area. Wormleaton et al (1982, ASCE, J. of Hyd. Div., Vol 108 No HY9, Sept, pp 975-994) suggest that diagonal boundaries or horizontal boundaries may be more appropriate for certain flow situations.

Estimating resistance from channel characteristics –

Strickler type equations –

$$n = \frac{d_s^{1/6}}{a}$$

where d_s is a representative roughness size and a is a parameter.

The term d_s is usually taken as a sediment grain size such as d_{50}, d_{65}, d_{84}, or d_{90} (i.e. d_{90} means 90% of a sample is composed of particles smaller than the given size, by weight)

A common estimator is

$$n = \frac{d_{50}^{1/6}}{31.3}$$

where d_{50} is in feet so n is in $(ft)^{1/6}$

For a 2mm size this gives a value of

$$n = \frac{\left(\frac{2}{304.8}\right)^{1/6}}{31.3} = 0.014$$

Monomial type equations –

$$\sqrt{\frac{8}{f}} = a\left(\frac{R}{k}\right)^{1/m}$$

Where a and m are parameters and k is often taken as d_{90}

Note that if $a \approx 8$, $m = 6$, and $k = d_{90}$ then

$$n = \frac{d_{90}^{1/6}}{30.4}$$

Which is close to a Strickler type formula

Semi logrithmic type equations –

$$\frac{1}{\sqrt{f}} = a \log\left(\frac{cR}{k}\right) \quad \text{(turbulent flow)}$$

where a and c are parameters.

$a \approx 2.0 \qquad \bar{c} \approx 12.0$

Manipulating this equation gives

$$\sqrt{\frac{8}{f}} = \frac{U}{U_f} = 6.10 + 5.66 \log\left(\frac{R}{k}\right)$$

which is similar to the velocity equation given before.

Values for k - manmade boundary

Surface		Value of k, ft
Very smooth, finished joint, concrete	-	0.001
Smooth finished gunite	-	0.005
untreated gunite	-	0.01-0.03

Values for k - natural alluvial boundaries (armored and loose)

Investigator	Value of k =
Ackers-White	1.25 d_{35}
Einstein	d_{65}
Engelund-Hansen	2.0 d_{65}
Hey	3.5 d_{84}
Kamphius	2.5 d_{90}
Parker and Peterson	2.0 d_{90}
Mahmood	5.1 d_{84}
Rijn	3.0 d_{90}

(See Rijn, 1982, J. of Hyd. Div. ASCE, Vol 108, No HY10, Oct, pp 1215-1218; for more details)

Such variation is partly a function of the form of the equation used and partly a function of the "best" variable (size)

Casting the above in terms of n yields

$$\frac{1}{n} = \frac{\sqrt{8}\,(3.8)\,a \log\left(\frac{CR}{k}\right)}{R^{1/6}}$$

$$= \frac{21.5 \log\left(\frac{12R}{k}\right)}{R^{1/6}}$$

This, of course, will necessitate a convergent (trial and error) solution if normal depth is to be found given Q, S, and channel shape (including k).

<u>Channels with mobile (loose) boundaries</u> will develop bedforms as the boundary shear stress (discharge) increases.

<u>Bed form</u>

Shear stress ↓

Plane bed, no sediment movement

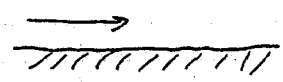

Ripples → dunes
increased form drag

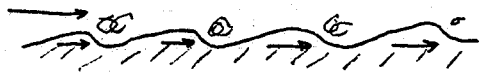

Plane bed, sediment movement

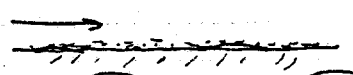

Standing waves

Breaking wave antidunes

Chutes and pools

Resistance varies with the bedform. In a loose boundary channel, the bed forms may vary across the section depending on flow conditions, e.g. standing waves in the center and plane bed on the sides.

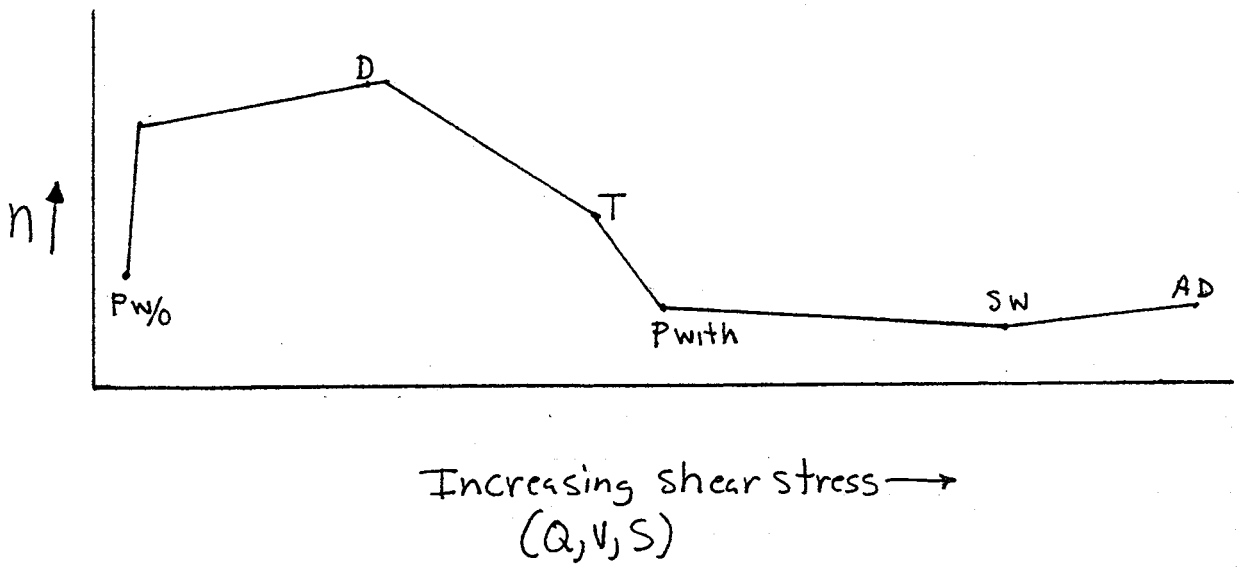

n values may go up to 0.033 for dunes and drop to 0.012 for standing waves

Therefore it is improper to choose only one n value when examing an alluvial channel.

Simons and Richardson (1966, US GS Prof. Paper 422J, 61 pages) describe flow resistance in alluvial channels with bed forms.

Plane bed - no sediment movement

$$\frac{1}{\sqrt{f}} = 16.69 \log\left(\frac{8.36D}{d_{85}}\right)$$

where D is the depth of flow

Plane bed - with appreciable sediment movement

$$\frac{1}{\sqrt{f}} = 20.93 \log\left(\frac{D}{d_{85}}\right)$$

Ripples -

$$\frac{1}{\sqrt{f}} = \left(21.67 - \frac{0.85}{U_f}\right) \log D + \frac{0.37}{U_f} + 31.11$$

Dunes and Antidunes (standing and breaking waves)

$$\frac{1}{\sqrt{f}} = 20.93 \log\left(\frac{D}{d_{85}}\right) \sqrt{1 - \frac{\Delta RS}{RS}}$$

The correction factor accounts for form drag and is related to grain size and flow factors.

Vegetated Channels -

Selection of appropriate resistance values for grassed (or other vegetation) channels is difficult because the vegetation is easily modified - cut or burned - and it grows. Similarly, it can be eroded if velocities are too high. The Soil Conservation Service ("Hand book for Channel Design for Soil and Water Conservation (1954, revised 1966); SCS TP-61) presents a method based on empirical data whereby n is related to VR for different classes of vegetation. This "retardance" method is directed at four (A, B, C, D, E - A is highest) classes of vegetation type - condition.

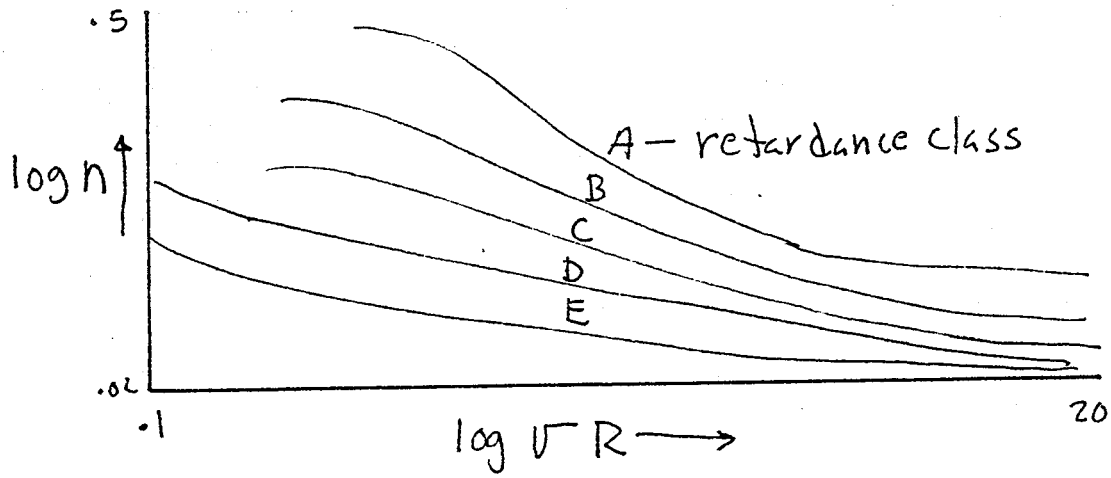

General form of n - VR relationship

More details can be found in Chow (1959, pp 179-188)

Kouwen et al (1981, Transactions of ASAE, Vol 23, No. 3, May-June pp 684-690, 698) suggest a new approach based upon the biomechanical properties of the vegetation. A outline of this new (needs more testing)

1) Pick slope $S = S_o$
2) Guess at a flow depth y_n (note that the method assumes that $R \approx y_n$ or that unit width flow is being used) This may necessitate using a composite channel. Units of meters.
3) Select a vegetation height, in meters, as h_v
4) Select an appropriate vegetation stiffness as MEI.

Retardance Class	MEI Newtons-m^2	Example
A	300	Weeping lovegrass, 760mm
B	20	Bermudagrass, 300mm
C	0.5	Bermudagrass, 150mm
D	0.05	Kentucky Bluegrass, 75mm
E	0.005	Bermudagrass 38 mm high

A more complete table can be found in the above reference.

5) Calculate

$$U_f = \sqrt{g\, y_n S} \quad (\text{in m/sec})$$

6) Calculate

$$k = 0.14\, h_v \left[\frac{\left(\frac{MEI}{9806\, y_n S} \right)^{1/4}}{h_v} \right]^{1.59}$$

7) Calculate

$U_{f\text{-critical}}$

$$= 0.028 + 6.33\,[MEI]^2 \quad \text{if } MEI \leq 0.16$$

$$= 0.23\,[MEI]^{0.106} \quad \text{otherwise}$$

8) Find parameters a and b with U_f and $U_{f\text{-critical}}$

Criteria	a	b
$\frac{U_f}{U_{f\text{-crit.}}} \leq 1.0$	0.15	1.85
$1.0 < \frac{U_f}{U_{f\text{-crit.}}} \leq 1.5$	0.20	2.70
$1.5 < \frac{U_f}{U_{f\text{-crit}}} \leq 2.5$	0.28	3.08
$2.5 < \frac{U_f}{U_{f\text{-Crit}}}$	0.29	3.50

9) Calculate

$$\frac{1}{\sqrt{f}} = a + b \log\left(y_n/k\right)$$

10) Calculate

$$n = \frac{y_n^{1/6}}{\sqrt{8g}\sqrt{\frac{1}{f}}}$$ (n is now in $\frac{sec}{m^{1/3}}$ if y_n in meters)

or $$n = \frac{y_n^{1/6}}{10.75\sqrt{\frac{1}{f}}}$$ (y_n in ft, n in $ft^{1/6}$, g is "absorbed")

11) Check to see if this n gives the right y_n (or R). If not, iterate. (Watch for excessive velocity)

Summary -

1) Resistance is result of energy dissipation
2) Surface drag and form drag are the two components of resistance.
3) Surface may be hydraulically smooth, transition, or roogh depending on flow conditions and size of roughness elements
4) There are numerous ways to estimate resistance coefficients.
5) Type of channel material and expected flow conditions dictate selection process.

Example of Simplified Slope - Area Method:

Use channel data from "Design of Small Dams" Fig. B-18, B-19, & B-21

$$\text{Average area} = \frac{208 + 209.1 + 224.6 + 206.9}{4} = 212.2 \text{ ft}^2$$

$$\text{Average slope} = \frac{16.35 - 13.73}{121 + 90 + 119} = \frac{2.62 \text{ ft}}{330 \text{ ft}} = .0079$$

$$\log Q = 0.366 + 1.33 \log A + 0.05 \log S - 0.056 (\log S)^2$$

$$\log Q = 0.366 + 3.095 - 0.105 - 0.248$$

$$= 3.108$$

$$Q = 1{,}280 \text{ cfs}$$

The avg. Q by slope - area = 1380 cfs (Fig. B-21)

Example of Simplified Slope-Area Method:

Use channel data from "Design of Small Dams"

Fig. B-23 & Table B-8

Elevation	Area	Q
30	95 ft^2	360
35	400	2,420
40	753	5,600
45	1160	9,960
50	1610	15,400

$$\log Q = 0.366 + 1.33 \log A + 0.05 \log .00395 - 0.056 (\log .00395)^2$$

$$= -0.0776 + 1.33 \log A$$

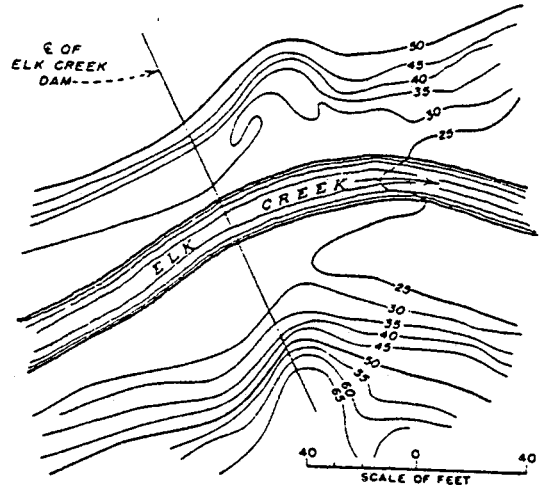

(A)

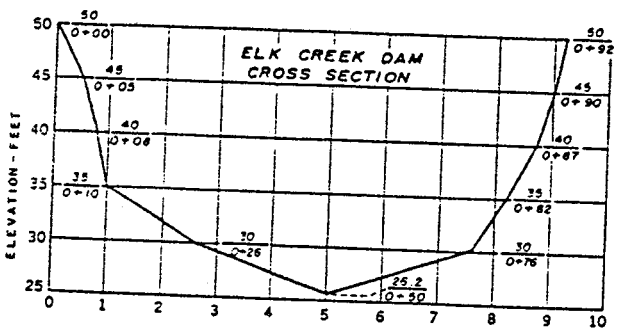

(B) 100 ft

Figure B–22. Plan and cross section of Elk Creek Dam site 288–D–2832.

by Simplified Slope-Area

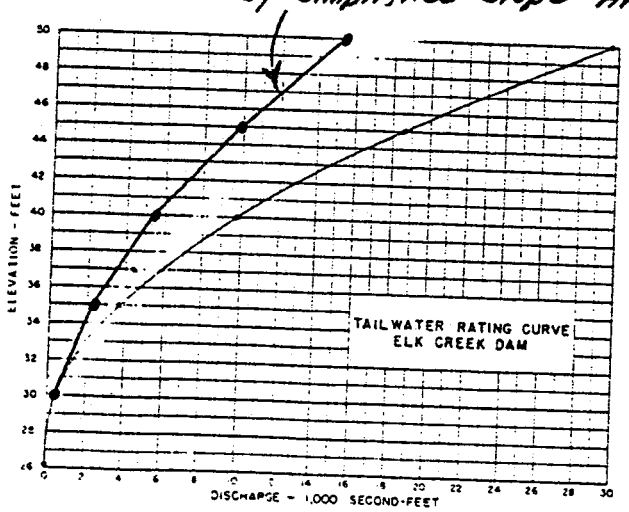

Figure B–23. Tailwater rating curve for Elk Creek Dam. 288–D–2560.

TABLE B–8.—*Computations for tailwater rating curve*

ELK CREEK DAM

Data: $n=0.030$ s_b=mean bed slope=0.00395

$$C=\frac{1.486}{n}=49.53 \quad s_b^{1/2}=0.0628$$

Elevation	a	p	r	$r^{2/3}$	C	K_d	$s_b^{1/2}$	Q
26.2	0	0	0	0				
30	95	50.6	1.88	1.523	49.53	7,170	0.0628	450
35	400	75.1	5.32	3.047	49.53	60,400	.0628	3,790
40	733	87.6	8.60	4.198	49.53	156,000	.0628	9,800
45	1160	99.2	11.70	5.154	49.53	296,000	.0628	18,600
50	1610	111.7	14.40	5.919	49.53	472,000	.0628	29,600

by the one-half power of the mean bed slope to compute the discharge at each elevation. The tailwater rating curve derived from the computations is shown in figure B-23.

(b) *Water Surface Profile Method.*—In studies where more exact tailwater curves are required, water surface profiles may be developed for a range of discharges. The computations in such studies are more involved and require a series of cross sections downstream from the damsite.

Several methods [1, 2, 8, 9] have been developed for computing water surface profiles; however, this discussion will be limited to Bureau of Reclamation Method A. This method is adaptable to irregular channels having various roughness segments and large variations in cross-section geometry. It is limited to the assumption that flow paths between cross sections are equal in length for all roughness segments. Other methods [8, 9] must be used for variable travel distances.

In Method A, a number of cross sections are selected at intervals below the damsite. The selection of the cross-section locations is probably the most important factor in preparing a good study. The sections should be located so the average area, hydraulic radius, and n values of any two sections will be representative of the reach length between them. Channels that are alternately wide and narrow should have sections located in the narrow and wide points so the average condition can be defined. Special attention should also be given to locating a section at each point that indicates a definite change in grade or a control such as a natural constriction or bridge. The cross sec-

Gradually Varied Flow

Assumptions:

1. steady flow
2. flow lines are essentially parallel; i.e., the one-dimensial energy equation is valid
3. the head loss for a short reach of channel can be approximated by assuming uniform flow.

Derivation of gvf Equations

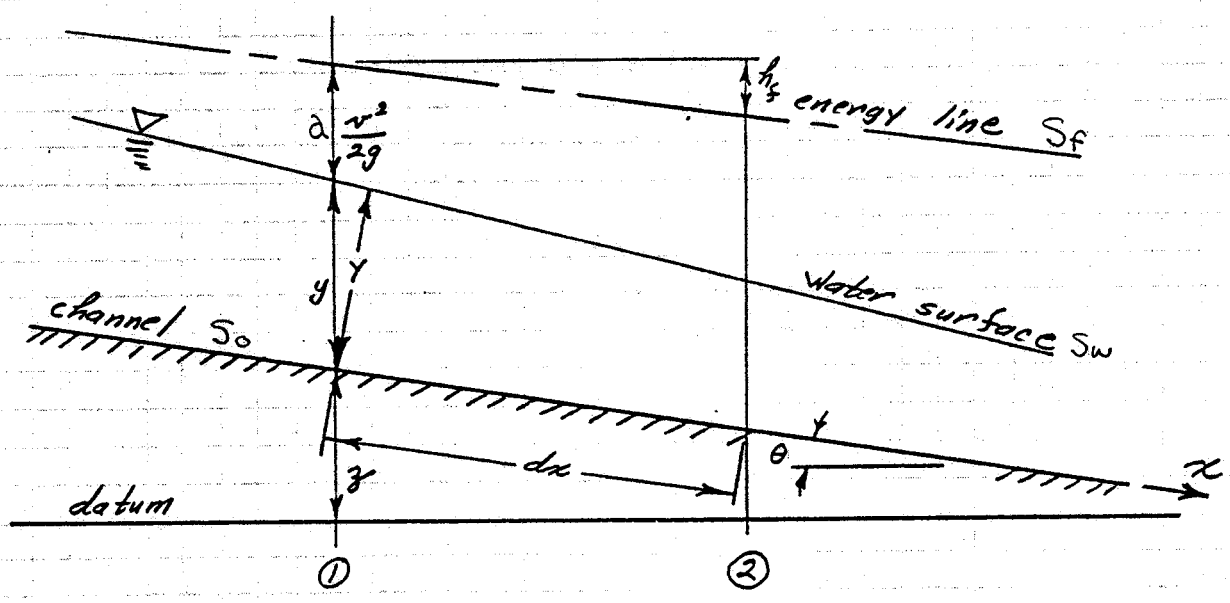

Total head @ ①:

$$H = \frac{\alpha v^2}{2g} + Y\cos\theta + z$$

$$\frac{dH}{dx} = \frac{d}{dx}\left(\frac{\alpha v^2}{2g}\right) + \frac{dY}{dx}\cos\theta + \frac{dz}{dx}$$

$$\frac{dH}{dx} = -S_f \quad \text{energy gradient}$$

$$\frac{dz}{dx} = -S_o \quad \text{channel slope}$$

$$\frac{d}{dx}\left(\frac{\alpha v^2}{2g}\right) = \frac{dY}{dx}\left[\frac{d}{dY}\left(\frac{\alpha v^2}{2g}\right)\right]$$

$$\left.\frac{dY}{dx} = \frac{S_o - S_f}{\cos\theta + \frac{d}{dY}\left(\frac{\alpha v^2}{2g}\right)}\right\} \text{gvf equation}$$

$\frac{dY}{dx}$ = slope of water surface w.r.t. channel bottom

This is not the most amenable expression and several computational forms are available. These are usually based on several additional assumptions:

1. θ is small, $\cos\theta \approx 1.0$, $\frac{dY}{dx} \approx \frac{dy}{dx}$
2. $\alpha = 1.0$
3. the channel is wide

$$Q = Tq$$

$$A = Ty$$

Substituting $v = \frac{Q}{A}$

$$\frac{d}{dY}\left(\frac{v^2}{2g}\right) = \frac{Q^2}{2g}\frac{d}{dY}\left(\frac{1}{A^2}\right)$$

$$= \frac{-Q^2}{gA^3}\frac{dA}{dY}$$

$$\frac{dA}{dY} = T$$

$$= \frac{-Q^2 T}{gA^3}$$

$$\frac{dy}{dx} = \frac{S_o - S_f}{1 - \frac{Q^2 T}{gA^3}}$$

let $Q = Tq$ & $A = Ty$

$$\frac{dy}{dx} = \frac{S_o - S_f}{1 - q^2/gy^3}$$

let $q^2 = g d_c^3$ d_c = critical depth

$$\frac{dy}{dx} = \frac{S_o - S_f}{1 - \left(d_c/y\right)^3}$$ } simple form of the gvf eq'n.

Other forms of the gvf equation are available. Water surface profiles are determined by numerically integrating a form of the gvf equation.

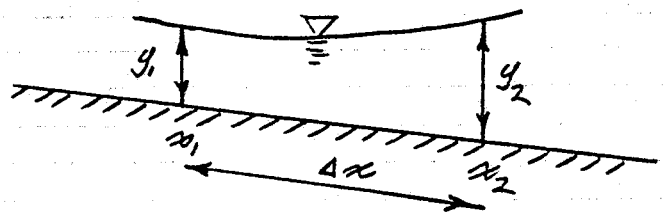

$$\Delta x = x_2 - x_1 = \int_{x_1}^{x_2} dx = \int_{y_1}^{y_2} \frac{dx}{dy}\, dy$$

The simple equation

$$\frac{dy}{dx} = \frac{S_o - S_f}{1 - \left(\frac{d_c}{y}\right)^3}$$

Can be manipulated using Manning's equation to yield:

$$\frac{dy}{dx} = S_o \left[\frac{1 - \left(\frac{d_n}{y}\right)^{10/3}}{1 - \left(\frac{d_c}{y}\right)^3} \right]$$

There are 5 slope types and 3 y, d_n, d_c combinations for 15 possible water surface profiles. However, when $S_o \leq 0$ then d_n is nonexistent which eliminates two profiles.

Classification of Water Surface Profiles

Water surface profiles are classified according to:

1. slope of channel
2. zone of flow

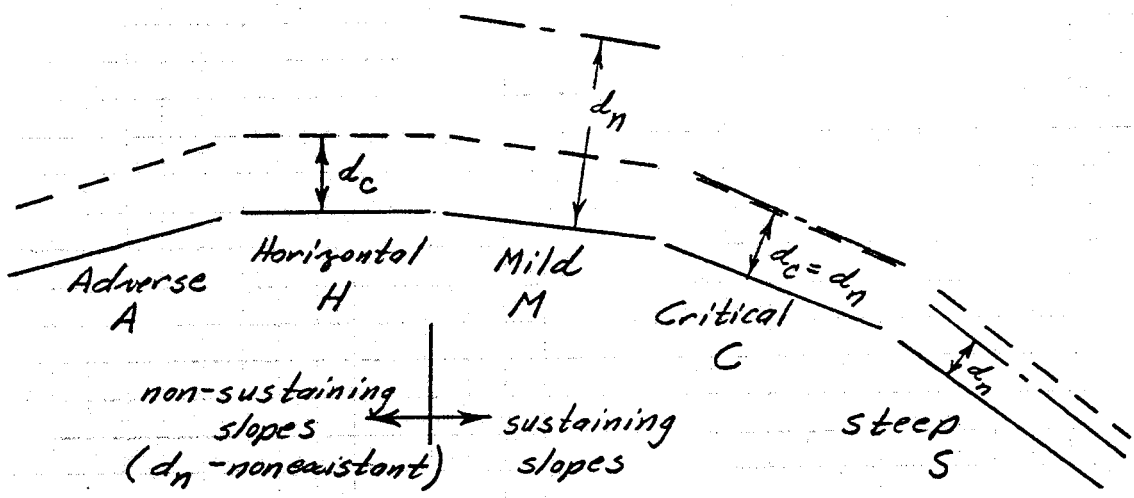

Zone 1 – $y > d_n$ & d_c

Zone 2 – y between d_n & d_c

Zone 3 – $y < d_n$ & d_c

Reference – Chow, Fig. 9-2

Control

Definition – A channel station or channel reach in which there is a unique relation between discharge and depth of flow.

Types of control:

1. critical flow
   a. at free overfall of mild channel
   b. at transition from mild to steep channels
   c. on critical slope channels
2. artificial controls
   a. weir
   b. sluice gate
   c. dam crest
   d. orifice
3. friction – uniform flow in a long channel
4. hydraulic jump

It is necessary to identify controls and classify the flow as either subcritical or supercritical. Water surface profiles for <u>subcritical</u> flow start at a control and progress <u>upstream.</u>
Water surface profiles for <u>supercritical</u> flow start at a control and progress <u>downstream.</u>

Direct Step Method

Beginning with the control section, the channel is divided into short reaches. Computations begin at the control and progress from one section to the next. This method is only applicable to prismatic channels.

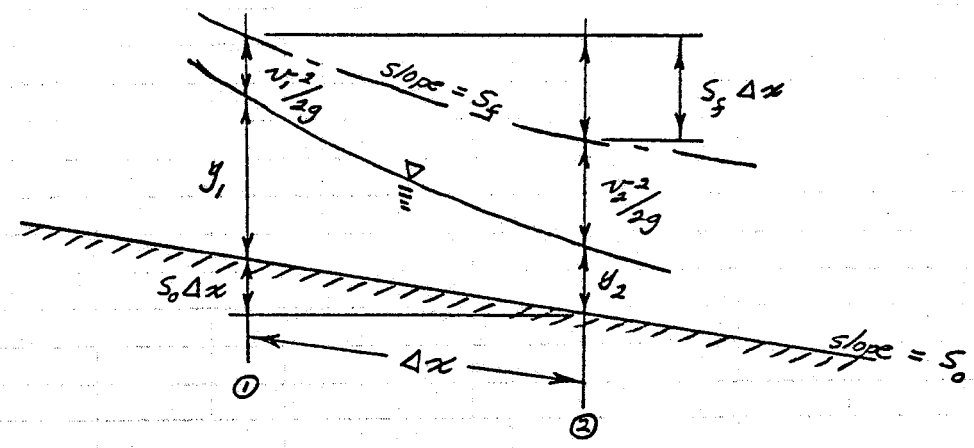

Total energy at ① = Total energy at ② + friction loss

$$S_0 \Delta x + \underbrace{\frac{v_1^2}{2g} + y_1}_{He_1} = S_f \Delta x + \underbrace{\frac{v_2^2}{2g} + y_2}_{He_2}$$

$$\Delta x = \frac{He_2 - He_1}{S_0 - S_f}$$

from Manning's Eq'n $\quad S_f = \dfrac{n^2 v^2}{2.22\, R^{4/3}}$

If S_f is not constant use $\quad \bar{S}_f = \dfrac{S_{f_1} + S_{f_2}}{2}$

Example of Direct Step Method

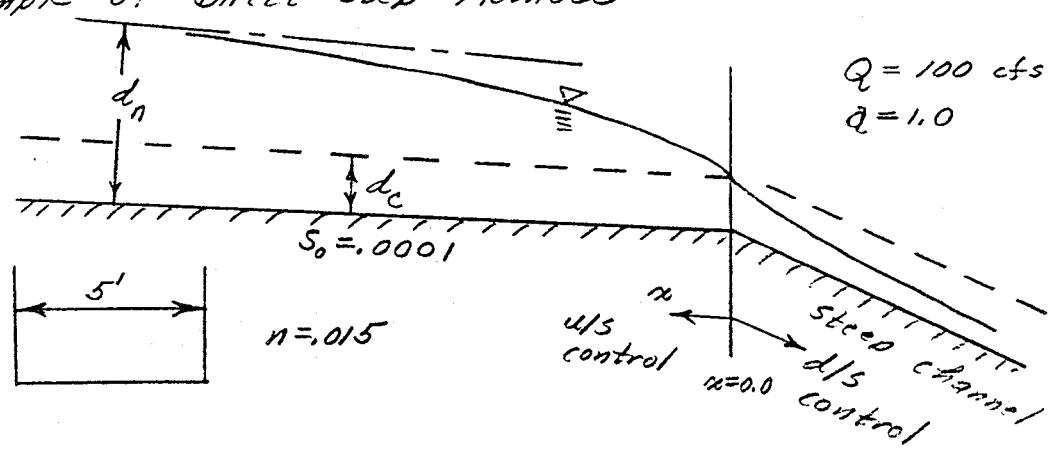

Determine the distance u/s of the control where the depth is 4.0 ft.

1. Calculate the critical depth.

$$q = (g d_c^3)^{1/2} \qquad d_c = \left(q^2/g\right)^{1/3}$$

$$q = \frac{100}{5} = 20 \text{ cfs/ft}$$

$$d_c = \left(\frac{20^2}{g}\right)^{1/3} = 2.31 \text{ ft}$$

2. Calculate the normal depth (use Chow, Fig. 6-1)

$$AR^{2/3} = \frac{nQ}{1.49\, S^{1/2}} = \frac{(.015)(100)}{1.49\,(.0001)^{1/2}} = 100.67$$

$$\frac{AR^{2/3}}{b^{8/3}} = \frac{100.67}{5^{8/3}} = 1.38$$

$$\frac{d_n}{b} = 2.4 \quad \text{from Fig 6-1}$$

$$\therefore \; d_n = 2.4(5) = 12.0 \text{ ft}$$

$d_n > d_c$ $\therefore$ the slope is mild, the flow will be in Zone 2 $\rightarrow$ M2 profile

y (1)	A (1)×5' (2)	$\bar{v}$ $\frac{100\,cfs}{(2)}$ (3)	$\frac{\bar{v}^2}{2g}$ (4)	H_e (1)+(4) (5)	ΔH_e (6)	S_f $\frac{n^2 v^2}{2.22\,R^{4/3}}$ (7)	$\bar{S}_f$ (8)	$S_o - \bar{S}_f$ (9)	Δx $\frac{(6)}{(9)}$ (10)	x (11)
2.31	11.55	8.66	1.16	3.47		.0060				0.0
					.02		.0054	-.0053	-3.8	
2.50	12.50	8.00	.99	3.49		.0048				-3.8
					.08		.0042	-.0041	-19.5	
2.75	13.75	7.27	.82	3.57		.0037				-23.3
					.12		.0034	-.0033	-36.4	
3.00	15.00	6.67	.69	3.69		.0030				-59.6
					.15		.0027	-.0026	-57.7	
3.25	16.25	6.15	.59	3.84		.0024				-117.3
					.17		.0022	-.0021	-81.0	
3.50	17.50	5.71	.51	4.01		.0020				-198.3
					.18		.0018	-.0017	-105.9	
3.75	18.75	5.33	.44	4.19		.0017				-304.2
					.20		.0016	-.0015	-133.3	
4.00	20.00	5.00	.39	4.39		.0014				-437.2

The channel must be less than 437 ft to keep the water from rising to over 4 ft depth.

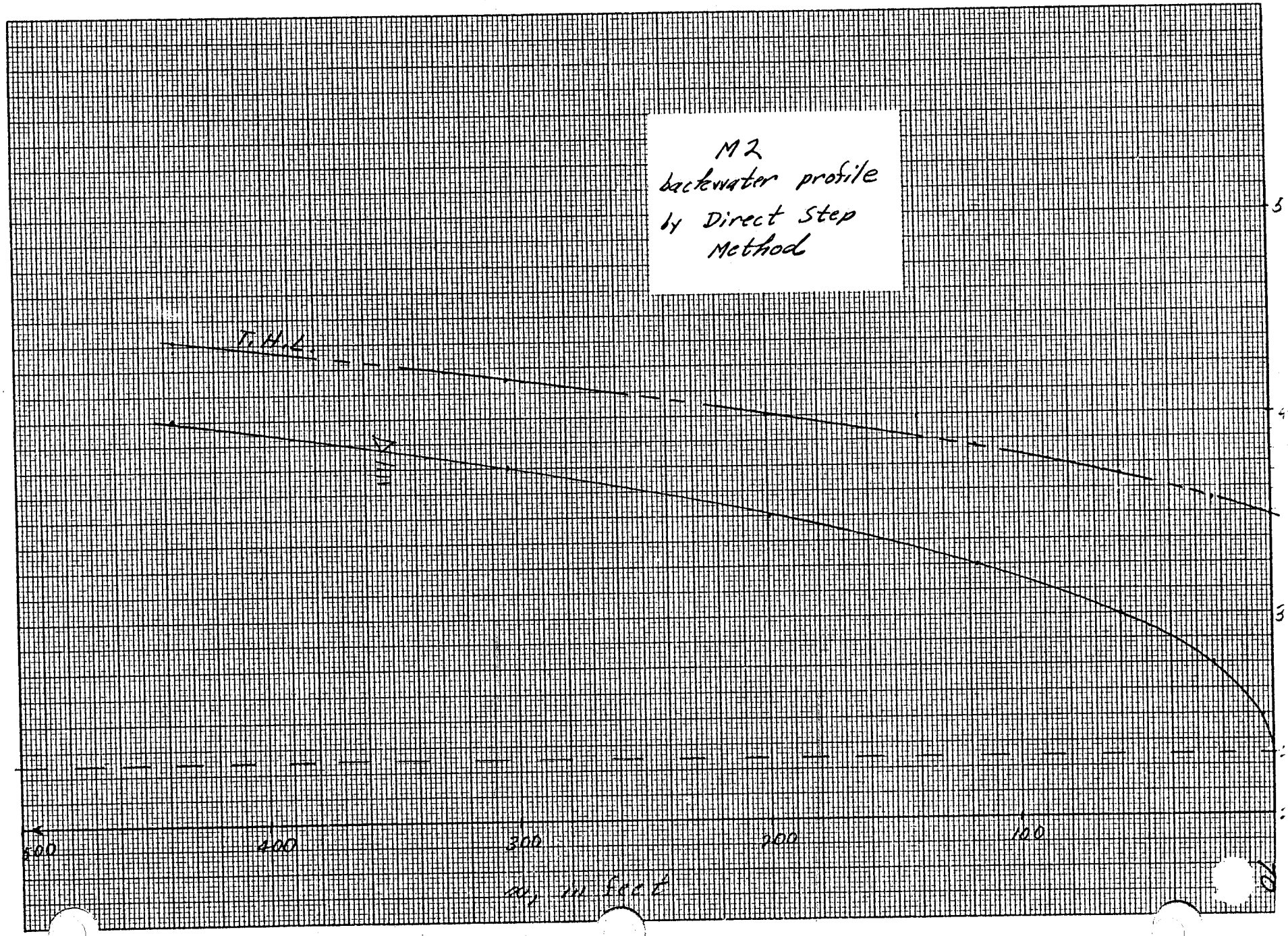

CITADEL® NO. 641 - SCIENCE - 10 SQUARES TO CENTIMETER

SPILLWAYS: Subcritical Water Surface Profiles

H2 (M2)

b = 100 ft
z = 2
n = 0.04

s_0 = 0.00

Ref.- SCS TR 39
Hydraulics of Broadcrested Weirs

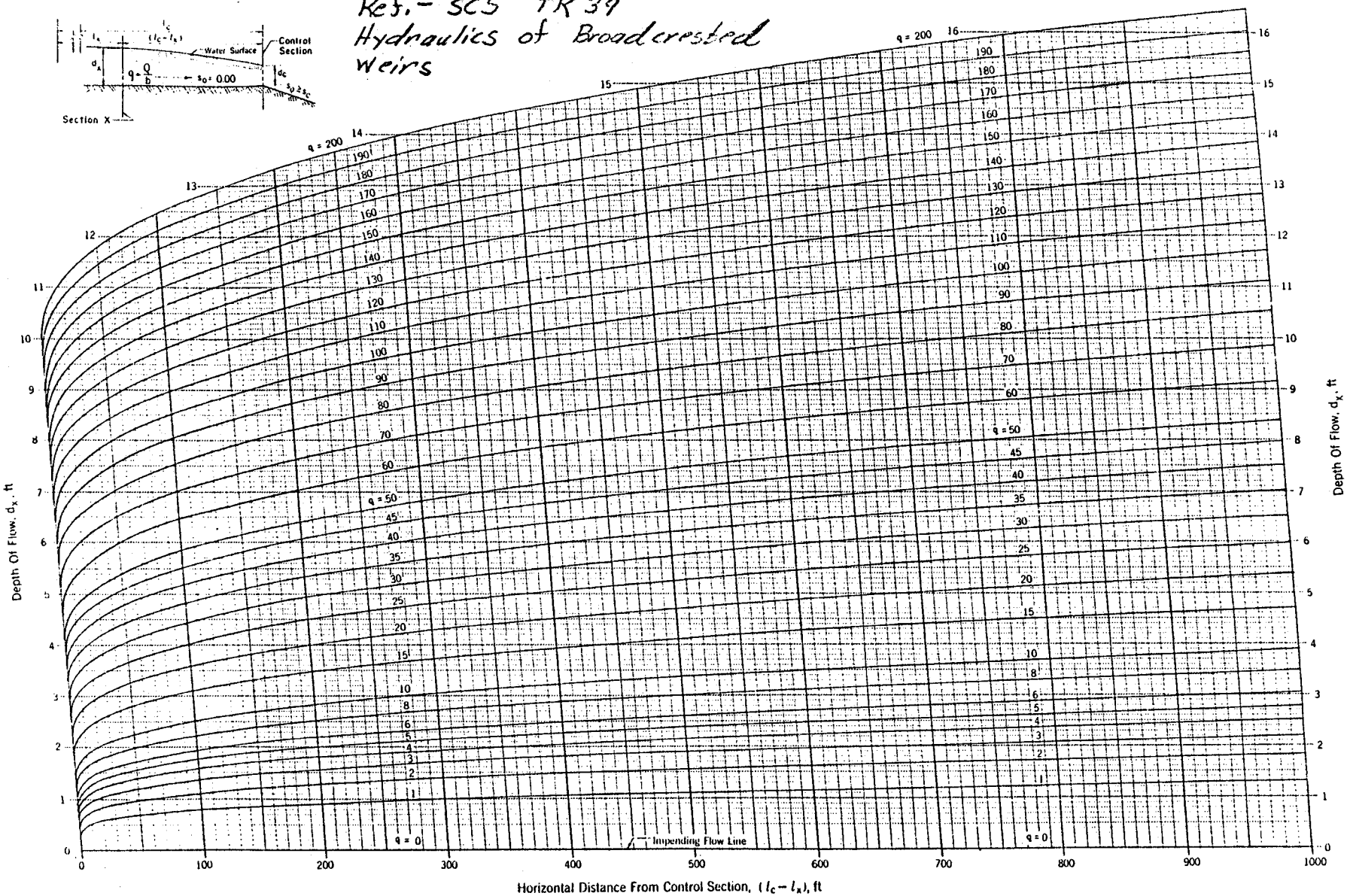

U. S. DEPARTMENT OF AGRICULTURE
SOIL CONSERVATION SERVICE
ENGINEERING DIVISION - DESIGN UNIT

STANDARD DWG. NO.
ES- 158
SHEET 1 OF 10
DATE 2-67

Example – Estimate the location of a hydraulic jump in an 8-ft square box upstream of a sluice gate.

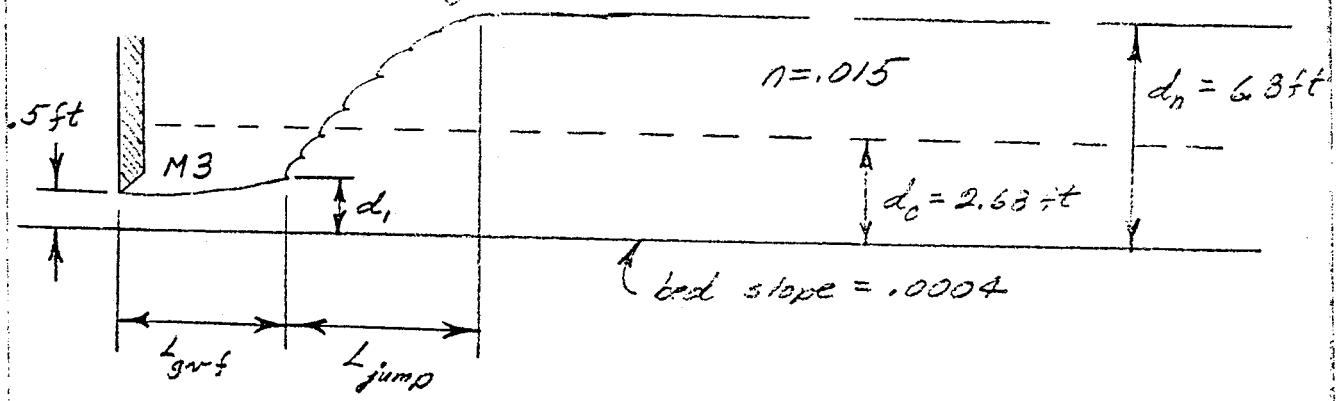

The jump will occur when the conjugate depth of d_1 is the normal depth (6.8 ft).

1. Determine d_1 for $d_2 = 6.8$ ft

$$d_2/d_1 = \frac{1}{2}\left(\sqrt{1+8F^2}-1\right)$$

d_1	$F = \frac{8/d}{\sqrt{gd}}$	$\frac{1}{2}\left(\sqrt{1+8F^2}-1\right)$	$d_2 = d_1$ (Col. (3))	
(1)	(2)	(3)	(4)	
.5	12.5	17.1	8.56	
1.0	4.4	5.8	5.8	
.8	6.1	8.2	6.6	
.75	6.8	9.1	6.8	OK

Jump will occur when d on M3 profile = .75 ft

```
d = 8.0000
B = 8.0000
Z1 = 0.0000
Z2 = 0.0000
SO = 0.0004
Q = 200.0000
n = 0.0150

Y = 0.5000
V = 50.0000
VH = 38.8199
X = 0.0000

Y = 0.5500
V = 45.4545
VH = 32.0825
X = 10.3038

Y = 0.6000
V = 41.6667
VH = 26.9582
X = 20.7673

Y = 0.6500
V = 38.4615
VH = 22.9703
X = 31.3587

Y = 0.7000
V = 35.7143
VH = 19.8061
X = 42.0503

Y = 0.7500
V = 33.3333
VH = 17.2533
X = 52.8171
```

$L_{surf} = 52.8$ ft

$L_{jump} = \frac{5.9}{d_2}$ (from [illegible])

$= (5.9)(6.8) = 40.1$ ft

∴ The total channel length from the sluice gate to normal flow is $52.8 + 40.1 = 92.9$ ft.

Standard Step Method

The standard Step Method is similar to the Direct Step Method, except that the channel does not have to be prismatic and miscellaneous losses can be incorporated. Total energy is used rather than specific energy.

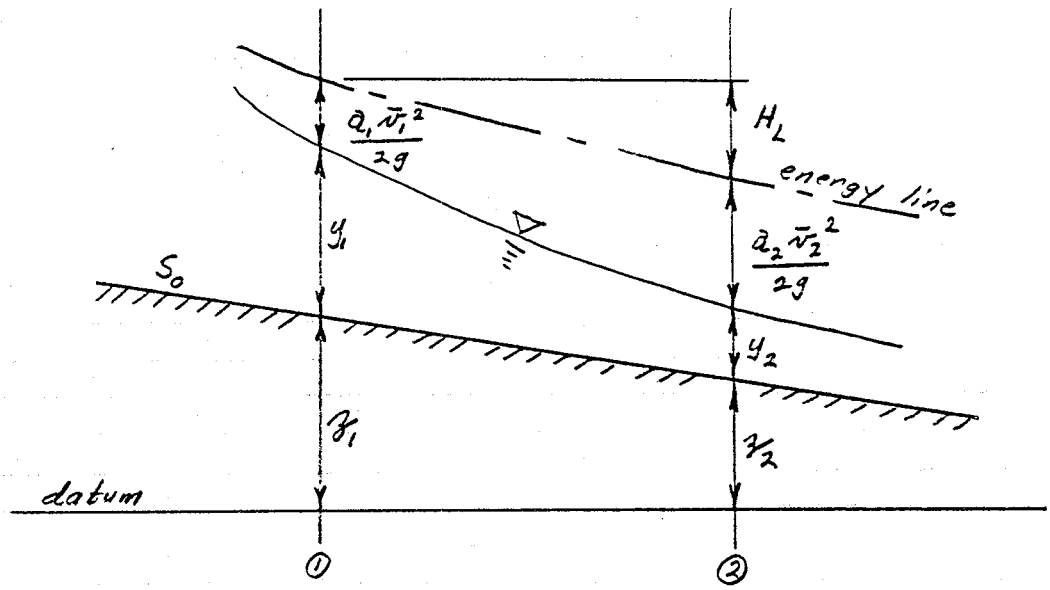

Total head @ ① = Total head @ ② + Σ losses

$$H_1 = \frac{a_1 \bar{v}_1^2}{2g} + y_1 + z_1$$

$$H_2 = \frac{a_2 \bar{v}_2^2}{2g} + y_2 + z_2$$

$$H_L = h_{friction} + \Sigma \text{ miscellaneous losses}$$

$$H_1 - H_2 - \underbrace{h_f - \Sigma h_e}_{} = 0$$

estimate based on an assumed y_2; repeat until the equation is solved.

Computation By Standard Step Method

This method is particularly suited to natural streams where channel cross-sectional geometry changes from point to point.

The classical approach to solving the standard step method is to, like the direct step method, build a table which can then be filled in at each trial.

It is imparative that the flow area and wetted perimeter can be expressed as a function of depth, via charts, tables or equations, at each section in order to facilitate computations.

When using the method it is necessary to assume that discharge is constant in the reach and that n, S_o, and α can be set constant for the entire reach or only have a slight variation.

Computations begin at a section with a known depth and proceed upstream (subcritical flow).

The following simplified table shows the steps needed in this method

Standard Step Method

① Section	② WS ft	③ Y ft	④ A ft^2	⑤ V ft^2/sec	⑥ VH ft	⑦ HI ft	⑧ R ft	⑨ SF —	⑩ SFAVG —	⑪ DX ft	⑫ HF ft	⑬ HE ft	⑭ HZ ft

① I.D. of section
② Water surface elevation—given for Section 1, solved for the rest
③ Maximum depth of flow at Section
④ Area of flow—related to depth
⑤ Average velocity = Q/A
⑥ Velocity head at section = $\frac{\alpha V^2}{2g}$
⑦ Total head = WS + VH
⑧ Hydraulic radius = A/P
P not given in this table
⑨ Friction slope = $\frac{(nV)^2}{2.22\,R^{4/3}}$
⑩ Average of current and previous section friction slopes
⑪ Distance between sections
⑫ Friction head loss = (DX)(SFAVG)
⑬ Eddy head loss = (K)(Averge of VH values at current and previous section)
K varies as to type of loss
⑭ Total head elevation = total head in previous reach + HF and HE in this reach

For each trial water surface, a flow depth is calculated from which the other values are derived. If the values of H1 and H2 do not agree within a specified error, then a new depth is calculated.

Henderson (page 143) has shown that an adjustment depth Δy can be found from

$$\Delta y = \frac{H1 - H2}{1-(1-K)Fr_2^2 + \frac{3(SF_2)(DX)}{2R_2}}$$

where Fr_2^2 = Froude number at current section

$$= \frac{{}^2T}{g \quad A}$$

T = channel top width

R_2 = hydraulic radius at current section

SF_2 = friction slope at current section

and the other variables were previously denoted

The new guess of y_{new} is

$$y_{new} = y - \Delta y$$

Convergence using this correction is very rapid.

Standard Step Example

The following four (4) sections were measured on a channel. Use the data to compute a backwater curve for the channel with a discharge of 1000 cfs.

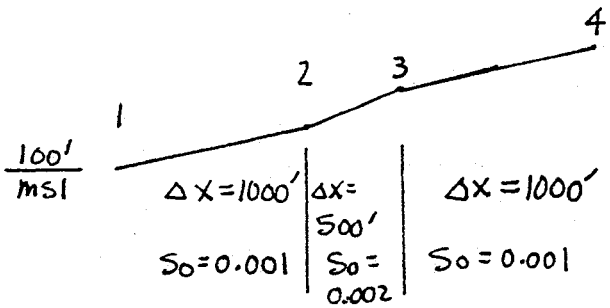

$n = 0.028$

$y_1 = 5'$

Section	Bottom width	Sideslope Z	α	K
1	40'	3	1.1	
				0.2
2	30	3	1.1	
				0.1
3	50	0	1.1	
				0.2
4	40	0	1.1	

Computational steps – refer to computer print out

Section 1 –

$WS = 100 + 5 = 105'$

$Y = Y_1 = 5'$

$A = 40(5) + 3(5)^2 = 275\,ft^2$

$V = Q/A = 1000/275 = 3.64\,fps$

$VH = \frac{1.1(3.64)^2}{2(32.2)} = 0.23$

$H1 = 105 + 0.23 = 105.23'\ (\approx 105.226)$

$R = A/P = \frac{275}{40 + 2(5)\sqrt{3^2+1}} = \frac{275}{71.86} = 3.84'$

$SF = \frac{(0.028(3.64))^2}{2.22(3.84)^{4/3}} = 0.000777$

SFAVG = Doesn't apply in this case
Same for DX, HF, HE

H2 = H1 for the first section

Section 2

$WS = 100 + S_o(DX) + y_1$

$= 100 + 0.001(1000) + 5 = 106'$ This is an initial guess

$y = y_1$ initial guess $= 5'$

$A = 30(5) + 3(5)^2 = 225\ ft^2$

$V = \frac{1000}{225} = 4.44\ fps$

$VH = \frac{1.1(4.44)^2}{2(32.2)} = 0.34'$

$H1 = 106 + 0.34 = 106.34' (\cong 106.337)$

$R = \frac{225}{30 + 2(5)\sqrt{3^2+1}} = \frac{225}{61.62} = 3.65'$

$SF = \frac{(0.028(4.44))^2}{2.22\ (3.65)^{4/3}} = 0.0001241$

$SFAVG = \frac{SF_1 + SF}{2} = \frac{0.000777 + 0.0001241}{2} = 0.0001009$

$HF = SFAVG(DX) = 0.0001009(1000) = 1.009'$

$HE = K(VH_{previous} + VH_{current})/2 = 0.2\ (0.23 + 0.34)/2 \cong 0.056$

$H2 = \text{Previous } H2 + HF + HE$

$= 105.226 + 1.009 + 0.056 = 106.291'$

$\Delta H = H1 - H2 = 106.337 - 106.291 = 0.046'$

$\longrightarrow$ Not acceptable because $|\Delta H| > 0.001' \longleftarrow$

Correction for next trial

$$\Delta y = \frac{0.046}{1 - (1-0.2)\left(\frac{(4.44)^2(30 + 2(3)(5))}{(32.2)\ 225}\right) + \frac{3(0.0001241)(1000)}{2\ (3.65)}}$$

$\Delta y \cong 0.050'$

(Although the program says 0.03 this is probably roundoff error.)

The new y is then

$$5.00 - \Delta y \cong 4.95'$$

The same proce are followed until

$|H1 - H2| < 0.001$ (or whatever you choose)

The profile is plotted on the next page.

CHANNEL NAME --- EXAMPLE FOR DEMONSTRATION

DISCHARGE, CFS = 1000 MANNING'S n = .028 BASE ELEVATION, FEET = 100

SECTION	WS	Y	A	V	VH	H1	R	SF	SFAVG	DX	HF	HE	H2
1.00	105.00	5.00	275.00	3.64	0.23	105.226	3.84	0.000777	0.000000	0.00	0.000	0.000	105.226
2.00	106.00	5.00	225.00	4.44	0.34	106.337	3.65	0.001241	0.001009	1000.00	1.009	0.056	106.291
2.00	105.97	4.97	222.96	4.49	0.34	106.309	3.63	0.001273	0.001025	1000.00	1.025	0.057	106.308
2.00	105.96	4.96	222.88	4.49	0.34	106.308	3.63	0.001274	0.001026	1000.00	1.026	0.057	106.308
3.00	106.96	4.96	248.23	4.03	0.28	107.242	4.14	0.000862	0.001068	500.00	0.534	0.031	106.873
3.00	106.62	4.62	230.85	4.33	0.32	106.937	3.90	0.001081	0.001177	500.00	0.589	0.033	106.930
3.00	106.61	4.61	230.52	4.34	0.32	106.932	3.89	0.001085	0.001180	500.00	0.590	0.033	106.932
4.00	107.61	4.61	184.42	5.42	0.50	108.113	3.75	0.001784	0.001435	1000.00	1.435	0.082	108.449
4.00	107.83	4.83	193.18	5.18	0.46	108.287	3.89	0.001547	0.001316	1000.00	1.316	0.078	108.326
4.00	107.86	4.86	194.25	5.15	0.45	108.309	3.91	0.001521	0.001303	1000.00	1.303	0.077	108.312
4.00	107.86	4.86	194.34	5.15	0.45	108.311	3.91	0.001518	0.001302	1000.00	1.302	0.077	108.311

Plot of Example Backwater Curve

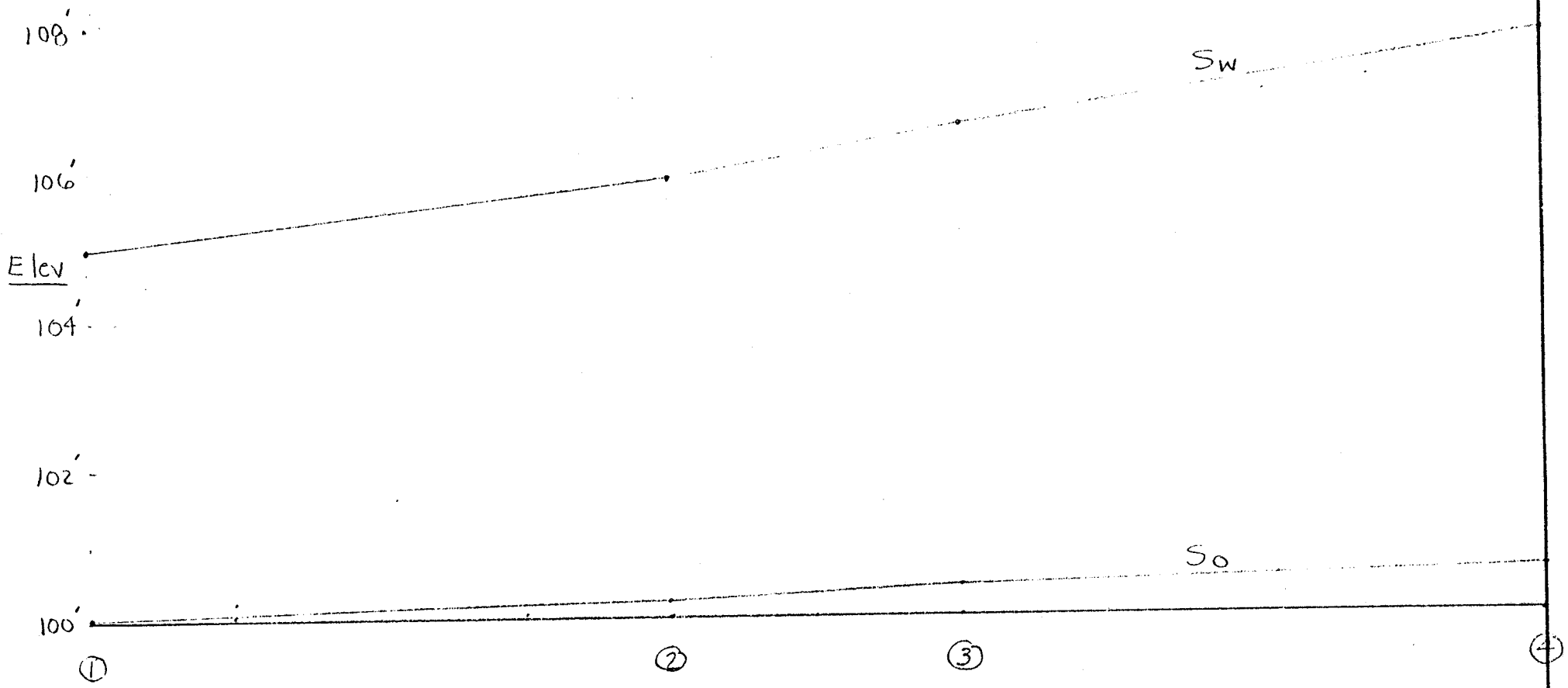

Cross Section

Plan & Profiles

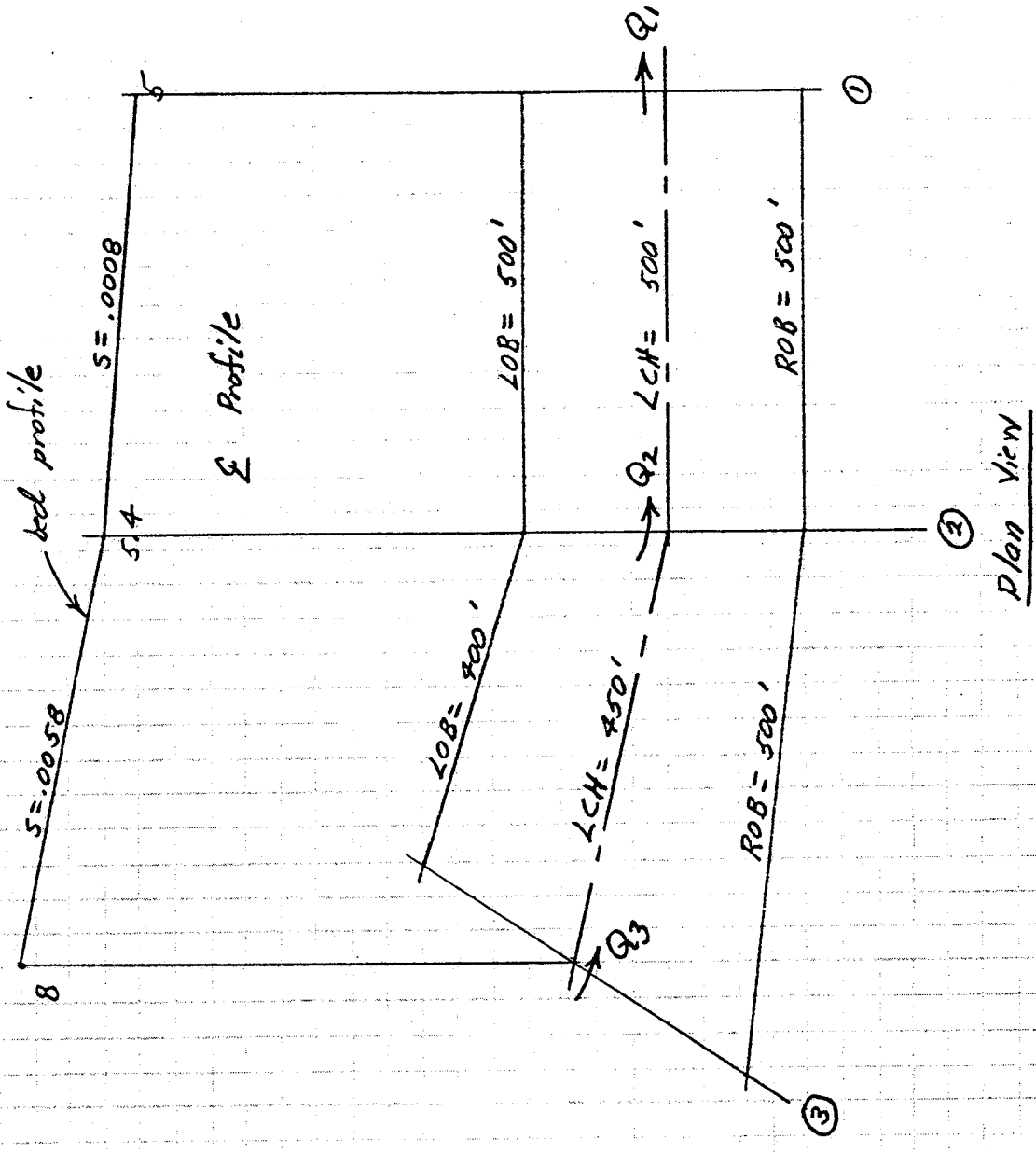

expansion coef. = .3

contraction coef. = .1

Cross-Sections

Section 1:

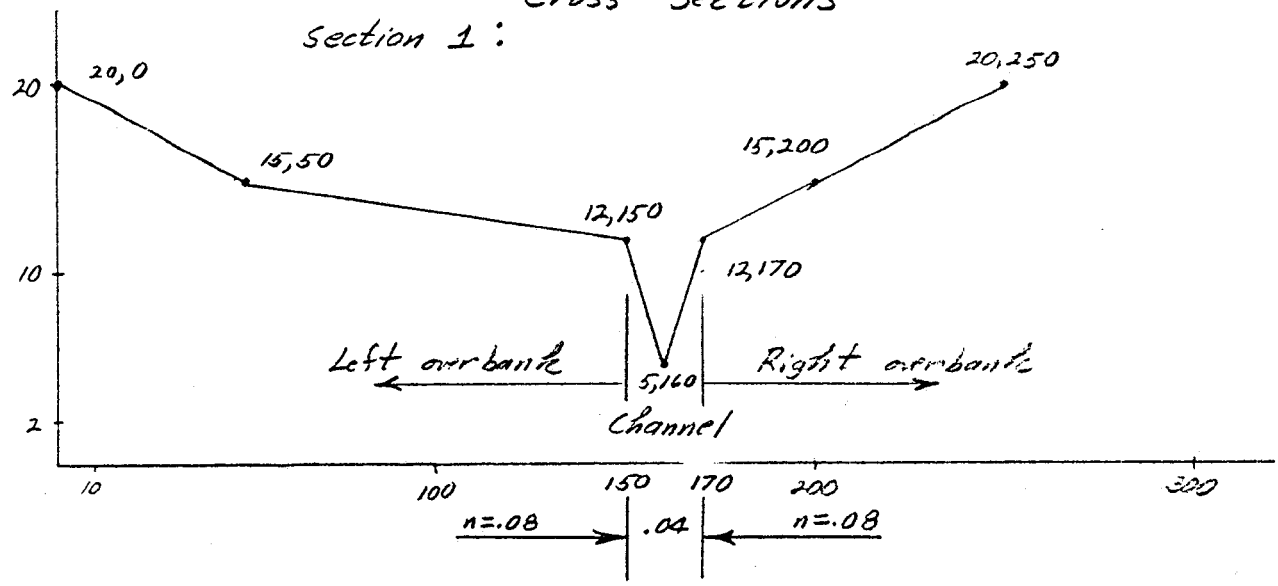

Section 2:

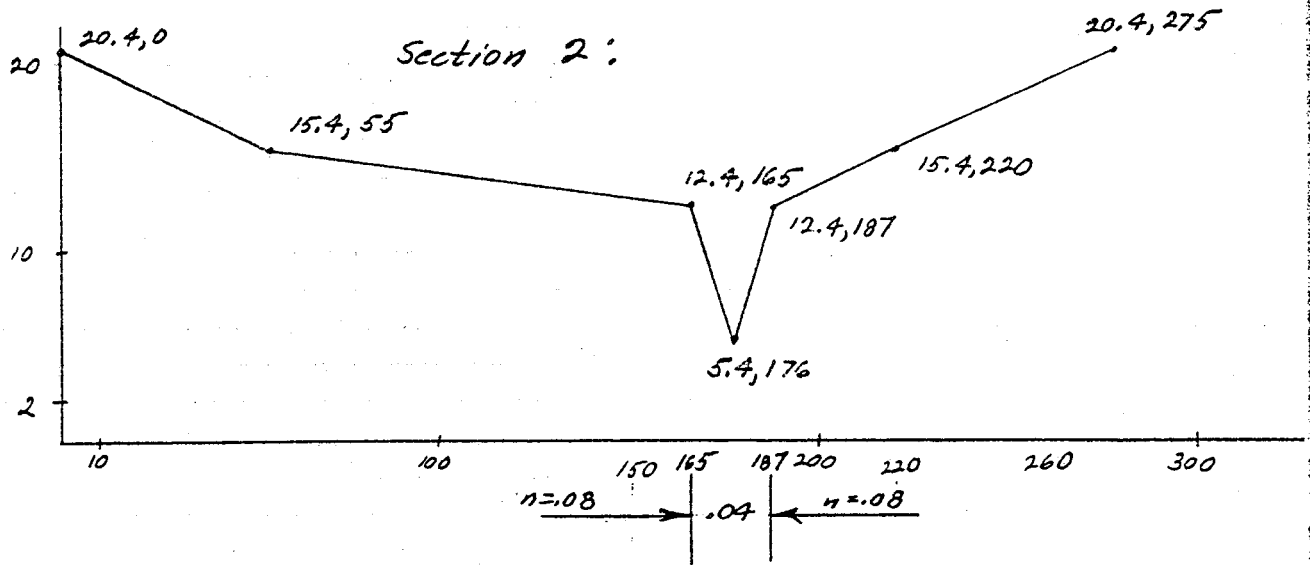

Section 3:

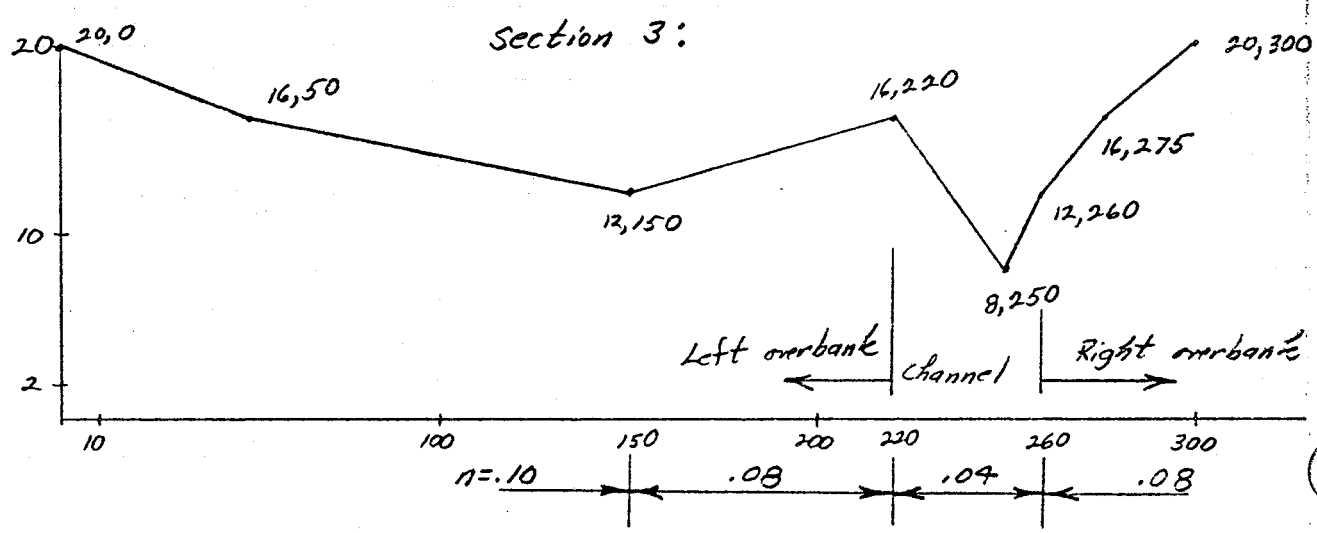

Input for Samples 1 & 2

	Card No.	Card ID	Field	
	1	T1		Title cards for first run
	2	T2		"
	3	T3		"
	4	J1	2	discharge from field 2 of the QT card will be used
			4	subcritical profile
			5	starts from known discharge
			9	starting elev. is 13-ft
section 1	5	QT	1	two discharges to be run
			2	first is 200 cfs
			3	second is 500 cfs
	6	NC	1	"n" for left overbank (LOB)
			2	"n" for right overbank (ROB)
			3	"n" for channel
			4	contraction coef.
			5	expansion coef.
	7	X1	1	section ID number
			2	7 sets of coord. define cross-section
			3	150 is coord. of left bank
			4	170 is coord. of right bank
	8,9	GR	1-10	cross-section coordinates (elev., station)
section 2	10	X1	1	section ID number
			2,3,4	blank, section remains the same as last section
			5	LOB length
			6	ROB "
			7	Channel "
			8	expand width of last section by factor 1.1
			9	raise bottom of section #2 0.4-ft above section #1
section 3	11	NH	1	number of "n" values across cross-section
			2	n = .10
			3	previous "n" from 0 to station 150
			4	n = .08
			5	previous "n" from 150 to 220
			6	n = .04
			7	220 to 260
			8	n = .08
			9	260 to 300
	12	QT	1	two discharges to be run
			2	first is 180 cfs
			3	second is 450 cfs

Section 3

13	X1	1	section ID number
		2	8 sets of coord. define cross-section
		3	220 is coord. of left bank
		4	260 is coord. of right bank
		5	400 LOB length
		6	500 ROB length
		7	450 Channel length
14	X3	1	10 calls for effective area option
15,16	GR	1-10	cross-section coordinates
17	EJ		ends first run
18	T1		title cards for second run
19	T2		"
20	T3		"
21	J1	2	discharge from field 3 of the QT card will be used
		4	subcritical
		5	starts from known depth
		9	starting elev. is 15-ft
22	J2	1	15 indicates last run & request summary
23			blank } ends input
24			blank } ends input
25			blank } ends input
26	ER		ends run } ends input

NEW MEXICO STATE UNIVERSITY COMPUTER CENTER

NAME: G. Sabol LOCATION: PHONE: DATE: 3-83

PROGRAM: HEC-2 Sample Problems 1 & 2 PAGE 1 OF 1

Card No. Field:

Card No.	0	1	2	3	4	5	6	7	8	9	10
1	T1		SAMPLE PROBLEM 1								
2	T2		FIRST RUN								
3	T3		SAMPLE CREEK 200 CFS								
4	J1		2		0		0			13	
5	QT	2	200	500							
6	NC	.08	.08	.04	.1		.3				
7	X1	1	7	150	170						
8	GR	20	0	15	50		12	150	5	160	12	170
9	GR	15	200	20	250						
10	X1	2				500		500	500	1.1	.4
11	NH	4	.1	150	.08		220	.04	260	.08	300
12	QT	2	180	450							
13	X1	3	8	220	260		400	500	450		
14	X3	10									
15	GR	20	0	16	50		12	150	16	220	8	250
16	GR	12	260	16	275		20	300			
17	EJ										
18	T1		SAMPLE PROBLEM 2								
19	T2		SECOND RUN								
20	T3		SAMPLE CREEK 500 CFS								
21	J1		3							15	
22	J2	15									
23											
24											
25											
26	ER										

```
*****************************************************
  HEC2 RELEASE DATED NOV 76 UPDATED FEB 1977
  ERROR CORR -  01
  MODIFICATION -  50,51,52
*****************************************************
```

Input

```
T1        SAMPLE PROBLEM 1
T2        FIRST RUN
T3        SAMPLE CREEK 200 CFS

J1   ICHECK     INQ        NINV       IDIR       STRT       METRIC     HVINS      Q          WSEL       FQ
        0.        2.         0.         0.   0.0        0.0        0.0        0.    13.000     0.0

QT       2.000   200.000   500.000      0.0        0.0        0.0        0.0        0.0        0.0        0.0
NC       0.080     0.080     0.040      0.100      0.300      0.0        0.0        0.0        0.0        0.0

X1 Section 1.000   7.000   150.000    170.000      0.0        0.0        0.0        0.0        0.0        0.0
GR      20.000     0.0      15.000     50.000     12.000    150.000     5.000    160.000     12.000    170.000
GR      15.000   200.000    20.000    250.000      0.0        0.0        0.0        0.0        0.0        0.0

X1section 2.000    0.0        0.0        0.0      500.000    500.000    500.000     1.100     0.400      0.0
NH       4.000     0.100   150.000      0.080     220.000      0.040    260.000     0.080   300.000      0.0
QT       2.000   180.000   450.000      0.0        0.0        0.0        0.0        0.0        0.0        0.0

X1section 3.000    8.000   220.000    260.000    400.000    500.000    450.000     0.0        0.0        0.0
X3      10.000     0.0       0.0        0.0        0.0        0.0        0.0        0.0        0.0        0.0
GR      20.000     0.0      16.000     50.000     12.000    150.000    16.000    220.000     8.000    250.000
GR      12.000   260.000    16.000    275.000     20.000    300.000     0.0        0.0        0.0        0.0
EJ       0.0       0.0       0.0        0.0        0.0        0.0        0.0        0.0        0.0        0.0
```

```
*PROF 1

CCHV=    0.100 CEHV=    0.300
*SECNO 1.000
   SECNO      DEPTH      CWSEL      CRIWS      WSELK      EG         HV         HL         OLOSS      BANK ELEV
   Q          QLOB       QCH        QROB       ALOB       ACH        AROB       VOL        TWA     LEFT/RIGHT
   TIME       VLOB       VCH        VROB       XNL        XNCH       XNR        WTN        ELMIN        SSTA
   SLOPE      XLOBL      XLCH       XLOBR      ITRIAL     IDC        ICCNT      CORAR      TOPWID       ENDST

     1.00       8.00      13.00        0.0      13.00      13.07       0.07        0.0        0.0      12.00
     200.         5.       194.         1.        17.        90.         5.         0.         0.      12.00
      0.0       0.28       2.15       0.28      0.080      0.040      0.080        0.0       5.00     116.67
 0.000590         0.         0.         0.          0          0          0        0.0      63.33     180.00

*SECNO 2.000
     2.00       7.88      13.28        0.0        0.0      13.35       0.06       0.28       0.00      12.40
     200.         4.       195.         1.        15.        97.         4.         1.         1.      12.40
     0.07       0.25       2.02       0.25      0.080      0.040      0.080      0.040       5.40     132.38
 0.000517       500.       500.       500.          1          0          0        0.0      64.40     196.79

1490 NH CARC USED
*SECNO 3.000                                                    elev. of left effective area
3495 OVERBANK AREA ASSUMED NON-EFFECTIVE,ELLEA=        16.00 ELREA=        12.00

     3.00       5.55      13.55        0.0        0.0      13.61       0.06       0.26       0.00      16.00
     180.         0.       178.         2.         0.        93.         4.         2.         1.      12.00
     0.14        0.0       1.92       0.39      0.080      0.040      0.080      0.040       8.00     229.22
 0.000649       400.       450.       500.          1          0          0        0.0      36.56     265.78
```

16

```
*************************************************
  HEC2 RELEASE DATED NOV 76 UPDATED FEB 1977
  ERROR CORR -  01
  MODIFICATION -  50,51,52
*************************************************

T1       SAMPLE PROBLEM 2
T2       SECOND RUN
T3       SAMPLE CREEK 500 CFS
J1  ICHECK    INQ      NINV     IDIR     STRT     METRIC   HVINS    Q        WSEL     FQ
       0.      3.       0.       0.  0.0           0.0      0.0      0.    15.000    0.0
J2  NPROF     IPLOT    PPFVS    XSECV    XSECH    FN       ALLDC    IBW      CHNIM    ITRACE
    15.000     0.0      0.0      0.0      0.0      0.0      0.0      0.0      0.0      0.0
```

```
*PROF 2

CCHV=    0.100 CEHV=    0.300
*SECNO 1.000
   SECNO      DEPTH      CWSEL      CRIWS      WSELK      EG         HV         HL         OLOSS      BANK ELEV
   Q          CLOB       QCH        QROB       ALOB       ACH        AROB       VOL        TWA     LEFT/RIGHT
   TIME       VLOB       VCH        VROB       XNL        XNCH       XNR        WTN        ELMIN        SSTA
   SLOPE      XLOBL      XLCH       XLOBR      ITRIAL     IDC        ICONT      CORAR      TOPWID       ENDST

      1.00      10.00      15.00       0.0       15.00      15.10       0.10       0.0        0.0       12.00
     500.        94.       378.        28.       150.       130.        45.        0.         0.        12.00
       0.0      0.62       2.91       0.62      0.080      0.040      0.080       0.0        5.00      50.00
 0.000660         0.         0.         0.          0          0          0       0.0      150.00     200.00

*SECNO 2.000
      2.00       9.92      15.32       0.0        0.0       15.41       0.09       0.30       0.00      12.40
     500.        89.       384.        27.       157.       141.        47.        4.         2.        12.40
      0.06      0.57       2.72       0.57      0.080      0.040      0.080      0.040       5.40      57.82
 0.000563       500.       500.       500.          1          0          0       0.0      161.33     219.15

1490 NH CARD USED
*SECNO 3.000

3495 OVERBANK AREA ASSUMED NON-EFFECTIVE,ELLEA=        16.00 ELREA=        12.00

      3.00       7.60      15.60       0.0        0.0       15.70       0.10       0.29       0.00      16.00
     450.         0.       432.        18.         0.       164.        24.        7.         3.        12.00
      0.11       0.0       2.63       0.75      0.080      0.040      0.080      0.040       8.00     221.53
 0.000772       400.       450.       500.          0          0          0       0.0       51.94     273.47
```

Tests 1 & 2

```
*************************************************
 HEC2 RELEASE DATED NOV 76 UPDATED FEB 1977
 ERROR CORR -  01
 MODIFICATION -  50,51,52
*************************************************
```

NOTE- ASTERISK (*) AT LEFT OF CROSS-SECTION NUMBER INDICATES MESSAGE IN SUMMARY OF ERRORS LIST

SAMPLE CREEK 200 CFS

SUMMARY PRINTOUT TABLE 150

SECNO	XLCH	ELTRD	ELLC	ELMIN	Q	CWSEL	CRIWS	EG	IOKWS	VCH	AREA	.01K
1.000	0.0	0.0	0.0	5.00	200.00	13.00	0.0	13.07	5.30	2.15	111.67	82.33
1.000	0.0	0.0	0.0	5.00	500.00	15.00	0.0	15.10	6.60	2.91	325.70	134.73
2.000	500.00	0.0	0.0	5.40	200.00	13.23	0.0	13.35	5.17	2.32	115.43	97.92
2.000	500.00	0.0	0.0	5.40	500.00	15.32	0.0	15.41	5.63	2.72	344.75	213.04
3.000	450.00	0.0	0.0	8.00	180.00	13.55	0.0	13.61	6.43	1.92	97.46	70.64
3.000	450.00	0.0	0.0	8.00	450.00	15.60	0.0	15.72	7.72	2.63	173.15	151.35

SAMPLE CREEK 200 CFS

SUMMARY PRINTOUT TABLE 150

SECNO	Q	CWSEL	DIFWSP	DIFWSX	DIFKWS	TOPWID	XLCH
1.000	200.00	13.00	0.0	0.0	0.0	63.33	0.0
1.000	500.00	15.00	2.00	0.0	0.0	150.00	0.0
2.000	200.00	13.28	0.0	0.28	0.0	64.40	500.00
2.000	500.00	15.32	2.03	0.32	0.0	161.33	500.00
3.000	180.00	13.55	0.0	0.26	0.0	36.56	450.00
3.000	450.00	15.60	2.05	0.28	0.0	51.94	450.00

SUMMARY OF ERRORS

Unsteady Flow

Definition: $\frac{\partial(\ )}{\partial t} \neq 0$ (unsteady) — some hydraulic property (Q, V, A, etc)

and $\frac{\partial(\ )}{\partial x} \neq 0$ (non uniform)

We typically deal with an unsteady, non uniform flow condition.

$\frac{\partial y}{\partial x}$ = "small" value – gradually varied flow – slow changes with distance

$\frac{\partial y}{\partial x}$ = "large" value – rapidly varied flow – surges, gate operation.

Unsteady flow deals with translatory waves such as flood waves

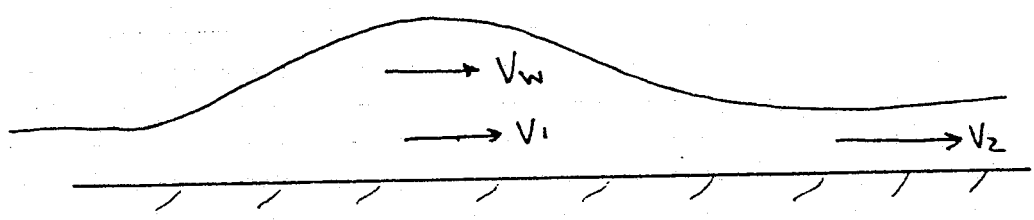

Governing equations -

Continuity:

Isolating a small "control volume"

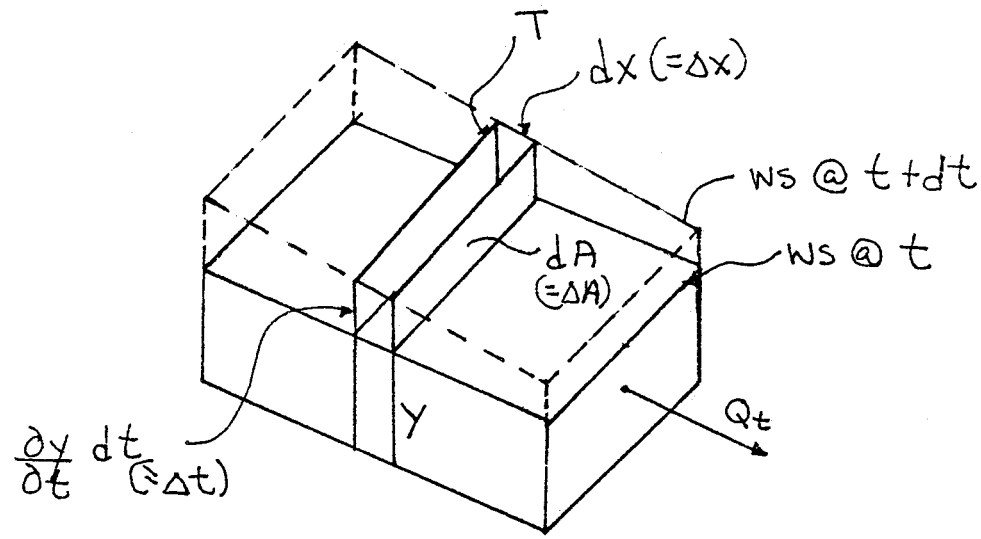

Continuity says $(I-O) = \frac{\Delta S}{\Delta t}$

$$I - O = \frac{\Delta Q}{\Delta X} \Rightarrow \frac{\partial Q}{\partial X}$$

and $\frac{\Delta S}{\Delta t} = \frac{\partial V}{\partial t} = \frac{\partial A}{\partial t}$

We can see this on the control volume

as $\left(\frac{\Delta Q}{\Delta X}\right) dX\, dt + dX \left(\frac{\Delta A}{\Delta t}\right) dt = 0$

or $\frac{\partial Q}{\partial X} + \frac{\partial A}{\partial t} = 0$ (= q_l for lateral inflows)

uniform term

steady term

Momentum:

$$\Sigma F = \rho Q (\beta_2 v_2 - \beta_1 v_1)$$

$$\Sigma F = \underbrace{(P_1 - P_2)}_{\text{Pressure force}} + \underbrace{W \sin\theta}_{\text{weight of water}} - \underbrace{F_f}_{\text{Resistance to flow from perimeter}}$$

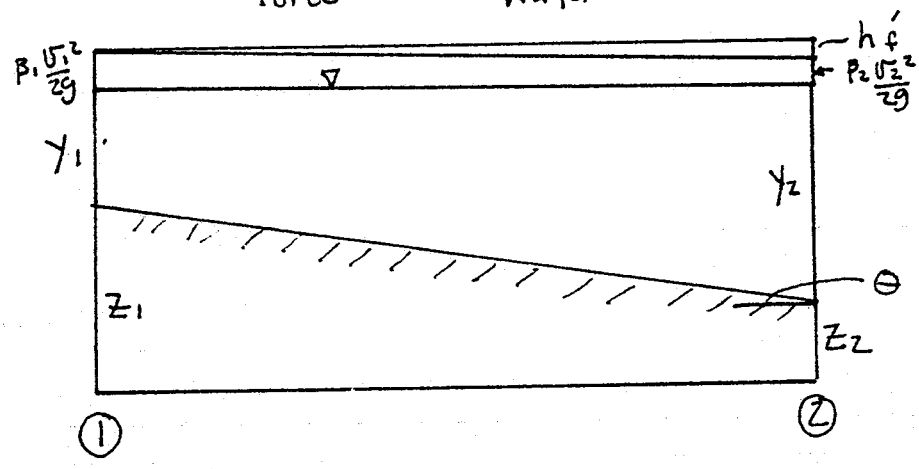

Although not exactly the same as the energy equation, the momentum equation is analogous for a rectangular (unit width) channel of small slope ($\sin\theta \approx 0$). as shown above (the components should sum to zero net)

Because of the analogy, the energy equation is sometimes used as a starting point.

From this starting point note that

$$h_f + z_2 + y_2 + \frac{V_2^2}{2g} = (\cancel{z_1} + dz) + (\cancel{y_1} + dy) + \left(\cancel{\frac{\alpha V_1^2}{2g}} + d\left(\frac{\alpha V^2}{2g}\right)\right) + \overset{h_f}{S_f dx}$$

$$= \cancel{z_1} + \cancel{y_1} + \cancel{\frac{\alpha V_1^2}{2g}}$$

from which

$$\frac{dz}{dx} + \frac{dy}{dx} + \frac{d}{dx}\left(\frac{\alpha V^2}{2g}\right) = -S_f$$

in Unsteady flow there is a component of loss related to acceleration or work

$$\text{Work} = F \cdot x = max$$

in the differential element form

$$\text{Work} = \frac{W}{g}\frac{\partial V}{\partial t} dx$$

work per unit weight then is

$$\frac{\text{Work}}{W} = \frac{1}{g}\frac{\partial V}{\partial t} dx$$

Now we get (using the partial notation)

$$\frac{\partial z}{\partial x} + \frac{\partial y}{\partial x} + \frac{\alpha V}{g}\frac{\partial V}{\partial x} + \frac{1}{g}\frac{\partial V}{\partial t} = -S_f$$

From this we can substitute

$S_o = \frac{-\partial z}{\partial x}$ (we talk about positive slopes)

to yield:

$$S_f = \underbrace{S_o}_{\text{bed slope}} - \underbrace{\frac{\partial y}{\partial x}}_{\text{Water surface slope}} - \underbrace{\frac{\alpha v}{g}\frac{\partial v}{\partial x}}_{\text{Convective acceleration}} - \underbrace{\frac{1}{g}\frac{\partial v}{\partial t}}_{\text{local acceleration}} = \frac{\bar{v}^2}{C^2 R}$$

terms → I II III IV

Wave type	Terms
Kinematic	$S_f = I$
Diffusion	$S_f = I - II$
Steady, nonuniform quasistate dynamic	$S_f = I - II - III$
Full dynamic unsteady, nonuniform	$S_f = I - II - III - IV$
Gravity wave	$0 = -II - III - IV$

The similarities and differences between these wave types will be discussed in a later section.

Assumptions and limitations associated with the dynamic wave equation:

1) Coordinate system is orthogonal to horizontal and vertical (gravity oriented)

2) $\alpha \approx \beta \approx 1.0$

3) Changes in internal stresses with respect to distance are negligible

4) Water surface elevation may be substituted for

$$\left(\frac{\partial y}{\partial x} - S_o\right)$$

5) Not reliable when assumptions are violated -

a) initial stages of a dam break

b) curvilinear flow

c) supercritical flow with surface instabilities

d) Froude number near 1.0

6) Good enough for most problems

7) Certain simplifying concepts reduce the complexity of the solution

8) Except for special cases solutions to the simultaneous equations of continuity and momentum are by finite difference schemes.

9) Solutions assume x and t are independent and V and y (Q and A) are dependent.

The Method of Characteristics -

In the MOC, "characteristic" curves are located in an x, t plane and the Ord. Diff. Eqns. on those curves are integrated to find the solutions

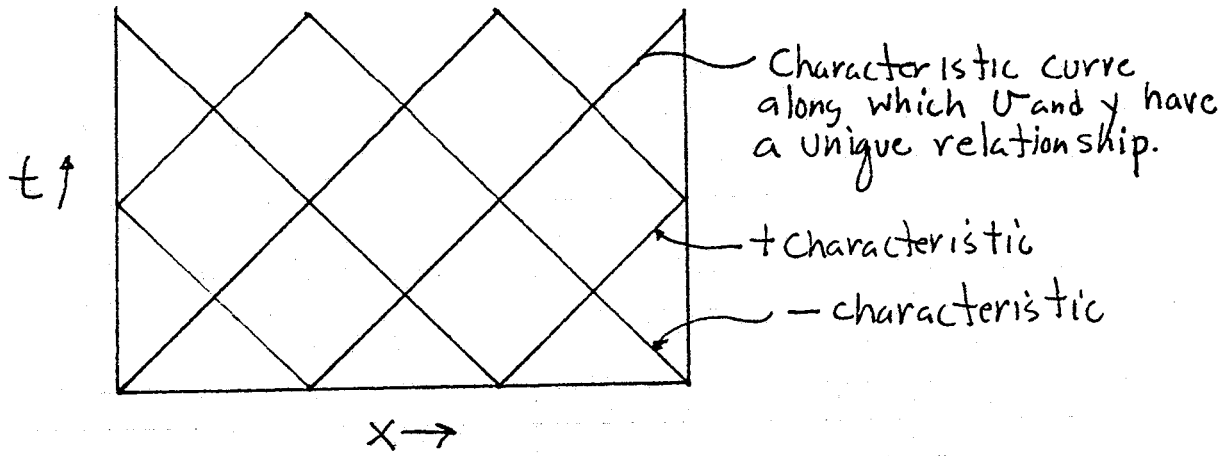

In terms of the governing equations we can recast them as

$$\frac{\partial y}{\partial x} + \frac{V}{g}\frac{\partial V}{\partial x} + \frac{1}{g}\frac{\partial V}{\partial t} = (S_o - S_f)$$

$$\frac{\partial V y}{\partial x} + \frac{\partial y}{\partial t} = 0$$

Using the fact that the celerity of a shallow water-wave, C, is

$$C = \sqrt{gy}$$

and that $\quad dx\frac{\partial C}{\partial x} + dt\frac{\partial C}{\partial t} = dC$

and $\quad dx\frac{\partial V}{\partial x} + dt\frac{\partial V}{\partial t} = dV$

total derivatives

A matrix of the form

$$\begin{pmatrix} 2(v+c) & 2 & v+c & 1 \\ -2(v-c) & -2 & v-c & 1 \\ dx & dt & 0 & 0 \\ 0 & 0 & dx & dt \end{pmatrix} \begin{pmatrix} \partial c/\partial x \\ \partial c/\partial t \\ \partial v/\partial x \\ \partial v/\partial t \end{pmatrix} = \begin{pmatrix} g(S_o - S_f) \\ g(S_o - S_f) \\ dc \\ dv \end{pmatrix}$$

Can be solved for the determinant to get two solutions (hyperbolic) of the form

$$\frac{dt}{dx} = \frac{1}{v+c} \qquad + \text{characteristic}$$

$$\frac{dt}{dx} = \frac{1}{v-c} \qquad - \text{characteristic}$$

Integrating along the characteristics gives

$$v + 2c = v_o + 2c_o + \int g(S_o - S_f)\,dt$$

$$v - 2c = v_o - 2c_o + \int g(S_o - S_f)\,dt$$

<u>For gravity waves</u> - such as when water surface slope and acceleration terms predominate,

$$S_o = S_f \approx 0$$

Then the solution is simple. Note that $S_o - S_f = 0$ is <u>not</u> the same thing!

Solutions for gravity waves using MOC include

1) Reservoir drawdown effects on inflowing rivers
2) Formation of surges from gate operation
3) Classic dam break problem

Summary –

1) Unsteady (and nonuniform) flow is a common occurrence in channels and must be considered.
2) The governing equations are continuity and dynamic (momentum/energy).
3) The dynamic equation is composed of specific "wave" types
4) The method of characteristics is a classic solution technique
5) There are certain assumptions and limitations to the dynamic wave, but they are not so restrictive as to preclude its use for many problems

Reservoir Routing

Storage Equation : $\bar{I} - \bar{O} = \frac{\Delta S}{\Delta t}$

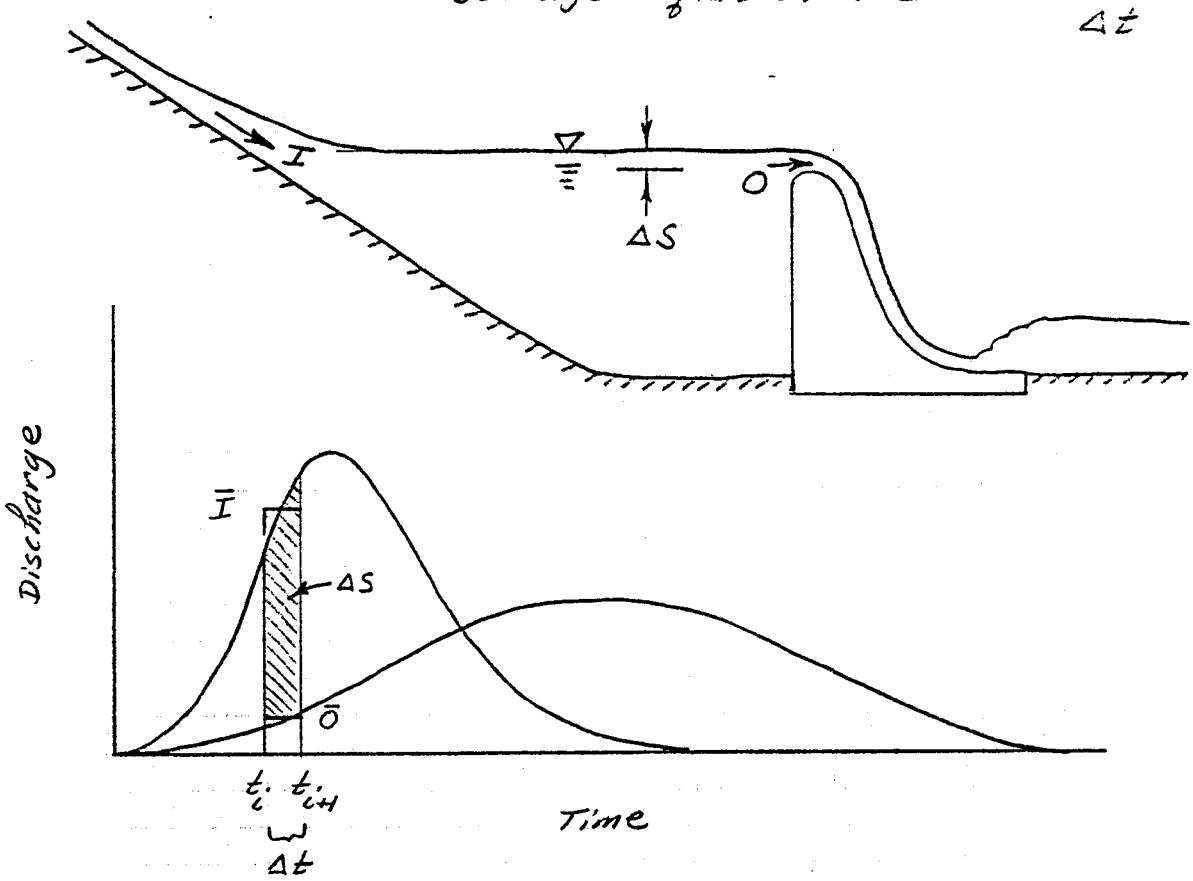

$$\bar{I} = \frac{I_i + I_{i+1}}{2} \qquad \bar{O} = \frac{O_i + O_{i+1}}{2}$$

$$\frac{I_i + I_{i+1}}{2} - \frac{O_i + O_{i+1}}{2} = \frac{S_{i+1} - S_i}{\Delta t}$$

$$\underbrace{I_i + I_{i+1} + \frac{2S_i}{\Delta t} - O_i}_{\text{calculate}} = \underbrace{\frac{2S_{i+1}}{\Delta t} + O_{i+1}}_{\text{determine relation between}}$$

$\left(\frac{2S}{\Delta t} + O\right)$ and O.

Needed :

1. Stage-volume relation
2. Stage - outflow relation
3. Outflow - $\left(\frac{2S}{\Delta t} + O\right)$ relation

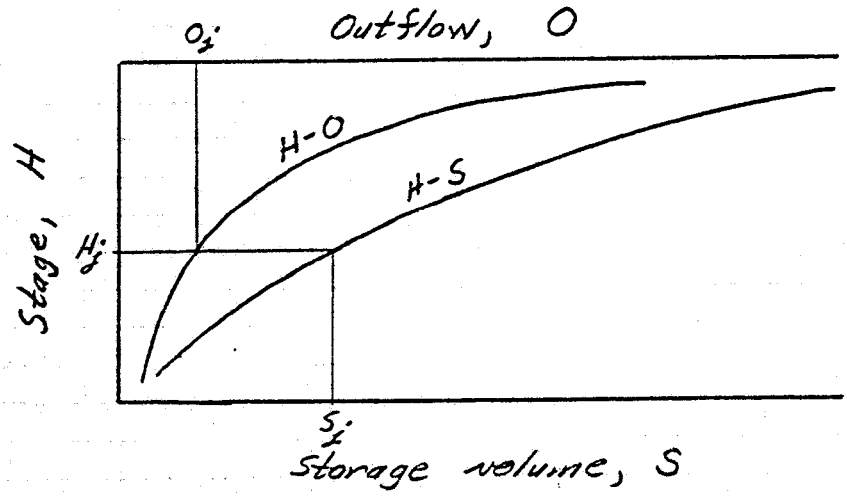

Set-up a table (choose a Δt):

H_j	S_j	O_j	$\frac{2S_j}{\Delta t} + O_j$
(1)	(2)	(3)	(4)
↓	↓	↓	↓

Plot $\frac{2S}{\Delta t} + O$ versus O :

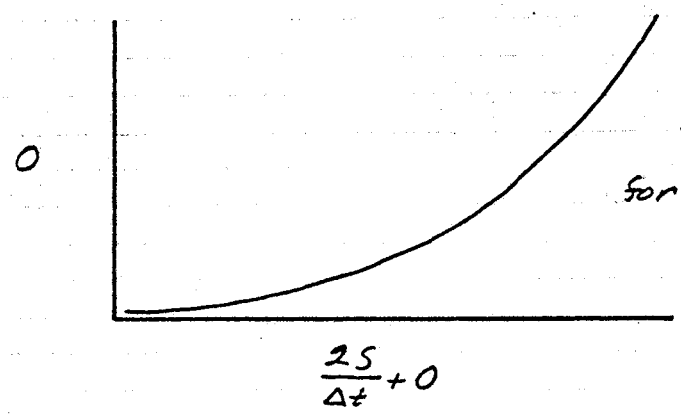

Note : This is for a specific Δt.

Prepare a table :

i (1)	I_i (2)	$\frac{S_i}{\Delta t}$ (3)	$\sum \frac{S_i}{\Delta t}$ (4)	$\frac{2\sum S_i}{\Delta t} - O_i$ (5)	$\frac{2\sum S_{i+1}}{\Delta t} + O_{i+1}$ (6)	O_i (7)	$\sum I_i$ (8)	$\sum O_i$ (9)	$\sum \frac{S_i}{\Delta t}$ (10)
0	I_0	I_0	I_0	I_0	I_0+I_1	0	0	0	0
1	I_1					O_1			
⋮	⋮								
i	I_i								
⋮	⋮								
N	I_N								

The table shows the initial information.

Column	Description
(1)	Increment number
(2)	Digitized inflow hydrograph
(3)	(2) - (7)
(4)	$(4)_{i-1} + (3)$
(5)	$2 \times (4) - (7)$
(6)	$(5) + (2) + (2)_{i+1}$
(7)	from $\frac{2S}{\Delta t} + O$ vs O curve @ $\frac{2S}{\Delta t} + O = (6)_{i-1}$
(8)	$\sum_{i=1}^{n} (2)$
(9)	$\sum_{i=1}^{n} (7)$
(10)	(8) - (9) this must equal (4)

Example - Reservoir routing

Route the inflow hydrograph through the reservoir with a 25.3 ft wide ogee crest spillway.

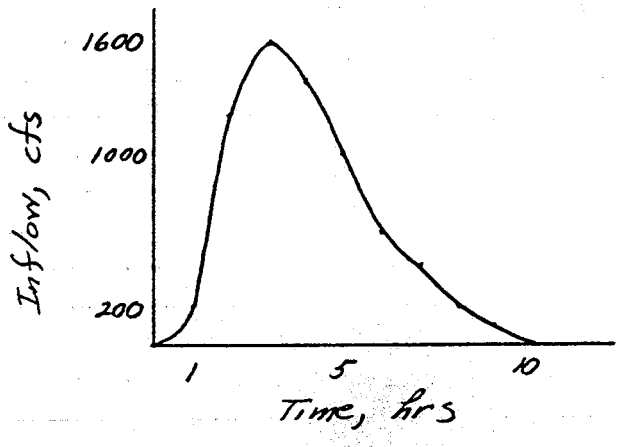

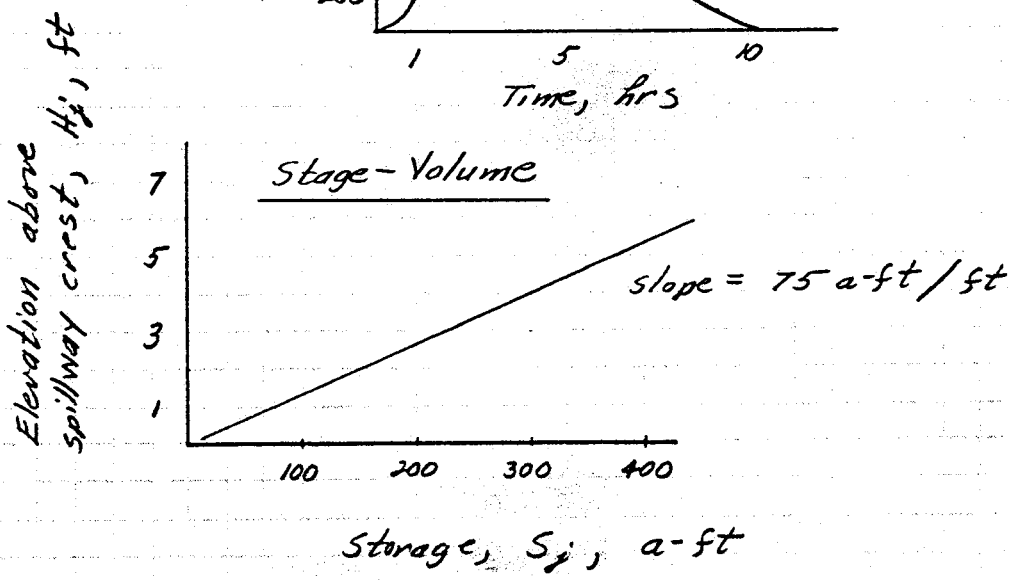

Stage-Outflow

$$O = C L H^{3/2}$$

$L = 25.3$ ft $\quad C = 3.95 \quad O_j = 100\, H_j^{3/2}$

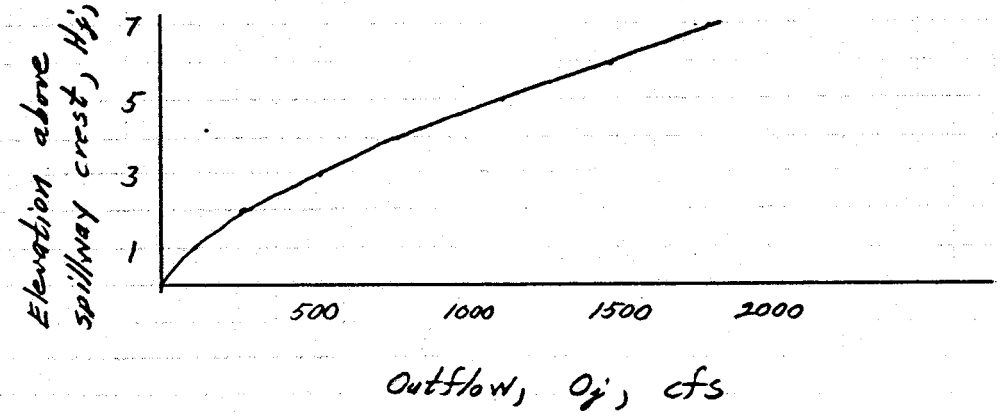

$\Delta t = 1\text{-hr}$

H_j, ft	S_j, $ft^3 \times 10^5$	O_j, cfs	$\frac{2S}{\Delta t} + O$, cfs
(1)	(2)	(3)	(4)
0	0	0	0
1	32.67	100	1008
2	65.34	280	2095
3	98.01	520	3242
4	130.68	800	4430
5	163.35	1120	5658
6	196.02	1470	6915
7	228.69	1850	8202
8	261.36	2260	9520

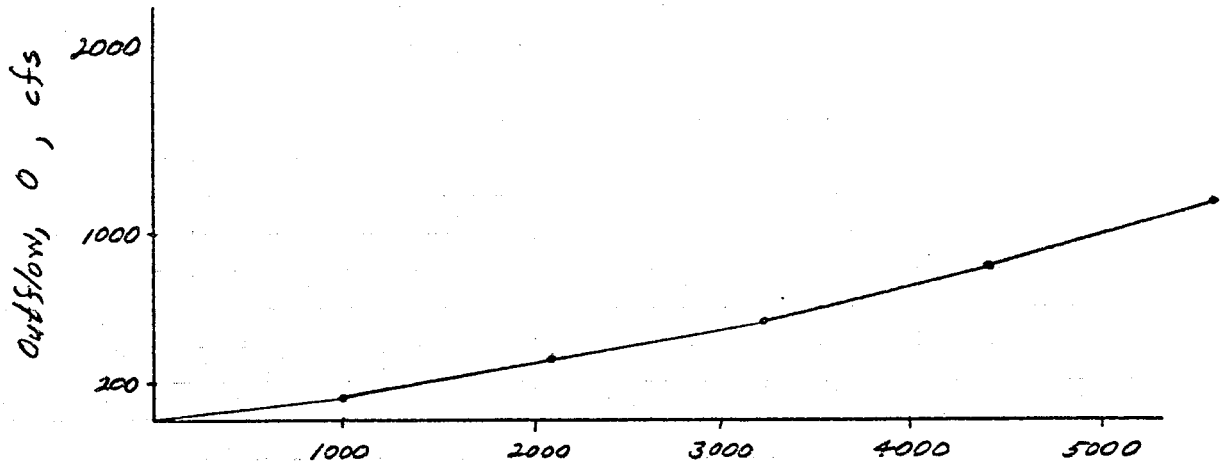

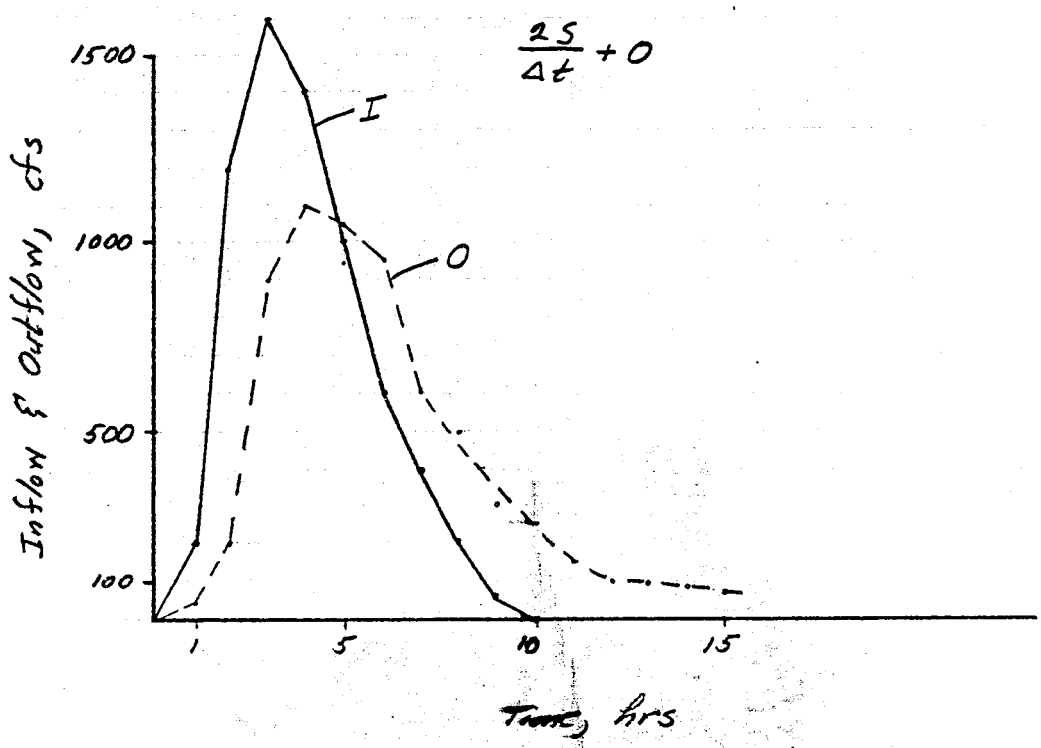

i (1)	I_i (2)	$\frac{S_i}{\Delta t}$ (3)	$\frac{\Sigma S_i}{\Delta t}$ (4)	$\frac{2\Sigma S_i}{\Delta t} - O_i$ (5)	$\frac{2\Sigma S_{i+1}}{\Delta t} + O_{i+1}$ (6)	O_i (7)	ΣI (8)	ΣO (9)	$\Sigma \frac{S}{\Delta t}$ (10)
0	0	0	0	0	0+200	0	0	0	0
1	200	160	160	280	1680	40	200	40	160
2	1200	1000	1160	2120	4920	200	1400	240	1160
3	1600	700	1860	2820	5820	900	3000	1140	1860
4	1400	300	2160	3220	5620	1100	4400	2240	2160
5	1000	−50	2110	3170	4770	1050	5400	3290	2110
6	600	−350	1760	2570	3570	950	6000	4240	1760
7	400	−200	1560	2520	3120	600	6400	4840	1560
8	200	−300	1260	2020	2270	500	6600	5340	1260
9	50	−250	1010	1720	1770	300	6650	5640	1010
10	0	−250	760	1270	1270	250		5890	760
11	0	−150	610	1070	1070	150		6040	610
12	0	−100	510	920	920	100		6140	510
13	0	−100	410	720	720	100		6240	410
14	0	−90	320	530	530	90		6330	320
15	0					60		6390	260

Flood Routing – Part 1

Two types of "routing" (moving water waves from one point to another) are commonly used:

1) Hydrologic routing using continuity only

2) Hydraulic routing using continuity <u>and</u> dynamic wave equations

These two ideas are analogous to an electrical system with capacitance and resistance

- Capacitance <u>stores</u> energy to be slowly released.
- Resistance retards the flow of energy and thereby changes the output.

Capacitance is responsible for the storage routing approach incorporated in hydrologic routing.

Hydrologic routing –

$$I - O = \frac{\Delta S}{\Delta t}$$

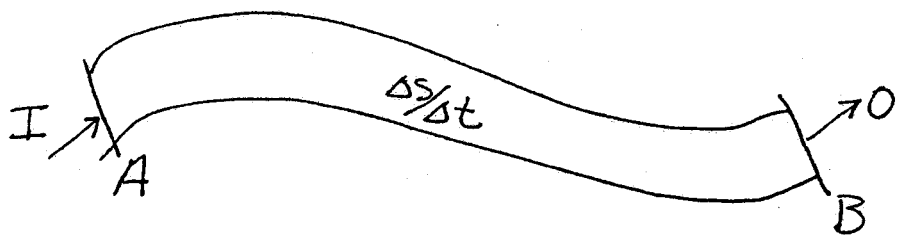

Input at A is modified to give output at B

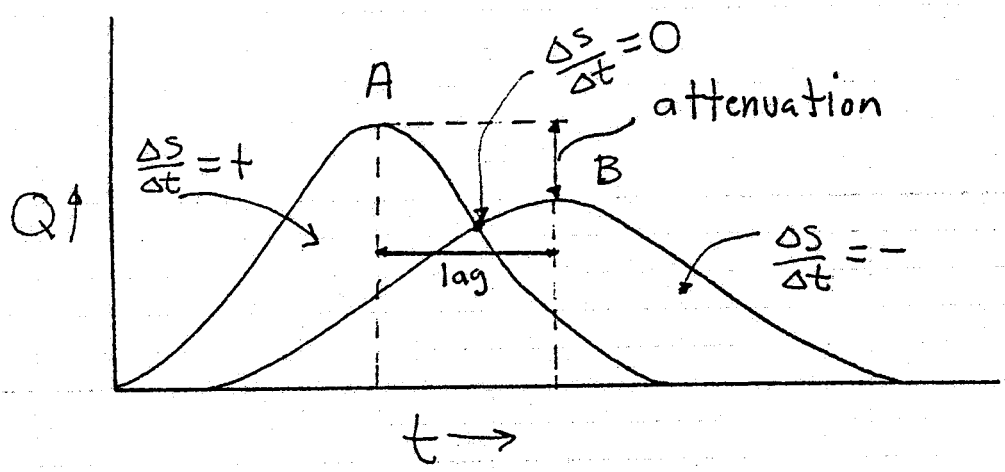

- lag = f_1(Channel geometry)
- attenuation = f_2 (Storage, resistance)
- Storage is important factor in hydrologic routing

SOCIETY OF CIVIL ENGINEERS FOUNDED 1852

For the Muskingum approach

Best when $S_o >> $ acceleration and other terms

$$I = Q_{in} = a_1 y_1^{n_1} \qquad O = Q_{out} = a_2 y^{n_2}$$

$$\text{Storage} = S_I = b_1 y_1^{m_1} \qquad S_o = b_2 y_2^{m_2}$$

For channels of similar cross section

$$a_1 \approx a_2 \quad b_1 \approx b_2 \quad n_1 \approx n_2 \quad m_1 \approx m_2$$

If we say

$$S = X S_I + (1-X) S_o$$

and substituting the above equations gives

$$S = K [X I^z + (1-X) O^z]$$

where $K = \dfrac{b}{a^z}$ $\quad z = m/n$

For wide prismatic channels $n = 5/3$; $m = 1$; $z \Rightarrow 0.6$

z is commonly assumed to be 1.0 yielding

$$S = K [X I - (1-X) O]$$

or $S = K [O + X (I - O)]$

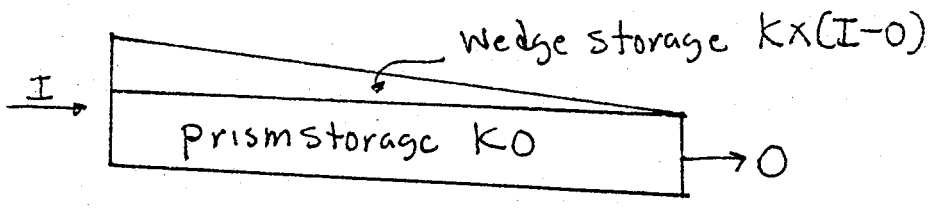

Earlier we say

$$\frac{I_2+I_1}{2} - \frac{O_2+O_1}{2} = \frac{S_2-S_1}{\Delta t}$$

substitution gives

$$O_2 = C_0 I_2 + C_1 I_1 + C_2 O_1$$

Where

$$C_0 = \frac{\frac{\Delta t}{K} - 2X}{\frac{\Delta t}{K} + 2(1-X)}$$

$$C_1 = \frac{\frac{\Delta t}{K} + 2X}{\frac{\Delta t}{K} + 2(1-X)}$$

$$C_2 = \frac{2(1-X) - \frac{\Delta t}{K}}{\frac{\Delta t}{K} + 2(1-X)}$$

$$C_0 + C_1 + C_2 \doteq 1.0$$

How to get K and X –

K = travel time in reach

X = weighting factor

$$\frac{K}{3} \le \Delta t \le K \quad \text{(typically)}$$

$$X \rightarrow 0 - 0.3 \quad \text{try } X = 0.2$$

1) From a inflow-outflow hydrograph pair compute:

$$\bar{I} = \frac{I_{i+1} + I_i}{2}$$

$$\bar{O} = \frac{O_{i+1} + O_i}{2}$$

$$S_{i+1} = \Delta t\,(\bar{I} - \bar{O}) + S_i$$

$$S_1 = 0 \text{ (arbitrary)}$$

2) Compute $Z_{i+1} = X I_{i+1} + (1-X) O_{i+1}$ for various X (.1 – .9)

3) Plot

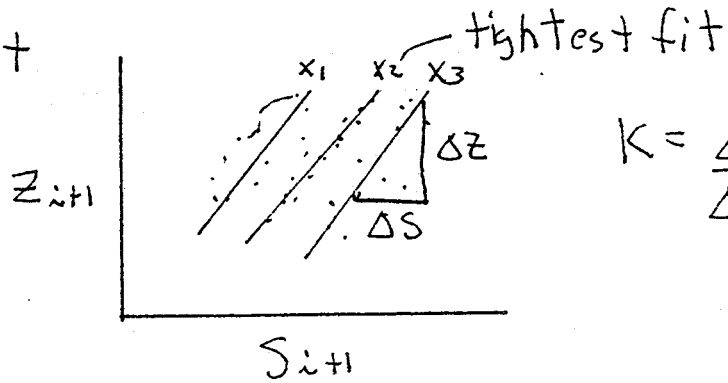

$$K = \frac{\Delta S}{\Delta Z}$$ for best X value

Muskingum-Cunge with Variable Parameters

K and x vary with discharge and channel geometry

In this case

$$K = \frac{\Delta x}{c}$$

$$x = \frac{1}{2}\left(1 - \frac{q}{S_o c \Delta x}\right)$$

where Δx = length of the reach
c = wave celerity
q = unit width discharge
S_o = channel bed slope in the reach

Now

$$c = \left.\frac{dQ}{dA}\right|_{j,n}$$

$$q = \left.\frac{Q}{B}\right|_{j,n}$$

where j = a space point
n = a time point

Values of c and q can be averaged for O_1, I_1, I_2 and then used to guess those for O_2 to be used in further iterations

The results are more physically meaningful as they indicate more of the controlling processes. (Refer to Ward, 1982 handout)

Summary -

1) Hydrologic routing is storage routing

2) The Muskingum method, and its variants, is the keystone of this technique.

Flood Routing - Part 2

Previously examined solutions for gravity waves where $S_o = S_f = 0$.

When this is not realistic, resistance then enters the picture in

$$v + 2c = \int (S_o - S_f)\,dt + v_o + 2c_o$$

$$v - 2c = \int (S_o - S_f)\,dt + v_o - 2c_o$$

This makes the characteristics curve

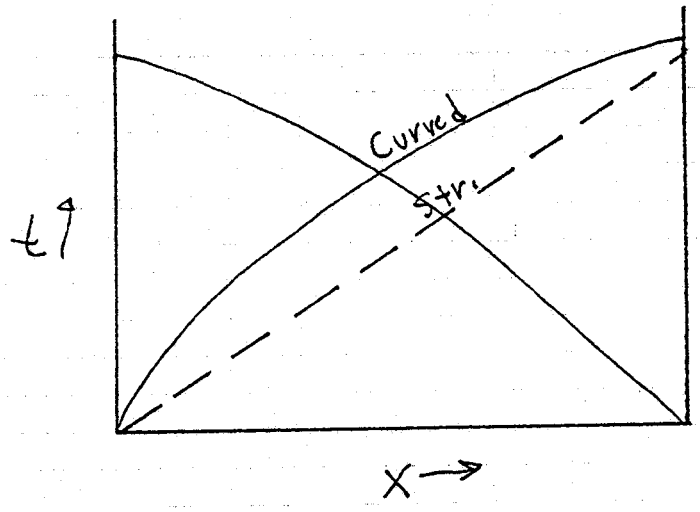

How do we now solve the differential equations?

Four approaches

1) Characteristic equations in explicit or implicit form using a finite difference approach on a curvilinear system

2) Characteristic equations as above but with a fixed grid system

3) Original equations, implicit finite difference scheme, fixed rectangular grid

4) Original equations as above but with an explicit scheme

Also finite element and finite boundary methods are available.

The <u>implicit</u> method is most widely used, and is the most stable.

Terms

Stability – Solution grows unbounded with time

Consistency – numerical scheme approximates the PDE

Convergence – numerical scheme reproduces the PDE terms so not to impair its accuracy.

Finite Difference Approach

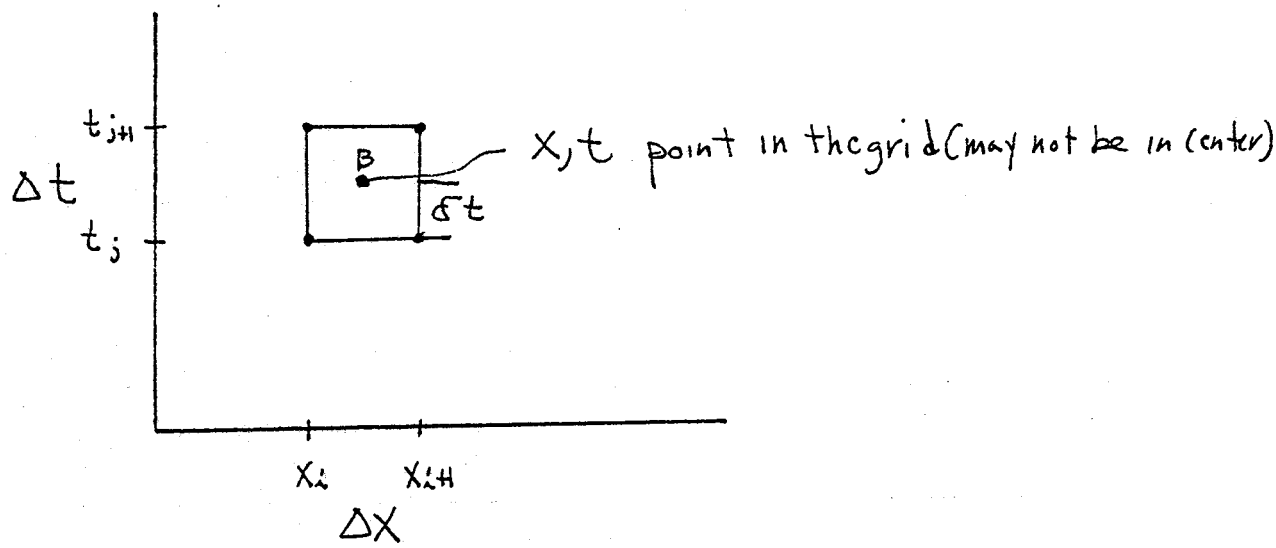

$$f_B(x,t) \cong \lambda \left(\frac{f_i^{j+1} + f_{i+1}^{j+1}}{2} \right) + (1-\lambda) \left(\frac{f_i^{j} + f_{i+1}^{j}}{2} \right)$$

$$\frac{\partial f}{\partial x} \cong \lambda \left(\frac{f_{i+1}^{j+1} - f_i^{j+1}}{\Delta x} \right) + (1-\lambda) \left(\frac{f_{i+1}^{j} - f_i^{j}}{\Delta x} \right)$$

$$\frac{\partial f}{\partial t} \cong \frac{1}{2} \left(\frac{f_i^{j+1} - f_i^{j}}{\Delta t} + \frac{f_{i+1}^{j+1} - f_{i+1}^{j}}{\Delta t} \right)$$

where $f_i^j = f_B(x_i, t_j)$; $f_{i+1}^{j+1} = f_B(x_{i+1}, t_{j+1})$ etc

(f_B is like u, v)

λ is a weighting factor $= \dfrac{\delta t}{\Delta t}$

$\lambda = 1/2$ Center implicit

$\lambda = 1$ fully implicit

$\lambda = 0$ fully explicit

A double sweep approach is often used to go forward from the upstream boundary setting up the equations in a matrix. When the down stream boundary condition (such as a stage-discharge relationship) is encountered then the coefficient matrix is solved and the intervening point values are uniquely determined.

<u>The method is stable for</u>

$0.5 < \lambda \leq 1.0$ (small damping)

weakly stable for

$\lambda = 0.5$ (typical case)

<u>Courant number defines convergence</u>

$$C = c \frac{\Delta t}{\Delta x}$$

$$c = \frac{L}{T}$$

L = Wave length

T = Wave period

$$\underset{\text{errors}}{10} \leq \frac{T}{\Delta t} \leq \underset{\text{inefficient}}{100}$$

For explicit schemes we need

$$\frac{\Delta t}{\Delta x} \leq \frac{1}{|V_0 + C_0|}$$

try to get $\frac{\Delta t}{\Delta x} < 1$ for stability reasons

Comparison of wave models –
(Ponce and Simons, 1977; J. of Hyd. Div. ASCE Vol 103 No HY 12, pp 1461–1476)

<u>Kinematic Wave</u> – 1) Celerity = $3/2\ V_0$ (= mean flow velocity)
($S_f = S_0$) 2) propagates downstream without dissipation

<u>Diffusion Wave</u> – 1) Celerity = $3/2\ V_0$
($S_f = S_0 - \frac{\partial y}{\partial x}$) 2) propagates downstream with dissipation

<u>Steady dynamic wave</u> – 1) Celerity = f(F_0, other terms)
$S_f = S_0 - \frac{\partial y}{\partial x} - \frac{1}{g}\frac{\partial V}{\partial x}$ 2) propagates downstream with dissipation

<u>Dynamic Wave</u> – 1) Celerity is complex
$S_f = S_0 - \frac{\partial y}{\partial x} - \frac{1}{g}\frac{\partial V}{\partial x} - \frac{1}{g}\frac{\partial V}{\partial t}$ 2) propagate <u>both</u> directions with dissipation

<u>Gravity Waves</u> – 1) Celerity = $V_0 \pm C_0$
$\frac{\partial y}{\partial x} + \frac{1}{g}\frac{\partial V}{\partial x} + \frac{1}{g}\frac{\partial V}{\partial t} = 0$ 2) propagate upstream and downstream without dissipation

Which wave is the best?

Kinematic waves are in vogue because they can be used for a wide variety of problems and they are easier to solve. Ponce et al (1978, J. of Hyd. Div., ASCE, Vol 104, No HY3, pp 353-360) present methods by which to choose.

When in doubt, and if practical, use the full dynamic wave. Most of the time, the kinematic will work.

Summary -

1) When friction and bed slope are no longer small, a more complex routing situation exists.

2) The implicit finite-difference method for solving the PDE's is most often used.

3) Certain space and time constraints determine the performance of a method.

4) The different waves perform differently and should be examined to see which is most applicable.

TABLE B-2.—*Velocity head and discharge at critical depths and static pressures in circular conduits partly full*

D = Diameter of pipe.
d = Depth of flow.
h_{v_c} = Velocity head for a critical depth of d.
Q_c = Discharge when the critical depth is d.
P = Pressure on cross section of water prism in cubic units of water. To get P in pounds, when d and D are in feet, multiply by 62.5.

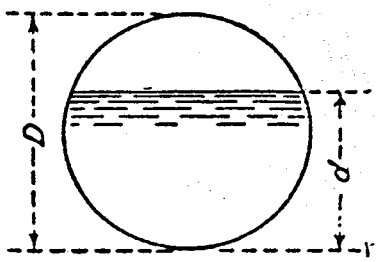

$\frac{d}{D}$	$\frac{h_{v_c}}{D}$	$\frac{Q_c}{D^{5/2}}$	$\frac{P}{D^3}$	$\frac{d}{D}$	$\frac{h_{v_c}}{D}$	$\frac{Q_c}{D^{5/2}}$	$\frac{P}{D^3}$	$\frac{d}{D}$	$\frac{h_{v_c}}{D}$	$\frac{Q_c}{D^{5/2}}$	$\frac{P}{D^3}$
1	2	3	4	1	2	3	4	1	2	3	4
0.01	0.0033	0.0006	0.0000	0.34	0.1243	0.6657	0.0332	0.67	0.2974	2.4464	0.1644
.02	.0067	.0025	.0000	.35	.1284	.7040	.0356	.68	.3048	2.5182	.1700
.03	.0101	.0055	.0001	.36	.1326	.7433	.0381	.69	.3125	2.5912	.1758
.04	.0134	.0098	.0002	.37	.1368	.7836	.0407	.70	.3204	2.6656	.1816
.05	.0168	.0153	.0003	.38	.1411	.8249	.0434	.71	.3286	2.7414	.1875
.06	.0203	.0220	.0005	.39	.1454	.8671	.0462	.72	.3371	2.8188	.1935
.07	.0237	.0298	.0007	.40	.1497	.9103	.0491	.73	.3459	2.8977	.1996
.08	.0271	.0389	.0010	.41	.1541	.9545	.0520	.74	.3552	2.9783	.2058
.09	.0306	.0491	.0013	.42	.1586	.9996	.0551	.75	.3648	3.0607	.2121
.10	.0341	.0605	.0017	.43	.1631	1.0458	.0583	.76	.3749	3.1450	.2185
.11	.0376	.0731	.0021	.44	.1676	1.0929	.0616	.77	.3855	3.2314	.2249
.12	.0411	.0868	.0026	.45	.1723	1.1410	.0650	.78	.3967	3.3200	.2314
.13	.0446	.1016	.0032	.46	.1769	1.1899	.0684	.79	.4085	3.4112	.2380
.14	.0482	.1176	.0038	.47	.1817	1.2399	.0720	.80	.4210	3.5050	.2447
.15	.0517	.1347	.0045	.48	.1865	1.2908	.0757	.81	.4343	3.6019	.2515
.16	.0553	.1530	.0053	.49	.1914	1.3427	.0795	.82	.4485	3.7021	.2584
.17	.0589	.1724	.0061	.50	.1964	1.3955	.0833	.83	.4638	3.8061	.2653
.18	.0626	.1928	.0070	.51	.2014	1.4493	.0873	.84	.4803	3.9144	.2723
.19	.0662	.2144	.0080	.52	.2065	1.5041	.0914	.85	.4982	4.0276	.2794
.20	.0699	.2371	.0091	.53	.2117	1.5598	.0956	.86	.5177	4.1465	.2865
.21	.0736	.2609	.0103	.54	.2170	1.6164	.0998	.87	.5392	4.2721	.2938
.22	.0773	.2857	.0115	.55	.2224	1.6735	.1042	.88	.5632	4.4056	.3011
.23	.0811	.3116	.0128	.56	.2279	1.7327	.1087	.89	.5900	4.5486	.3084
.24	.0848	.3386	.0143	.57	.2335	1.7923	.1133	.90	.6204	4.7033	.3158
.25	.0887	.3667	.0157	.58	.2393	1.8530	.1179	.91	.6555	4.8725	.3233
.26	.0925	.3957	.0173	.59	.2451	1.9146	.1227	.92	.6966	5.0603	.3308
.27	.0963	.4259	.0190	.60	.2511	1.9773	.1276	.93	.7459	5.2726	.3384
.28	.1002	.4571	.0207	.61	.2572	2.0409	.1326	.94	.8065	5.5183	.3460
.29	.1042	.4893	.0226	.62	.2635	2.1057	.1376	.95	.8841	5.8118	.3537
.30	.1081	.5225	.0255	.63	.2699	2.1716	.1428	.96	.9885	6.1787	.3615
.31	.1121	.5568	.0266	.64	.2765	2.2386	.1481	.97	1.1410	6.6692	.3692
.32	.1161	.5921	.0287	.65	.2833	2.3067	.1534	.98	1.3958	7.4063	.3770
.33	.1202	.6284	.0309	.66	.2902	2.3760	.1589	.99	1.9700	8.8263	.3848
								1.00	------	------	.3927

Tables B-3 and B-5 give areas and hydraulic radii for partially full conduits and coefficients which can be applied in the solution of the Manning equation. If $A = k_6 \frac{\pi D^2}{4}$ and $r = k_7 D$, Manning's equation can be written:

$$Q' = \frac{1.486}{n}\left(k_6 \frac{\pi D^2}{4}\right)(k_7 D)^{2/3} s^{1/2},$$

or

$$\frac{Qn}{D^{8/3} s^{1/2}} = k_6 \frac{1.486\pi}{4}(k_7)^{2/3} = k, \qquad (39)$$

TABLE B-3.—*Uniform flow in circular sections flowing partly full*

d = Depth of flow.
D = Diameter of pipe.
A = Area of flow.
r = Hydraulic radius.
Q = Discharge in second-feet by Manning's formula.
n = Manning's coefficient.
s = Slope of the channel bottom and of the water surface.

$\frac{d}{D}$	$\frac{A}{D^2}$	$\frac{r}{D}$	$\frac{Qn}{D^{8/3}s^{1/2}}$	$\frac{Qn}{d^{8/3}s^{1/2}}$	$\frac{d}{D}$	$\frac{A}{D^2}$	$\frac{r}{D}$	$\frac{Qn}{D^{8/3}s^{1/2}}$	$\frac{Qn}{d^{8/3}s^{1/2}}$
1	2	3	4	5	1	2	3	4	5
0.01	0.0013	0.0066	0.00007	15.04	0.51	0.4027	0.2531	0.239	1.442
.02	.0037	.0132	.00031	10.57	.52	.4127	.2562	.247	1.415
.03	.0069	.0197	.00074	8.56	.53	.4227	.2592	.255	1.388
.04	.0105	.0262	.00138	7.38	.54	.4327	.2621	.263	1.362
.05	.0147	0325	.00222	6.55	.55	.4426	.2649	.271	1.336
.06	.0192	.0389	.00328	5.95	.56	.4526	.2676	.279	1.311
.07	.0242	.0451	.00455	5.47	.57	.4625	.2703	.287	1.286
.08	.0294	.0513	.00604	5.09	.58	.4724	.2728	.295	1.262
.09	.0350	.0575	.00775	4.76	.59	.4822	.2753	.303	1.238
.10	.0409	.0635	.00967	4.49	.60	.4920	.2776	.311	1.215
.11	.0470	.0695	.01181	4.25	.61	.5018	.2799	.319	1.192
.12	.0534	.0755	.01417	4.04	.62	.5115	.2821	.327	1.170
.13	.0600	.0813	.01674	3.86	.63	.5212	.2842	.335	1.148
.14	.0668	.0871	.01952	3.69	.64	.5308	.2862	.343	1.126
.15	.0739	.0929	.0225	3.54	.65	.5404	.2882	.350	1.105
.16	.0811	.0985	.0257	3.41	.66	.5499	.2900	.358	1.084
.17	.0885	.1042	.0291	3.28	.67	.5594	.2917	.366	1.064
.18	.0961	.1097	.0327	3.17	.68	.5687	.2933	.373	1.044
.19	.1039	.1152	.0365	3.06	.69	.5780	.2948	.380	1.024
.20	.1118	.1206	.0406	2.96	.70	.5872	.2962	.388	1.004
.21	.1199	.1259	.0448	2.87	.71	.5964	.2975	.395	0.985
.22	.1281	.1312	.0492	2.79	.72	.6054	.2987	.402	.965
.23	.1365	.1364	.0537	2.71	.73	.6143	.2998	.409	.947
.24	.1449	.1416	.0585	2.63	.74	.6231	.3008	.416	.928
.25	.1535	.1466	.0634	2.56	.75	.6319	.3017	.422	.910
.26	.1623	.1516	.0686	2.49	.76	.6405	.3024	.429	.891
.27	.1711	.1566	.0739	2.42	.77	.6489	.3031	435	.873
.28	.1800	.1614	.0793	2.36	.78	.6573	.3036	.441	.856
.29	.1890	.1662	.0849	2.30	.79	.6655	.3039	.447	.838
.30	.1982	.1709	.0907	2.25	.80	.6736	.3042	.453	.821
.31	.2074	.1756	.0966	2.20	.81	.6815	.3043	.458	.804
.32	.2167	.1802	.1027	2.14	.82	.6893	.3043	.463	.787
.33	.2260	.1847	.1089	2.09	.83	.6969	.3041	.468	.770
.34	.2355	.1891	.1153	2.05	.84	.7043	.3038	.473	.753
.35	.2450	.1935	.1218	2.00	.85	.7115	.3033	.477	.736
.36	.2546	.1978	.1284	1.958	.86	.7186	.3026	.481	.720
.37	.2642	.2020	.1351	1.915	.87	.7254	.3018	.485	.703
.38	.2739	.2062	.1420	1.875	.88	.7320	.3007	.488	.687
.39	.2836	.2102	.1490	1.835	.89	.7384	.2995	.491	.670
.40	.2934	.2142	.1561	1.797	.90	.7445	.2980	.494	.654
.41	.3032	.2182	.1633	1.760	.91	.7504	.2963	.496	.637
.42	.3130	.2220	.1705	1.724	.92	.7560	.2944	.497	.621
.43	.3229	.2258	.1779	1.689	.93	.7612	.2921	.498	.604
.44	.3328	.2295	.1854	1.655	.94	.7662	.2895	.498	.588
.45	.3428	.2331	.1929	1.622	.95	.7707	.2865	.498	.571
.46	.3527	.2366	.201	1.590	.96	.7749	.2829	.496	.553
.47	.3627	.2401	.208	1.559	.97	.7785	.2787	.494	.535
.48	.3727	.2435	.216	1.530	.98	.7817	.2735	.489	.517
.49	.3827	.2468	.224	1.500	.909	.7841	.2666	.483	.496
.50	.3927	.2500	.232	1.471	1.00	.7854	.2500	.463	.463

B. FLOW IN NATURAL CHANNELS

B-5. General.—This portion of the appendix presents briefly the hydraulic theory and analyses of natural stream channel flow as related to the design of small dams. These analyses are all directed toward the goal of establishing rating curves (stage-discharge relation) at some desired location within the stream channel. One of the more important uses of the rating curve is in connection with establishing tailwater conditions in the design of stilling basins.

The hydraulic conditions discussed herein involve only the conditions of steady and nonuniform flow. A steady flow condition is said to prevail when the discharge is the same at all sections along the channel and remains constant with respect to time. The flow is defined as nonuniform when the grade of the water surface is different from that of the channel bottom, which implies accelerating or decelerating flow. Both conditions generally prevail in natural channels. The flows may be confined to the main channel portion of the stream, but generally overbank or flood plain discharge will occur at design discharges.

Suggested procedures are given for the collection of an adequate set of field data to define each of the components in Manning's formula or Bernoulli's theorem which are used in the hydraulic computations. The accuracy of the results is very much dependent on gathering the field data representative of the prevailing hydraulic conditions and analyzing them through reasonable assumptions and interpretations. An accuracy of 0.5 foot is ordinarily a reasonable limit for the computation of water surfaces for low flows. The degree of accuracy expected for higher discharges involving overbank flow is about 1.0 foot. The loss in accuracy for overbank flow conditions is due to more difficult definition of overbank n values and flow distances between sections.

B-6. Collection of Data.—(a) *Streamflow Records.*—Records of streamflow taken from established U.S. Geological Survey (USGS) gaging stations furnish valuable information for the required hydraulic analysis. A check of the USGS water supply papers and the water resources data published annually for each State will show the available streamflow data for each station. Detailed descriptions of gaging stations can be studied in Water Supply Paper 888 [10].

Damsites are occasionally located near gaging stations. The rating curve of a station can be transposed to a cross section at or near the damsite if the hydraulic conditions of the reach between the damsite and the station are relatively uniform. A reasonable distance between the damsite and the gaging station for transposing the curve probably should not exceed 1,000 feet. Extreme changes in grade of the streambed, cross-sectional dimensions, and n values destroy the uniformity of the channel reach and consequently reduce the accuracy of the transposed rating curve.

(b) *Topographic Maps and Aerial Photographs.*—A topographic map and aerial photographs, if available, also provide useful information for rating curve development or water surface profile computation. For rough studies, the hydraulic properties of the stream at the damsite can be determined for a cross section as plotted from the topographic map. An example is included in section B-8 showing how this is done. The topographic map is also useful in studies involving water surface profile computations, where it can be used to locate a series of cross sections below the damsite. Flow distances between such cross sections can be measured from the map.

Aerial photographs can be used to assist in selecting the location of the cross sections. Further, the n coefficients can be evaluated by observing the areal coverage of vegetation and the meandering pattern of the stream.

(c) *Field Surveys.*—The field work required to define the hydraulic dimensions of a single cross section is relatively simple and generally inexpensive. Essentially, the procedure involves setting up a level or transit in direct line with the cross section and taking intermittent soundings and distance measurements across the section. Concurrently, levels can be run along the stream thalweg (lowest points in the streambed) or water surface (intermittent

shots may be taken at water's edge along both banks) to define a slope for use in Manning's formula; a distance of 200 to 300 feet downstream and upstream from the cross section will usually be sufficient. Elevations to the nearest tenth of a foot are satisfactory for cross-sectional data; however, it may be necessary to establish water surface elevations to the nearest hundredth of a foot on streams having relatively flat gradients. Horizontal distances measured to the nearest foot are usually adequate for the other cross-sectional coordinate.

If water surface profiles are to be computed for a more precise determination of a rating curve, a series of cross sections downstream from the dam will be needed. The sections should be spaced so that there will be a drop of no more than 2 feet in water surface between cross sections and a total drop of 8 to 10 feet in the study reach.

High water marks may be used to define the water surface slope. Field observations of these marks should be made immediately following the occurrence of any flows of sufficient magnitude to leave discernible high water marks. An example of their use in a slope-area computation is shown in the next section.

(d) *Determination of n Values.*—The selection of n values for use in the Manning formula requires considerable judgment. Table B-6 gives values of n for average channels of various conditions. Table B-7 presents a procedure for computing a mean n value by systematically considering the factors which are involved.

The following publications will serve as guides in the proper selection of n values:

1. "Hydraulic and Excavation Tables," Bureau of Reclamation, eleventh edition, 1957, U.S. Government Printing Office, Washington, D.C.
2. "Handbook of Hydraulics," King, H. W. and Brater, E. F., fifth edition, 1963, McGraw-Hill, New York, N.Y.
3. "Hydrologic and Hydraulic Analyses, Computation of Backwater Curves in River Channels," Part CXIV, Ch. 9, Engineering Manual, Civil Works Construction, May 1952, Department of the Army, Corps of Engineers, Office of the Chief of Engineers.
4. "Flow of Water in Drainage Channels," Ramser, C. E., Technical Bulletin No. 129, November 1929, U.S. Department of Agriculture, Washington, D.C.
5. "Flow of Water in Irrigation and Similar Canals," Scobey, F. C., Bureau of Agricultural Engineering, U.S. Department of Agriculture, Washington, D.C., February 1939.
6. "Design Criteria for Interrelated Highway and Agricultural Drainage and Erosion Control," Tentative ASAE Recommendation, Agricultural Engineers Yearbook, 1958, American Society of Agricultural Engineers.
7. "Roughness Characteristics of Natural Channels," Water Supply Paper 1849, U.S. Department of the Interior, Geological Survey, 1967.

B-7. *Slope-Area Method of Computing Streamflow.*—The slope-area method is utilized primarily to determine the discharge of a stream from specific field data. However, if the discharge is known, the method can be used to compute the value of n. Field procedures required to obtain needed data for the slope-area method include:

1. Selecting a representative reach of river channel: (a) The length of the reach should be at least 75 times the mean depth in the channel.
   (b) The fall in the reach should be equal to or greater than the velocity head or at least 0.50 foot.
2. Defining channel cross sections:
   (a) A minimum of three cross sections is recommended.
3. Measuring the water surface slopes from observed high water marks:
   (a) Average the elevations on both banks at each cross section.
4. Selecting a suitable roughness factor, n.

With these data, the discharge can be determined by Manning's formula,

$$Q = \frac{1.486}{n} a r^{2/3} s^{1/2} \qquad (53)$$

where:

Q=total discharge in cubic feet per second,
n=a roughness coefficient,
a=the cross-sectional area of the channel in square feet,
r=hydraulic radius in feet, and
s=energy gradient.

This procedure involves combining such factors as the area, hydraulic radius, and n to compute the conveyance capacity, K_d, for each section, defined by the equation:

$$K_d=\frac{1.486}{n}\,ar^{2/3} \tag{54}$$

From equations (53) and (54), it can be seen that

$$Q=K_d\,s^{1/2} \tag{55}$$

The Manning equation was developed for conditions of uniform flow, but it has been assumed that the equation is also valid for nonuniform reaches that are characteristic of natural channels, if the energy gradient is modified to reflect only the losses due to boundary friction. Figure B-17 is a definition sketch of a two-section slope-area reach, from which the energy equation can be written:

$$Z_2+d_2+h_{v_2}=Z_1+d_1+h_{v_1}+h_f+k(\Delta h_v) \tag{56}$$

where:

Z=channel bottom elevation,
d=depth of water,
h_v=velocity head $=\frac{\alpha V^2}{2g}$,
h_f=energy loss due to boundary friction,
Δh_v=upstream velocity head minus the downstream velocity head, and
$k(\Delta h_v)$=energy loss due to acceleration or deceleration in a contracting or expanding reach.

Adding $Z+d$ gives the water surface elevation, h, and equation (56) may be written:

$$h_2+h_{v_2}=h_1+h_{v_1}+h_f+k(\Delta h_v) \tag{57}$$

The friction slope may now be solved:

$$s=\frac{h_f}{L}=\frac{\Delta h+\Delta h_v-k(\Delta h_v)}{L} \tag{58}$$

where Δh is the difference in water surface elevation at the two sections and L is the length of the reach.

The reach discharge can now be computed

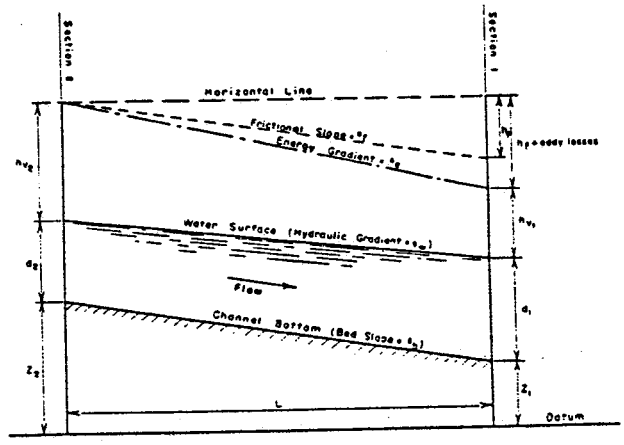

Figure B-17. Energy of open-channel flow. 288—D—2827.

using the friction slope and the geometric mean of the cross-section conveyances, or

$$Q=\sqrt{K_{d_1}\cdot K_{d_2}\cdot s} \tag{59}$$

The velocity head (h_v) at each section is computed as

$$h_v=\frac{\alpha V^2}{2g} \tag{60}$$

where V is the mean velocity in the section and α is the velocity-head coefficient. The value of α is assumed to be 1.0 if the section is not subdivided. The value of α in subdivided channels is computed as

$$\alpha=\frac{\Sigma(Kd_i/a_i^2)}{K_{d_T}{}^3/a_T{}^2} \tag{61}$$

where the subscript i refers to the conveyance or area of the individual subsections and T to the area or conveyance of the entire cross section.

The energy loss due to contraction or expansion of the channel in the reach is assumed to be equal to the difference in velocity heads at the two sections (Δh_v) times a coefficient, k. The value of k has been set at zero for contracting reaches and 0.5 for expanding reaches by the U.S. Geological Survey [12]. The value of Δh_v is computed as the upstream velocity head minus the downstream velocity head; therefore, the friction slope to be used in the

Manning equation is computed algebraically as

$$s=\frac{\Delta h+(\Delta h_v/2)}{L} \text{ (when } \Delta h_v \text{ is positive)} \quad (62)$$

and

$$s=\frac{\Delta h+\Delta h_v}{L} \quad \text{(when } \Delta h_v \text{ is negative)} \quad (63)$$

The U.S. Geological Survey publication [12] contains discharge equations for slope-area computations developed from the above basic equations. The general equation and the equation for a two-section reach are presented here.

Two sections:

$$Q=K_{d_1}\sqrt{\frac{\Delta h}{\frac{K_{d_1}}{K_{d_2}}L+\frac{K_{d_1}^2}{2gA_1^2}\left[-\alpha_2\left(\frac{A_1}{A_2}\right)^2(1-k)+\alpha_1(1-k)\right]}} \quad (64)$$

where:

Q=Total discharge in cubic feet per second, and

A=Total cross-sectional area in square feet.

Multiple sections (n=number of sections):

$$Q=K_{d_1}\sqrt{\frac{\Delta h}{X+Y}} \quad (65)$$

where:

$$X=K_{d_1}{}^2\frac{L_{[n-(n-1)]}}{K_{d_n}K_{d_{(n-1)}}}+K_1{}^2\frac{L_{[(n-1)-(n-2)]}}{K_{d_{(n-1)}}K_{d_{(n-2)}}}+\cdots$$

$$\frac{K_{d_1}{}^2L_{3-2}}{K_{d_3}K_{d_2}}+\frac{K_{d_1}{}^2L_{2-1}}{K_{d_2}K_{d_1}}, \text{ and}$$

$$Y=\frac{K_{d_1}{}^2}{A_1{}^2 2g}\left[-\alpha_n\left(\frac{A_1}{A_n}\right)^2(1-k_{n-(n-1)})+\right.$$

$$\alpha_{n-1}\left(\frac{A_1}{A_{n-1}}\right)^2(k_{(n-1)-(n-2)}-k_{n-(n-1)})+$$

$$\alpha_{(n-2)}\left(\frac{A_1}{A_{n-2}}\right)^2(k_{(n-2)-(n-3)}-k_{(n-1)-(n-2)})+\cdots+$$

$$\left.\alpha_2\left(\frac{A_1}{A_2}\right)^2(k_{2-1}-k_{3-2})+\alpha_1(1-k_{2-1})\right].$$

Using the data from the USGS publication [12] (see figures B-18, B-19, and B-20), the following procedure is used to compute the discharge. The conveyance (K_d), the velocity head coefficient for each cross section (α), and the weighted conveyance (K_w) of each subreach are computed and tabulated on the form shown in figure B-21. It should be noted that the subscripting is in reverse order of that used in the definition sketch and discharge formulas. Next, use the two-section formula given above to compute directly the discharge for each two-section subreach. The computed values will most likely differ for each subreach. Then, using the appropriate discharge as the "assumed" value on the form, complete for each subreach the computation of the various heads, slope, and "computed" discharge. The "computed" discharge must agree exactly with the "assumed" if all computations have been made correctly.

Using the multiple section equation, the final value of discharge can then be computed for the total reach. After this value is determined, it is used to compute the subsection discharges for subdivided sections, the corresponding velocities, and the mean velocities for all sections. Enter the computations in the two columns at the right of the computation form (fig. B-21). Gross errors can be often recognized if velocities are greatly different from those anticipated based on inspection of the channel after the flood.

A check should be made for critical or supercritical flow conditions at each section. This matter will be discussed in further detail in section **B-9**.

If the discharge is known, an analysis similar to the above can be used to arrive at the appropriate n value to assign to the channel sections. A trial and error solution will be necessary.

B-8. *Development of Rating Curves.*—(a) *Approximate Method.*—The field data required for development of a rating curve are similar to those used in a slope-area analysis. A determination must be made of the hydraulic properties for the section under consideration. Data required include channel cross-section geometry, channel bottom or water surface

TABLE B-6.—*Coefficient of roughness, average channels*

Value of n	*Channel condition*
0.016–0.017	Smoothest natural earth channels, free from growth, with straight alinement.
0.020	Smooth natural earth channels, free from growth, little curvature.
0.0225	Average, well-constructed, moderate-sized earth channels in good condition.
0.025	Small earth channels in good condition, or large earth channels with some growth on banks or scattered cobbles in bed.
0.030	Earth channels with considerable growth. Natural streams with good alinement, fairly constant section. Large floodway channels, well maintained.
0.035	Earth channels considerably covered with small growth. Cleared but not continuously maintained floodways.
0.040–0.050	Mountain streams in clean loose cobbles. Rivers with variable section and some vegetation growing in banks. Earth channels with thick aquatic growths.
0.060–0.075	Rivers with fairly straight alinement and cross section, badly obstructed by small trees, very little underbrush or aquatic growth.
0.100	Rivers with irregular alinement and cross section, moderately obstructed by small trees and underbrush. Rivers with fairly regular alinement and cross section, heavily obstructed by small trees and underbrush.
0.125	Rivers with irregular alinement and cross section, covered with growth of virgin timber and occasional dense patches of bushes and small trees, some logs and dead fallen trees.
0.150–0.200	Rivers with very irregular alinement and cross section, many roots, trees, bushes, large logs, and other drift on bottom, trees continually falling into channel due to bank caving.

TABLE B-7.—*A method of computing mean n value for a channel*

(Used by U.S. Soil Conservation Service)

Steps

1. Assume basic n
2. Select modifying n for roughness or degree of irregularity
3. Select modifying n for variation in size and shape of cross section
4. Select modifying n for obstructions such as debris deposits, stumps, exposed roots, and fallen logs
5. Select modifying n for vegetation
6. Select modifying n for meandering
7. Add items 1 through 6

Aids in Selecting Various n Values

1. Recommended basic n values

Channels in earth	0.010	Channels in fine gravel	0.014
Channels in rock	0.015	Channels in coarse gravel	0.028

2. Recommended modifying n value for degree of irregularity

Smooth	0.000	Moderate	0.010
Minor	0.005	Severe	0.020

3. Recommended modifying n value for changes in size and shape of cross section

Gradual	0.000	Frequent	0.010 to 0.015
Occasional	0.005		

4. Recommended modifying n value for obstructions such as debris, roots, etc.

Negligible effect	0.000	Appreciable effect	0.030
Minor effect	0.010	Severe effect	0.060

5. Recommended modifying n values for vegetation

Low effect	0.005 to 0.010	High effect	0.025 to 0.050
Medium effect	0.010 to 0.025	Very high effect	0.050 to 0.100

6. Recommended modifying n value for channel meander

L_s = Straight length of reach L_m = Meander length of reach

L_m/L_s	n
1.0–1.2	0.000
1.2–1.5	0.15 times n_s
>1.5	0.30 times n_s

where n_s = items 1+2+3+4+5

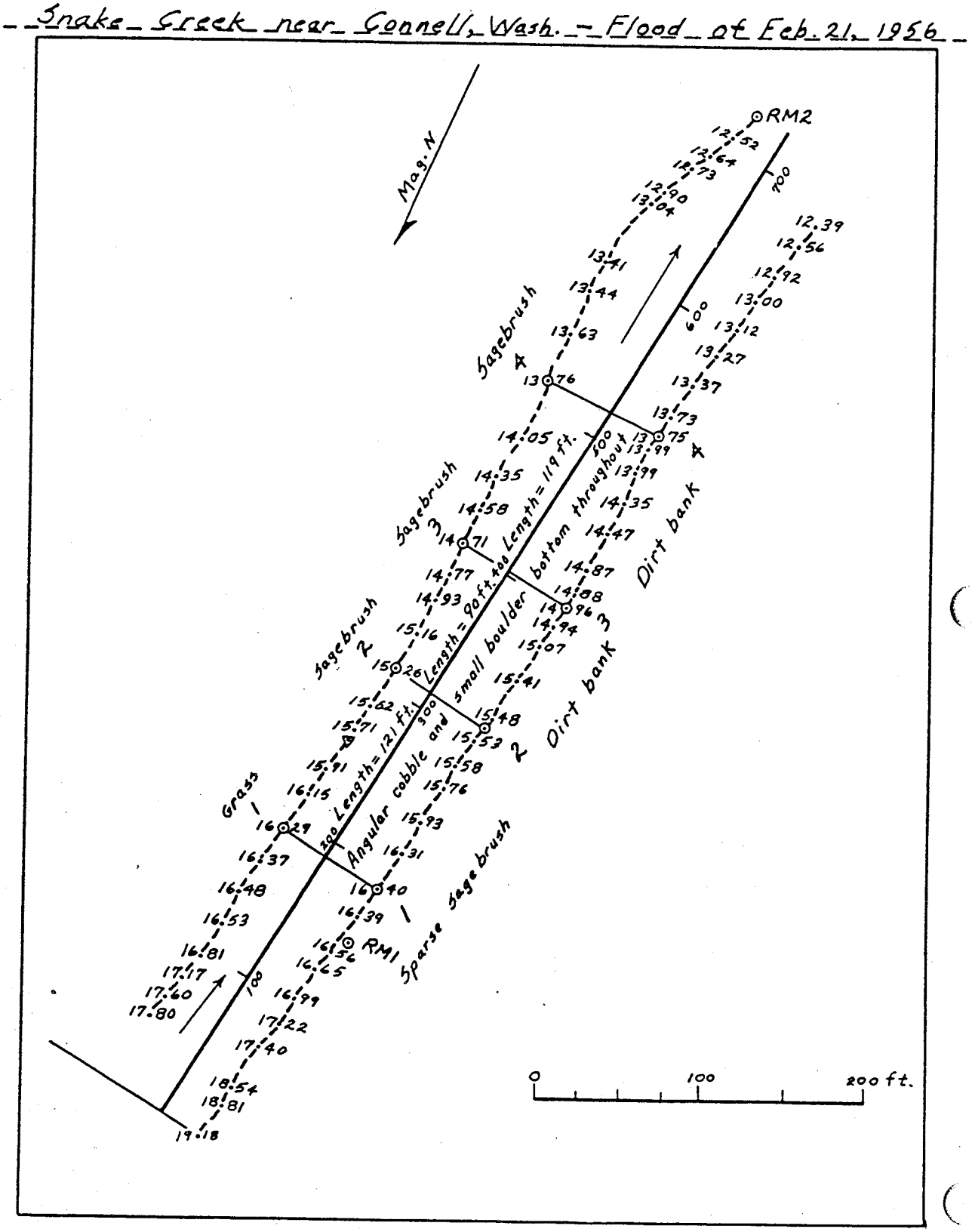

Figure 8–18. Sample slope-area computation, plan view of reach. 288–D–2828.

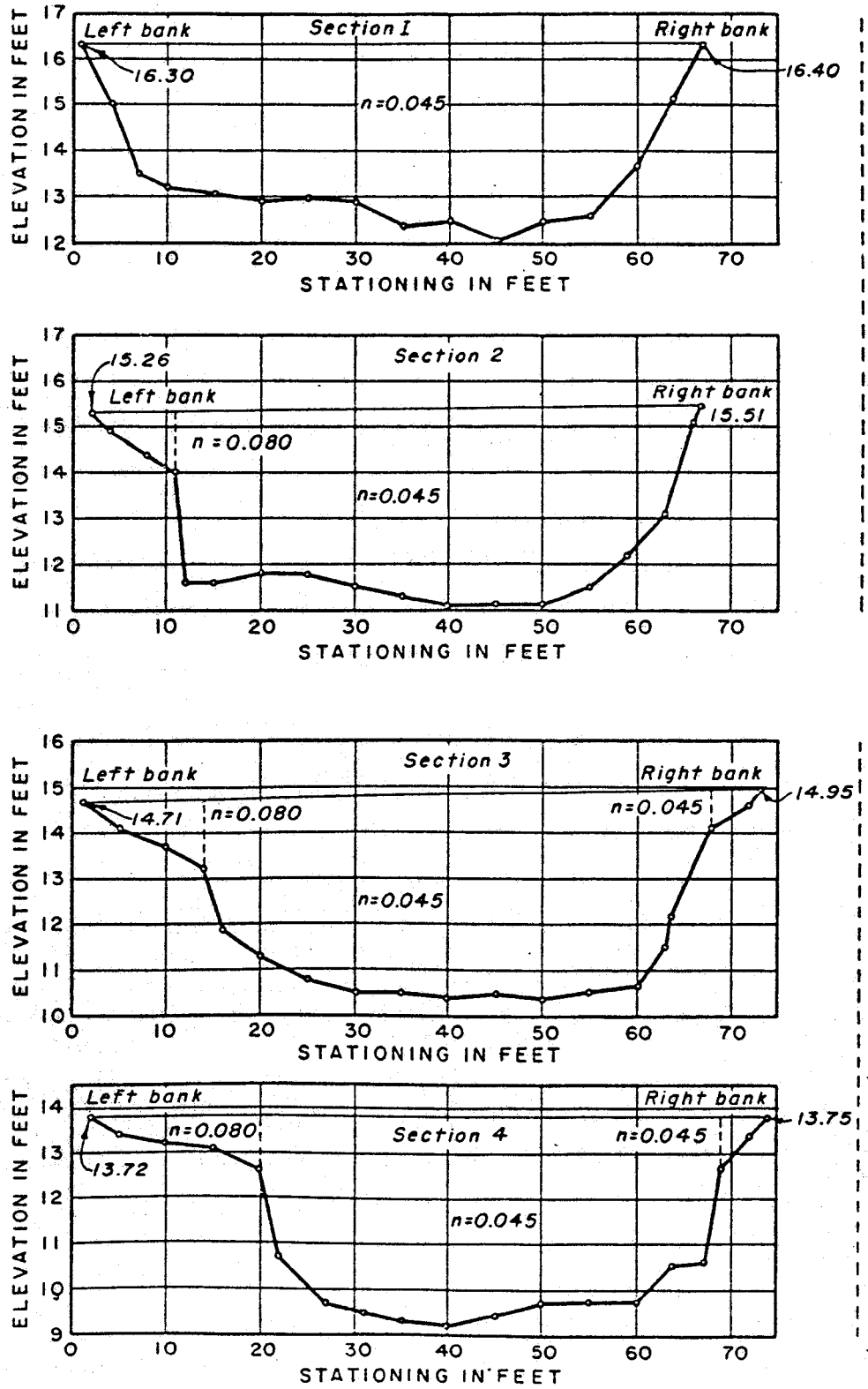

Figure 8–19. Sample slope-area computation, cross sections. 288–D–2829.

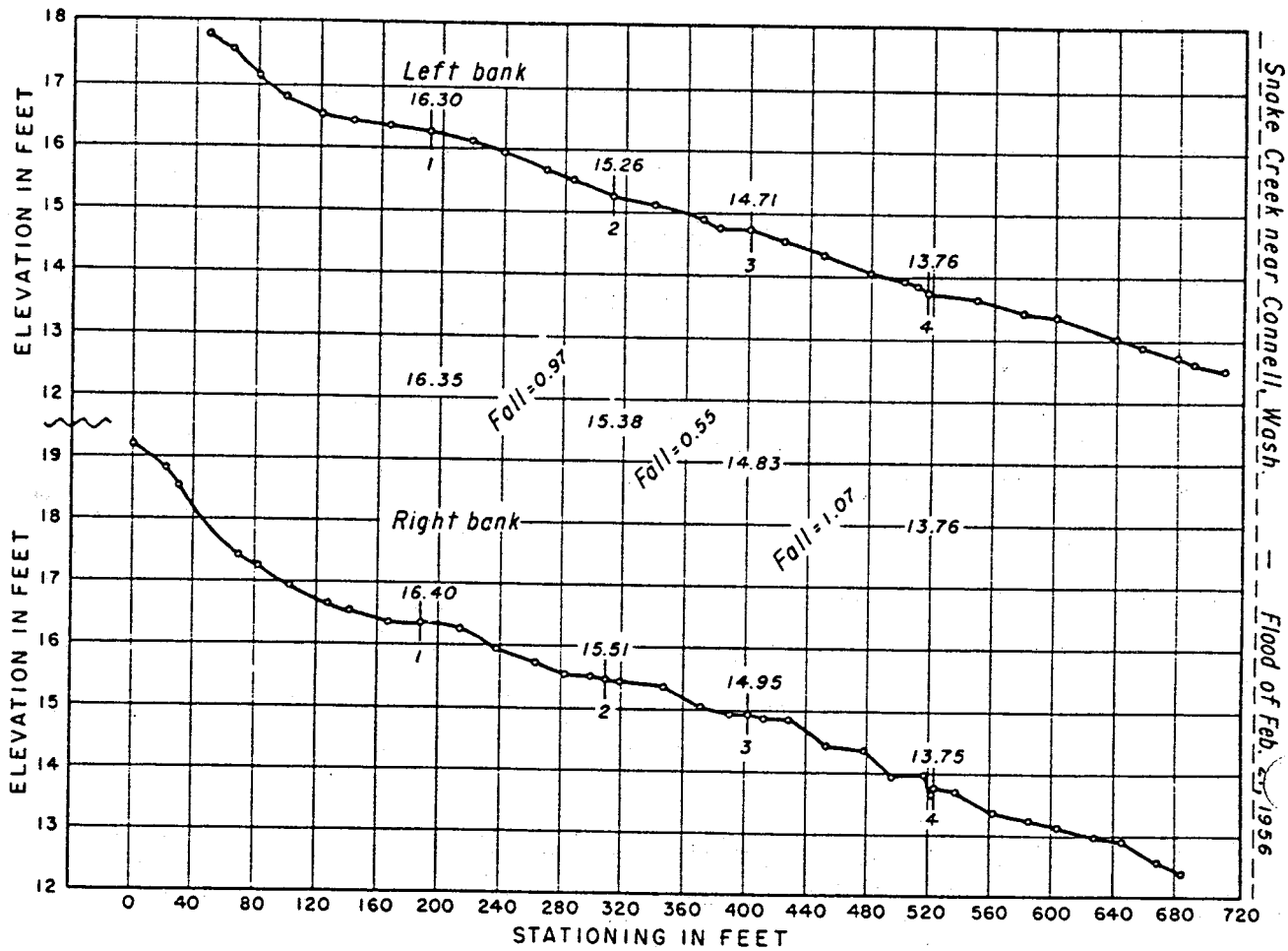

Figure B–20. Sample slope-area computation, high-water profile. 288–D–2830.

slope, and assignment of n value(s) to the affected area.

When economics or time will not permit detailed field measurements to be taken, the curve must be developed from whatever pertinent data are available. A topographic map might be used for determining the cross section and possibly the channel bed profile. Other sources of information, such as photographs, may provide data from which a selection of an n value can be made.

Figures B-22 and B-23 and table B-8 illustrate the preparation of a rating curve from a topographic map. The procedures shown are also applicable if the cross section is established from a field survey. First, the centerline of the dam was located on the topographic map available for the area, as shown in (A) of figure B–22. The cross section in (B) was then developed by scaling the distances between contours on the map. The low point in the streambed was determined by interpolation between contours. The mean bed slope of the stream was obtained from map-scaled measurements of distances between contours crossing the stream channel. A value of n of 0.030 was selected on the basis of various descriptions and field observations that considerable growth of vegetation was present in a stream of relatively straight alinement. The computations were then performed as shown in table B–8 on page 582.

The conveyance capacity method illustrated under the slope-area discussion has been utilized in the computations. From the geometric properties of the section and an n of 0.030, the conveyance capacity, K_n, is computed for various elevations. These values are multiplied

9-193
Slope-area measurement
December 1960

UNITED STATES DEPARTMENT OF THE INTERIOR
GEOLOGICAL SURVEY
WATER RESOURCES DIVISION

File _____

Meas. No. _____

Slope-area measurement of Snake Creek near Connell, Wash. (Miscellaneous site) for flood of Feb. 21, 1956

Reach between sections	1-2	2-3	3-4		
Length of reach (L), ft	121	90	119	Gage height,	— ft
Fall in reach (Δh), ft	0.97	0.55	1.07	Discharge[1],	1,380 cfs
				Drainage area,	115 sq mi

SECTION PROPERTIES

Section	n	1.486/n	a	r	$r^{2/3}$	$K=\frac{1.486}{n}ar^{2/3}$	K^3/a^2	[2] α	[3] q	v
1 Sta. 1-67	.045	33.0	208	3.09	2.12	14,550		1.00	1,380	6.64
2 2-11	.080	18.6	6.1	.68	.77	90	0.196		8	1.31
11-67	.045	33.0	203	3.47	2.29	15,340	876		1,370	6.75
			209.1			15,430	876 .196	1.04		
							842			
3 1-14	.080	18.6	10.0	.77	.84	160	.410		13	1.30
14-68	.045		212	3.83	2.45	17,140	1122		1,360	6.42
68-73	.045		2.6	.51	.64	50	.185		4	1.54
			224.6			17,350	1122 .595	1.08		
							1035			
4 2-20	.080	18.6	11.1	.62	.73	150	.274		13	1.17
20-69	.045		193	3.79	2.43	15,480	996		1,360	7.05
69-74	.045		2.8	.55	.67	60	.275	1.10	4	1.43
			206.9			15,690	996 .549			
							901			

Weighted conveyance[4] (K_w). 1-2 14,930 2-3 16,360 3-4 16,500

COMPUTATION OF DISCHARGE

Reach	Assumed Q	[5] h_v	[6] Δh_v	[7] h_f	$s=h_f/L$	$s^{1/2}$	Computed Q $=K_w s^{1/2}$
1-2	1,330	Upstr. .636 / Dwnstr. .655	-0.019	0.951	0.00786	0.0887	1,330
2-3	1,320	Upstr. .645 / Dwnstr. .580	.065	.582	.00647	.0804	1,320
3-4	1,460	Upstr. .710 / Dwnstr. .852	-.142	.928	.00780	.0883	1,460

[1] DISCHARGE (by formula) 1,380, or

FORMULAS

2 $\alpha = \Sigma (K^3/a^2) \div K^3_{total}/A^2_{total}$

3 $q = Q\ (K/K_{total})$

4 $K_w = \sqrt{K_{Upstr.} \times K_{Dwnstr.}}$

5 $h_v = \alpha\ V^2/2g$

6 $\Delta h_v = \text{Upstr. } h_v - \text{Dwnstr. } h_v$

7 When Δh_v is positive, $h_f = \Delta h + \frac{1}{2}\Delta h_v$
When Δh_v is negative, $h_f = \Delta h + \Delta h_v$

Summary of factors influencing measuring conditions (floodmarks, surge, scour, fill, channel configuration, angle of flow, selection of n, etc.): _____

Sheet No. 11 of 13 Sheets. Prepared by E.L.S. Date 3-19-56 Checked by E.G.P. Date 5-14-56

Figure B-21. Sample slope-area computation, discharge. 288-D-2831.

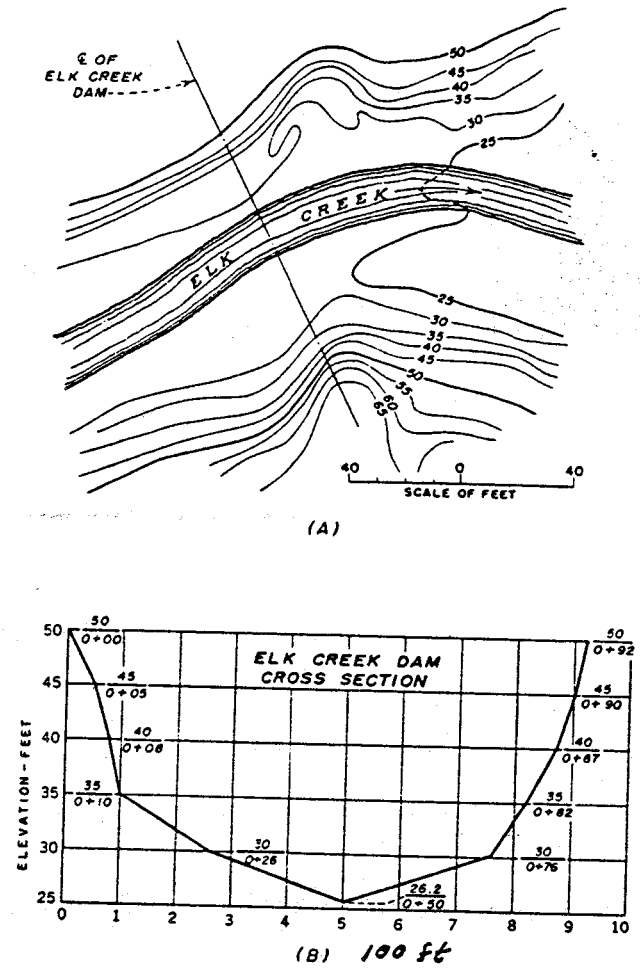

Figure 8–22. Plan and cross section of Elk Creek Dam site 288–D–2832.

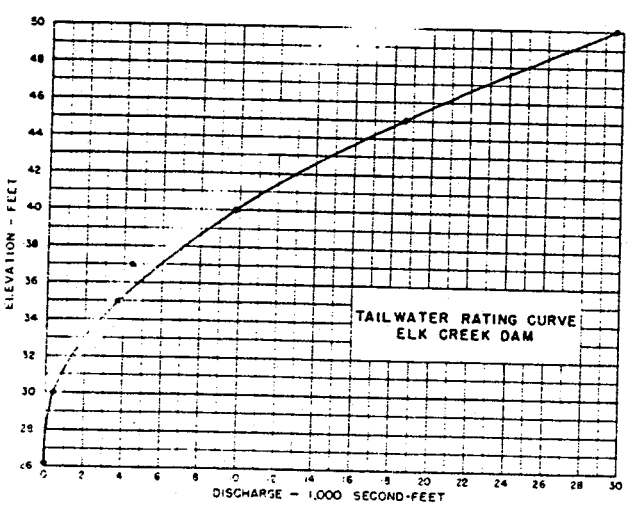

Figure 8–23. Tailwater rating curve for Elk Creek Dam. 288–D–2560.

TABLE B–8.—*Computations for tailwater rating curve*

ELK CREEK DAM

Data: $n=0.030$ s_b=mean bed slope=0.00395

$$C=\frac{1.486}{n}=49.53 \quad s_b^{1/2}=0.0628$$

Elevation	a	p	r	$r^{2/3}$	C	K_d	$s_b^{1/2}$	Q
26.2	0	0	0	0	.....	.....	.....	.....
30	95	50.6	1.88	1.523	49.53	7,170	0.0628	450
35	400	75.1	5.32	3.047	49.53	60,400	.0628	3,790
40	753	87.6	8.60	4.198	49.53	156,000	.0628	9,800
45	1160	99.2	11.70	5.154	49.53	296,000	.0628	18,600
50	1610	111.7	14.40	5.919	49.53	472,000	.0628	29,600

by the one-half power of the mean bed slope to compute the discharge at each elevation. The tailwater rating curve derived from the computations is shown in figure B-23.

(b) *Water Surface Profile Method.*—In studies where more exact tailwater curves are required, water surface profiles may be developed for a range of discharges. The computations in such studies are more involved and require a series of cross sections downstream from the damsite.

Several methods [1, 2, 8, 9] have been developed for computing water surface profiles; however, this discussion will be limited to Bureau of Reclamation Method A. This method is adaptable to irregular channels having various roughness segments and large variations in cross-section geometry. It is limited to the assumption that flow paths between cross sections are equal in length for all roughness segments. Other methods [8, 9] must be used for variable travel distances.

In Method A, a number of cross sections are selected at intervals below the damsite. The selection of the cross-section locations is probably the most important factor in preparing a good study. The sections should be located so the average area, hydraulic radius, and n values of any two sections will be representative of the reach length between them. Channels that are alternately wide and narrow should have sections located in the narrow and wide points so the average condition can be defined. Special attention should also be given to locating a section at each point that indicates a definite change in grade or a control such as a natural constriction or bridge. The cross sec-

tions should be surveyed and segmented according to roughness (n) characteristics. A minimum of five cross sections should be selected, with no more than 2 feet of fall between the sections.

Reference is again made to figure B-17 and the basic hydraulic equations presented in section B-7. Equation (55) can be rearranged to give

$$s_f=\left(\frac{Q}{K_d}\right)^2 \tag{66}$$

in which K_d is the total conveyance capacity of the main channel and overbank areas. Now the discharge in each subdivision of the cross section can be determined as follows:

$$Q=K_d\, s_f^{1/2} \tag{67}$$

$$\text{and } Q_s=K_{d_s}\, s_f^{1/2} \tag{68}$$

where:

Q=total discharge
s_f=slope of the friction gradient
K_d=total conveyance
and Q_s and K_{d_s}=corresponding elements for partial discharge and conveyance capacity of the subdivision under consideration.

Dividing one equation by the other

$$\frac{Q}{Q_s}=\frac{K_d}{K_{d_s}}$$

and solving for Q_s:

$$Q_s=\frac{Q\cdot K_{d_s}}{K_d} \tag{69}$$

The friction head, h_f, is determined by averaging the computed friction slopes at sections 1 and 2 and multiplying by the length as below:

$$h_f=L\left(\frac{s_{f_1}+s_{f_2}}{2}\right) \tag{70}$$

The velocity head, h_v, is derived by a weighting process using the partial discharges occurring in each subdivision of the cross section. Velocities in each segment are computed by the equation $V_s=Q_s/a_s$ where a_s is the area of the segment. The velocity head results from the following equation:

$$h_v=\frac{\Sigma(V_s^2\, Q_s)}{2gQ} \tag{71}$$

It should be noted that this equation gives the same result as equation (60).

Method A deviates slightly at this point from the slope-area computation in that a coefficient of 0.1 is used to determine the eddy losses in contracting reaches. A coefficient of 0.5 is also used here to compute losses in expanding reaches.

The following example shows the procedure required to establish a rating curve by Method A:

(1) Seven cross sections designated by numbers 1 through 7 were selected from figure B-24, and their geometric properties were determined by field survey.
(2) Area and hydraulic radius curves were developed for each cross section, similar to the one shown in figure B-25. It should be noted that a separate curve is drawn for each subsection.
(3) A set of conveyance curves was developed for each section similar to the one shown in figure B-26.
(4) A rating curve for the lowermost cross section, section 1 (fig. B-27), was determined by the approximate method described in section B-8(a) of this appendix.
(5) Water surface profiles were computed for several discharges to define the required tailwater rating curve. The computations shown in table B-9 are for Q=11,100 cubic feet per second.
(6) Section 1 is the starting point of the profile computation. The starting elevation 5714.0 in column 2 was taken from the rating curve in figure B-27. The area values in column 3 were read from the area curve for section 1 (not shown). The distance between sections 1 and 2 was entered in column 4 and the K_d values were read from

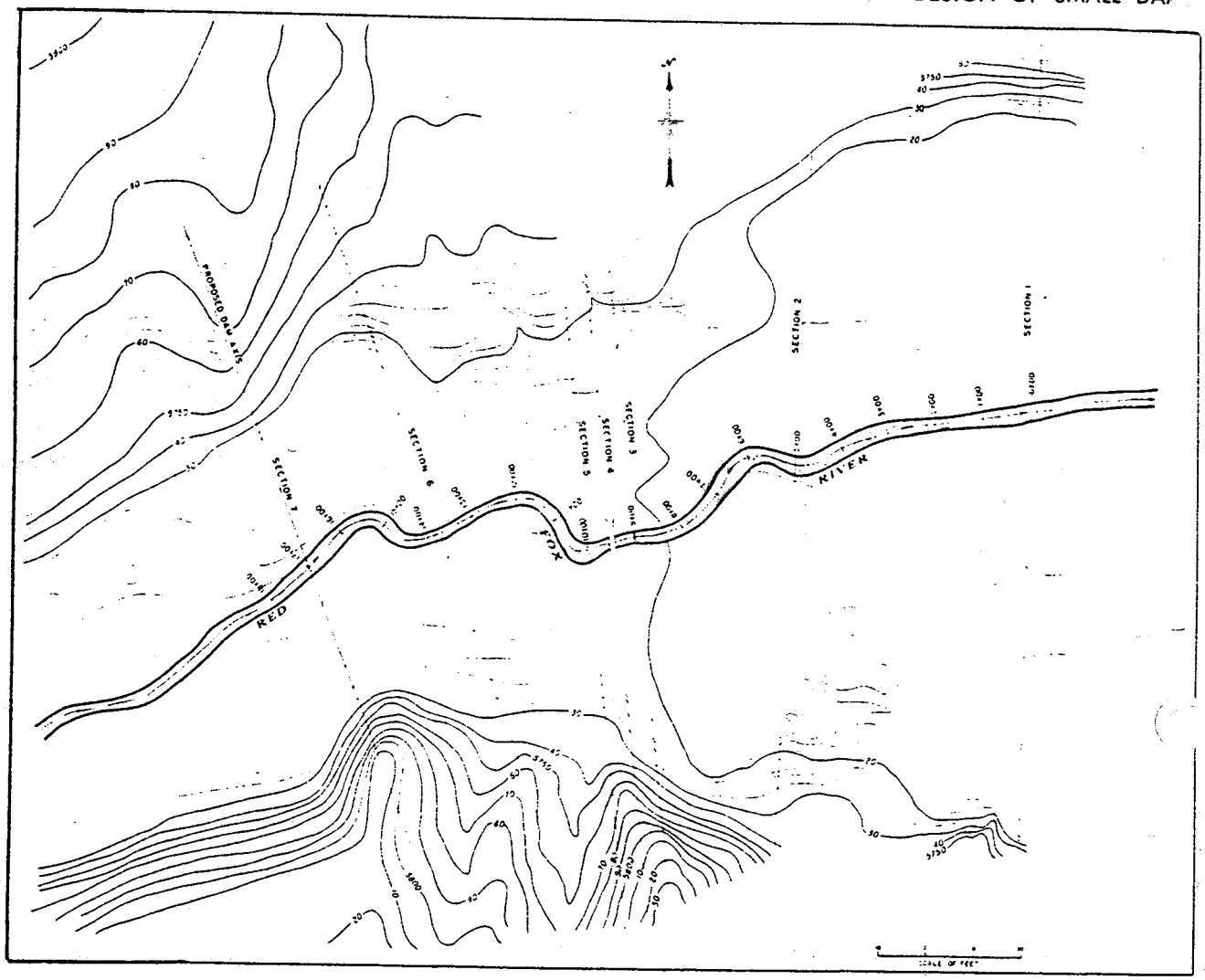

Figure 8–24. Cross sections used to establish a rating curve by Method A. 288–D–2833.

the conveyance capacity curve for section 1 (not shown) at elevation 5714.0.

(7) Next, the s_f value was computed for section 1 using equation (66).

(8) Q_x values were computed for each subsection of section 1 using equation (69).

(9) The velocity in each subsection was computed using $V=Q/A$, and the values V^2Q were computed and placed in column 11 and totaled.

(10) The h_v value was next derived for section 1 using equation (71).

(11) The elevation 5714.0 was repeated in column 17.

(12) A trial water surface elevation was then placed in column 2 for section 2 and steps 6 and 7 were repeated based on the data for section 2.

(13) A mean friction slope was computed for the reach by averaging the friction slopes computed for sections 1 and 2.

(14) The friction head loss, h_f, between sections 1 and 2 was then arrived at by multiplying the mean friction slope by the distance L.

(15) Steps 8, 9, and 10 were then repeat for section 2 data.

(16) The algebraic difference in velocity head was then entered in column 13.

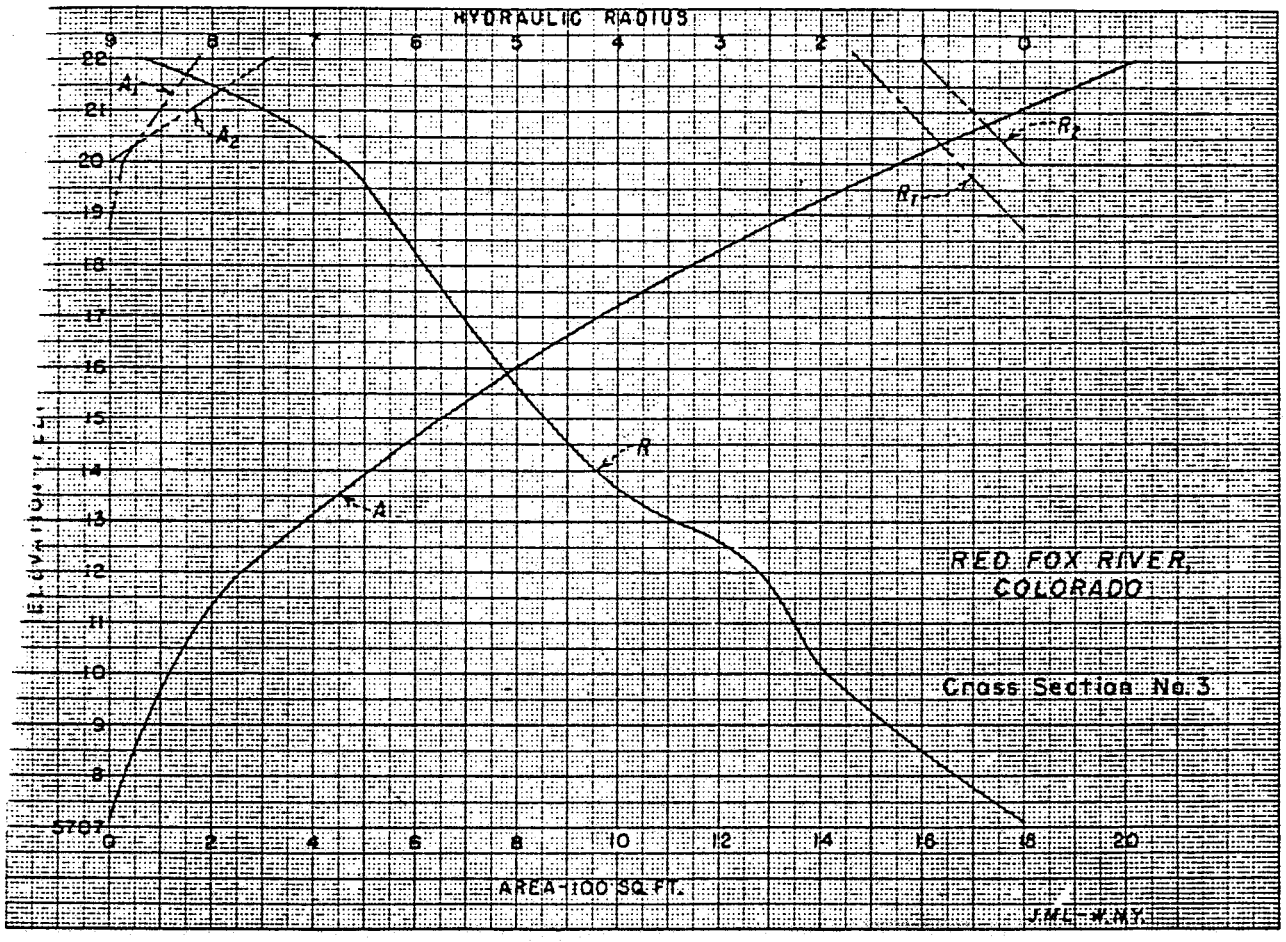

Figure 8–25. Area and hydraulic radius curves—Section 3—Red Fox River. 288–D–2834.

The upstream velocity head is subtracted from the downstream value.

(17) The eddy loss is assumed to be 0.1 and 0.5 of the absolute value of the difference in velocity heads for contracting and expanding reaches, respectively. Thus, if the Δh_v is -1.0 foot, the eddy loss is 0.5 foot and if the Δh_v is $+1.0$ foot, the eddy loss is 0.1 foot. The eddy loss value was placed in column 14.

(18) The total loss is equal to the friction head loss plus the eddy loss. The ΔH value is the algebraic sum of the total head loss and the change in velocity head.

(19) The water surface elevation in column 17 is the sum of the water surface elevation at section 1 and the ΔH. If the computed water surface elevation in column 17 agrees with the assumed elevation within a tenth of a foot, the computation is completed and computations are begun for the next upstream section.

When a sufficient number of profiles have been computed, a rating curve can be developed from the computed water surface elevations at any given section. This method is more reliable than the approximate method previously described, because if the first section does not typify the average stream channel hydraulics the variations are recognized as the profiles are continued upstream. This may be proven by changing the starting elevation at the first section and computing a new profile. It will be found that a considerable change in the starting elevation at section 1 will make much

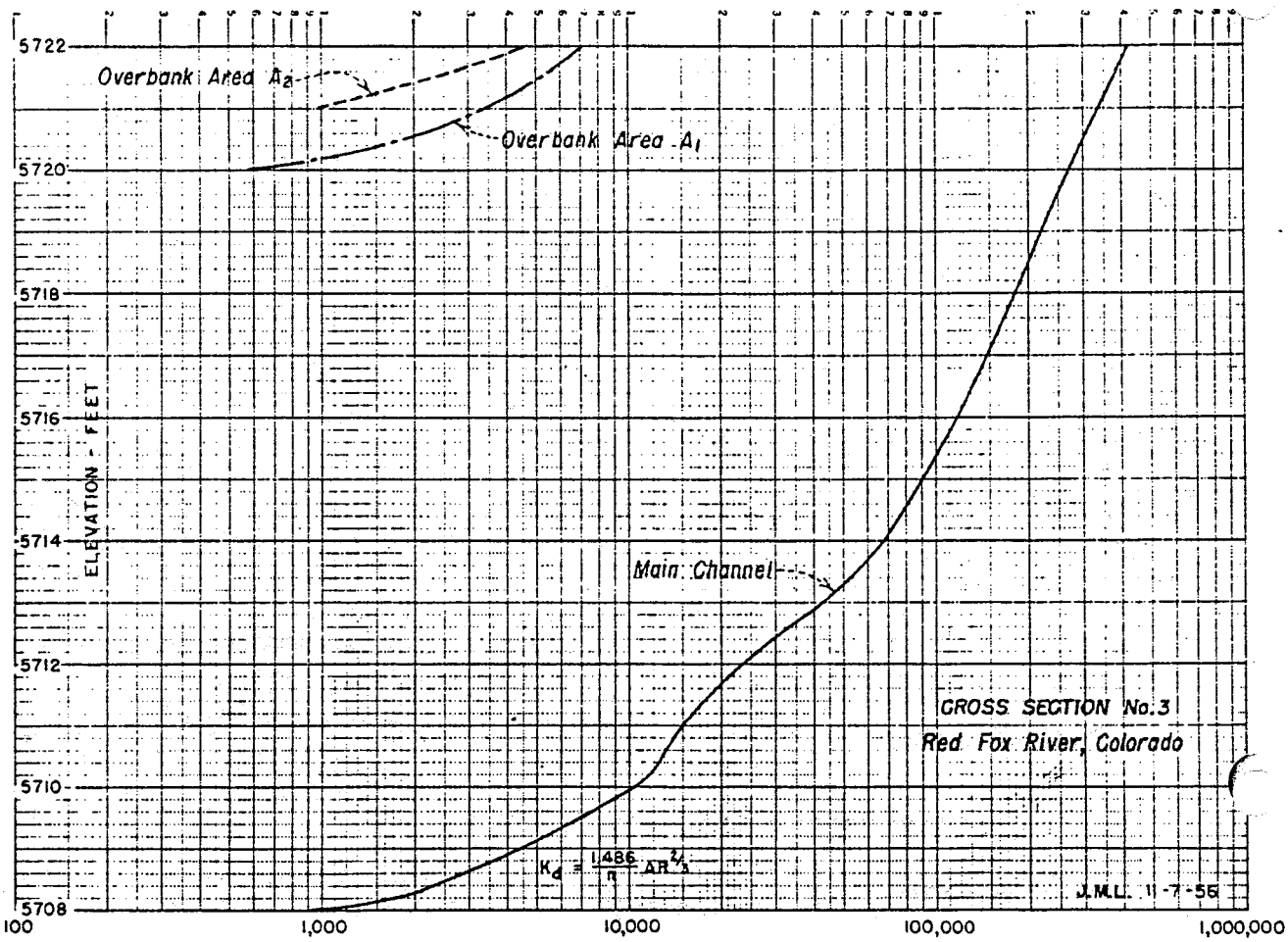

Figure B–26. Conveyance (K_d) curves—Section 3—Red Fox River. 288–D–2835.

less difference in the computed elevation for section 7.

B-9. *Critical Flow.*—The hydraulic analysis of flow in open channels becomes more complex when critical conditions can occur at some point along the river reach under consideration. The conditions of critical flow can be commonly observed at a "control" section in the channel. Such controls occur at locations where there is a material change in the cross section causing a constriction of the flow. These constrictions may be natural, or artificial such as bridges. Another cause may be a significant change in bottom grade. Vortices, eddies, cross currents, and large standing waves are some of the characteristics indicating critical flow conditions. A field reconnaissance of the hydraulic reach under investigation should include the location of any critical sections.

Whenever a computed velocity appears very high, a check should be made to see if the velocity exceeds critical velocity. This is true if the elevation has been arrived at by the approximate method or by an energy balance. Equation (14) of this appendix,

$$V_c = 5.67\sqrt{\frac{a}{T}}, \qquad (14)$$

can be used to determine the critical velocity and, when the velocity at the computed elevation exceeds critical, it may be assumed that a control exists. Other methods may be used for checking critical flow but they are not discussed because all are based on different ways of analyzing equation (7)

$$\frac{Q^2}{g} = \frac{a^3}{T}$$

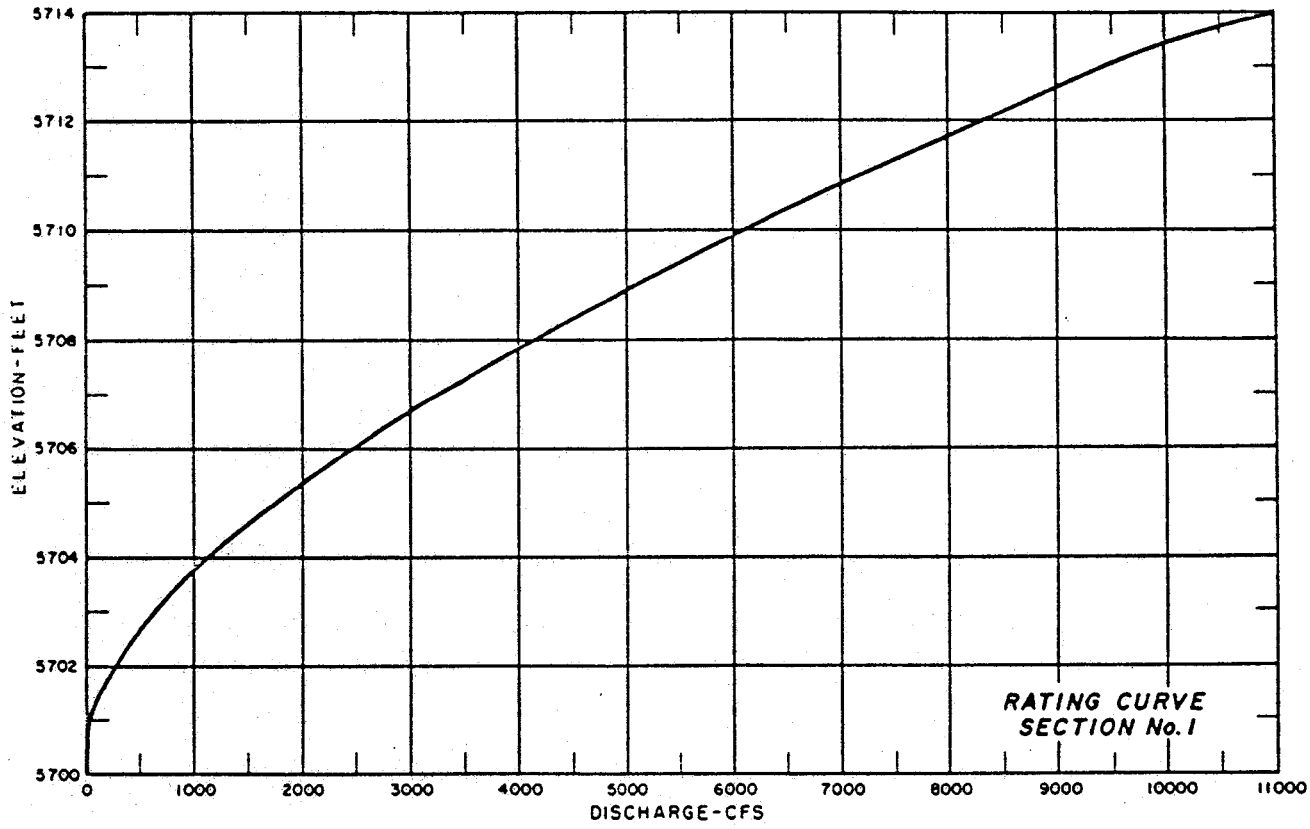

Figure 8–27. Rating curve—Section No. 1. 288–D–2836.

When the depth of flow is greater than critical depth throughout the reach under study and a control point is not evident at some relatively close distance downstream from the reach, the computed water surface profiles are acceptable. If a control point is located downstream from the reach, the reach should be extended to the control, and profile computations started at that point. When the control point is encountered within the study reach, the critical depth elevation is determined and the profile computation is started again at the critical discharge elevation. Generally, in most streams, supercritical flow conditions will occur only in the immediate vicinity of a control section.

The above discussion involves the analysis of critical flow as applied to water surface profile computations. It may be required to develop a critical rating curve for a control section which is located at or near a damsite. In this event the critical velocities are computed by equation (14) and multiplied by the area to determine the discharge. This is done for several elevations and a curve of critical flow stage versus discharge plotted.

It is advisable to consider only the main channel portion of subdivided cross sections because the overbank areas will tend to lower the mean cross-section velocity and not depict the velocities attained in the channel itself.

B-10. *Computer Applications.*—The necessary trial-and-error solution of the energy balance equation involving iterative processes is ideally suited to digital computer applications. The Bureau of Reclamation has made use of several computer programs for computing water surface profiles; however, all are based upon an energy balance procedure and differ only in degree of sophistication.

TABLE B-9.—*Water surface profile computations—Method A.* 288-D-2859.

WATER SURFACE PROFILE COMPUTATIONS – METHOD A

SUBJECT: Red Fox River, Colorado Discharge = 11,100 cfs

COMPUTED BY: DATE: CHECKED BY: DATE: SHEET OF

1	2	3	4	5	6	7	8	9	10	11	12	13	14	15	16	17
STATION	Assumed Water Surface Elev.	Area a	Dist. L	$K_d = \frac{1.486}{n} a r^{2/3}$	$S_f = \left(\frac{Q}{K_d}\right)^2$	Mean S_f	Mean S_f × L = h_f	Q	V	V^2Q	h_v	$h_{v_1} - h_{v_2}$	Eddy Loss	Total Loss	ΔH	W.S. El.
Section 1	5714.0	524		125,000				10,700	18.0	3,460,000						
		192		4,150				400	2.08	1,730						
				129,150	0.00735			11,100		3,461,730	4.85					5714.0
			500													
Section 2	5720.9	843		230,000				5,540	6.60	275,000						
		1,170		130,000				3,370	2.88	28,000						
		1,000		25,000				550	0.65	274						
		1,500		43,000				1,120	0.75	630						
				428,000	0.000673	0.00401	2.00	11,100		304,904	0.43	-0.42	0.44	2.44	5.85	5720.85
			400													
Section 3	5721.2	1,832		360,000				11,000	6.00	396,000						
		115		2,700				70	0.61	26						
		185		1,250				30	0.16	8						
				363,950	0.00108	0.000877	0.35	11,100		396,034	0.56	-0.13	0.07	0.42	0.23	5721.45
			100													
Section 4	5721.2	1,300		158,000	0.00493	0.00301	0.30	11,100	8.54		1.13	-0.57	0.27	0.57	0.00	5721.20
			100													
Section 5	5722.1	1,481		220,000	0.00254	0.00374	0.37	11,100	6.60		0.66	-0.45	0.05	0.42	0.67	5722.87
			400													
Section 6	5722.8	1,018		174,000				10,900	10.7	1,250,000						
		130		3,350				190	1.46	405						
		20		141				10	0.50	3						
				177,541	0.00391	0.00328	1.31	11,100		1,250,408	1.75	-1.07	0.54	1.85	0.78	5722.69
			500													
Section 7	5725.3	844		124,000				10,500	12.5	1,640,000						
		58		1,400				110	1.12	138						
		220		5,800				490	2.23	2,440						
				131,200	0.00714	0.00553	2.77	11,100		1,642,578	2.30	-0.55	0.28	3.05	2.50	5725.35

C. BIBLIOGRAPHY

B-11. *Bibliography.*—

[1] King, H. W., and Brater, E. F., "Handbook of Hydraulics," fifth edition, McGraw-Hill Book Co., Inc., New York, N.Y., 1963.

[2] Woodward, S. B., and Posey, C. J., "Steady Flow in Open Channels," John Wiley & Sons, Inc., fourth printing, September 1949.

[3] Bakhmeteff, B. A., "Hydraulics of Open Channels," McGraw-Hill Book Co., Inc., New York, N.Y., 1932.

[4] Binder, R. C., "Fluid Mechanics," third edition, Prentice-Hall, Inc., Englewood Cliffs, N.J., 1955.

[5] Rouse, Hunter, "Engineering Hydraulics," John Wiley & Sons, Inc., New York, N.Y., 1950.

[6] "Friction Factors for Large Conduits Flowing Full," Engineering Monograph No. 7, Bureau of Reclamation, 1965.

[7] Bradley, J. N., and Peterka, A. J., "The Hydraulic Design of Stilling Basins," ASCE Proceedings, vol. 83, October 1957, Journal of Hydraulics Division, No. HY 5, Papers No. 1401 to 1404, inclusive.

[8] "Guide for Computing Water Surface Profiles," Bureau of Reclamation, November 1957.

[9] "Hydrologic and Hydraulic Analyses—Computation of Backwater Curves in River Channels," Engineering Manual, Department of the Army, Corps of Engineers, pt. CXIV, ch. 9, May 1952.

[10] "Stream Gaging Procedure," Water Supply Paper 888, U.S. Department of the Interior, Geological Survey, 1945.

[11] Ramser, C. E., "Flow of Water in Drainage Channels," Technical Bulletin No. 129, U.S. Department of Agriculture, 1929.

[12] Dalrymple, Tate, and Benson, M. A., "Measurement of Peak Discharge by the Slope-Area Method," Techniques of Water Resources Investigations of the U.S. Geological Survey, A2, U.S. Department of the Interior, Geolo[illegible] Survey, 1967.

[13] "Water Measurement Manual," Bureau of Reclamation, second edition, 1967.

Jour. Research U.S. Geol. Survey
Vol. 4, No. 3, May–June 1976, p. 285–291

A SIMPLIFIED SLOPE-AREA METHOD FOR ESTIMATING FLOOD DISCHARGES IN NATURAL CHANNELS

By H. C. RIGGS, Reston, Va.

Abstract.—Discharge of a stream may be computed from the slope of the water surface, the cross-sectional area, and an estimate of channel roughness. This, the slope-area method, is widely used to compute flood peak discharges from high-water marks. Reliability of a computed discharge depends largely on the roughness coefficient, which must be estimated. This paper shows that results of comparable accuracy can be obtained from area and slope alone in natural channels; a roughness coefficient is not needed because roughness and slope are related. The estimating equation and suggestions for application of the simplified method are included.

The slope-area method is widely used to compute peak discharge after the passage of a flood. A reach of uniform channel is selected on which the flood profile on both banks can be defined from high-water marks. Surveys of these high-water marks and of channel cross sections and estimates of the roughness coefficient in the Manning equation are required. The method is described by Benson and Dalrymple (1968) and by Dalrymple and Benson (1967).

Although judgment is required in selecting the stream reach and in interpreting the profiles from high-water marks, the major subjectivity is in selection of the roughness coefficient n in the Manning equation

$$Q=\frac{1.49}{n}AR^{2/3}S^{1/2}$$

where Q is discharge in cubic feet per second, A is cross-sectional area in square feet, R is the hydraulic radius in feet (cross-sectional area divided by the wetted perimeter), and S is the slope of the energy gradient. Guides to selection of n are given in many texts. The guide by Barnes (1967) for estimating the roughness coefficient in natural channels includes color photographs of stream reaches for which the coefficients have been computed from channel surveys and known peak discharges.

Study of the photographs and the computed (verified) values of n in Barnes' (1967) report will show some apparent inconsistencies; for example, between Cache Creek and Boundary Creek. These inconsistencies are thought to arise from two sources. First, the roughness coefficient of a natural channel is due to bed roughness, bank irregularity, effect of vegetation(if any), depth of water, channel slope, and perhaps other factors. No objective way of evaluating and combining these factors into one coefficient is available. Second, a verified value of a roughness coefficient is affected by the inaccuracies in each of the other variables in the Manning equation. Inaccuracies may arise because of a poorly defined water-surface profile or nonrepresentative cross sections. A poorly defined profile may be caused by poor high-water marks, bank irregularity at the high-water line, or a changing cross-sectional area and shape throughout the reach. In rough cross sections the detail to which the cross section is surveyed will affect the computed area and thus the computed roughness coefficient.

Several investigators have related the verified roughness coefficients to channel bed roughness and to the vertical velocity distribution. See Boyer (1954), Graf (1966), and Limerinos (1970). However, such relations have limited use because bed roughness is only part of the total roughness in most channels, and the vertical velocity distribution generally is not known at sites where a slope-area measurement is made.

Thus the roughness coefficient still must be selected by judgment based on guidelines and experience. Whether this is a disadvantage or not depends on the accuracy of results. How accurate are slope-area measurements? This has been a subject of discussion for many years. Opinions range from claims of high accuracy to the comment of a prominent (unnamed) hydraulic engineer who was quoted by Henry Beckman (written commun., 1925) as saying that, whenever results obtained by the slope-area method came nearer than 25 percent to the correct result, it was due either to accident or to a second choice of factors to use in the formula after the first choice had gone amiss. Fifty years later, wide differences of opinion as to the accuracy of the method still exist.

Those with experience in slope-area measurements can recognize reaches where good results can be ex-

pected. But how good is good? An answer to this is now possible. Estimates of the roughness coefficient were recorded on field notes of some surveys of channel reaches for which the coefficient was computed from known peak discharge. Estimated roughness coefficients by each individual and the computed (verified) coefficients are shown in table 1. All reaches listed in table 1 are ones in which the flow was contained in a single channel.

Table 1 shows a surprisingly small difference among estimates by individual observers for most of the streams. That table also indicates that estimates of roughness coefficient tend to be better on some types of reaches than on others. Estimates were poor on Salt-Roca, Cache–Lower Lake, Cachuma–Santa Ynez, Sycamore–McDowell, and Hominy–Candler. One might conclude from this table that experienced observers can make acceptable subjective estimates of the roughness coefficients in channels typified by that of W. Fk. Bitterroot–Conner but that better guidelines are needed for unusual channels. Nearly all the estimates in table 1 were made by observers with extensive experience in this type of work. Less experienced observers would do less well on the average. Thus, a less subjective method is needed.

Some measurable channel characteristic related to the roughness coefficient might permit an objective selection of the latter. Channel (or water-surface) slope is one such characteristic. It has been known for years

TABLE 1.—*Estimated and verified values of the channel roughness coefficient* n

[The first 20 streams are included in Barnes' (1967) report; the rest are from unpublished verifications]

Stream reach	Estimated n				Verified n
Clark Fork–St. Regis, Mont	0.035	0.030	0.035	0.035	0.028
Clark Fork above Missoula, Mont	.035	.035	.035	----	.030
Salt–Roca, Nebr	.045	.045	----	----	.030
Blackfoot—Ovando, Mont	.035	----	----	----	.031
Coeur d Alene–Prichard, Idaho	.035	.038	.040	.030	.032
Rio Chama–Chamita, N. Mex	.035	.025	----	----	.032
Clearwater–Kamiah, Idaho	.035	.035	.035	----	.033
W. Fk. Bitterroot–Conner, Mont	.040	.035	.035	----	.036
Yakima–Umtanum, Wash	.032	----	----	----	.036
Wenatchee–Plain, Wash	.037	.035	.030	.035	.037
Moyie–Eastport, Idaho	.030	.035	.035	.030	.038
Spokane–Spokane, Wash	.038	.035	.035	----	.038
M. Fk. Flathead–Essex, Mont	.038	.040	.038	----	.041
Catherine—Union, Oreg	.042	.045	.040	.040	.043
Chiwawa–Plain, Wash	.038	----	----	----	.043
Grande Ronde–LaGrande, Oreg	.038	.040	.040	.038	.043
S. Fk. Clearwater–Grangeville, Idaho	.050	.045	.048	----	.051
Cache–Lower Lake, Calif	.082	.074	----	----	.053
Boundary–Porthill, Idaho	.065	.075	----	----	.073
Rock–Darby, Mont	.070	.065	.075	----	.075
Salmon–Whitebird, Idaho	.04	.04	.04	----	.040
Sulfur Fork Red–Adams, Tenn	.05	.09	----	----	.050
Cachuma–Santa Ynez, Calif	.045	.055	----	----	*.07
Sycamore–McDowell, Ariz	.032	----	----	----	.020
Salt–Lincoln, Nebr	.035	.042	----	----	*.03
Bijou–Wiggins, Colo	.025	----	----	----	*.025
Deckers–Morgantown, W. Va	.035	----	----	----	.035
Millers–Erving, Mass	.037	.042	----	----	.037
Neversink–Godeffroy, N. Y	.035	----	----	----	.035
Hominy–Candler, N. C	.045	----	----	----	.060

* Varies depending on interpretation of data.

that the roughness coefficient is related to slope i natural channels but, in practice, the two have bee considered independent. The degree of relation betwe roughness coefficient, n, and the square roo tl water-surface slope is shown in figure 1 usi da from Barnes' (1967) report. A relation of this ty might be used to modify an estimated n according slope; or one might conclude that the two variables a so highly related that only one of the two is needed computing discharge. The latter is the basis for tl simplified method described in the next section.

THE SIMPLIFIED METHOD

The existence of a relation between channel roug ness and water-surface slope in natural channels su gests that discharge might be computed without usi a roughness coefficient and without defining the rel tion of roughness coefficient to slope. Assuming th

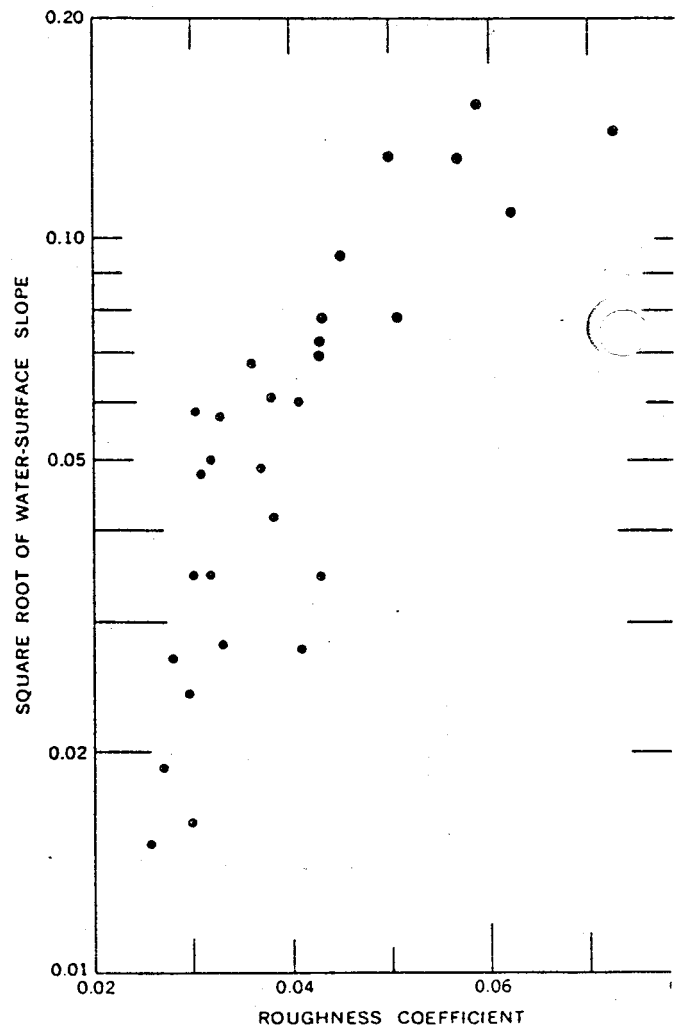

FIGURE 1.—Relation of roughness coefficient to squa root water-surface slope.

the slope will replace n and that the hydraulic radius, R, is closely related to cross-sectional area, A, the Manning equation is reduced to the model

$$Q = aA^bS^c$$

if S is redefined as water-surface slope.

Using areas and slopes from Barnes' (1967) report, the following equation was derived (Riggs, 1974):

$$\log Q = 0.53 + 1.295 \log A + 0.316 \log S \qquad (1)$$

where Q is in cubic metres per second. A is in square metres, and S is dimensionless. The standard error is about 20 percent.

Subsequent study of the data indicated that the relation with slope is not log linear. Accordingly the data were reanalyzed in English units with the following result which is the basis for the simplified method:

$$\boxed{\log Q = 0.366 + 1.33 \log A + 0.05 \log S - 0.056 (\log S)^2} \qquad (2)$$

where Q is in cubic feet per second, A is in square feet, and S is dimensionless. The standard error is about the same as before but this latter equation fits the data better throughout the range. Comparison of results from equation 2 with those that would have been obtained by the conventional slope-area method is possible for stream reaches (table 1) for which the survey-party members selected n values prior to verification. These reaches are listed in table 2 along with the mean of the estimates of n for each reach, the known discharge, the discharge computed by the conventional slope-area method using the mean n, and the discharge computed by the simplified method (eq 2). Results are plotted in figure 2. These plots indicate little difference in relia-

TABLE 2.—*Evaluation of slope-area method and simplified method*

[See table 1 for reach locations and estimated n values]

Stream reach	Mean, $\bar{n}$, of estimated n values	Discharge: Known	Discharge: Using $\bar{n}$	Discharge: By eq 2
Clark Fork	0.034	68,900	56,700	59,300
Clark Fork	.035	31,500	27,000	31,100
Salt	.045	1,860	1,240	1,620
Blackfoot	.035	8,200	7,300	8,510
Coeur d'Alene	.036	11,300	9,400	9,660
Rio Chama	.030	1,060	1,130	1,110
Clearwater	.035	99,000	93,400	114,000
W. Fk. Bitterroot	.037	3,880	3,780	3,460
Yakima	.032	27,700	31,200	26,200
Wenatchee	.034	22,700	24,700	22,900
Moyie	.032	8,030	9,400	8,360
Spokane	.036	39,600	42,200	43,300
M. Fk. Flathead	.039	14,500	15,400	14,800
Catherine	.042	1,740	1,790	1,410
Chiwawa	.038	5,880	6,650	6,170
Grande Ronde	.039	4,620	5,100	4,720
S. Fk. Clearwater	.048	12,600	13,400	13,800
Cache	.078	3,840	2,610	3,630
Boundary	.07	2,530	2,640	3,180
Rock	.07	1,500	1,600	1,580
Salmon	.04	101,000	101,000	114,000
Sulfur Fork Red	.07	10,100	7,220	10,100
Cachuma	.05	776	------	1,120
Sycamore	.032	2,300	1,440	1,420
Salt	.038	29,200	------	21,700
Bijou	.025	7,900	------	8,830
Deckers	.035	3,100	3,100	2,630
Millers	.040	5,700	5,350	7,470
Neversink	.035	10,100	10,100	11,000
Hominy	.045	6,800	5,100	8,140

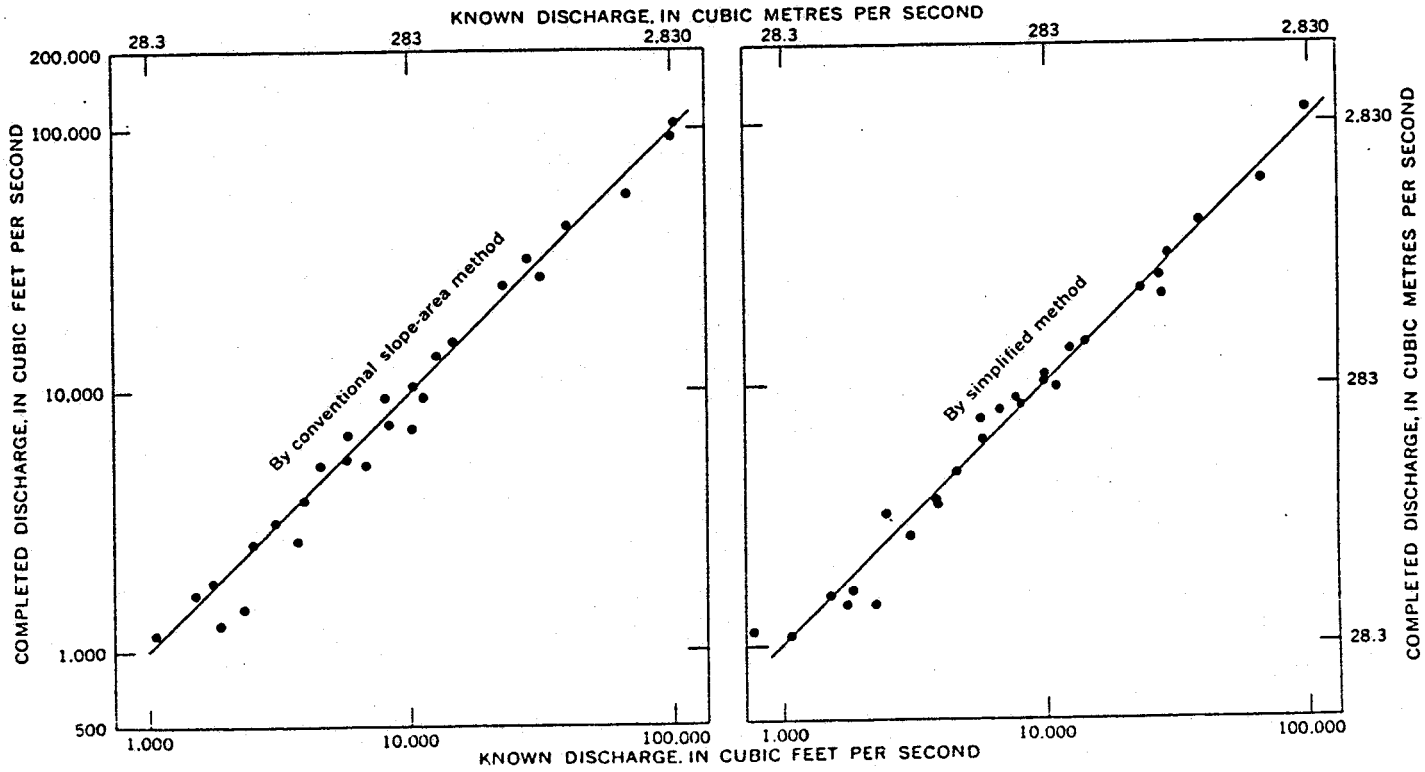

FIGURE 2.—Comparison of known peak discharges with those computed by two methods (data from table 2).

bility of the two methods. Most of the channel reaches used in this test were favorable for use of the slope-area method, and the hydrologists who made most of the surveys had broad experience in selecting n.

The applicability of the simplified method was further tested on 44 slope-area verifications not used in its derivation. Data from these verifications and the discharge computed by the simplified method are shown in table 3. Some of these verifications are of poor quality because of unfavorable channel characteristics, poor high-water marks, channel modification by man, or backwater. However, the peak discharges should be reliable because they are based on discharge measurements or short rating extensions. Comparisons of known discharge with discharge computed by equation 2 are shown in figure 3. These computed discharges are less reliable than those in figure 2 because the reaches used were not as good. However, no bias is indicated. The data on which table 3 and figure 3 are based did not include estimated values of n; thus the discharges cannot be computed by the conventional slope-area method for comparison with those by the simplified method. However, the verified n is indefinite for some stream reaches in table 3, and it could not be computed at all for others. This indicates that, had n been estimated at each of these streams, the discharge computed by the slope-area method also would have been considerably in error.

A FURTHER SIMPLIFICATION

In developing the simplified method it was found that, for nearly full channels of a certain type, discharge may be computed reliably from mean cross-sectional area alone. The relation, shown in figure 4, is

TABLE 3.—*Application of the simplified method to data not used in its derivation*

Stream	Date	Area	Slope	Verified n	Discharge	
					Known	By eq 2
Red Willow, Nebr	8-25-50	297	0.00067	0.015	1,790	855
Rio Grande, N. Mex	5-12-52	1,057	.00091	.015	6,380	5,230
Rio Grande, N. Mex	6-17-52	1,036	.00113	--------	6,100	5,530
Bijou, Colo	8-22-52	1,097	.00343	.02-0.03	7,900	8,830
Pecos, N. Mex	6-24-51	258	.00032	0.25	457	518
S. Fk. Cheyenne, Wyo	5-23-52	1,279	.00185	.026	7,900	8,780
Elkhorn, Nebr	6-26-56	1,240	.00043	.016	6,960	4,760
Lance, Wyo	6-27-52	1,010	.002	.027	5,400	6,590
Little Colorado, Ariz	7-27-40	2,681	.0028	.015	20,100	[illegible]00
Little Colorado, Ariz	7-27-40	2,037	.00725	.05-0.055	20,100	0
Trinity, Tex	5-06-50	[1] 5,547	.00055	.065-0.07	25,000±	[illegible]00
Wissahickon, Pa	2-26-62	577	.00158	(?)	2,460	2,880
Cullasaja, N.C	6-16-49	1,702	.00133	.07	8,450	11,400
Deckers, W. Va	4-13-48	391	.00573	.035	3,100	2,630
French Broad, N.C	8-28-49	2,312	.00079	.047	10,100	14,000
Croton, N.Y	3-31-51	726	.0103	.063	4,670	7,090
Cane, N.C	3-28-48	339	.0010	(?)	1,360	1,190
Hominy, N.C	6-16-49	1,219	.00179	.060	6,800	8,140
John Day, Oreg	5-23-48	2,896	.00188	.032	23,000	26,200
Millers, N.Y	3-22-48	912	.00438	.037	5,700	7,470
Mills, N.C	6-16-49	954	.00145	(?)	5,300	5,440
Neversink, N.Y	3-22-48	1,366	.00279	.035	10,100	11,000
Antelope, Nebr	6-17-54	85.4	.00278	(?)	445	277
Captina, Ohio	2-27-62	796	.00047	(?)	3,630	2,740
Antelope, Nebr	5-23-54	18.4	.0021	.029	45	33
Antelope tributary, Nebr	5-01-54	6.3	.0072	.063	10.8	12
Tenaya, Calif	5-17-50	170	.005	.034	886	833
Tenaya, Calif	5-16-50	184	.00202	.033	920	687
Merced, Calif	5-17-50	380	.0097	.067	1,990	2,950
Merced, Calif	5-17-50	464	.00453	.060	1,990	3,070
Merced, Calif	5-20-50	694	.0104	.088	3,950	6,690
Sulfur, Tenn	5-12-49	1,900	.00067	.050	10,100	[2] 10,100
Twelvepole, W. Va	2-14-48	2,496	.00045	.05+	9,350	12,300
San Gabriel, Calif	1-04-64	112	.00109	.032	211	283
Alder, Ariz	2-11-63	36.2	.0181	.067	117	152
Piru, Calif	7-24-62	66.6	.0042	.031	281	227
Cachuma, Calif	2-11-62	171	.0136	(?)	776	1,120
Sycamore, Ariz	2-11-63	240	.0064	.020	2,300	1,420
Salmon, N.Y	4-02-52	141	.0109	.05-0.066	676	814
Salmon, N.Y	4-08-52	136	.0109	.05-0.066	623	776
Salmon, Idaho	6-03-48	9,371	.00148	.040	101,000	114,000
Powder, Wyo	5-24-52	2,110	.00107	--------	22,000	[illegible],900
Salt, Nebr	5-09-50	3,704	.0005	(?)	29,200	700
Paradise, Wash	2-28-48	41.8	.0009	.030	90.4	66

[1] Main channel.
[2] Overflow (10 percent) not included.

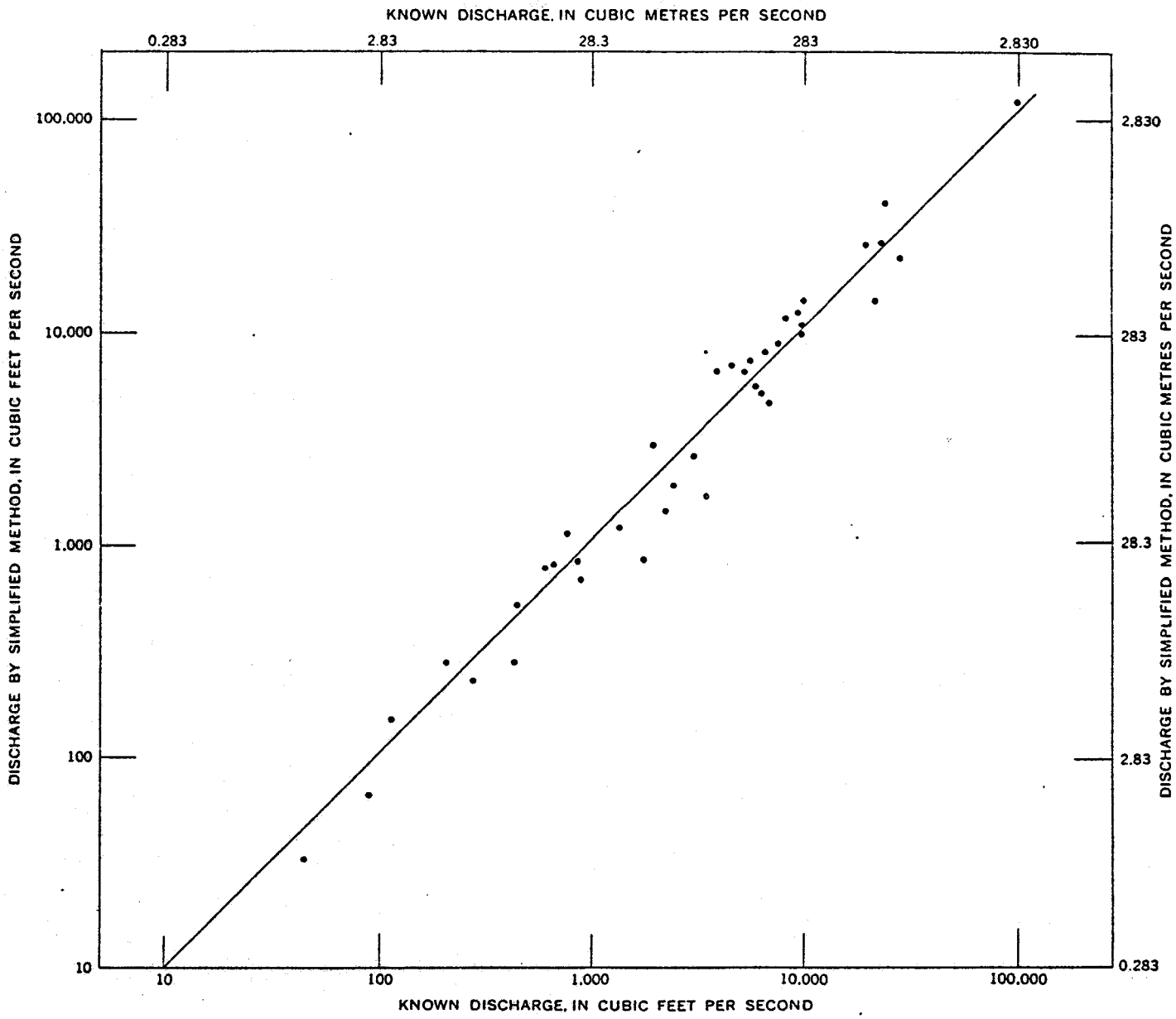

FIGURE 3.—Further evaluation of the simplified method (data from table 3).

based largely on channels in the Pacific Northwest and applies to full channels. Part-full discharges in these channels will be less than the discharges shown by the relation.

Study of the photographs of streams in Barnes' (1967) report should lead to the ability to recognize such stream channels. Figure 4 provides a reconnaissance tool for estimating discharge of near bankfull channels of this type; it is not the simplified method.

APPLICATION OF THE SIMPLIFIED METHOD

Criteria

The reach should be selected according to the same criteria used for a conventional slope-area measurement except that a uniform cross-sectional area throughout is preferable to a contracting reach. Ideally, the reach should be 4 or 5 channel widths long in order that the water-surface slope can be measured accurately. The method has been verified only for nearly full natural channels without substantial overbank flow and without backwater from constrictions or a flooding tributary. Thus it is recommended only for such channels at this time.

These criteria are not as restrictive as they may seem. Necessity often forces the use of the best available reach, which may have undesirable characteristics both for the simplified method and for the conventional slope-area method. Thus a reach which does not meet

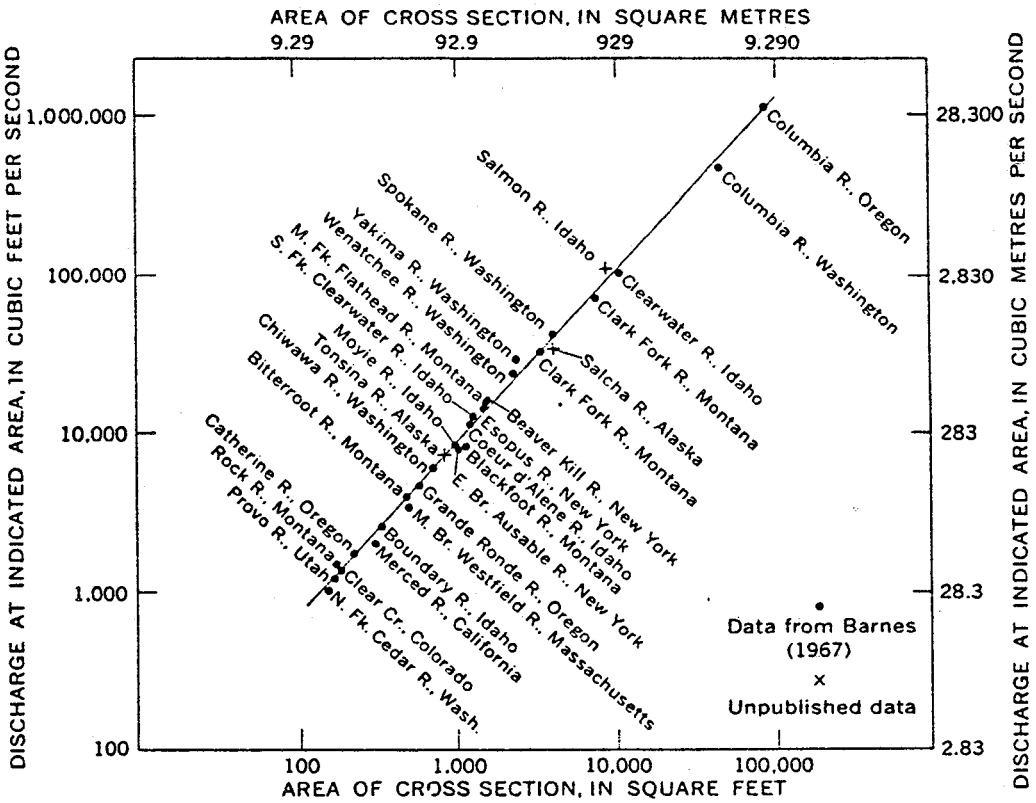

Figure 4.—Relation of discharge to channel cross-sectional area for full channels typified by those in Pacific Northwest.

the criteria is used when there is no better way to estimate the flood peak. Table 3 and figure 3 indicate the accuracy attainable by the simplified method from poor or unusual channel reaches.

Procedure

1. To determine peak discharge of a flood from high-water marks:
   (a) Define slope of water surface from high-water marks as a straight line throughout the reach.
   (b) Measure three cross sections so located that their average defines the average cross-sectional area in the reach.
   (c) Apply equation.
2. To determine discharge corresponding to a specific stage, either arbitrarily selected or from a few high-water marks:
   (a) Define water-surface slope as bed slope or slope of water surface at existing stream stage.
   (b) Project defined water-surface slope through specified stage.
   (c) Survey three cross sections and average the areas.
   (d) Apply equation.

Advantages

1. No subjective estimate of a roughness coefficient required; both cross-sectional area and slope ca be measured.
2. A water-surface profile based on high-water marl throughout the reach is desirable, but well-defin water-surface elevations at the ends of the rea may be adequate.
3. Computation of discharge is simple; and one a swer is obtained. There is little room for subje tive judgments either by the originator or by tl reviewer.
4. Two or more measurements at different stages the same reach will give consistent answers.
5. The method can be applied where only one hig water mark is found.
6. The method appears to give results comparable accuracy to those from the slope-area method f natural streams.

REFERENCES CITED

Barnes, H. H., Jr., 1967, Roughness characteristics of natu channels: U.S. Geol. Survey Water-Supply Pa 18 213 p.

Benson, M. A., and Dalrymple, Tate, 1968, General field and and office procedures for indirect discharge measurements: U.S. Geol. Survey Techniques Water-Resources Inv., book 3, chap. A1, 30 p.

Boyer, M. C., 1954, Estimating the Manning coefficient from an average bed roughness in open channels: Am. Geophys. Union Trans., v. 35, no. 6, pt. 1, p. 957–961.

Dalrymple, Tate, and Benson, M. A., 1967, Measurement of peak discharge by the slope-area method: U.S. Geol. Survey Techniques Water-Resources Inv., book 3, chap. A2, 12 p.

Graf, W. H., 1966, On the determination of the roughness coefficient in natural and artificial waterway: Internat. Assoc. Sci. Hydrology Bull., 11th year, no. 1, p. 59–68.

Limerinos, J. T., 1970, Determination of the Manning coefficient from measured bed roughness in natural channels: U.S. Geol. Survey Water-Supply Paper 1898–B, 47 p.

Riggs, H. C., 1974, Proposed hydrologic analyses of streamflow for Brazil: U.S. Geol. Survey open-file rept., 18 p.

Example of Simplified Slope - Area Method:

Use channel data from "Design of Small Dams" Fig. B-18, B-19, & B-21

$$\text{Average area} = \frac{208 + 209.1 + 224.6 + 206.9}{4} = 212.2 \text{ ft}^2$$

$$\text{Average slope} = \frac{16.35 - 13.73}{121 + 90 + 119} = \frac{2.62 \text{ ft}}{330 \text{ ft}} = .0079$$

$$\log Q = 0.366 + 1.33 \log A + 0.05 \log S - 0\ 056\ (\log s)^2$$

$$\log Q = 0.366 + 3.095 - 0.105 - 0.248$$

$$= 3.108$$

$$Q = 1{,}280 \text{ cfs}$$

The avg. Q by slope - area = 1380 cfs (Fig. B-21)

Example of Simplified Slope-Area Method:

Use channel data from "Design of Small Dams"

Fig. B-23 & Table B-8

Elevation	Area	Q
30	95 ft^2	360
35	400	2,420
40	753	5,600
45	1160	9,960
50	1610	15,400

$$\log Q = 0.366 + 1.33 \log A + 0.05 \log .00395 - 0.056 (\log .00395)^2$$

$$= -0.0776 + 1.33 \log A$$

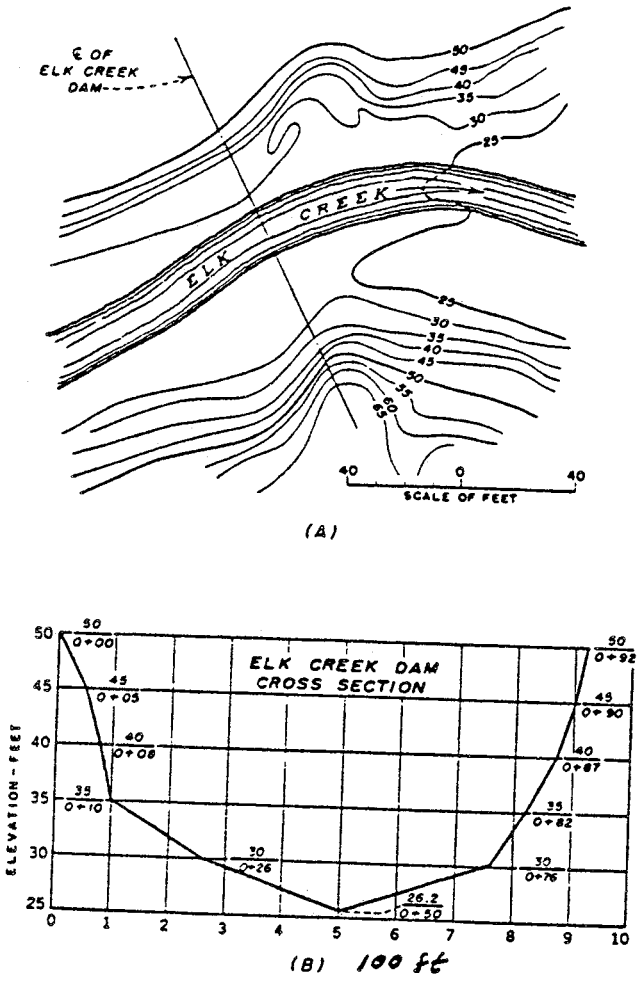

Figure B–22. Plan and cross section of Elk Creek Dam site 288–D–2832.

by Simplified Slope-Area

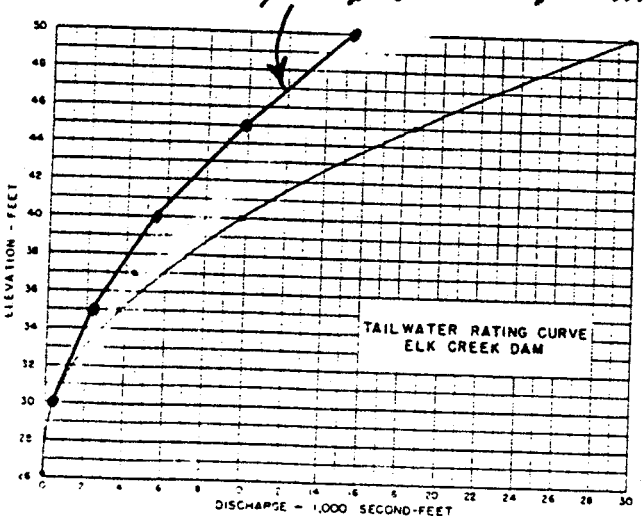

Figure B–23. Tailwater rating curve for Elk Creek Dam. 288–D–2560.

TABLE B–8.—*Computations for tailwater rating curve*
ELK CREEK DAM

Data: $n=0.030$ s_b=mean bed slope=0.00395

$$C=\frac{1.486}{n}=49.53 \quad s_b^{1/2}=0.0628$$

Elevation	a	p	r	$r^{2/3}$	C	Ka	$s_b^{1/2}$	Q
26.2	0	0	0	0	.....	.....	.....	.....
30	95	50.6	1.88	1.523	49.53	7,170	0.0628	450
35	400	75.1	5.32	3.047	49.53	60,400	.0628	3,790
40	753	87.6	8.60	4.198	49.53	156,000	.0628	9,800
45	1160	99.2	11.70	5.154	49.53	296,000	.0628	18,600
50	1610	111.7	14.40	5.919	49.53	472,000	.0628	29,600

by the one-half power of the mean bed slope to compute the discharge at each elevation. The tailwater rating curve derived from the computations is shown in figure B-23.

(b) *Water Surface Profile Method.*—In studies where more exact tailwater curves are required, water surface profiles may be developed for a range of discharges. The computations in such studies are more involved and require a series of cross sections downstream from the damsite.

Several methods [1, 2, 8, 9] have been developed for computing water surface profiles; however, this discussion will be limited to Bureau of Reclamation Method A. This method is adaptable to irregular channels having various roughness segments and large variations in cross-section geometry. It is limited to the assumption that flow paths between cross sections are equal in length for all roughness segments. Other methods [8, 9] must be used for variable travel distances.

In Method A, a number of cross sections are selected at intervals below the damsite. The selection of the cross-section locations is probably the most important factor in preparing a good study. The sections should be located so the average area, hydraulic radius, and n values of any two sections will be representative of the reach length between them. Channels that are alternately wide and narrow should have sections located in the narrow and wide points so the average condition can be defined. Special attention should also be given to locating a section at each point that indicates a definite change in grade or a control such as a natural constriction or bridge. The cross sec-

JOURNAL OF THE
HYDRAULICS DIVISION

Critical Flow in Rivers with Flood Plains

By Sylvester Petryk[1] and Edgar U. Grant,[2] Associate Members, ASCE

Introduction

Reasonably accurate evaluation of critical flow is required in a large variety of hydraulic projects including evaluation of flood control alternatives, prediction of channel erosion and deposition patterns, and determining correct operating conditions for hydraulic structures.

Critical flow is quantitatively defined by the "critical depth of flow," or simply "critical depth" that is measured with respect to the channel thalweg. It is conventionally taken as the depth that results in the minimum specific energy of flow. Experience has shown that this definition is satisfactory for canals and rivers with relatively steep banks. However, for rivers with flood plains, the specific energy curve can take on odd shapes where more than one minimum may occur.

This paper examines the problems encountered in evaluating the conventional critical depth. Example computations show that a composite channel can have at least two minimums in its specific energy curve. A study of physical flow characteristics in rivers with flood plains shows that this definition of critical depth is both inaccurate and lacks mathematical definition.

A new method of computing critical depth is proposed. Composite sections are used to compute the Froude number in each subsection. Critical depth is defined as the depth where the discharge weighted Froude number is equal to 1.00.

The corresponding computational procedure is presented in a form that is easily adaptable to existing backwater computer programs. Example computations are carried out for a river with its two flood plains. The numerical results of the proposed method are compared with the two existing conventional methods.

Note.—Discussion open until October 1, 1978. To extend the closing date one month, a written request must be filed with the Editor of Technical Publications, ASCE. This paper is part of the copyrighted Journal of the Hydraulics Division, Proceedings of the American Society of Civil Engineers, Vol. 104, No. HY5, May, 1978. Manuscript was submitted for review for possible publication on July 15, 1977.

[1]Sr. Hydr. Engr., Lalonde, Girouard, Letendre and Assocs., Montreal, Quebec, Canada.
[2]Design Engr., City of Tallahassee, Fla.

General.—Critical flow is the transition point between subcritical and supercritical flow. Subcritical and supercritical flows have radically different characteristics, particularly with respect to wave pattern and disturbance propagation properties (3). More appreciation for the difference between subcritical flow and supercritical flow is realized when one studies the hydraulic and aerodynamic analogy between: (1) Subcritical flow and subsonic flow; (2) supercritical flow and supersonic flow; and (3) critical flow and sonic flow.

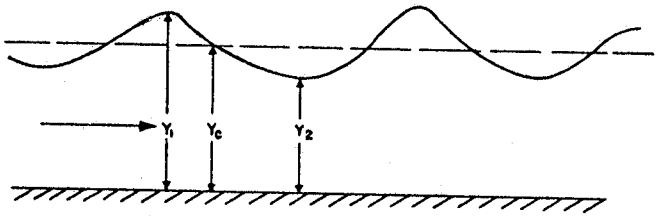

FIG. 1.—Unstable Critical Flow at Normal Depth

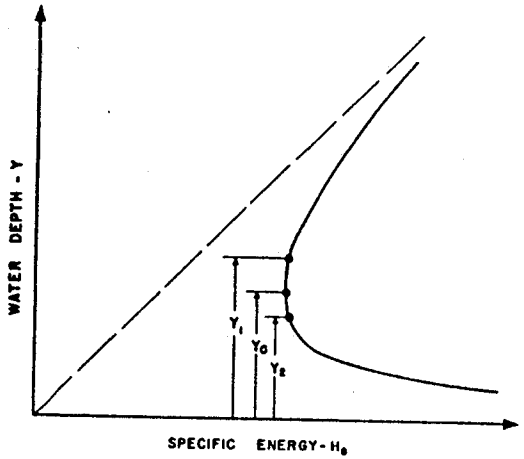

FIG. 2.—Specific Energy Curve Showing Unstable Critical Flow

In open channel flow, critical flow normally occurs only at certain points where transition from subcritical to supercritical or vice versa occurs. The transition from subcritical flow to supercritical is normally smooth such as in the case of flow over a broad crested weir. However, the transition from supercritical flow to subcritical flow is normally abrupt, taking place through a hydraulic jump, sometimes in a sudden well defined form and sometimes in a weak form through a series of undular waves.

Flow sustained for a long distance at or near critical depth has a very wavy pattern to it as shown on Fig. 1. Here in fact the flow is alternating from supercritical to subcritical in the form of a series of waves. The waves are relatively long and stable in position because of channel boundary irregularities

varying size. In fluvial channels the wave pattern changes because of channel ›undary changes with time. This wave pattern should not be confused with ıdular waves that may or may not have a hydrostatic pressure distribution, ıd that cause large fluctuations in discharge with time and position.

The reason for the unstable flow pattern at critical depth is shown in Figs. and 2. Small disturbances in the channel cause the flow to oscillate between ›nditions Y_1 and Y_2. The total energy of the flow with respect to the bottom the channel remains relatively constant while the depth oscillates between ıe subcritical Y_1 value and the supercritical Y_2 value. The oscillating flow creases friction losses and form losses as illustrated by Leopold, et al. (4). ı other words, the overall friction factor is higher for flows near critical depth ıan for flows completely subcritical or completely supercritical. This is particu- rly true in natural streams. As a result, critical flow in nature normally does ›t occur over long distances. It normally occurs at specific drops in the channel, ıd it is only in unusually steep mountain streams that one observes streams owing near critical or supercritical over long channel distances.

RITICAL FLOW IN SIMPLE CHANNEL

A "simple channel" here refers to an open channel flow condition where ıe velocity is reasonably uniform over the cross section and the energy coefficient close to unity. This contrasts with a typical alluvial river and its flood plain here the flow is best analyzed in a "composite channel" form. Here definable ıanges in velocity occur in subsections of the channel.

In a simple channel, the specific energy of flow is:

$$H_s = Y + \frac{Q^2}{2gA^2} \quad \text{(1)}$$

ı which Y = water depth; Q = discharge: G = gravitational constant; and = cross-sectionl area of flow. It should be emphasized that the energy coefficient assumed to be 1.00 in Eq. 1.

As shown in Fig. 2, it is well accepted that the critical condition occurs ı which H_s is a minimum or $dHs/dY = 0$. The critical condition, found by ifferentiating Eq. 1 with respect to Y, is:

$$\frac{Q^2 T}{gA^3} = 1 \quad \text{(2a)}$$

ı which T = top width of the channel. Alternatively, it is conventional to xpress the critical condition in Froude number form which is:

$$F_r = \frac{Q}{A\sqrt{g\frac{A}{T}}} = 1 \quad \text{(2b)}$$

ELATION OF CRITICAL DEPTH TO SLOPE OF ENERGY GRADE LINE

It is often important to understand what slope of energy grade line is required o produce critical flow depths. For example, it is good design practice to avoid

flows near critical depth over long distances in rock excavated channels because the wave action tends to dislodge rocks, and thus increases the erosion action beyond normal.

It will now be shown how, for a given discharge per unit width, the critical depth varies as a function of roughness and slope of the energy grade line.

Consider a wide channel flowing under gradually varying flow conditions at a critical flow section. The Manning formula conventionally gives the energy loss per unit length in the form:

$$\frac{q}{Y} = \frac{1.485}{n} Y^{2/3} S_e^{1/2} \quad \text{(3)}$$

in which q = discharge per unit width in cubic feet per second; Y = depth of flow in feet; n = Manning's n value; and S_e = slope of the energy gradeline.

The critical flow condition is:

$$\frac{q}{Y} = \sqrt{gY} \quad \text{(4)}$$

Equating Eq. 3 to Eq. 4 one obtains for the critical slope:

$$S_e = \frac{g n^2}{(1.485)^2 Y^{1/3}} \quad \text{(5)}$$

Eq. 5 shows that the critical slope is very sensitive to roughness factor n and weakly dependent on flow depth Y. It shows that the wide channels may flow critical or supercritical in the center of the channel and subcritical towards the banks where: (1) The depth is lower; and (2) the roughness is higher. Likewise, to study the variation of Froude number as a function of depth, roughness, and slope the Manning equation is divided by $\sqrt{gY}$ or

$$F_r = \frac{\frac{q}{Y}}{\sqrt{gY}} = \frac{1.485\, Y^{1/6} S^{1/2}}{n\sqrt{g}} \quad \text{(6)}$$

From a Froude number point of view the right-hand side of Eq. 6 says that the Froude number is higher in the center of a wide channel because its depth is higher and its vegetation roughness is lower than near the banks.

The conclusions agree with what is normally observed in nature, particularly during flood flow. Fig. 3 shows a typical example. The higher Froude number of the flow in the center of the channel causes large waves in the center of the channel as the flow tends to approach critical.

CRITICAL FLOW IN COMPOSITE CHANNEL SECTIONS

Composite channel analysis is normally used where a total flow cross section can be broken down into different subsections, each having a different mean velocity. Flood flow through rivers with flood plains is typically evaluated by composite sections.

Normally the river channel is treated as one subsection, and the two flood plains are subdivided into two or more subsections. This analysis is often

conveniently treated in computer form, such as offered in excellent computer programs developed by the Corps of Engineers' Hydrologic Engineering Center (6) and the Soil Conservation Service (5).

Eq. 6 shows that the Froude number in the channel will be much higher than in the flood plain for two main reasons: (1) The mean depth is higher in the channel; and (2) the flood plain roughness is normally higher. Therefore, critical flow will almost always occur in the channel before the flood plain.

From a critical flow point of view, the preceding examination illustrates that subsections of a channel tend to behave independently of each other, just as they are often considered independent for flow resistance analysis.

Problems with Existing Computational Procedures

Existing computational methods determine critical depths by one of two analytical procedures. The first procedure treats the channel and flood plain together as a simple channel section, and Eqs. 1, 2*a* or 2*b* are applied. As

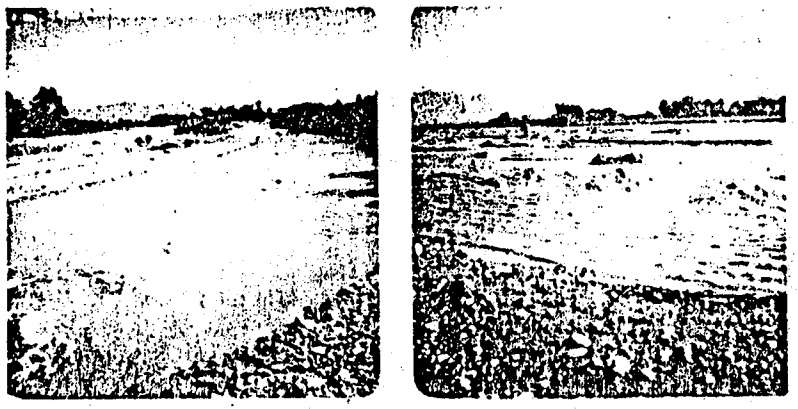

FIG. 3.—Flow Instability in Central Part of Channel

examined in Ref. 5, large errors can occur in the evaluated critical depth because the velocity in the flood plain is assumed to be the same as in the channel. From Eqs. 2*a* and 2*b*, it is seen that multiple critical depths can occur for one given discharge. At a relatively low depth the flow may be defined as critical because the area of flow A is small in relation the top width T. At another relatively high depth, the flow may also be defined as critical where the top width T is very large, and thus the area of flow can also be very large.

The second procedure uses composite channel sections with the specific energy equation

$$H'_s = Y + \frac{\alpha Q^2}{2gA^2} \quad (7)$$

in which α = energy coefficient; it is computed from the conveyance in each subsection, as described in detail by Chow (1). The critical depth is calculated

from the minimum value in H'_s, as detailed by Eichert (2).

Each of the preceding computational procedures can result in unrealistically high evaluated critical depths. Also, more than one depth can be defined as critical; physically this is practically impossible in nature, and highly undesirable and difficult from a computational point of view.

Proposed Method

The proposed method of computing critical depth in a river and its flood plain is based on the following considerations:

1. The composite channel method is used to subdivide the discharge and velocity in the major channel and its subsections. This implies that the slope of the energy gradeline is the same in the major channel as in the overbank sections. This also implies that changes in the channel sections are not abrupt in plan or profile, or both.
2. The Froude number in the major channel is independent of the Froude number in the overbank sections. Each value is dependent on the total discharge, conveyance value of each section, and slope of the energy grade line.
3. For a fixed energy grade-line slope, the flow becomes critical at each subsection at different elevations. Normally, the flow in the river channel becomes critical at the lowest elevation while the overbank sections are subcritical. As the water level rises the Froude number increases in all subsections, the flow becomes supercritical in the river channel while the flow in overbank sections remains subcritical until it too reaches the critical condition. In other words, there is a critical elevation for each subsection.
4. The existing known open channel backwater and flood routing procedures work with only one overall critical depth, defined for the river and its overbank sections. Therefore, it is necessary to find one overall depth which can be defined as critical for computational purposes. In fact, at this critical depth, some of the subsections will be flowing subcritical and some of the subsections will be flowing supercritical. Until detailed experimental data becomes available, the following discharge weighted Froude number model is proposed.

$$QF_r = Q_1 F_{r1} + Q_2 F_{r2} + Q_3 F_{r3} + \ldots \quad (8)$$

in which Q = total discharge; F_r = overall channel cross section Froude number; Q_i = discharge in the ith subsection; and F_{ri} = Froude number in the ith subsection.

The overall Froude number is found from Eq. 8 to be:

$$F_r = \frac{\sum_{i=1}^{N} Q_i F_{ri}}{Q} \quad (9)$$

And the critical elevation occurs when $F_r = 1$, or

$$1 = \frac{\sum_{i=1}^{N} Q_i F_{ri}}{Q_c} \quad (10)$$

in which Q_c = the critical discharge at a given depth.

The total critical discharge is:

$$Q_c = \sum_{i=1}^{N} Q_i \quad \text{or} \quad Q_c = \sum_{i=1}^{i=N} K_i S_c^{1/2} \qquad (11)$$

in which K_i = conveyance in the ith subsection at given elev tion; and S_c = overall critical slope of the energy gradeline where the wei ted Froude number is equal to 1.00.

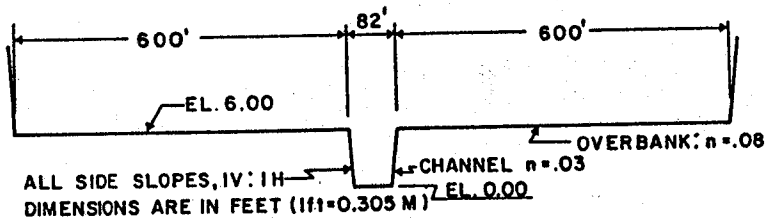

FIG. 4.—Example River Cross Section

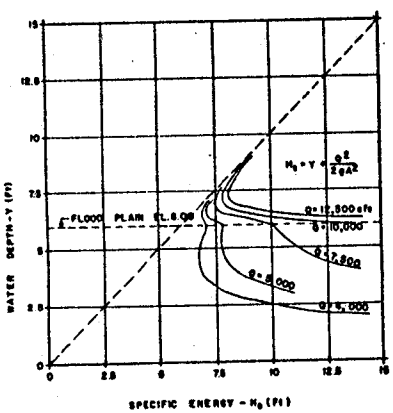

FIG. 5.—Specific Energy Curves—Simple Section Method (1 ft = 0.305 m; 1 cfs = 0.0283 m³/s)

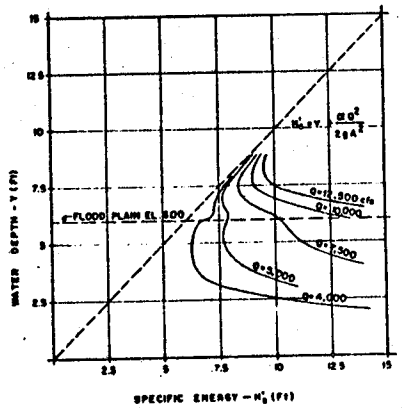

FIG. 6.—Specific Energy Curves—Composite Section Method (1 ft = 0.305 m; 1 cfs = 0.0283 m³/s)

By equating Eqs. 10 and 11, one obtains

$$S_c^{1/2} \sum_{i=1}^{N} K_i = \sum_{i=1}^{N} Q_i F_{ri} \qquad (12)$$

in which the Froude number in each subsection is

$$F_{ri} = \frac{Q_i}{A_i \sqrt{\dfrac{gA_i}{T_i}}} \qquad (13)$$

By combining Eqs. 12 and 13 the critical slope is found to be

$$S_c = g \left(\frac{\sum_{i=1}^{i=N} K_i}{\sum_{i=1}^{i=N} \dfrac{K_i^2 T_i^{1/2}}{A_i^{3/2}}} \right)^2 \qquad (14)$$

The total critical discharge at a given elevation is found from Eq. 11 to be

$$Q_c = \frac{g^{1/2} \left(\sum_{i=1}^{i=N} K_i \right)^2}{\sum_{i=1}^{i=N} \dfrac{K_i^2 T_i^{1/2}}{A_i^{3/2}}} \qquad (15)$$

If the Manning formula in the English system is used to express conveyance K_i, Eq. 14 reduces to

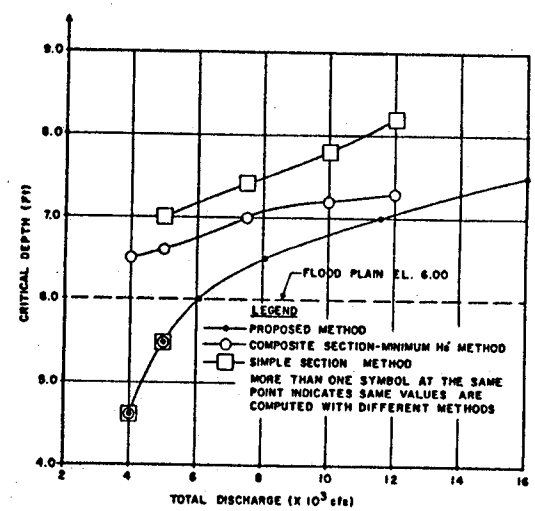

FIG. 7.—Comparison of Computation Methods for Critical Flow (1 ft = 0.305 m; 1 cfs = 0.0283 m³/s)

$$S_c = 14.60 \left(\frac{\sum_{i=N}^{i=N} \dfrac{A_i^{5/3}}{n_i P_i^{2/3}}}{\sum_{i=1}^{i=N} \dfrac{A_i^{11/6} T_i^{1/2}}{n_i^2 P_i^{4/3}}} \right)^2 \qquad (16)$$

And the critical discharge is expressed as:

$$Q_c = \frac{5.67 \left(\sum_{i=N}^{i=N} \dfrac{A_i^{5/3}}{n_i P_i^{2/3}} \right)^2}{\sum_{i=N}^{i=N} \dfrac{A_i^{11/6} T_i^{1/2}}{n_i^2 P_i^{4/3}}} \qquad (17)$$

Sample Calculation

Fig. 4 shows a sample cross section that will be used to illustrate the computations. It is simple to analyze, and representative of some of the sections found on Back Creek, Virginia.

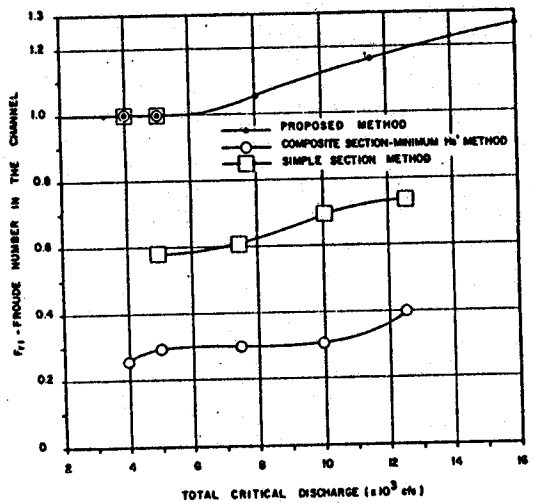

FIG. 8.—Comparison of Computed Froude Numbers in Channel (1 cfs = 0.0283 m³/s)

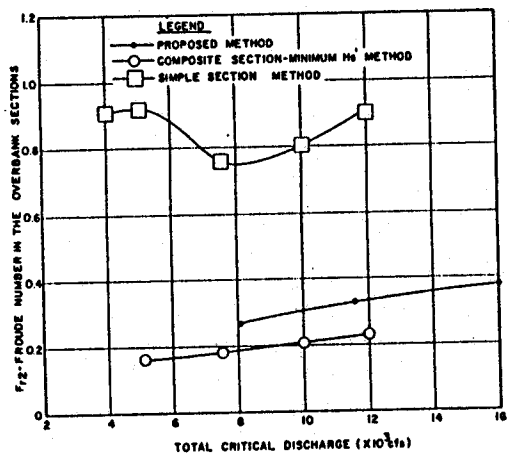

FIG. 9.—Comparison of Computed Froude Numbers in Overbank Sections (1 cfs = 0.0283 m³/s)

Fig. 5 shows the specific energy curves for five discharges when the specific energy is based on the simple channel method where the velocity in the flood plain is assumed the same as in the river channel, clearly a poor model in this case. For the discharges between 4,000 cfs and 5,000 cfs (113 m³/s and

142 m³/s) two minimums in the specific energy curve occur. For example, at 4,000 cfs (113 m³/s), the two critical depths are 4.6 ft (1.40 m) and 6.5 ft (1.98 m). The latter is over 40% deeper than the first one.

Fig. 6 shows the specific energy curves plotted according to Eq. 7 with α evaluated according to composite cross section method. Here the velocity distribution is reasonably accurately represented. However, if critical flow is based on the minimum in the specific energy curves, one again obtains two critical depths 5.5 ft (1.68 m) and 7.0 ft (2.14 m), or a difference of about 25% in the critical depth of flow at a discharge of 5,000 cfs (142 m³/s). The corresponding differences in the critical slopes are more than two times the preceding error in critical depth.

Fig. 7 presents the critical depths according to the proposed method, and compares the results with the two existing conventional methods. The computational advantage of the proposed method is that only one critical depth can be evaluated for a given discharge.

At the computed critical flow conditions, Figs. 8 and 9 present the Froude numbers in the channel and the overbank sections for the three methods of analysis. For the two conventional methods, with overbank flow, the Froude numbers in the main channel and overbank sections were always less than one. For the proposed method, the Froude numbers in the main channel were greater than one while the Froude numbers in overbank were less than 1.

These results show that the existing conventional computational methods can result in excessively high critical depths. The proposed method results in lower and more reasonable computed critical depths. Here some of the flow is normally supercritical in the channel and some of the flow is subcritical in the overbank sections.

Detailed experimental work would be very valuable to confirm the proposed method or derive a better critical flow model.

Future research may enable hydraulicians to use the composite section method directly in backwater and flood routing computations. In such a model, supercritical flow could exist in the main channel while subcritical flow would exist in the overbank sections. No single critical depth would occur for the whole cross section, but each subsection would have its own critical depth, as water flow computations proceed along the river.

Summary and Conclusion

The two existing conventional methods of computing critical depths are based on the minimum specific energy method. For typical rivers with adjoining flood plains, two major problems may result. The first one is that more than one minimum can occur in the specific energy curves. Example computations show that the difference between the two minimums may result in critical depths which differ by 25% to 40%. The second problem is that existing computational methods can produce excessively high critical depths in which the Froude number in each subsection of the channel is substantially less than 1.00.

A new method for computing critical flow conditions is proposed. It defines critical flow as the condition in which the discharge weighted Froude number is equal to 1.00. That is, at the critical water surface elevation, some of the

subsections are flowing at supercritical flow and some of sections are flowing at subcritical flow.

Equations are developed for the proposed method which can easily be applied to existing computer backwater programs. For composite section channels, the proposed results are much easier to apply than the minimum specific energy method. At the same time, the previously mentioned problems with existing conventional methods are eliminated.

Example computations are carried out for a typical river and flood plain. They illustrate the proposed computational procedure, and compare the results obtained by the three methods of analysis.

Acknowledgments

The writers are grateful to John E. Priest for bringing the problem to the writers' attention, to Harza Engineering Co., and University of Florida for supporting the work, and to Lalonde, Girouard, Letendre and Associates for preparing the document in final form.

Appendix I.—References

1. Chow, V. T., *Open Channel Hydraulics*, McGraw-Hill Book Co., Inc., New York, N.Y., 1959.
2. Eichert, B. S., "Critical Water Surface by Minimum Specific Energy Using the Parabolic Method," Hydrologic Engineering Center, Sacramento, Calif.
3. Henderson, F. M., *Open Channel Flow*, 3rd ed., The Macmillan Co., New York, N.Y., 1969.
4. Leopold, L. B., et al., "Flow Resistance in Sinuous or Irregular Channel," Geological Survey Professional Paper 282-D, 1960.
5. Maclay, R. E., "WSP2-Water Surface Profile Program, User's Guide," Soil Conservation Service, Washington, D.C., Nov., 1973 (Distributed by National Technical Information Service under No. PB-233-774).
6. *Water Surface Profiles*, Hydrologic Engineering Center, Corps of Engineers, Computer Program 723-X6 L202A, Sacramento, Calif., 1973.

Appendix II.—Notation

The following symbols are used in this paper:

A = total cross-sectional area of flow;
F_r = Froude number of flow;
g = gravitational constant (32.2 ft/sec^2);
H_s = specific energy of flow based on simple channel section method;
H'_s = specific energy of flow based on composite section method;
i = subscript, refers to ith channel subsection of total cross section;
K = conveyance of channel subsection at given water surface elevation;
P = wetted perimeter of flow;
Q = total discharge;
Q_c = critical discharge for given water surface elevation;
q = discharge per unit of width;
S = slope of energy grade line;
S_c = critical slope of energy grade line;

T = top width of channel section, or subsection, at given water surface elevation;
Y = depth of flow; and
α = energy coefficient.

Geo Labol

GENERALIZED COMPUTER PROGRAM

HEC-2
WATER SURFACE PROFILES

USERS MANUAL

JANUARY 1981

HEC HYDROLOGIC ENGINEERING CENTER

Water Resources Support Center U.S. Army Corps of Engineers

HEC-2
WATER SURFACE PROFILES
USERS MANUAL

Chapter 1

INTRODUCTION

1. PROGRAM DEVELOPMENT

The HEC-2 computer program was developed in the Hydrologic Engineering Center by Bill S. Eichert. The version documented herein, dated November 1976, is intended to replace all earlier versions. The basic computational capabilities for calculating water surface profiles and the data input requirements remain essentially unchanged. However, capabilities have been added for a) encroachment analysis (methods 5 and 6), b) summarizing output with pre-defined or user-defined summary tables, c) creating a permanent record of study results on an "archival" tape and d) calculating friction loss with one of five alternative approaches. The version also has reduced storage requirements and increased potential for usage on interactive computer terminals.

2. OVERVIEW OF PROGRAM CAPABILITIES

The program is intended for calculating water surface profiles for steady gradually varied flow in natural or man-made channels. Both subcritical and supercritical flow profiles can be calculated. The effects of various obstructions such as bridges, culverts, weirs, and structures in the flood plain may be considered in the computations. The computational procedure is based on the solution of the one-dimensional energy equation with energy loss due to friction evaluated with Manning's equation. The computational procedure is generally known as the Standard Step Method. The program is also designed for application in flood plain management and flood insurance studies to evaluate floodway encroachments and to designate flood hazard zones. Also, capabilities are available for assessing the effects of channel improvements and levees on water surface profiles. Input and output units may be either English or Metric.

3. SUPPLEMENTARY PROGRAMS

A data edit program (EDIT-2) which checks the data cards for various input errors is available. EDIT-2 is described in Appendix VIII.

A Fortran graphics program (Hydraulics Graphics Package) which produces HEC-2 cross section and profile plots in interactive or batch modes is also available. Documentation for the Hydraulics Graphics Package may be obtained from the Hydrologic Engineering Center.

4. COMPUTER EQUIPMENT REQUIREMENTS

The HEC-2 computer program was written for use on the CDC 6600, but may be used with little or no change on most medium to large computers such as the IBM 370 and UNIVAC 1108. The following table shows approximate memory requirements and compilation and execution times for various computers.

TABLE 1
COMPUTER MEMORY AND TIME REQUIREMENTS

Computer	Memory Requirement Words (Decimal)	Time Requirements: Compile	Time Requirements: Standard Tests* Execution
CDC 7600	32000	3.9 sec	3.7 sec
CDC 6600	32000	24.1 sec	22.3 sec
UNIVAC 1108	32000	35.0 sec	35.0 sec
IBM 370/168	1/	121.4 sec	27.0 sec
HONEYWELL CS6058	46000	59.6 sec	85.7 sec
HARRIS S120	96000 2/	6 min 42.0 sec	74.0 sec

*Standard Tests are contained in Exhibit 1 of the HEC-2 Water Surface Profiles, Programmers Manual, November 1976.

1/ OS/VS2; 248 K bytes virtual memory

2/ 3 bytes/word

Chapter 2

THEORETICAL BASIS FOR PROFILE CALCULATION

1. GENERAL

This section describes methodology used in HEC-2 for the calculation of water surface profiles. Topics discussed include equations used for basic profile calculation, cross section subdivision for determining conveyance and velocity distribution, friction loss evaluation, iterative procedure for solving the basic equations and critical depth determination. Computational methodology for calculating flow through bridges is presented in Appendix IV. Methodology used by HEC-2 to determine and evaluate flood plain encroachments is contained in Appendix II.

2. EQUATIONS FOR BASIC PROFILE CALCULATION

The following two equations are solved by an iterative procedure (the standard step method) to calculate an unknown water surface elevation at a cross section:

$$WS_2 + \frac{\alpha_2 V_2^2}{2g} = WS_1 + \frac{\alpha_1 V_1^2}{2g} + h_e \qquad (1)$$

$$h_e = L\,\bar{S}_f + C \left| \frac{\alpha_2 V_2^2}{2g} - \frac{\alpha_1 V_1^2}{2g} \right| \qquad (2)$$

where:

WS_1, WS_2	=	water surface elevations at ends of reach (see Figure 1)
V_1, V_2	=	mean velocities (total discharge ÷ total flow area) at ends of reach
α_1, α_2	=	velocity coefficients for flow at ends of reach
g	=	acceleration of gravity
h_e	=	energy head loss
L	=	discharge-weighted reach length
$\bar{S}_f$	=	representative friction slope for reach
C	=	expansion or contraction loss coefficient

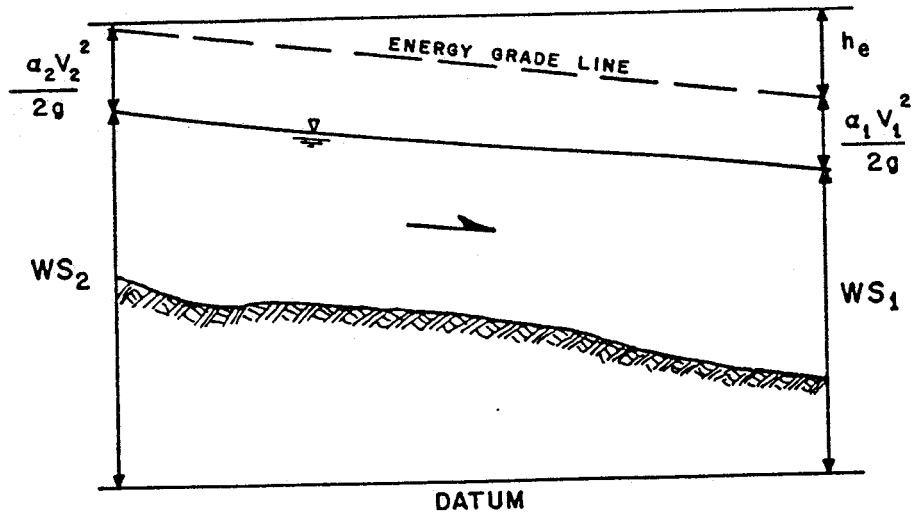

Figure 1. Representation of Terms in Energy Equation

The discharge-weighted reach length, L, is calculated as:

$$L = \frac{L_{lob}\bar{Q}_{lob} + L_{ch}\bar{Q}_{ch} + L_{rob}\bar{Q}_{rob}}{\bar{Q}_{lob} + \bar{Q}_{ch} + \bar{Q}_{rob}} \qquad (3)$$

where:

L_{lob}, L_{ch}, L_{rob} = reach lengths specified for flow in the left overbank, main channel and right overbank, respectively

$\bar{Q}_{lob}$, $\bar{Q}_{ch}$, $\bar{Q}_{rob}$ = arithmetic average of flows at the ends of the reach for the left overbank, main channel, and right overbank, respectively

Determination of a representative friction slope, $\bar{S}_f$, is discussed in Section 4. Selection of appropriate magnitudes for expansion and contraction coefficients is discussed in Chapter 2, Section 5 and Appendix IV.

3. CROSS SECTION SUBDIVISION

The determination of total conveyance and the velocity coefficient for a cross section requires that flow be subdivided into units for which the velocity is uniformly distributed. The approach used in HEC-2 is to subdivide flow in the overbank areas using the input cross section stations (X-coordinates) as the basis for subdivision. Conveyance is calculated within each subdivision by the equation (based on English units):

$$k = \frac{1.486}{n} a r^{2/3} \tag{4}$$

where:

k = conveyance for subdivision

n = Manning's 'n' for subdivision

a = flow area for subdivision

r = hydraulic radius for subdivision (area divided by wetted perimeter)

Flow in the main channel is not subdivided in normal applications. The total conveyance for the cross section is obtained by summing the incremental conveyances.

The velocity coefficient, α, is obtained with the following equation:

$$\alpha = \frac{(A_t)^2 \left[(K_{lob})^3/(A_{lob})^2 + (K_{ch})^3/(A_{ch})^2 + (K_{rob})^3/(A_{rob})^2\right]}{(K_t)^3} \tag{5}$$

where:

A_t = total flow area of cross section

A_{lob}, A_{ch}, A_{rob} = flow areas of left overbank, main channel and right overbank, respectively

K_t = total conveyance of cross section

K_{lob}, K_{ch}, K_{rob} = conveyances of left overbank, main channel and right overbank, respectively

4. FRICTION LOSS EVALUATION

Friction loss is evaluated in HEC-2 as the product of $\bar{S}_f$, and L, where $\bar{S}_f$ is the representative friction slope for a reach and L is defined with equation (3). Alternative expressions for $\bar{S}_f$ available in HEC-2 are as follows:

Average Conveyance Equation

$$\bar{S}_f = \left(\frac{Q_1 + Q_2}{K_1 + K_2} \right)^2 \qquad (6)$$

Average Friction Slope Equation

$$\bar{S}_f = \frac{S_{f_1} + S_{f_2}}{2} \qquad (7)$$

Geometric Mean Friction Slope Equation

$$\bar{S}_f = \sqrt{S_{f_1} \cdot S_{f_2}} \qquad (8)$$

Harmonic Mean Friction Slope Equation

$$\bar{S}_f = \frac{2\, S_{f_1} \cdot S_{f_2}}{S_{f_1} + S_{f_2}} \qquad (9)$$

Equation (6), which has been used in HEC-2 since 1971, is the 'default' equation used by the program; that is, it is used automatically unless use of a different equation is requested by input. The program also contains an option by which one of the above equations is automatically selected on a reach by reach basis depending on flow regime and profile type (e.g., S1, M1, etc.). Further discussion of the alternative methods for evaluating friction loss is contained in Chapter 4, Optional Capabilities.

5. COMPUTATION PROCEDURE

The unknown water surface elevation at a cross section is determined by an iterative solution of equations (1) and (2). The computational procedure is as follows:

1. Assume a water surface elevation at the upstream cross section (or downstream cross section if a supercritical profile is being calculated).

2. Based on the assumed water surface elevation, determine the corresponding total conveyance and velocity head.

3. With values from step 2, compute $\bar{S}_f$ and solve equation (2) for h_e.

4. With values from steps 2 and 3, solve equation (1) for WS_2.

5. Compare the computed value of WS_2 with the values assumed in step 1; repeat steps 1 through 5 until the values agree to within .01 feet (or .01 meters).

Criteria used to assume water surface elevations in the iterative procedure varies from trial to trial. Generally the first trial is based on projecting the previous cross section's water surface elevation on the average of the friction slopes from the previous two cross sections. The second trial is an arithmetic average of the computed and assumed elevations from the first trial. The third and subsequent trials are generally based on a "secant" method of projecting the rate of change of the difference between computed and assumed elevations for the previous two trials to zero. The change from one trial to the next is constrained to a maximum of ±50% of the assumed depth from the previous trial.

Once a 'balanced' water surface elevation has been obtained for a cross section, checks are made to ascertain that the elevation is on the 'right' side of the critical water surface elevation (e.g., above the critical elevation if a subcritical profile is being calculated). If the balanced elevation is on the 'wrong' side of the critical water surface elevation, critical depth is assumed for the cross section and a message to that effect is printed by the program. The program user should be aware of critical depth assumptions and determine the reasons for their occurrence, because in many cases they result from reach lengths being too long or from misrepresentation of the effective flow areas of cross sections.

For a subcritical profile, a preliminary check for proper flow regime involves the following equation:

$$\left(\frac{V^2}{2g}\right)_{test} = \frac{A_t}{2T} \qquad (10)$$

where:

$\left(\frac{V^2}{2g}\right)_{test}$ = velocity head that would exist if critical conditions existed at the balanced water surface elevation and $\alpha = 1$.

A_t = total flow area

T = water surface width

If the calculated velocity head, $\alpha \frac{V^2}{2g}$, is less than 94% of $\left(\frac{V^2}{2g}\right)_{test}$ the balanced water surface elevation will be accepted for the cross section. If the calculated velocity head is greater than 94% of the test value, the critical water surface elevation will be determined (by a procedure discussed in section 6) so that a direct comparison of balanced elevation versus critical elevation can be made.

For a supercritical profile, critical depth is automatically calculated for every cross section, which enables a direct comparison between balanced and critical elevations.

6. CRITICAL DEPTH DETERMINATION

Critical depth for a cross section will be determined if any of the following conditions are satisfied:

(1) The supercritical flow regime has been specified.

(2) Calculation of critical depth has been requested with the program's critical depth option.

(3) This is the first cross section and critical depth starting conditions have been specified.

(4) The critical depth check for a subcritical profile indicates that critical depth needs to be determined to verify the flow regime associated with the balanced elevation.

The total energy head for a cross section is defined by:

$$H = WS + \frac{\alpha V^2}{2g} \qquad (11)$$

where:

H = total energy head

WS = water surface elevation

$\frac{\alpha V^2}{2g}$ = velocity head

The critical water surface elevation is the elevation for which the total energy head is a minimum. The critical elevation is determined with an iterative procedure whereby values of WS are assumed and corresponding values of H are determined with equation (11) until a minimum value for H is reached.

To speed the iteration process, a parabolic interpolation procedure is followed. The procedure basically involves determining values of H for three values of WS that are spaced at equal ΔWS intervals. The WS corresponding to the minimum value for H defined by a parabola passing through the three points (on the H versus WS plane) is used as the basis for the next assumption of a value for WS.

It is presumed that critical depth has been obtained when there is less than a 2.5% change in depth from one iteration to the next and provided the energy head has either decreased or has not increased by more than .01 feet. The tolerance of 2.5% may be changed by program input.

7. PROGRAM LIMITATIONS

The following assumptions are implicit in the analytical expressions used in the program:

(1) Flow is steady

(2) Flow is gradually varied

(3) Flow is one dimensional (i.e., velocity components in directions other than the direction of flow are not accounted for)

(4) River channels have 'small' slopes, say less than 1:10

Flow is assumed to be steady because time-dependent terms are not included in the energy equation (1). Flow is assumed to be gradually varied because equation (1) is based on the premise that a hydrostatic pressure distribution exists at each cross section. Flow is assumed to be one-dimensional because equation (4) is based on the premise that the total energy head is the same for all points in a cross section. Small channel slopes are assumed because the pressure head which is a component of WS in equation (1) is represented by the water depth measured vertically.

The program does not have the capability to deal with movable boundaries (i.e., sediment transport) and requires that energy losses be definable with the terms contained in equation (2) or by using criteria described in Appendix IV for bridge, culvert or weir flow.

Chapter 3

BASIC DATA REQUIREMENTS

1. GENERAL

A major portion of the programming in HEC-2 is devoted to providing a large variety of input and data manipulation options. The program objective is quite simple -- compute water surface elevations at all locations of interest for given flow values. The data needed to perform these computations include: flow regime, starting elevation, discharge, loss coefficients, cross section geometry, and reach lengths. The options available for providing and manipulating input are discussed in the following sections.

2. FLOW REGIME

Profile computations begin at a cross section with known or assumed starting conditions and proceed upstream for subcritical flow or downstream for supercritical flow. The direction of flow is specified on the J1 card (first job card) by setting variable IDIR equal to one for supercritical flow or zero (or blank) for subcritical flow. Subcritical profiles computed by the program (IDIR = 0) are constrained to critical depth or above, and supercritical profiles (IDIR = 1) are constrained to critical depth or below. The program will not allow profile computations to cross critical depth except for certain bridge analysis problems. In cases where flow passes from one flow regime to another as shown in Figure 2 below, it is necessary to compute the profile twice, alternately assuming subcritical and supercritical flow. Results of a subcritical profile, (shown as ⊙ in Figure 2) computed for the example stream would plot at critical depth (above the actual water surface profile) in the steep reach of stream. Results from a supercritical profile computation (shown as x in Figure 2)

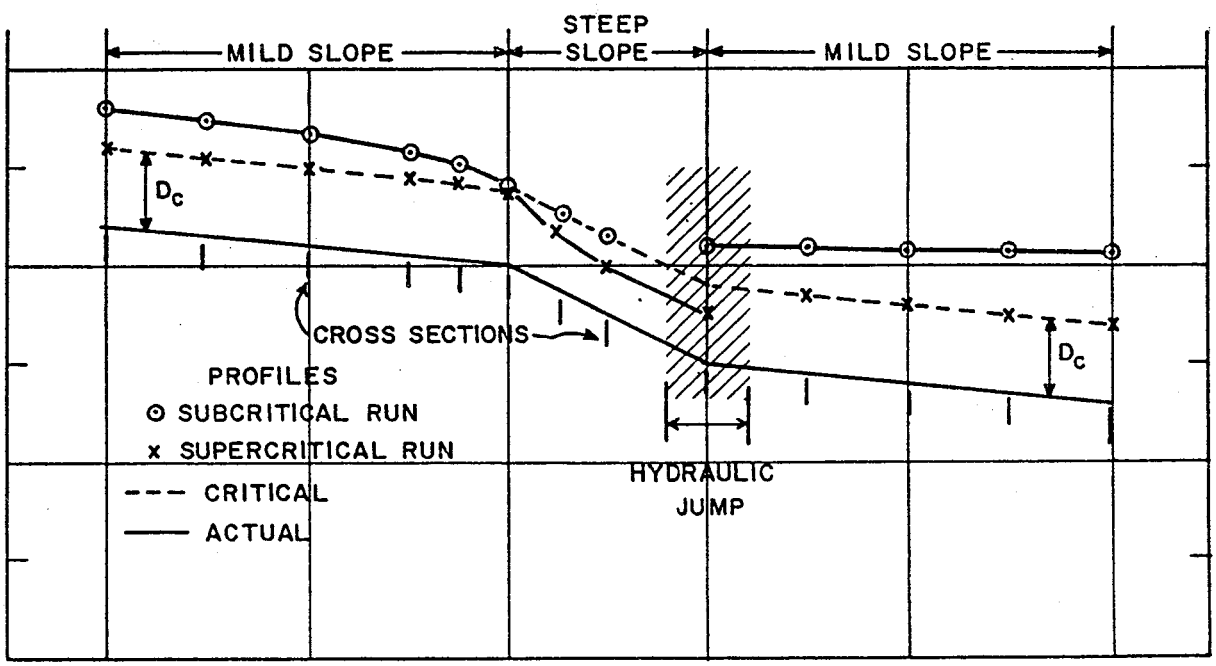

Figure 2. Profiles Calculated for Subcritical and Supercritical Flows

would plot at critical depth (below the actual water surface profile) for both mild reaches of the stream. The final plotted profile should incorporate computed results from both computations and an analysis of the hydraulic jump. HEC-2 does not contain the capability to determine the position of the hydraulic jump or energy losses associated with the jump.

3. STARTING ELEVATION

The water surface elevation for the beginning cross section may be specified in one of three ways: (1) as critical depth, (2) as a known elevation, (3) by the slope area method. By setting the variable STRT on the J1 card equal to minus one, critical depth will be computed and used as the starting water surface elevation. This method is appropriate at locations where critical or near critical conditions are known to exist for the range of discharges being computed, e.g., a waterfall, weir or a section of rapids. When a rating curve is available, the appropriate starting elevation can be specified by variable WSEL on the J1 card.

For beginning by the slope area method, STRT is set equal to the estimated slope of the energy grade line (must be a positive value) and WSEL is used as the initial estimate of the water surface elevation. The flows computed for the fixed slope are compared with the starting flow and the depth is adjusted until the computed flow is within one percent of the starting flow. The water surface elevation thus determined is used as the starting water surface elevation for subsequent water surface profile computations.

4. DISCHARGE

Discharge may be specified and altered in several ways. Variable Q on the first job card (J1 card) to specify the starting discharge for single profile runs. When it is desired to change the discharge for a single profile run, the variable QNEW on the X2 card can be used to permanently change the discharge at any cross section.

An alternate procedure utilizes the QT cards (discharge table) and may be used to specify from one to nineteen discharge values for single or multiple profile runs. QT cards may be used to specify starting discharges and to permanently change discharges at any cross section in a data set. Variable INQ on the J1 card directs the program to the field of the QT card that contains the discharge for that profile. When a value of FQ is entered, all discharges on the X2 cards and discharges in the specified INQ of the QT cards are multiplied by the value.

5. ENERGY LOSS COEFFICIENTS

Several types of loss coefficients are utilized by the program to evaluate head losses: (1) Manning's 'n' values for friction loss, (2) contraction and expansion coefficients to evaluate transition (shock) losses, and (3) bridge loss coefficients to evaluate losses related to weir shape, pier configuration, and pressure flow.

Because Manning's coefficient of roughness 'n' depends on such factors as type and amount of vegetation, channel configuration and stage; several options are available to vary 'n'. When three 'n' values are sufficient to describe the channel and overbank roughness, the first three fields of the NC card ('n' value change) are used. Any of the 'n' values may be permanently changed at any cross section by using another NC card. Often three values are not enough to adequately describe the lateral roughness variation in the cross section in which case the NH card ('n' value - horizontal) is used. The number of 'n' values used to describe the roughness is entered as variable NUMNH in the first field and the 'n' values and corresponding cross section stations are entered in subsequent fields. These 'n' values will be used for all subsequent cross sections unless changed by another NH card. Normally the NH card 'n' values should be redefined for each cross section with new geometry.

Data indicating the variation of Manning's 'n' with river stage may be used in the program. Manning's 'n' and the corresponding stage elevation (beginning with the lowest elevation) are entered on the NV card ('n' value - vertical), beginning in the second and third fields, respectively. Variable NUMNV in field one is the number of 'n' values input on the NV cards. This 'n' value option applies only to the channel area.

If for subsequent jobs of the same run it is desired to modify the 'n' values specified on the NC, NH, and NV cards by a factor, variable FN on the J2 card may be used. The desired factor is entered as variable FN for each job. If the value of FN is negative, the factor is multiplied by the channel 'n' values on the NC card but the overbank 'n' values are not changed.

Reference 1 shows Manning's 'n' values for average channels. A more extensive compilation of 'n' values for streams and flood plains is listed in reference 2. References 3 and 4 use pictures of selected streams as a guide to 'n' value determination.

Contraction or expansion of flow due to changes in the channel cross section is a common cause of energy losses within a reach. Whenever this occurs, the loss may be computed by specifying the contraction and expansion coefficients as variables CCHV and CEHV, respectively, on the NC card. The coefficients are multiplied by the absolute difference in velocity heads between the cross sections to give the energy loss caused by the transition. Where the change in river cross section is small, coefficients CCHV and CEHV are typically on the order of 0.1 and 0.3, respectively. When the change in effective cross section area is abrupt such as at bridges, CCHV and CEHV may be as high as 0.6 and 1.0, respectively. These values may be changed at any cross section by inserting a new NC card. These new values will be used until changed again by another NC card. For additional information concerning transition losses and for information on bridge loss coefficients see Appendix IV.

Boundary geometry for the analysis of flow in natural streams is specified in terms of ground surface profiles (cross sections) and the measured distances between them (reach lengths). Cross sections are located at intervals along a stream to characterize the flow carrying capability of the stream and its adjacent flood plains. They should extend across the entire flood plain and should be perpendicular to the anticipated flow lines (approximately perpendicular to contour lines). Occasionally it is necessary to layout cross sections in a curved or dog-leg alignment to meet this requirement. Every effort should be made to obtain cross sections that accurately represent the stream and flood plain geometry. However, ineffective flow areas of the flood plain such as stream inlets, small ponds or indents in the valley floor should generally not be included in the cross section geometry.

Cross sections are required at representative locations throughout a stream reach and at locations where changes occur in discharge, slope, shape, or roughness; at locations where levees begin or end and at bridges or control structures such as weirs. Where abrupt changes occur, several cross sections should be used to describe the change regardless of the distance. Cross section spacing is also a function of stream size, slope, and the uniformity of cross section shape. In general, large uniform rivers of flat slope normally require the fewest number of cross sections per mile. The purpose of the study also affects spacing of cross sections. For instance, navigation studies on large relatively flat streams may require closely spaced (e.g., five hundred feet) cross sections to analyze the effect of local conditions on low flow depths, whereas cross sections for sedimentation studies to determine deposition in reservoirs may be spaced at intervals of up to five or ten miles.

The choice of friction loss equation may also influence the spacing of cross sections. For instance, cross section spacing may be maximized when calculating an M1 profile with the average friction slope equation or when the harmonic mean friction slope equation is used to compute M2 profiles.

Each cross section in an HEC-2 data set is identified and described by X1 and GR cards. Variable SECNO on the X1 card is the cross section identification number which may correspond to stationing along the channel, mile points, or any fictitious numbering system, since it is only used to identify output and is not used in the computations. Each data point in the cross section is given a station number corresponding to the horizontal distance from a zero point on the left. The elevation and a corresponding station number of each data point are input as variables EL(I) and STA(I) on GR cards. Up to one hundred data points may be used to described cross section geometry for most program applications. When the encroachment options are utilized, no more than ninety-five data points should be used, since they generate additional data points automatically to define the encroachment limits. The channel improvement option also should be used with fewer than one hundred data points since it will generate data points (four or more depending on the geometry).

Cross section data is traditionally oriented looking downstream since the program considers the left side of the stream to have the lowest station numbers and the right side to have the highest. The left and right stations separating the channel from the overbank areas are specified as variables STCHL and STCHR on the X1 card. End points of a cross section that are too low (below the computed water surface elevation) will automatically be extended vertically and a note indicating the extension amount will be printed.

Numerous program options are available to allow the user to easily add or modify cross section data. For example, when the user wishes to repeat a surveyed cross section, a single X1 card may be input to identify the cross section and to provide reach length information. X1 card variables, PXSECR and PXSECE, allow the user to modify the horizontal and vertical dimensions of the repeated cross section data. Other program options to modify cross section data to model improved channel sections, encroachments and ineffective flow areas are described in detail in the following chapter.

7. REACH LENGTHS

The measured distances between cross sections are referred to as reach lengths. The reach lengths for the left overbank, right overbank and channel used in computations are specified on the X1 card by variables XLOBL, XLOBR, and XLCH, respectively. Channel reach lengths are typically measured along the thalweg. Overbank reach lengths should be measured along the anticipated path of the center of mass of the overbank flow. Often these three values will be equal. There are however, conditions where they will differ, such as at river bends, or where the channel meanders considerably and the overbanks are straight. Where the distances between cross sections for channel and overbanks are different, a discharge-weighted reach length is determined based on the discharges in the main channel and left and right overbank segments of the reach (see Equation 3, page 4).

Chapter 4

OPTIONAL CAPABILITIES

1. GENERAL

HEC-2 has numerous optional capabilities that allow the program user to determine flood plains, floodways, and flood hazard zones; to evaluate energy losses at obstructions such as weirs, culverts, and bridges; and to analyze improvements to drainage systems. Detailed descriptions of options associated with encroachments, determination of flood hazard zones, and bridges are contained in Appendices II, III, and IV, respectively. Other program options include the capability to select from alternative friction loss equations; calculate critical depth; solve directly for Manning's 'n'; automatically insert program generated cross sections; specify ineffective flow areas; analyze tributary streams; and perform multiple profile analysis in a single execution of the program. These options are described in detail in the following sections.

2. MULTIPLE PROFILE ANALYSIS

HEC-2 can in a single run compute up to fourteen profiles using the same cross sectional data. Variables NPROF on the J2 card controls the reading of data cards. For a multiple profile run, the NPROF for the first profile is set equal to one or left blank to read in cross section data cards. For all remaining profiles NPROF equals the profile number, i.e., 2, 3, 4, ..., and only T1, T2, T3, J1 and J2 are required (cards NC through EJ are omitted). If NPROF is set equal to fifteen for the last profile of a multiple profile run, a summary printout will be generated which provides a concise summary of results for all profiles for each cross section. If a summary printout is required for a single profile run, NPROF should be set equal to minus one.

3. CRITICAL DEPTH

Several options related to the computation of critical depth are available in HEC-2. Critical depth may be requested for <u>each</u> cross section of a sub-critical run by coding a value of -1 for variable ALLDC of the J2 card. As described previously in section 6 of Chapter 2, the normal tolerance used to terminate critical depth trial calculations is 2.5 percent of the depth. Other tolerances may be specified by coding a <u>minus</u> percent value for variable ALLDC. For instance, if a user desires critical depth to be computed at each cross section with a tolerance of 1.5 percent, a value of -1.5 should be entered for ALLDC.

As indicated in section 5 of Chapter 2, critical depth is calculated automatically for cross sections of subcritical profiles whenever the calculated velocity head exceeds a test velocity head. The tolerance normally used is also 2.5 percent of the depth. The user can specify an alternative tolerance to be used for the automatic calculation of critical depth by indicating a positive value for ALLDC.

4. EFFECTIVE FLOW OPTIONS

A series of program capabilities are available to restrict flow to the effective flow areas of cross sections. Among these capabilities are options to simulate sediment deposition, to confine flows to leveed channels, to block out road fills and bridge decks, and to analyze flood plain encroachments. These program options are illustrated in Figure 3 below.

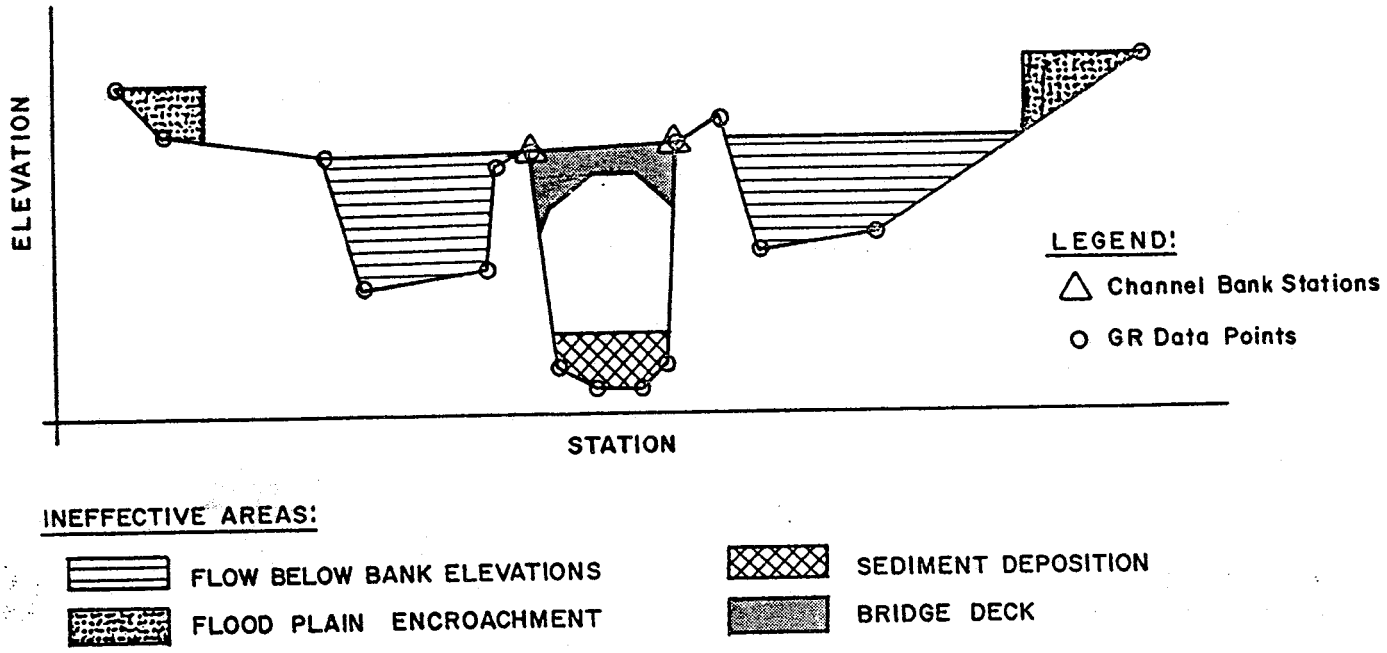

Figure 3. Types of Effective Flow Options

Sediment deposition may be specified by variable ELSED on the X3 card. The specified elevation (ELSED) is extended horizontally across the cross section and the area below this elevation is not considered by the program to carry flow.

Cross sections with low overbank areas or levees, require special consideration in computing water surface profiles because of possible overflow into areas outside the main channel. Normally the computations are based on the assumption that all area below the water surface elevation is effective in passing the discharge. However, if the water surface elevation at a particular cross section is less than the top of levee elevations, and if the water cannot enter or leave the overbanks upstream of that cross section, then the flow areas in these overbanks should not be used in the computations. Variable IEARA on the X3 card and the bank stations coded in fields three and four on the X1 card are used for this condition. By setting IEARA equal to ten the program will consider only flow confined by the levees,

unless the water surface elevation is above the top of one or both of the levees, in which case flow area or areas outside the levee(s) will be included. If this option is employed and the water surface elevation is close to the top of a levee, it may not be possible to balance the assumed and computed water surface elevations due to the changing assumptions of flow area when just above and below the levee top. When this condition occurs a note will be printed that states that the assumed and computed water surface elevations for the cross section cannot be balanced. A water surface elevation equal to the elevation which came closest to balancing will be adopted. It is then up to the program user to determine the appropriateness of the assumed water surface elevation and start the computation over again at that cross section if required.

It is important for the user to study carefully the flow pattern of the river where levees exist. If, for example, a levee were open at both ends and flow passed behind the levee without overtopping it, IEARA equals zero or blank should be used. Also, assumptions regarding effective flow areas may change with changes in flow magnitude. Where cross section elevations outside the levee are considerably lower than the channel bottom, it may be necessary to set IEARA equal to ten to confine the flow to the channel. For further information on this option see Appendix IV, paragraph 8, Effective Area Option. The effective flow capabilities of the bridge and encroachment routines are described in the following paragraphs and in Appendices IV and II, respectively.

5. BRIDGE LOSSES

Energy losses caused by structures such as bridges and culverts are computed in two parts. First, the losses due to expansion and contraction of the cross section on the upstream and downstream sides of the structure are computed in the standard step calculations. Secondly, the loss through the structure itself is computed by either the normal bridge or the special bridge methods.

The normal bridge method handles the cross section at the bridge just as it would any river cross section with the exception that the area of the bridge below the water surface is subtracted from the total area and the wetted perimeter is increased where the water surface elevation exceeds the low chord. The normal bridge method is particularly applicable for bridges without piers, bridges under high submergence, and for low flow through circular and arch culverts. Whenever flow crosses critical depth in a structure, the special bridge method should be used. The normal bridge method is automatically used by the computer, even though data was prepared for the special bridge method, for bridges without piers and under low flow control.

The special bridge method can be used for any bridge, but should be used for bridges with piers where low flow controls, for pressure flow, and whenever flow passes through critical depth when going through the structure. The special bridge method computes losses through the structure for low flow, weir flow and pressure flow or for any combination of these. Refer to Appendix IV for a detailed explanation of HEC-2 bridge capabilities.

6. ENCROACHMENT OPTIONS

Six methods of specifying encroachments for floodway studies can be used. Stations and elevations of the left and/or right encroachment (method 1) can be specified for individual cross sections as desired. A floodway with a fixed top width (method 2) can be specified which will be used for all cross sections until changed. The left and right encroachment stations are made equidistant from the centerline of the channel, which is half-way between the left and right banks stations. Encroachments can be specified by percentages (method 3) which indicate the desired proportional reduction in the natural discharge carrying capacity of each cross section.

Encroachments can be determined so that each modified cross section will have the same discharge carrying capacity (at some higher elevation) as the natural cross section (method 4). This higher elevation is specified as a fixed amount above the natural (e.g., 100-year) profile. The encroachments are determined so that an equal loss of conveyance (at higher elevation) occurs on each side of the channel, if possible.

Encroachment method 5 is an optimization solution of encroachment method 4. It determines water surfaces elevation differences between the natural and encroached conditions such that the target difference is obtained as near as possible.

Encroachment method 6 is an optimization solution similar to method 5; however, method 6 optimizes on differences in the energy grade line elevations. Refer to Appendix II for a detailed explanation of encroachment methods 1 through 6.

7. OPTIONAL FRICTION LOSS EQUATIONS

The friction loss between adjacent cross sections is computed as the product of the representative rate of friction loss (friction slope) and the weighted reach length. The program allows the user to select from the following previously defined (see page 6) friction loss equations:

(1) Average Conveyance

(2) Average Friction Slope

(3) Geometric Mean Friction Slope

(4) Harmonic Mean Friction Slope

Any of the above friction loss equations will produce satisfactory estimates provided that reach lengths are not too long. The advantage sought in alternative friction loss formulations is to be able to maximize reach lengths without sacrificing profile accuracy.

Equation (1), the Average Conveyance equation, is the friction loss formulation that has been standard in all HEC-2 source decks since 1971. Previous HEC-2 source decks utilized equation (2), the Average Friction Slope equation. Research by Reed and Wolfkill (reference 5), indicates that equation (2) is the most suitable for M1 profiles. (Suitability as indicated by Reed and Wolfkill is the most accurate determination of a

known profile with the least number of cross sections.) Equation (3) is the friction loss formulation presently used in the U.S.G.S. Step-Backwater programs E431 amd J635. Equation (4) has been shown by Reed and Wolfkill to be the most suitable for M2 profiles.

Another feature of this option is the capability of the program to select the most appropriate of the preceding four equations on a reach by reach basis depending on flow conditions (e.g., M1, S1, etc.) within the reach. It is anticipated that this capability may be incorporated into the program as a standard feature at sometime in the future. At present, however, the criteria shown in Table 2 below, do not select the best equation for friction loss analysis in reaches with significant lateral expansion, such as the reach below a contracted bridge opening.

TABLE 2
CRITERIA UTILIZED TO SELECT FRICTION EQUATION

Profile Type	Is friction slope at current cross section greater than friction slope at preceding cross section?	Equation Used
Subcritical (M1, S1)	Yes	(2)
Subcritical (M2)	No	(4)
Supercritical (S2)	Yes	(2)
Supercritical (M3, S3)	No	(3)

The friction loss equation is controlled by variable IHLEQ on the J6 card as follows:

Value of IHLEQ (J6.1)	Friction Loss Equation Used
0	(1) Average Conveyance
1	Program selects equation based on flow conditions (see Table 2).
2	(2) Average Friction Slope
3	(3) Geometric Mean Friction Slope
4	(4) Harmonic Mean Friction Slope

When using this option, it is appropriate to also use a J3 card to request printout of the variable IHLEQ to identify the equation used for each reach.

8. CHANNEL IMPROVEMENT

Cross section data may be modified automatically by the CHIMP option of the program to analyze improvements made to natural stream sections. The CHIMP option simulates channel improvement by trapezoidal excavation. This option is requested by the CI card which specifies the location of the centerline (CLSTA), the elevation of the improved invert (CELCH), a new channel reach length (XLCH), a new 'n' value (CNCH), the left side slope (XLSS), the right side slope (RSS) and a bottom width (BW). Up

to five different bottom widths may be specified for the execution of a single run on each CI card. A maximum of three CI cards may be used at each cross section. By using more than one CI card, a pilot channel can be defined. Figure 4 shows a sample application of the CHIMP option; note that improved section is modified only by excavation and not by fill. The old channel can be filled prior to the excavation by entering a negative channel bottom width.

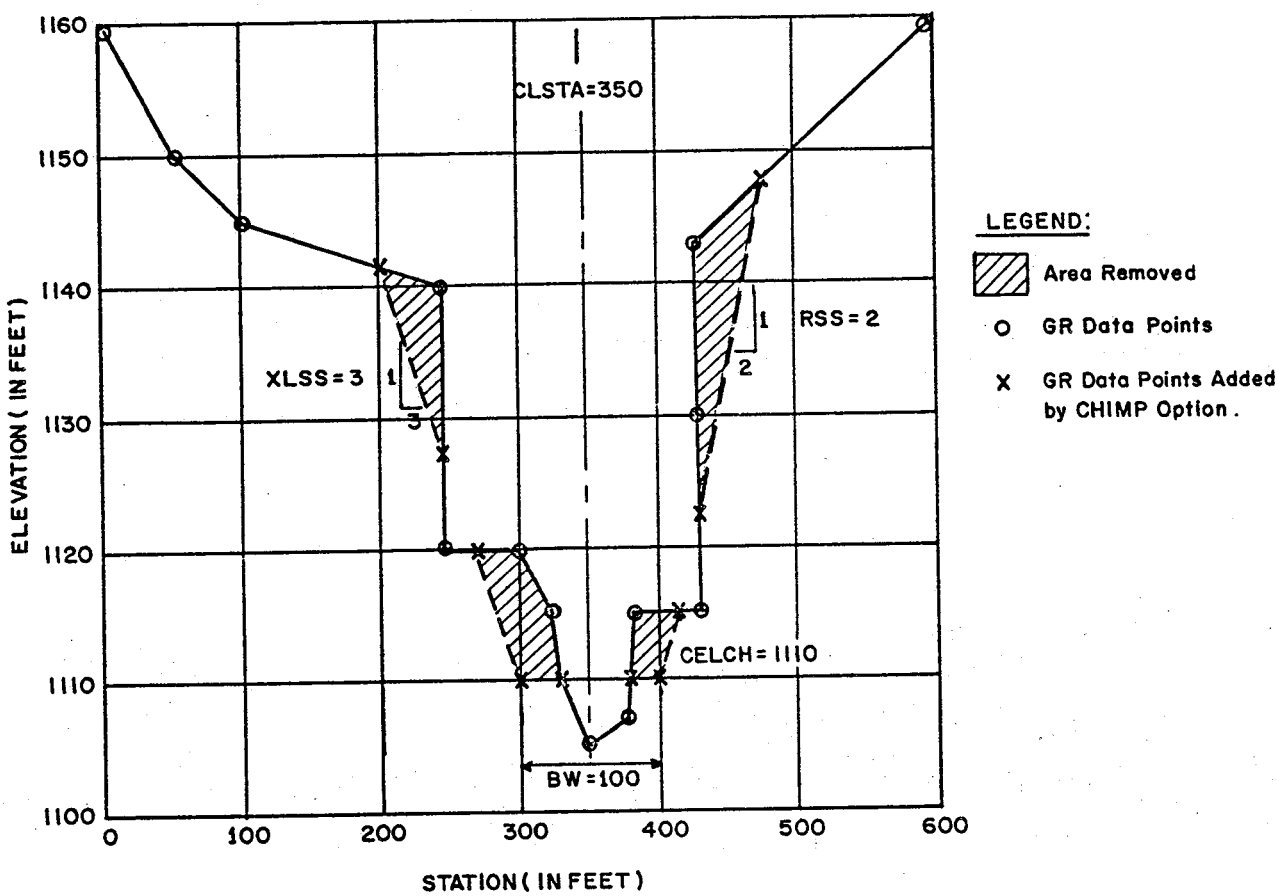

Figure 4. A Stream Cross Section Before and After CHIMP Modification

9. INTERPOLATED CROSS SECTIONS

Occasionally it is necessary to insert cross sections between those specified by input, because the change in velocity head (ΔHV) is too great to accurately determine the energy gradient. Additional cross sections may be coded manually or a program option may be requested to input interpolated cross sections. The option specified by the variable HVINS on the J1 card will insert up to three interpolated cross sections between two adjacent input cross sections. HVINS is the user specified maximum allowable change in velocity head between adjacent cross sections. When the program determines that ΔHV between the current cross section and the previous cross section exceeds the user specified criterion, the program will automatically insert one to three cross sections (depending on the magnitude of (ΔHV/HVINS) - 1).

Interpolated cross sections are determined by raising or lowering and expanding or contracting the current cross section's shape. They are inserted uniformly between the two input cross sections. A proportion of the elevation difference determined from the minimum elevations of the two input cross sections is added (or subtracted) to the elevation coordinates (on GR cards) of the current cross section.

The modification of the horizontal coordinates is a function of the ratio of the channel areas of the two input cross sections. The channel area (between bank stations) of the current cross section is determined with the depth of flow from the previous cross section.

Interpolated cross sections will be identified in the output by section numbers of 1.01, 1.02, and 1.03. The option will not add interpolated cross sections in the following cases: 1) if reach lengths between input cross sections are less than fifty feet, 2) if encroachments have been encountered in the run, or 3) if the previous cross section is a special bridge cross section.

When there is a substantial difference in shape between the previous and current cross sections, interpolated cross sections generated automatically by the program may not be representative of the actual stream geometry. The user should always check the reasonableness of interpolated cross sections.

The number of interpolated cross sections added to each profile may vary with discharge; therefore, it is advisable not to request them for multiple profile runs because analysis should be made using exactly the same cross section data.

10. TRIBUTARY STREAM PROFILES

Subcritical profiles may be computed for tributary stream systems for single or multiple profiles in a single execution of the program. In general data sets are arranged to compute profiles for the main stream (reach 1) from the most downstream point to the study limit on the main stream. Data for a tributary stream (reach 2), whose starting water surface elevation was determined when reach 1 was calculated, follows the data for reach 1. The first section number for reach 2 is negative and refers to the section number in reach 1 where the starting water surface elevation for reach 2 was determined. When a negative section number (on the X1 card) is encountered the program will search its memory for the computed water surface elevation that corresponds to the negative section number. The program will then start computing the profile for reach 2 with the previously determined water surface elevation.

Occasionally it may be desireable to calculate, in a single run, a profile for a stream system with a second order tributary (a tributary to a tributary). This may be accomplished if data for the tributary with the tributary is treated as a portion of the main stream and the main stream beyond the junction of the two streams is treated as a tributary. This is illustrated in the following figure on the next page; numbers one through eight locate cross sections on the main stream, numbers eleven through sixteen are cross sections on the first order tributary and numbers twenty-one through twenty-two are cross sections on the second order tributary.

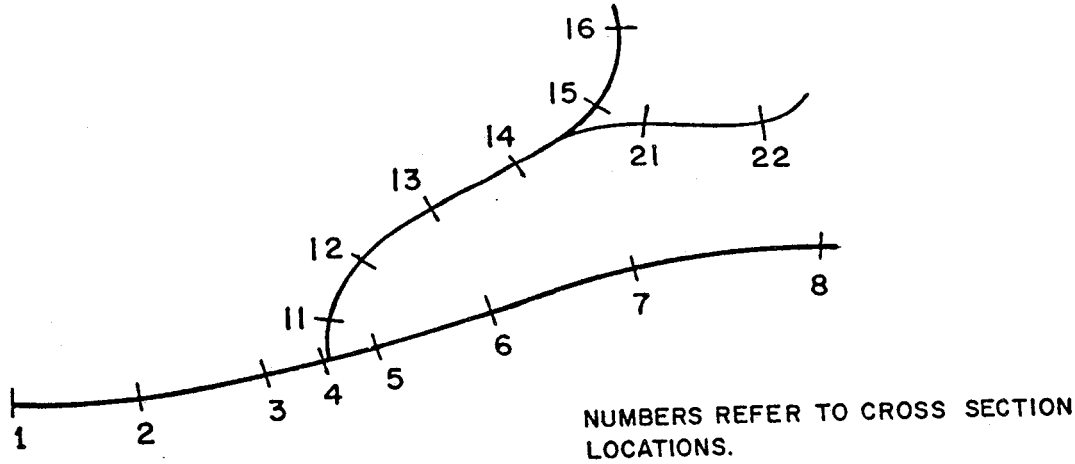

Figure 5. Second Order Stream System

The arrangement of cross section data (X1 and GR cards) for the stream system in Figure 5 for a tributary analysis in a single execution of the program is as follows: 1, 2, 3, 4, 11, 12, 13, 14, 15, 16, -4, 5, 6, 7, 8, -14, 21, and 22.

Tributary stream profiles should not be calculated simultaneously with encroachment methods 3 - 6.

11. SOLVING FOR MANNING'S 'n'

The program can be utilized in two ways to solve for Manning's 'n'. HEC-2 can compute 'n' values automatically from high water data if the discharge, relative ratios of the 'n' values for the channel and overbanks and the water surface elevation at each cross section are known. The "best estimate" of 'n' for the first cross section must be entered on the NC card since it is not possible to compute an 'n' value for this cross section. The relative ratio of 'n' between channel and overbank is set by the first cross section and will be used for all subsequent cross sections unless another NC card is used to change this ratio. High water marks are used for the computed water surface elevation by setting variable NINV on the J1 card equal to one and entering the known water surface elevation as variable WSELK on the X2 card for each cross section. The average friction slope equation (see J6 card description) is utilized by the program to solve for 'n' values. If one of the other friction equations is to be utilized for profile analysis then the program-determined 'n' values should be verified using the appropriate friction equation. Because of the sensitivity of calculated results to slight errors in observed high water marks, a weighted 'n' (WTN) value is also calculated at each cross section. WTN is the length weighted channel 'n' calculated from the first cross section to the current cross section. When an adverse slope is encountered, computations restart using 'n' values from the previous section, but WTN computations continue.

Another method is to specify the discharge and an assumed set of 'n' values, and have the program compute a water surface profile which can be compared with the high water profile. For this method WSELK may be input on the X2 card, without entering the computations, so that it can be easily compared with the computed water surface elevation on the output. The variable FN (J2.6 card) may be utilized to vary the assumed 'n' values for multiple profile trials.

12. STORAGE-OUTFLOW DATA

Punched cards can be obtained from HEC-2 for stream routing by the Modified Puls Method using program HEC-1. The cards punched are Y, 2, and 3 cards (see program description for HEC-1). This option can be used only if multiple profiles are computed from the same cross sectional data and if the summary printout is requested. Interpolated cross sections determined by the computer may be used. Routing reach sections may not be interpolated sections. However, it may not be wise to use interpolated cross sections since a different number of cross sections might be interpolated between two given cross sections for different magnitudes of discharge which could cause inconsistencies in the incremental storage volumes. The ability to repeat the previous cross section by using only an X1 card (i.e., field two on the X1 card is blank) can be used where additional cross sections are needed at the ends of routing reaches and in place of the interpolated cross sections. The J4 card calls for this option.

10. INTRODUCTION

After the cross sections are located and the method of solution is determined, the program user has to select coefficients associated with the method chosen. For the normal bridge method the Manning's 'n' values are used to determine the friction loss. The contraction and expansion losses caused by the bridge are estimated using contaction and expansion coefficients.

11. CONTRACTION AND EXPANSION COEFFICIENTS

These coefficients are used to compute energy losses associated with changes in the shape of river cross sections (or effective flow areas). The loss due to expansion of flow is usually much larger than the contraction loss, and losses from short abrupt transitions are larger than losses from gradual transitions. The transition loss is computed by multiplying a coefficient times the absolute difference in velocity heads between cross sections. If the values for the coefficients are being redefined to account for contraction and expansion through a bridge, the new values are read on the NC card prior to the section where the change in velocity head is evaluated. Referring back to Figure 6, on a subcritical profile, the new values should be read in just before section two and changed back to the original values after section four. Typical values are shown below.

	Coefficients	
	Contraction	Expansion
No transition loss computed	0.0	0.0
Gradual transitions	0.1	0.3
Bridge sections	0.3	0.5
Abrupt transitions	0.6	0.8

The maximum value for the expansion coefficient would be one (1.0).

12. SPECIAL BRIDGE COEFFICIENTS

When using the special bridge method, coefficients must be read in for the Yarnell equation, the orifice equation, and the weir equation. The following discussion provides suggested values and methods for estimating the required coefficients.

Pier Shape Coefficient XK is used in Yarnell's energy equation for computing the change in water surface elevation through a bridge for class A low flow. Because the calculation is based on the presence of piers, both the coefficient and a total width (BWP) must be read on the SB card. If there are no piers, both variables can be left blank and the program will use a standard step solution for low flows. The

following table gives values of XK for various pier shapes.

Pier Shape		K
Semicircular nose and tail	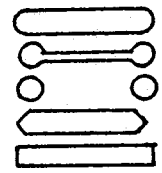	0.90
Twin-cylinder piers with connecting diaphragm		0.95
Twin-cylinder piers without diaphragm		1.05
90° triangular nose and tail		1.05
Square nose and tail		1.25

The Yarnell equation is a semi-empirical equation based on hydraulic model data. As such, it probably should not be applied in cases where the flow obstruction is something other than a pier; for example, the fill separating twin circular culverts.

Loss Coefficient XKOR is used in the orifice flow equation, $Q = A\sqrt{2gH/K}$. This form of the equation can be derived by applying the energy equation from a point just downstream from the bridge (2) to a point just upstream (1).

$$y_1 + Z_1 + \alpha_1 \frac{V_1^2}{2g} = y_2 + Z_2 + \alpha_2 \frac{V_2^2}{2g} + H_L \qquad (1)$$

where:

y = depth of water

Z = invert elevation

$\alpha \frac{V_2^2}{2g}$ = velocity head

H_L = head loss

Defining the head (H) on the orifice as the difference between the upstream energy elevation and the downstream water surface elevation (the definition used in HEC-2) produces:

$$H = (y_1 + Z_1 + \frac{\alpha_1 V_1^2}{2g}) - (y_2 + Z_2) \qquad (2)$$

Substituting H from equation 2 into equation 1 produces:

$$H = \frac{\alpha_2 V_2^2}{2g} + H_L \qquad (3)$$

just downstream can be defined by an expansion coefficient K_e and the change in velocity head.

$$H_L = K_b \frac{V_b^2}{2g} + K_e \left(\frac{V_b^2}{2g} - \frac{\alpha_2 V_2^2}{2g} \right) \qquad (4)$$

where:

b = subscript designating the bridge

The head loss equation 4 then can be used to define H_L in equation 3:

$$H = \frac{\alpha_2 V_2^2}{2g} + K_b \left(\frac{V_b^2}{2g} \right) + K_e \left(\frac{V_b^2}{2g} - \frac{\alpha_2 V_2^2}{2g} \right) \qquad (5)$$

If the expansion coefficient (K_e) is taken as 1.0, the equation can be rewritten into the form of the orifice equation by adding the continuity equation (Q = VA).

$$Q = A\sqrt{2gH/K} \qquad (6)$$

where:

$K = K_b + 1$

The loss coefficient used in the program's orifice equation can be related to the loss coefficient C from another commonly used orifice flow equation, $Q = CA\sqrt{2gH}$. The conversion ($XKOR = 1/C^2$) can be used for tabulated values of C. However, care must be taken to insure the definition of H used in the various formulations is applicable.

The Bureau of Public Roads (reference 1) shows experimental values for C for fully submerged conditions to vary from 0.7 to 0.9. A value of 0.8 is recommended as being applicable for the average two to four lane concrete girder bridge. The definition of H is consistent with that used in HEC-2. In the absence of calibration data, a value of 1.56 for XKOR (C = 0.8) would be applicable to most bridges and short culverts. For longer culverts, the coefficient can be calculated by the sum of XKOR shown below.

$XKOR = k_e + k_f + 1$

where:

k_e = entrance loss coefficient

k_f = friction loss coefficient

The coefficient for friction loss (k_f) can be computed from Manning's equation by equating two equations for friction loss in the culvert.

$$k_f \frac{V_b^2}{2g} = S_f \cdot L \tag{7}$$

where:

S_f = the average friction slope

L = the length of the culvert

Manning's equation for the velocity in the culvert is rearranged to define S_f.

$$V_b = \frac{1.49}{n} R^{2/3} S_f^{1/2}$$

$$S_f = \frac{V_b^2 n^2}{2.22R^{4/3}} \tag{8}$$

By substituting equation 8 for equation 7, the coefficient k_f can be defined based on culvert parameters.

$$k_f = \frac{V_b^2 n^2}{2.22R^{4/3}} \cdot L \cdot \frac{2g}{V_b^2}$$

$$k_f = 29n^2L/R^{4/3} \tag{9}$$

Typical values of the coefficients are shown below:

Description	k
Intake (k_e)	0.1 to 0.9
Intermediate piers	0.05
Friction (Manning's equation)	k_f
	XKOR = $\Sigma k + 1$

where:

English $k_f = 29n^2L/R^{4/3}$

Metric $k_f = 19.6n^2L/R^{4/3}$

King's Handbook (reference e), in its discussion on pipe culverts gives an entrance loss of .1 for a flush inlet, and 0.15 for a projecting inlet for concrete pipes. Inlet loss coefficients as high as 0.9 for a projecting entrance and corregated metal pipes are indicated. All the coefficients were applied to the velocity head for the pipe.

For Multiple Culverts, an equivalent coefficient can be computed to apply in cases where all culverts are flowing full.

$$Q = \sqrt{2gh}\ AT\sqrt{1/K_{equiv}}$$

where:

$$K_{equiv} = \frac{AT^2}{\left[\sum_{i=1}^{n} \sqrt{\frac{A_i^{\,2}}{K_i}}\right]^2}$$

AT = total area

A_i = area of individual culvert

K_i = coefficient for individual culvert

n = number of culverts

Coefficient of Discharge, COFQ is used in the standard weir equation: $Q = CLH^{3/2}$. Under free flow conditions (discharge independent of tailwater) the coefficient of discharge "C", ranges from 2.5 to 3.1 (1.39 - 1.72 metric) for broad-crested weirs depending primarily upon the gross head on the crest ("C" increases with head). Increased resistance to flow caused by obstructions such as trash on bridge railings, crubs, and other barriers would decrease the value of C. With submerged flow (discharge affected by tailwater), the coefficient "C" should be reduced. This is done automatically by the program using the Waterways Experiment Station Design Chart 1114. The correction is based on model studies with a low ogee crest weir.

Tables of weir coefficients (C) are given for broad-crested weirs in King's Handbook with the value of C varying with measured head (H) and breadth of weir. For rectangular weirs with a breadth of 15 feet and a H of one foot or more, the given value is 2.63. Trapezoidal shaped weirs generally have a larger coefficient with typical values ranging from 2.7 to 3.8.

Hydraulics of Bridge Waterways (reference i) provides a curve of C versus the head on the roadway. The roadway section is shown as a trapezoid and the coefficient rapidly changes from 2.9 for a very small H to 3.03 for H = 0.6 feet. From there, the curve levels off near a value of 3.05.

With very little prototype data available, it seems the assumption of a rectangular weir for flow over the bridge deck (assuming the bridge can withstand the forces) and a coefficient of 2.6 would be reasonable. If the weir flow is over the roadway approaches to the bridge, a value of 3.0 would be consistent with available data. If weir flow occurs a combination of bridge and roadway, an average coefficient (weighted by weir length) could be used.

SECPROP User's Guide for HP-41C

SECPROP calculates section proporties for a composite channel cross-section as shown in Figure 1.

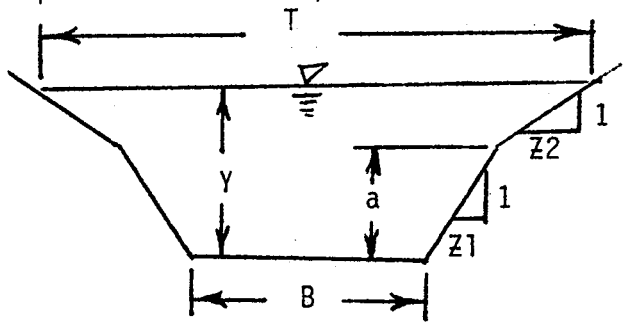

Figure 1 - Definition sketch for SECPROP.

The section proporties are:

A - cross-sectional area
T - top width
D - hydraulic depth, $D=\frac{A}{T}$
ZG - critical flow section factor, $ZG=A\sqrt{gD}$
P - wetted perimeter
RH - hydraulic radius, $RH=\frac{A}{D}$
AR - uniform flow section factor, $AR = (A)\ (RH)^{2/3}$

Procedure:

1. Read program into calculator
2. Place calculator in USER Mode
3. ASN "SECPROP" to "A"
4. XEQ "CLRG"
5. Input section geometry:

   a
   ENTER
   B
   ENTER
   Z1
   ENTER
   Z2
   "A"

6. Input depth, Y
7. If $Y<a$, use "C"
   If $Y\geq a$, use "B"
8. Program will calculate and print the section proporties
9. Steps 6 through 9 are repeated for additonal depths.

Notes:

1. Units should be in feet. This is because in calculating ZG the value of $g=32.2$ ft/sec^2 is used in the program. A simple reprogramming would be necessary for the metric system. Any other homogeneous units could be used; however, the ZG factor would be in error or need to be corrected.

2. If the section is a simple trapezoid, use a=o and Z1=0.

3. XEQ "CLRG" before inputing a new section geometry.

4. Subsequent depth's (Y) can be either larger or smaller than the previous depth.

Program Listing for SECPROP for HP-41C

```
01♦LBL "SECPROP"
02 STO 12
03 RDN
04 STO 13
05 RDN
06 STO 11
07 RDN
08 STO 10
09 ENTER↑
10 *
11 RCL 12
12 RCL 13
13 -
14 *
15 STO 00
16 RCL 10
17 2
18 *
19 RCL 13
20 RCL 12
21 -
22 *
23 RCL 11
24 +
25 STO 01
26 RCL 13
27 ENTER↑
28 *
29 1
30 +
31 SQRT
32 RCL 10
33 *
34 2
35 *
36 RCL 11
37 +
38 STO 02
39 RCL 12
40 ENTER↑
41 *
42 11
43 SQRT
44 2
45 *
46 STO 03
47 "SECPROP"
48 SF 12
49 PRA
50 CF 12
51 ADV
52 ADV
53 SF 13
54 RCL 10
55 "A = "
56 ARCL X
57 AVIEW
58 CF 13
59 RCL 11
60 "B = "
61 ARCL X
62 AVIEW
63 RCL 13
64 "Z1 = "
65 ARCL X
66 AVIEW
67 RCL 12
68 "Z2 = "
69 ARCL X
70 AVIEW
71 ADV
72 "Y?"
73 PROMPT
74 STOP
75♦LBL B
76 "Y = "
77 ARCL X
78 AVIEW
79 STO 15
80 ENTER↑
81 *
82 RCL 12
83 *
84 RCL 15
85 RCL 01
86 *
87 +
88 RCL 00
89 +
90 STO 04
91 "A = "
92 ARCL X
93 AVIEW
94 RCL 12
95 2
96 *
97 RCL 15
98 *
99 RCL 01
100 +
101 "T = "
102 ARCL X
103 AVIEW
104 RCL 04
105 /
106 1/X
107 "D = "
108 ARCL X
109 AVIEW
110 SQRT
111 5.67
112 *
113 RCL 04
114 *
115 "ZG = "
116 ARCL X
117 AVIEW
118 RCL 15
119 RCL 10
120 -
121 RCL 03
122 *
123 RCL 02
124 +
125 STO 05
126 "P = "
127 ARCL X
128 AVIEW
129 RCL 04
130 /
131 1/X
132 STO 06
133 "RH = "
134 ARCL X
135 AVIEW
136 2
137 ENTER↑
138 3
139 /
140 Y↑X
141 RCL 04
142 *
143 "AR = "
144 ARCL X
145 AVIEW
146 ADV
147 "Y?"
148 "PROMPT"
149 STOP
150♦LBL C
151 "Y = "
152 ARCL X
153 AVIEW
154 STO 15
155 ENTER↑
156 *
157 RCL 13
158 *
159 RCL 11
160 RCL 15
161 *
162 +
163 STO 04
164 "A = "
165 ARCL X
166 AVIEW
167 RCL 15
168 RCL 13
169 *
170 2
171 *
172 RCL 11
173 +
174 "T = "
175 ARCL X
176 AVIEW
177 RCL 04
178 /
179 1/X
180 "D = "
181 ARCL X
182 AVIEW
183 SQRT
184 5.67
185 *
186 RCL 04
187 *
188 "ZG = "
189 ARCL X
190 AVIEW
191 RCL 13
192 ENTER↑
193 *
194 1
195 +
196 SQRT
197 RCL 15
198 *
199 2
200 *
201 RCL 11
202 +
203 STO 05
204 "P = "
205 ARCL X
206 AVIEW
207 RCL 04
208 /
209 1/X
210 STO 06
211 "RH = "
212 ARCL X
213 AVIEW
214 2
215 ENTER↑
216 3
217 /
218 Y↑X
219 RCL 04
220 *
221 "AR = "
222 ARCL X
223 AVIEW
224 ADV
225 "Y?"
226 PROMPT
227 STOP
228 .END.
```

Example Problem using SECPROP

For Q=2200 cfs, n=.03, and S_o=.005, what is the normal depth and critical depth?

SECPROP

a = 3.00
B = 50.00
Z1 = 2.00
Z2 = 4.00

Y = 2.00
A = 108.00
T = 58.00
D = 1.86
ZG = 835.61
P = 58.94
RH = 1.83
AR = 161.71

Y = 3.00
A = 168.00
T = 62.00
D = 2.71
ZG = 1,568.02
P = 63.42
RH = 2.65
AR = 321.65

Y = 4.00
A = 234.00
T = 70.00
D = 3.34
ZG = 2,425.82
P = 70.05
RH = 3.34
AR = 522.90

Y = 5.00
A = 308.00
T = 78.00
D = 3.95
ZG = 3,470.26
P = 76.68
RH = 4.02
AR = 778.25

Y = 3.75
A = 216.75
T = 68.00
D = 3.19
ZG = 2194.15
P = 68.39
RH = 3.17
AR = 467.66

Y = 3.76 ← critical depth
A = 217.43
T = 68.08
D = 3.19
ZG = 2203.20
P = 68.46
RH = 3.18
AR = 469.81

For critical depth

$$Q = A\sqrt{gD} = \text{"ZG"}$$

For normal depth

$$\frac{Qn}{1.49\,S_o^{1/2}} = A r_h^{2/3} = \text{"AR"}$$

$$\frac{Qn}{1.49\,S_o^{1/2}} = 626.4$$

Y = 4.40
A = 262.64
T = 73.20
D = 3.59
ZG = 2820.78
P = 72.70
RH = 3.61
AR = 618.35

Y = 4.41
A = 263.37
T = 73.28
D = 3.59
ZG = 2831.04
P = 72.77
RH = 3.62
AR = 620.85

Y = 4.43
A = 264.84
T = 73.44
D = 3.61
ZG = 2851.62
P = 72.90
RH = 3.63
AR = 625.86

BKWTR User's Guide for HP-41C

BKWTR calculates water surface profiles for a composite channel cross-section as shown in Figure 1.

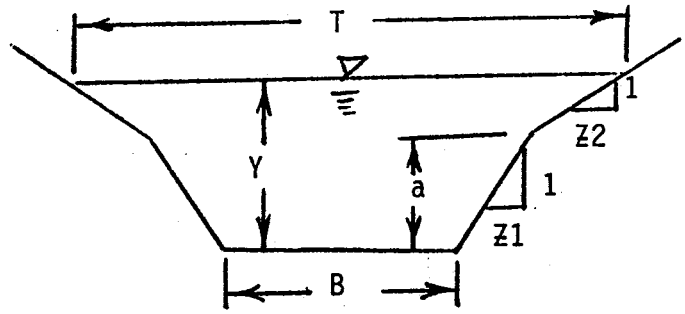

Figure 1. - Definition sketch for BKWTR.

The program will begin at the control and progress upstream (-x's) for subcritical flow or downstream (+x's) for supercritical flow as shown in Figure 2.

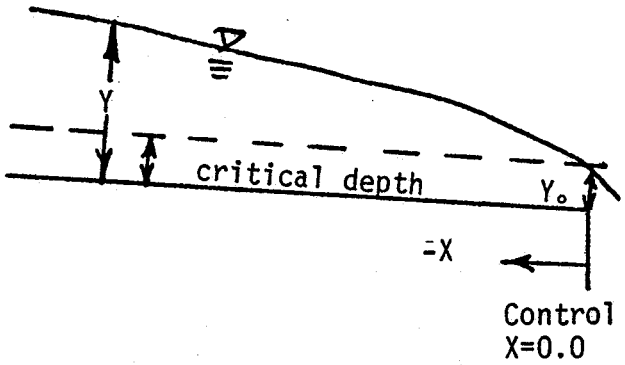

Subcritical flow, calculations progress upstream.

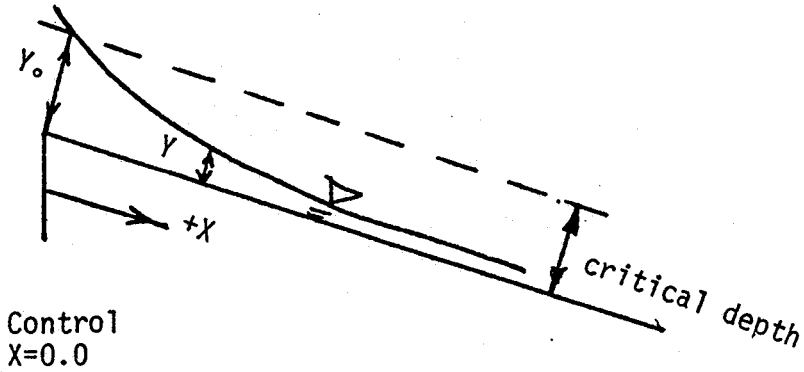

Supercritical flow, calculations progress downstream.

Figure 2. - Control for subcritical and supercritical channels.

Procedure:

1. Read program into calculator
2. Place calculator in USER Mode
3. ASN "BKWTR" to "A"
4. XEQ "CLRG"
5. Input section geometry:
   a, in feet
   ENTER
   B, in feet
   ENTER
   Z1
   ENTER
   Z2
   "A"

6. Input channel proporties:
   S_o - bed slope, as a decimal
   ENTER
   Q - discharge, in dvs
   ENTER
   n - Manning's coefficient
   "B"

7. Input the depth at the control section, Y.
   Y_o, in feet
   "C"
   "D"

8. Input the next depth, Y
   Y, in feet
   "C"
   "E"

9. Output is printed

10. Steps 8 and 9 are repeated for subsequent depths

    Output:
    Y- depth, in feet
    V- mean velocity, in feet per second
    VH- velocity head, in feet $VH=\frac{V^2}{2g}$
    X- distance from control, in feet

Notes:

1. Calculate critical depths and normal depths before beginning program executior

2. Plan the range of depths for which the water surface profile is required.

3. All values must be in English units. Programming changes are necessary for the metric system.

4. Each Y must be continuously increasing or decreasing.

5. If the section is a simple trapezoid, use a=o and Z1=0.

6. If the section is rectangular, use Z1=0 and Z2=0.

7. XEQ "CLRG" before inputing a new channel geometry.

Program Listing for BKWTR for HP-41C

```
01♦LBL "BKWTR"
02 STO 04
03 RDN
04 STO 03
05 RDN
06 STO 02
07 RDN
08 STO 01
09 STOP
10♦LBL B
11 STO 07
12 RDN
13 STO 08
14 RDN
15 STO 09
16 "BKWTR"
17 SF 12
18 PRA
19 CF 12
20 ADV
21 ADV
22 SF 13
23 RCL 01
24 "A = "
25 ARCL X
26 AVIEW
27 CF 13
28 RCL 02
29 "B = "
30 ARCL X
31 AVIEW
32 RCL 03
33 "Z1 = "
34 ARCL X
35 AVIEW
36 RCL 04
37 "Z2 = "
38 ARCL X
39 AVIEW
40 RCL 09
41 "SO = "
42 ARCL X
43 AVIEW
44 RCL 08
45 "Q = "
46 ARCL X
47 AVIEW
48 SF 13
49 RCL 07
50 "N = "
51 ARCL X
52 AVIEW
53 CF 13
54 ADV
55 RCL 01
56 ENTER↑
57 *
58 RCL 04
59 RCL 03
60 -
61 *
62 STO 16
63 RCL 01
64 2
65 *
66 RCL 03
67 RCL 04
68 -
69 *
70 RCL 02
71 +
72 STO 17
73 RCL 03
74 ENTER↑
75 *
76 1
77 +
78 SQRT
79 RCL 01
80 *
81 2
82 *
83 RCL 02
84 +
85 STO 18
86 RCL 04
87 ENTER↑
88 *
89 1
90 +
91 SQRT
92 2
93 *
94 STO 19
95 STOP
96♦LBL C
97 STO 15
98 "Y = "
99 ARCL X
100 AVIEW
101 RCL 01
102 X<>Y
103 X<=Y?
104 GTO c
105 RCL 15
106 ENTER↑
107 *
108 RCL 04
109 *
110 RCL 15
111 RCL 17
112 *
113 +
114 RCL 16
115 +
116 STO 10
117 RCL 15
118 RCL 01
119 -
120 RCL 19
121 *
122 RCL 18
123 +
124 RCL 10
125 /
126 1/X
127 STO 11
128 STOP
129♦LBL c
130 RCL 15
131 ENTER↑
132 ENTER↑
133 RCL 03
134 *
135 RCL 02
136 +
137 *
138 STO 10
139 RCL 03
140 ENTER↑
141 *
142 1
143 +
144 SQRT
145 RCL 15
146 *
147 2
148 *
149 RCL 02
150 +
151 RCL 10
152 /
153 1/X
154 STO 11
155 STOP
156♦LBL D
157 RCL 08
158 RCL 10
159 /
160 STO 00
161 "Y = "
162 ARCL X
163 AVIEW
164 ENTER↑
165 *
166 64.4
167 /
168 "YH = "
169 ARCL X
170 AVIEW
171 RCL 15
172 +
173 STO 05
174 RCL 07
175 ENTER↑
176 *
177 RCL 00
178 ENTER↑
179 *
180 *
181 RCL 11
182 4
183 ENTER↑
184 3
185 /
186 Y↑X
187 /
188 2.22
189 /
190 STO 06
191 RCL 20
192 "X = "
193 ARCL X
194 AVIEW
195 ADV
196 STOP
197♦LBL E
198 RCL 08
199 RCL 10
200 /
201 STO 00
202 "Y = "
203 ARCL X
204 AVIEW
205 ENTER↑
206 *
207 64.4
208 /
209 "YH = "
210 ARCL X
211 AVIEW
212 RCL 15
213 +
214 STO 13
215 RCL 07
216 ENTER↑
217 *
218 RCL 00
219 ENTER↑
220 *
221 *
222 RCL 11
223 4
224 ENTER↑
225 3
226 /
227 Y↑X
228 /
229 2.22
230 /
231 STO 14
232 RCL 13
233 RCL 05
234 -
235 STO 12
236 RCL 06
237 RCL 14
238 +
239 2
240 /
241 RCL 09
242 -
243 CHS
244 RCL 12
245 /
246 1/X
247 ST+ 20
248 RCL 20
249 "X = "
250 ARCL X
251 AVIEW
252 ADV
253 RCL 13
254 STO 05
255 RCL 14
256 STO 06
257 STOP
258 .END.
```

Example Problem using BKWTR

Using the same channel as the SECPROP Example. Calculate an M2 profile starting with critical flow at the control.

BKWTR

a = 3.0000
B = 50.0000
Z1 = 2.0000
Z2 = 4.0000
SO = 0.0050
Q = 2,200.0000
n = 0.0300

Y = 3.76 ← critical depth
V = 10.12
VH = 1.59
X = 0.00

Y = 3.80
V = 9.99
VH = 1.55
X = -0.21

Y = 3.85
V = 9.84
VH = 1.50
X = -0.98

Y = 3.90
V = 9.69
VH = 1.46
X = -2.43

Y = 4.00
V = 9.40
VH = 1.37
X = -7.77

Y = 4.10
V = 9.13
VH = 1.29
X = -17.76

Y = 4.20
V = 8.87
VH = 1.22
X = -35.23

Y = 4.30
V = 8.62
VH = 1.15
X = -66.54

Y = 4.35
V = 8.49
VH = 1.12
X = -93.20

Y = 4.40
V = 8.38
VH = 1.09
X = -135.35

Y = 4.43 ← normal depth
V = 8.31
VH = 1.07
X = -177.59

Y = 4.50
V = 8.15
VH = 1.03
X = -527.33

Y = 4.60
V = 7.93
VH = 0.98
X = -333.79

Notice that the solution "blows'up" for depths greater than normal depth.

Example - use of SECPROP

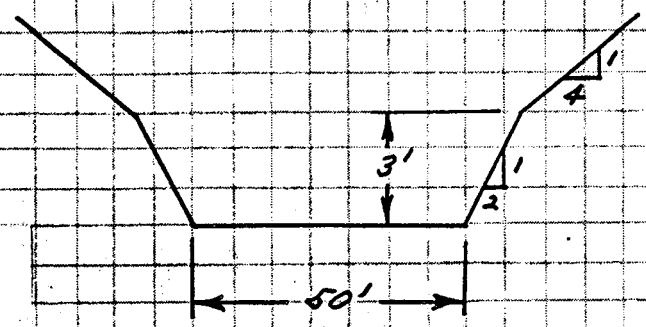

SECPROP

a = 3.0000
B = 50.0000
Z1 = 2.0000
Z2 = 4.0000

Y = 0.5000
A = 25.5000
T = 52.0000
D = 0.4904
ZG = 101.2492
P = 52.2361
RH = 0.4882
AR = 15.8096

Y = 1.0000
A = 52.0000
T = 54.0000
D = 0.9630
ZG = 289.3285
P = 54.4721
RH = 0.9546
AR = 50.4146

Y = 1.5000
A = 79.5000
T = 56.0000
D = 1.4196
ZG = 537.0809
P = 56.7082
RH = 1.4019
AR = 99.5821

Y = 2.0000
A = 108.0000
T = 58.0000
D = 1.8621
ZG = 835.6121
P = 58.9443
RH = 1.8322
AR = 161.7131

Y = 2.5000
A = 137.5000
T = 60.0000
D = 2.2917
ZG = 1,180.2160
P = 61.1803
RH = 2.2475
AR = 235.9192

Y = 3.00
A = 168.00
T = 62.00
D = 2.71
ZG = 1,568.02
P = 63.42
RH = 2.65
AR = 321.65

Y = 3.00
A = 168.00
T = 62.00
D = 2.71
ZG = 1,568.02
P = 63.42
RH = 2.65
AP = 321.65

Y = 3.50
A = 200.00
T = 66.00
D = 3.03
ZG = 1,974.04
P = 66.73
RH = 3.00
AR = 415.74

Y = 4.00
A = 234.00
T = 70.00
D = 3.34
ZG = 2,425.82
P = 70.05
RH = 3.34
AR = 522.90

Y = 4.50
A = 270.00
T = 74.00
D = 3.65
ZG = 2,924.24
P = 73.37
RH = 3.68
AR = 643.59

Y = 5.00
A = 308.00
T = 78.00
D = 3.95
ZG = 3,470.26
P = 76.68
RH = 4.02
AR = 778.25

Y = 6.00
A = 390.00
T = 86.00
D = 4.53
ZG = 4,709.02
P = 83.32
RH = 4.68
AR = 1,091.33

Y = 7.00
A = 480.00
T = 94.00
D = 5.11
ZG = 6,150.00
P = 89.95
RH = 5.34
AR = 1,465.78

Y = 8.00
A = 578.00
T = 102.00
D = 5.67
ZG = 7,801.44
P = 96.58
RH = 5.98
AR = 1,905.23

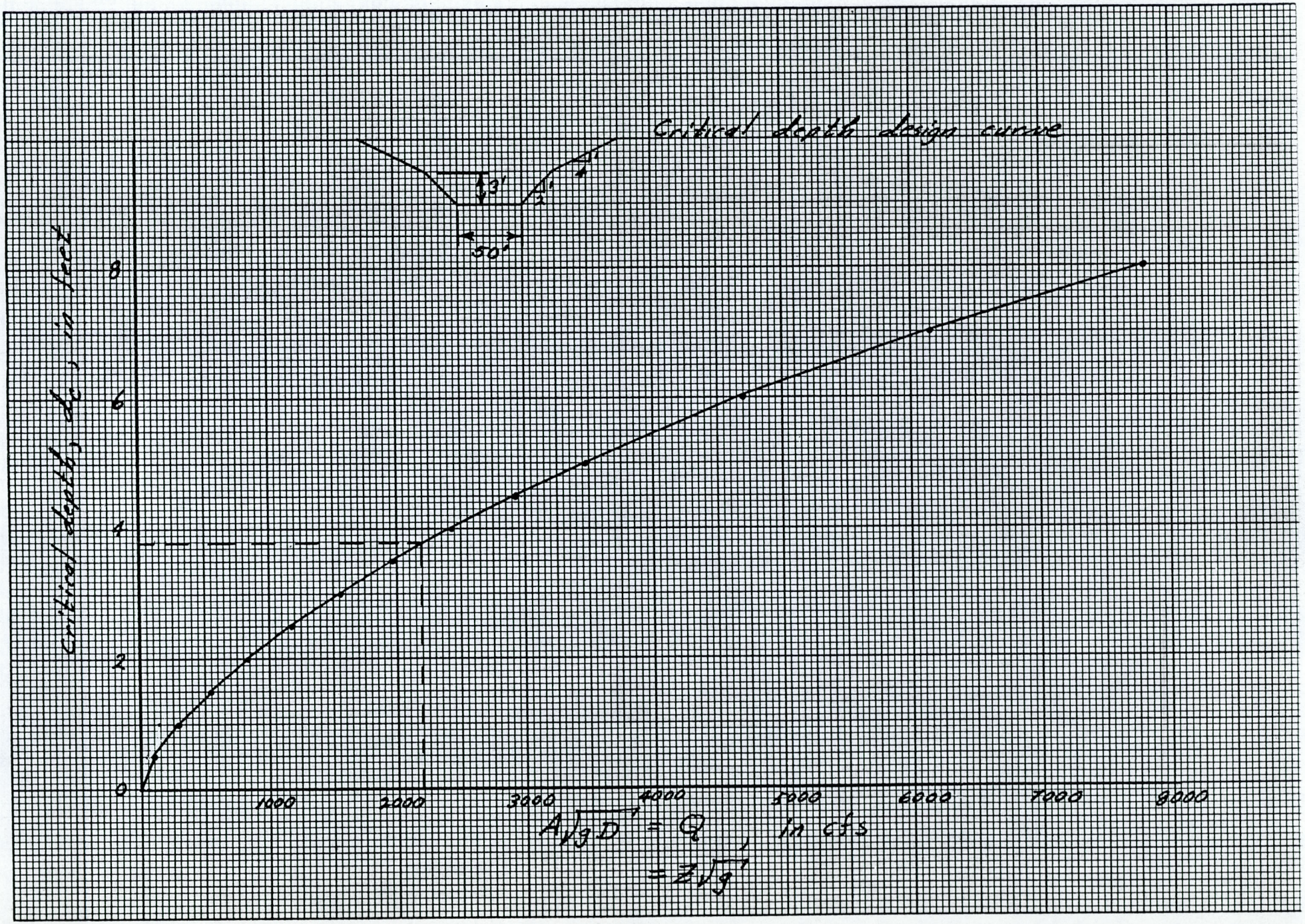

CITADEL® NO. 643 - CROSS SECTION - 20 SQUARES TO INCH

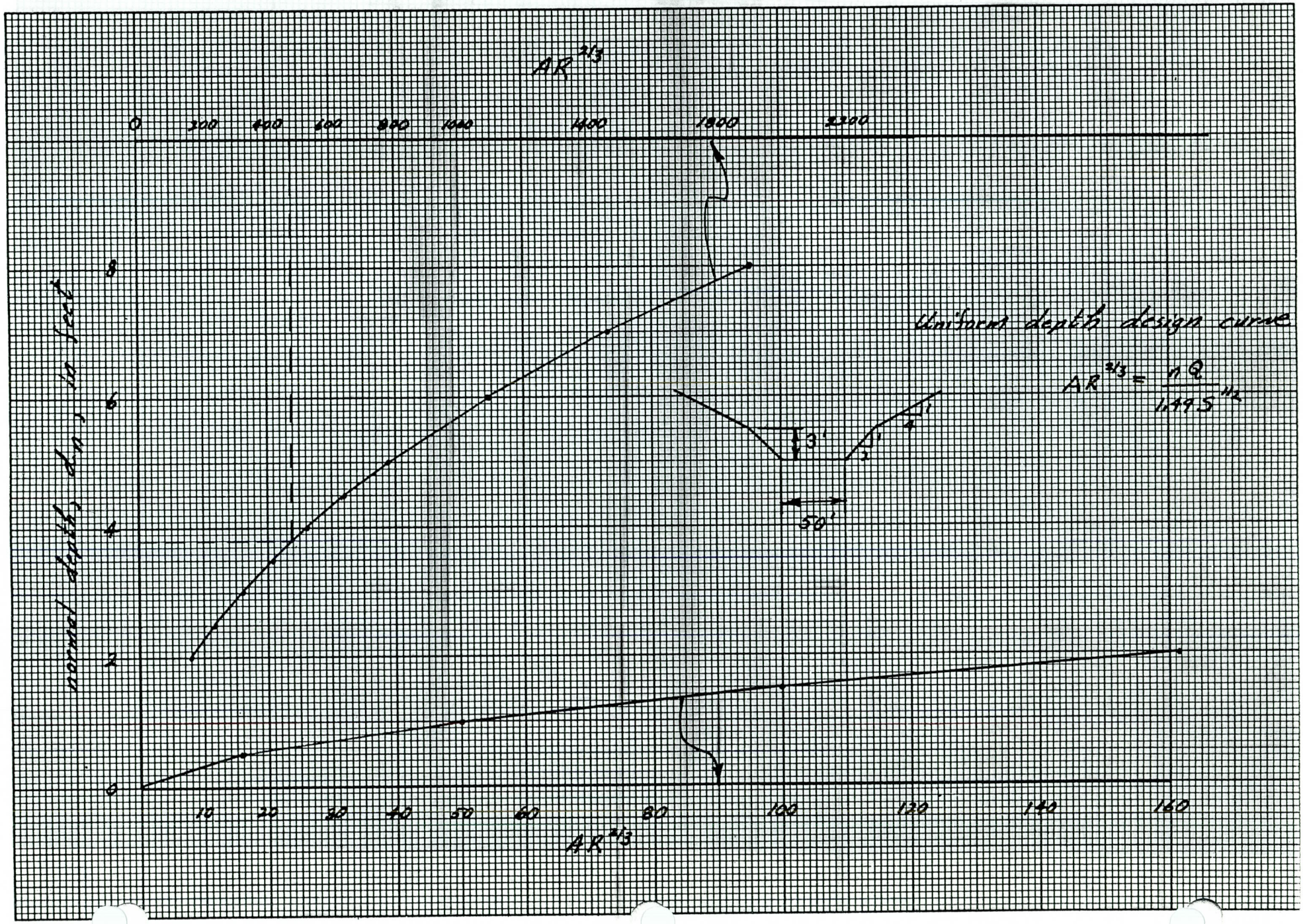

CITADEL® NO. 643 - CROSS SECTION - 20 SQUARES TO INCH

Design discharge = 2200 cfs

Riprap lined lower bank, earthen upper bank, and sand bed channel.

Practical range of n .02 → .04 ?

1. What is the critical depth for 2200 cfs ?

$$\underline{\underline{d_c = 3.8 \text{ ft}}}$$

2. If the bed slope is .5%, what is the normal depth ?

$$AR^{2/3} = \frac{nQ}{1.49 S^{1/2}}$$

$$= n \frac{2200}{1.49 (.005^{1/2})}$$

$$= n (20,881)$$

n	$AR^{2/3}$	d_n	comment
.02	417	3.5	supercritical
.025	522	4.0	subcritical
.03	626	4.5	subcritical
.035	730	4.7	subcritical
.04	835	5.2	subcritical

This channel could easily fluctuate between subcritical and supercritical flow, with waves 2 ft high!

3. What is the critical slope ?

@ $d_c = d_n = 3.8$ ft, $AR^{2/3} = 480 = \frac{nQ}{1.49 S_c^{1/2}}$

$\hookrightarrow S_c = n^2(9.46)$

n	S_c
.02	.0038
.025	.0059
.03	.0085
.035	.0116
.04	.0151

channel slopes from .3% to 1.5% could be critical!

4.6.4 Routing Procedure

For the storage facilities involved in urban highway drainage, it will be assumed that the water surface in the impoundment is horizontal, that the overflow and storage are each functions of the stored water elevation. Under such circumstances, the continuity equation becomes (for short

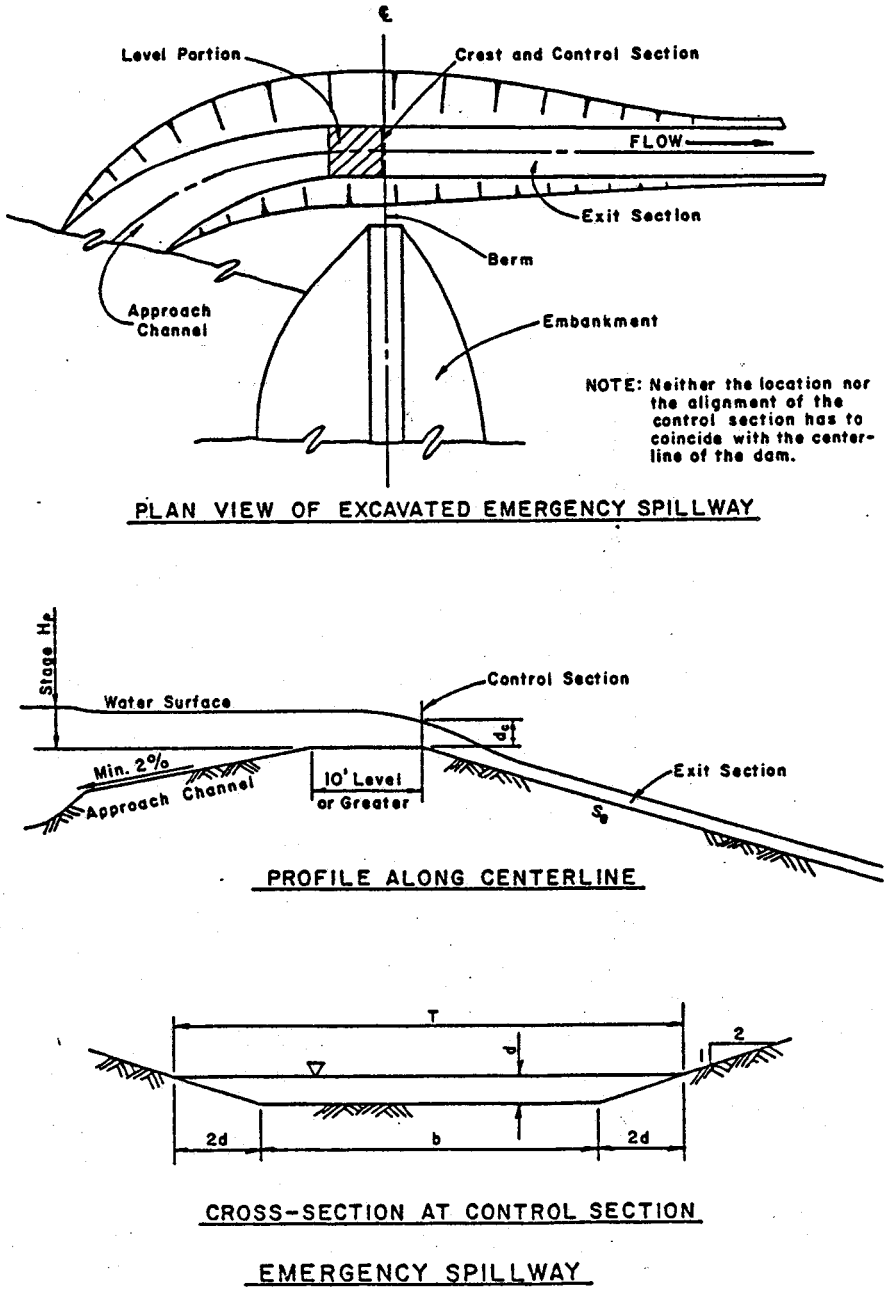

FIG. 4-3

finite time periods Δt, in minutes, the hydrograph may be taken as a straight line):

$$\frac{I_1 + I_2}{2} \; 60 \; \Delta t - \frac{O_1 + O_2}{2} \; 60 \; \Delta t = S_2 - S_1 \qquad (4\text{-}20)$$

in which I_1 and I_2 are the inflow rates in cfs at the beginning and end of the time period Δt in minutes; O_1 and O_2 are the outflow rates at the beginning and end of the same time period Δt (the factor 60 converts the time period to seconds); S_2 and S_1 are the storage volumes in cubic feet at the beginning and end of the time period Δt. In short: inflow mass less outflow mass equals change in storage. This can be rearranged as follows:

$$\frac{I_1 + I_2}{2} + \frac{S_1}{60 \; \Delta t} - \frac{O_1}{2} = \frac{S_2}{60 \; \Delta t} + \frac{O_2}{2} \qquad \text{.....(4-21)}$$

At the beginning of any routing period t, all parameters on the left side of the equation are known. Fortunately, the right side parameters are directly related in the storage-discharge curve, if it is assumed that the water surface of the impoundment is horizontal (with no significant backwater). I_1 and I_2 can be obtained from the inflow hydrograph and S_1 is known for the starting depth; the outflow for the amount of storage at the starting depth can be calculated or obtained from the discharge-storage curve or relationship.

The following examples illustrate the relative simplicity of solving equation 4-21:

4.6.4.1 <u>Example 4-1</u>

Given: Area = 210 acres or 0.33 square miles

L = 0.85 mile

L_{ca} = 0.59 mile

Traversed by highway 2000 feet long, 240 feet wide; 11-acre right-of-way;

5.1-acre pavement;

Impervious area = 40%

Pervious area = 60%

Assume unit duration = 10 minutes

Storage basin equivalent to one with bottom dimensions of 170 feet by 340 feet and 2:1 side slopes; a single outlet draining the lowest point; and a broad-crested overflow spillway.

Determine outflow hydrograph with peak no greater than 60% of the maximum inflow with inflow hydrograph based upon 10-year 30-minute rainfall at Denver, Colorado. Excess precipitation the same as was used in Table 3-9.

Step 1: Using the Denver Synthetic Unit Hydrograph formulas (Equations 3-15 and 3-16), develop the 10-minute unit hydrograph

$$C_t = 7.81/40^{.78} = 0.44$$

$$t_p = 0.44(0.85 \times 0.59)^{.3} = .36 \text{ hour} = 22 \text{ minutes}$$

$$C_p = 0.89 \times .44^{.46} = 0.61$$

$$q_p = \frac{640 \times 0.61}{.36} = 1084 \text{ cfs/sm}$$

$$Q_p = 1084 \times 0.33 = 358 \text{ cfs}$$

$$T_p = 22 + 10/2 = 27 \text{ minutes} = 0.45 \text{ hour}$$

Step 2: With unit hydrograph Q assumed as 358 cfs and T_p as 0.45 hour, the CSC dimensionless unit hydrograph results in the inflow hydrograph of Fig. 4-4 with 10-minute ordinates as given in column 14 of Table 4-2.

Step 3: Using FHWA HEC-5 and HEC-10 select an outlet pipe size and assuming a maximum outflow of 220 cfs with a maximum water depth of 8 to 10 feet (and a culvert length of 70 feet), determine the head-discharge relationship. Chart 2 of HEC-5 indicates a 60-inch pipe under 8 feet total head above its invert would handle about 220 cfs, so it is decided to develop the head-discharge curve for a 60-inch pipe. Fig. 4-5 and column 2 of Table 4-3 give the curve and tabulation of the data.

Step 4: Assume a detention basin with a depth-volume curve such as would result from a rectangular basin with a bottom 170 feet by 340 feet and 2:1 side slopes. Such a curve is given by Fig. 4-5. The surface area of the pond structure at 10-foot depth would be 79,800 square feet or 1.8 acres; at 8-foot depth 75,144 square feet or 1.7 acres; and 70,616 square feet (almost 1.6 acres) at 6-foot depth. Table 4-3 column 3 gives the total storage below each foot of elevation up to a depth of 10 feet. Note that storage is given in cfs-minutes which is the actual cubic feet of storage divided by 60.

FIG. 4-4

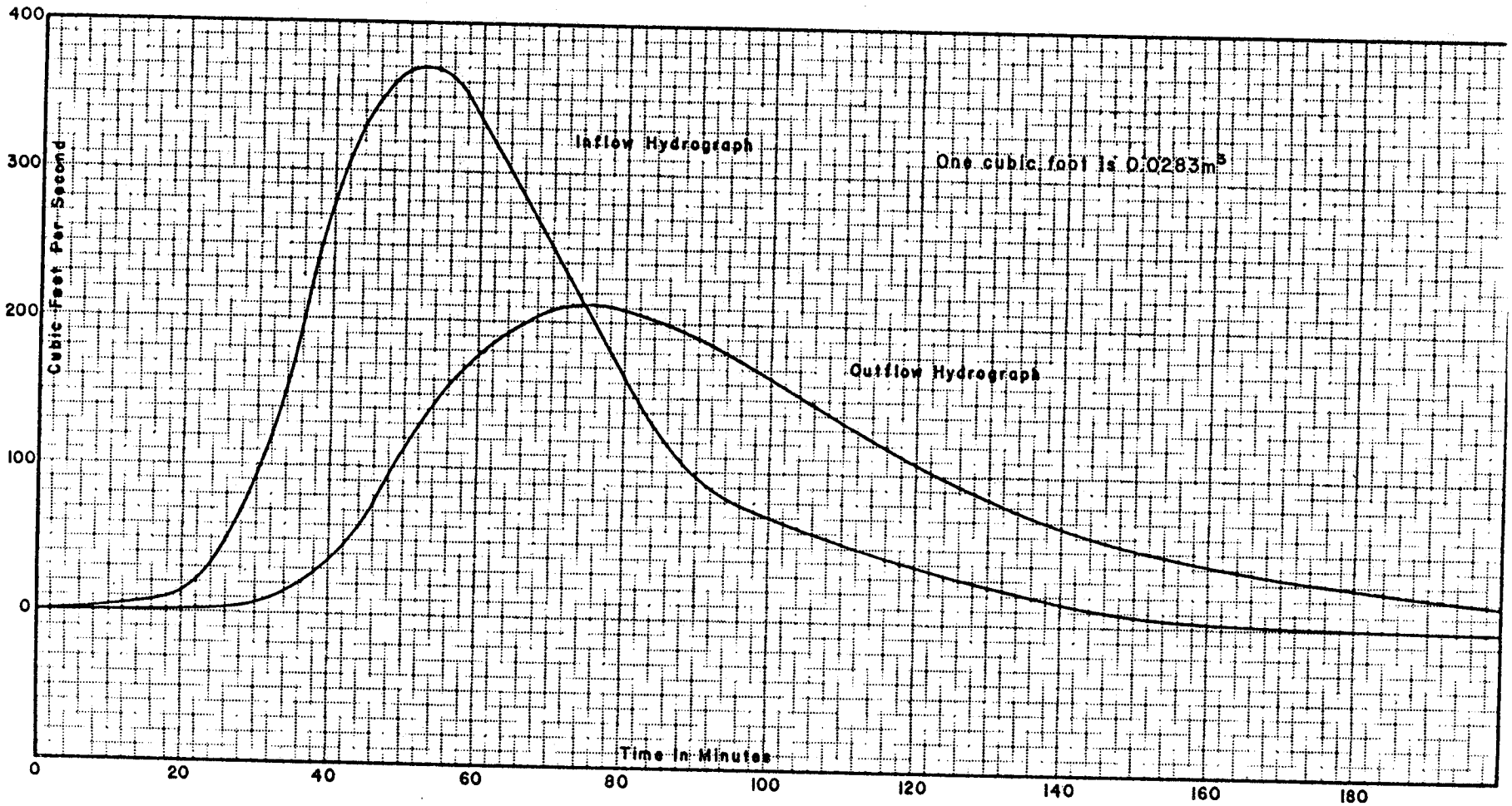

INFLOW AND OUTFLOW HYDROGRAPHS

STORAGE ROUTING EXAMPLE NO. 4-1

DETERMINATION OF STORM HYDROGRAPH
(EXAMPLE 4-1)

Time (Min.) (1)	Unit Hydrograph (cfs) (2)	Excess Precipitation in Inches											Hydrograph (cfs) (14)
		.02 (3)	.05 (4)	.74 (5)	.24 (6)	.17 (7)	06 (8)	03 (9)	03 (10)	02 (11)	02 (12)	02 (13)	
0	0												0
10	98	2.0											2.0
20	309	6.2	5.0										11.2
30	350	7.0	15.4	73									95.4
40	250	5.0	17.5	229	23.5								275
50	129	2.6	12.5	259	74	16.7							365
60	72	1.4	6.5	185	84	52	5.9						334.8
70	38.3	0.8	3.6	95	60	60	18.5	2.9					259
80	21.2	0.4	1.9	53	31	43	21.0	9.3	2.9				162
90	11.7	0.2	1.1	28	17.3	22	15.0	10.3	9.3	2.0			95
100	6.4	0.1	0.6	15.6	9.2	12.2	7.7	7.5	10.3	6.2	2.0		71
110	5.1	0.1	0.3	8.7	5.1	6.5	4.3	3.9	7.5	7.0	6.2	2.0	52
120	3.7	0.1	0.3	4.7	2.8	3.6	2.3	2.2	3.9	5.0	7.0	6.2	38
130	0	0	0.2	3.8	1.5	2.0	1.3	1.1	2.2	2.6	5.0	7.0	26
140			0	2.7	1.2	1.1	0.7	0.6	1.1	1.4	2.6	5.0	16
150				0	0.9	0.9	0.4	0.4	0.6	0.8	1.4	2.6	8
160					0	0.6	0.3	0.2	0.4	0.4	0.8	1.4	4
170						0	0.2	0.2	0.2	0.2	0.4	0.8	2
180							0	0.1	0.2	0.1	0.2	0.4	1
190								0	0.1	0.1	0.1	0.2	0.5
200									0	0.1	0.1	0.1	0.3
210										0	0.1	0.1	0.2
220											0	0.1	0.1
230												0	0

One inch is 25.4mm. One cubic foot is $0.0283m^3$

TABLE 4-2

EXAMPLE 4-1
HEAD-STORAGE & HEAD-DISCHARGE
STORAGE ROUTING COMPUTATIONS

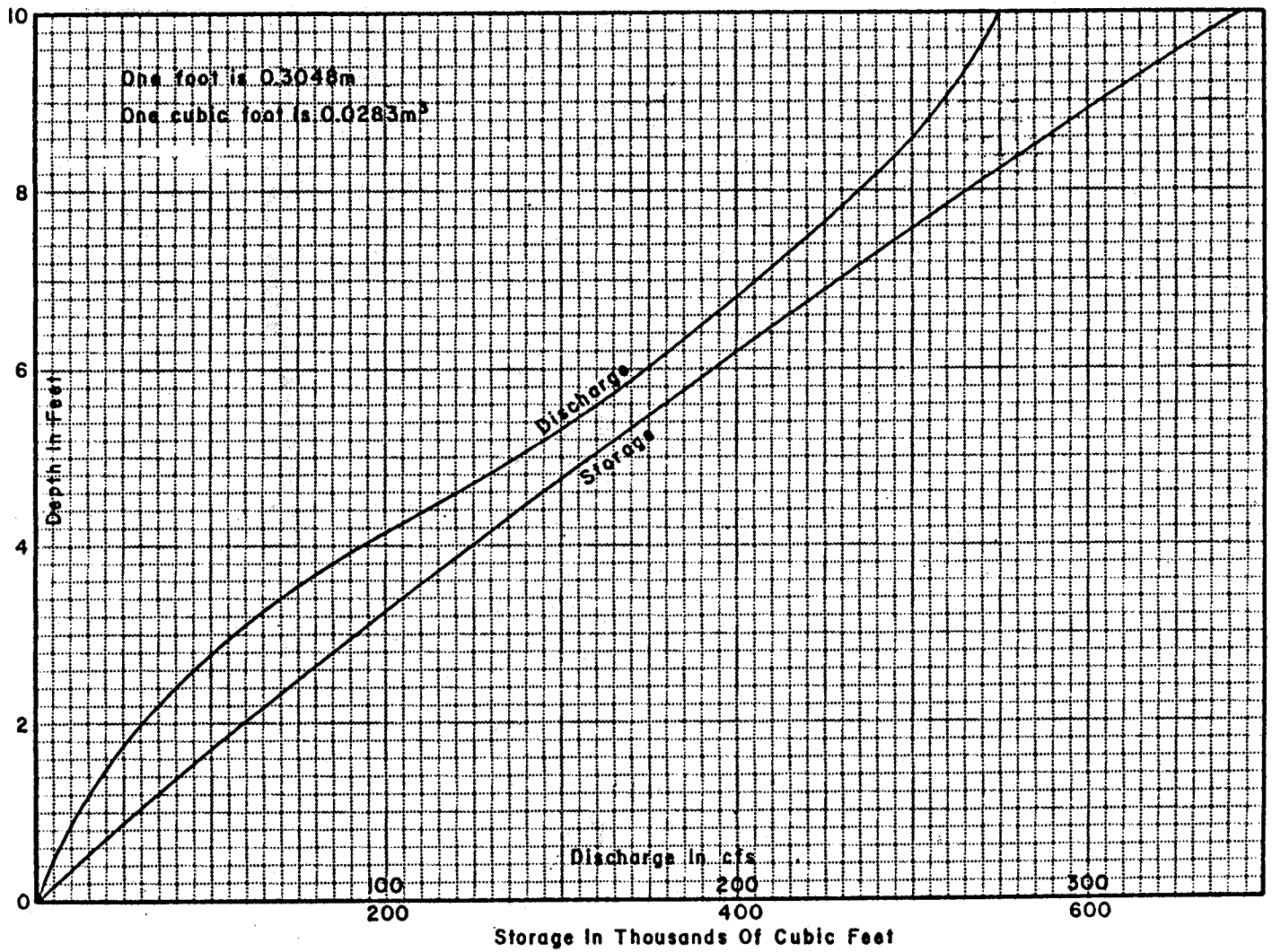

FIG. 4-5

STORAGE-INDICATION COMPILATION TABLE
EXAMPLE 4-1

Elevation (ft.) (1)	Discharge O_2 (cfs) (2)	Storage S_2 (cfs-min) (3)	$\frac{O_2}{2}$ (cfs) (4)	$\Delta t = 10$ min. $\frac{S_2}{\Delta t}$ (cfs) (5)	$\frac{S_2}{\Delta t}+\frac{O_2}{2}$ (cfs) (6)
0	0				
1	14	980.5	7	98.0	105.0
2	32	1995.7	16	199.6	215.6
3	57	3046.6	28.5	304.7	333.2
4	94	4167	47	416.7	463.7
5	137	5269	68.5	526.9	595.4
6	175	6422	87.5	642.2	729.7
7	205	7622	102.5	762.2	864.7
8	235	8863	117.5	886.3	1003.8
9	260	10144	130	1014.4	1144.4
10	275	11467	137.5	1146.7	1284.2

TABLE 4-3

One cubic foot is $0.0283m^3$
One foot is 0.3048m

STORAGE ROUTING COMPUTATIONS
EXAMPLE 4-1

Routing Interval (1)	Time min. (2)	Inflow cfs (3)	Avg. Inflow cfs (4)	$S_1/\Delta t+O_1/2$ cfs (5)	O_1 cfs (6)	$S_2/\Delta t+O_2/2$ cfs (7)	O_2 cfs (8)
1	0	0	0	0	0	0	0
2	10	2.0	1.0	0	0	1.0	0.1
3	20	11.2	6.6	1.0	0.1	7.5	1
4	30	95	53.1	7.5	1	59.6	7.7
5	40	275	185	59.6	7.7	236.9	36
6	50	365	320	236.9	36.0	520.9	112
7	60	335	350	520.9	112	758.9	175
8	70	259	297	759	175	881	208
9	80	162	210.5	881	208	883.5	209
10	90	95	128.5	883.5	209	803	191
11	100	71	83	803	191	695	164
12	110	52	61.5	695	164	593	136
13	120	38	45	593	136	502	106
14	130	26	32	502	106	428	84
15	140	16	21	428	84	365	65
16	150	8	6	365	65	312	52
17	160	4	3	312	52	266	42
18	170	2	1.5	266	42	227	34
19	180	1	0.75	227	34	191	28
20	190	0.5	0.4	191	28	164	26
21	200	0.3	0.25	164	26	138	19
22	210	0.2	0.15	138	19	119	16
23	220	0.1	0.05	119	16	103	14
24	230	0	0	103	14	89	12
25	240			89	12	77	10
26	250			77	10	67	8.8
27	260			67	8.8	58.2	7.5
28	270			58.2	7.5	50.7	6.4
29	280			50.7	6.4	44.3	5.7
30	290			44.3	5.7	38.6	4.8
31				38.6	4.8	33.8	4.2

TABLE 4-4

Step 5: Complete Table 4-3 by computing the proper values to be inserted in columns 4, 5 and 6. Then plot on Fig. 4-6 the curve of $S_2/\Delta t + O_2/2$ against O_2.

Step 6: Set up and complete storage routing, Table 4-4.

Column 1 - routing interval sequence for ease of reference.

Column 2 - insert cumulative time in 10-minute intervals.

Column 3 - from inflow hydrograph as developed in Step 2.

Column 4 - average inflow in each 10-minute interval.

Column 5 - start with 0 in routing interval No. 1. Each subsequent figure in this column is the same as that in column 7 on the line immediately preceding.

Column 6 - start with 0 in routing interval No. 1. Each subsequent figure in this column is the same as that in column 8 of the preceding line.

Column 7 - column 4 plus column 5 minus column 6.

Column 8 - enter the curve on Fig. 4-6 with the value in column 7 and read off the related value of O_2 which is inserted in column 8.

Note that Table 4-4 is a tabular way of solving the storage equation 4-21. The O_2 at the end of each routing interval becomes the O_1 at the beginning of the following interval. The value of $S_2/\Delta t + O_2/2$ at the end of each routing interval becomes the value of $S_1/\Delta t + O_1/2$ at the beginning of the next interval. And when O_1 (column 6) is subtracted from $S_1/\Delta t + O_1/2$ (column 5), it becomes $S_1/\Delta t - O_1/2$. This added to the average inflow (column 4) results in $S_2/\Delta t + O_2/2$ (column 7), all as given by equation 4-21.

Step 7: From the discharge-storage and depth-discharge curves of Fig. 4-5 the maximum storage required for the peak outflow rate of 209 cfs will be 466,000 cubic feet which occurs at a depth of 7.12 feet. This suggests that the emergency overflow spillway could be set at 8 feet.

Step 8: Estimate the probable maximum emergency spillway rate. Precipitation data are to be obtained from the most recent National Weather Service publication (Table 2-1 and Figs. 2-14, 2-15, 2-16) applicable to the area under study. The

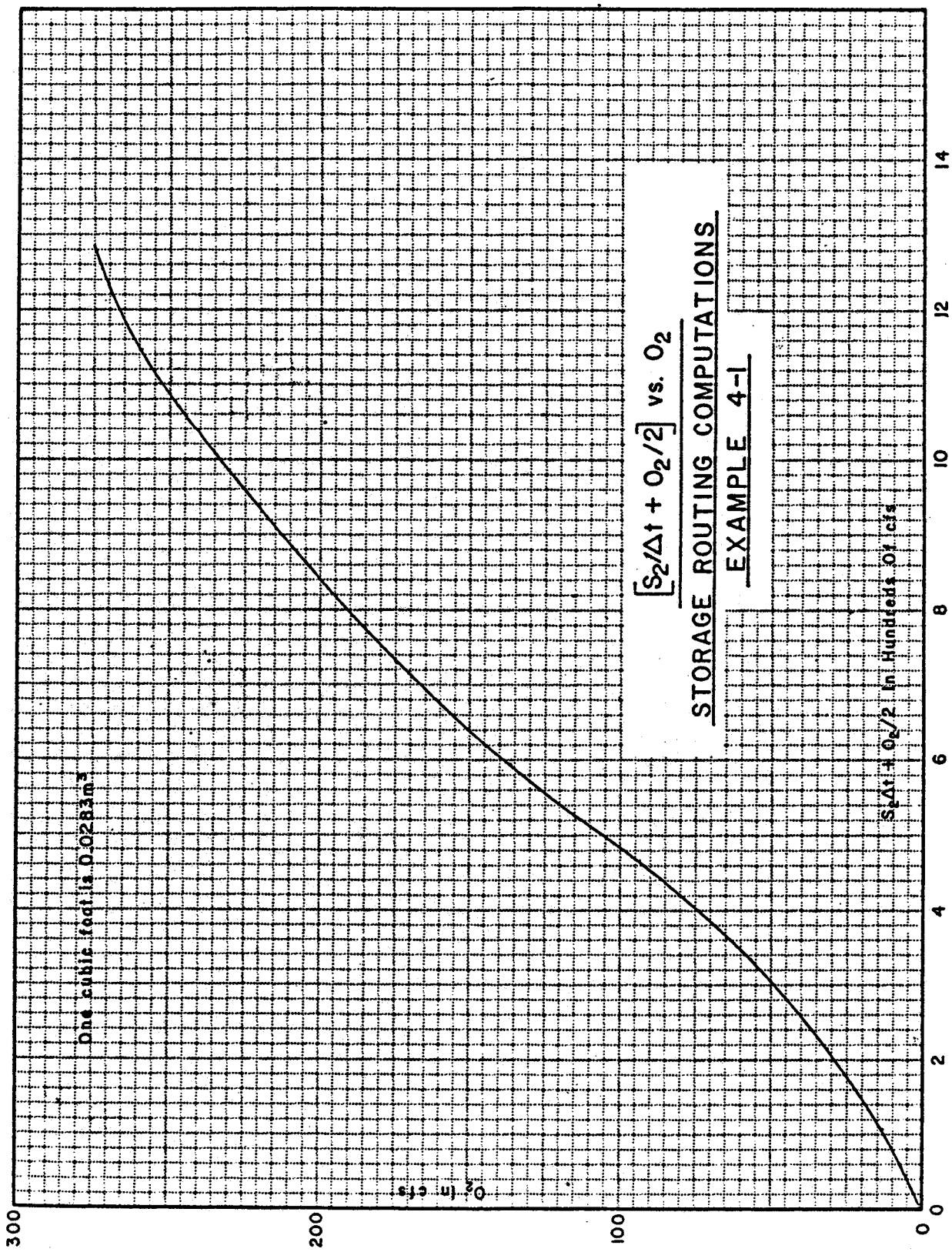
[S2/Δt + O2/2] vs. O2
STORAGE ROUTING COMPUTATIONS
EXAMPLE 4-1
One cubic foot is 0.0283m3
O2 in cfs
S2Δt + O2/2 in Hundreds Of cfs
0
100
200
300
0
2
4
6
8
10
12
14

FIG. 4-6

1-hour 100-year rainfall will often be the desirable basis of design of the principal or emergency spillway, although where lives or high property values would be endangered by a breached detention basin, the probable maximum precipitation (PMP)(Table 2-1, Section C) should be used. The methods of runoff determination discussed in Chapter 3 may be used.

For this example the 60-minute 100-year precipitation at Denver of 2.25 inches will be used. A rational method C of 0.95 will be assumed. The peak 100-year 60-minute runoff will then be 0.95 x 2.25 x 210 = 449 cfs. Should it be desirable to assume the PMP, it would be 0.95 x 21.5 x 210 or 4300 cfs. The former of these would be reduced somewhat (perhaps 30%) by the assumed storage but the great size of the PMP assures complete flooding of the assumed storage with an outflow rate equal to the inflow rate. Actually, a specific design for so great an outflow would make it essential to carry out thorough detailed studies to have confidence that the spillway provided was satisfactory. The entire dam probably would become an overflow spillway and would need to be constructed accordingly.

Assuming the available storage would reduce the 100-year peak to about 315 cfs, the emergency spillway could then be designed as follows:

Using equation 4-14 with the assumption of C_{es} of 3.0 and H_p of 3.0, b is found to be 61 feet. If an H_p of 4.0 can be tolerated, the length of the weir could be shortened to 53 feet. Each foot of height of the dam increases its base width by 4 feet so it becomes a matter of the economic choice of broad-crested weir depth as opposed to critical velocity of flow through the weir and cost of dam fill. The 3-foot deep flow would have a critical velocity (assuming a turf n of 0.04) of 5.5 fps and a critical slope of 2.4%; the 4-foot deep flow would involve a critical velocity of 5.8 fps and 2.3% critical slope. While these velocities are a bit high for turf, the rare 1% frequency of their likelihood makes it feasible to decide upon a dem height of 12 feet assuming the sill of the overflow weir at 8-foot depth plus an overflow depth of 3 feet (and a related 61-foot length of weir along the axis of the dam or related thereto as topography best dictates) with a 1-foot freeboard.

For a thorough treatment of the design of emergency spillways for small dams refer to Refs. 4-11 and 4-12.

JOURNAL OF THE
HYDRAULICS DIVISION

Shallow Wave Propagation in Open Channel Flow

By Victor Miguel Ponce,[1] M. ASCE and Daryl B. Simons,[2] F. ASCE

Introduction

Over the years, several investigators have attempted to clarify the phenomenon of propagation of shallow waves in open channel flow. Perhaps the most illuminating of these studies is that reported in the classical paper by Lighthill and Whitham (5), which analyzed in detail the concept of kinematic wave and contrasted it to the dynamic wave. The Lagrange formula (3) for the celerity of shallow gravity waves has also been a subject of considerable attention in the literature. Despite the progress made in the understanding of the physical phenomenon, a coherent theory that accounts for celerity as well as attenuation characteristics has yet to be formulated. In this respect, the theory of linear stability (6) can be used as an effective tool not only to furnish a first approximation analysis but also to provide valuable insight into the underlying physics of the problem.

The analysis presented herein endeavors to apply the theory of linear stability to the set of equations governing the motion in open channel flow. The equations are the so-called Saint Venant equations (1), which are analytical expressions of the principle of mass and momentum conservation. The conclusions relate to the magnitude of celerity and attenuation of various types of shallow water waves, expressed as a function of the Froude number of the steady uniform flow and a dimensionless wave number of the unsteady component of the motion.

Governing Equations

The governing equations for the one-dimensional unsteady flow in broad

Note.—Discussion open until May 1, 1978. To extend the closing date one month, a written request must be filed with the Editor of Technical Publications, ASCE. This paper is part of the copyrighted Journal of the Hydraulics Division, Proceedings of the American Society of Civil Engineers, Vol. 103, No. HY12, December, 1977. Manuscript was submitted for review for possible publication on February 7, 1977.

[1] Asst. Prof. of Civ. Engrg., Colorado State Univ., Fort Collins, Colo.

[2] Prof. of Civ. Engrg., and Assoc. Dean of Research, Colorado State Univ., Fort Collins, Colo.

annels of rectangular cross section, expressed per unit of channel width, : (4) equation of continuity

$$\frac{\partial d}{\partial x} + d\frac{\partial u}{\partial x} + \frac{\partial d}{\partial t} = 0 \quad (1)$$

d equation of motion

$$\frac{\partial u}{\partial t} + \frac{u}{g}\frac{\partial u}{\partial x} + \frac{\partial d}{\partial x} + (S_f - S_o) = 0 \quad (2)$$

which u = velocity averaged in a vertical section; d = depth of flow; g acceleration of gravity; S_f = friction slope; and S_o = bed slope.

he friction slope S_f is directly related to the bottom shear stress τ by the ression (2):

$$= \frac{\tau}{\gamma d} \quad (3)$$

which γ is the unit weight of water.

n the usual manner of stability calculations (7), Eqs. 1 and 2 must satisfy unperturbed flow for which $u = u_o$; $d = d_o$; and $\tau = \tau_o$, as well as the turbed flow for which $u = u_o + u'$; $d = d_o + d'$; and $\tau = \tau_o + \tau'$. superscript in the flow variables represents a small perturbation to the dy uniform flow. Thus, all quadratic terms in the fluctuating components be neglected due to an order of magnitude reasoning.

ubstitution of the perturbed variables in Eqs. 1, 2, and 3 yields, after arization (5):

$$\frac{\partial d'}{\partial x} + d_o\frac{\partial u'}{\partial x} + \frac{\partial d'}{\partial t} = 0 \quad (4)$$

$$\frac{\partial u'}{\partial t} + \frac{u_o}{g}\frac{\partial u'}{\partial x} + \frac{\partial d'}{\partial x} + S_o\left(\frac{\tau'}{\tau_o} - \frac{d'}{d_o}\right) = 0 \quad (5)$$

hich $S_o = \dfrac{\tau_o}{\gamma d_o}$ (6)

he boundary shear stress τ can be related to the mean velocity by

$$f\rho u^2 \quad (7)$$

hich $f = \dfrac{g}{C_f^2}$ (8)

re C_f is the Chezy coefficient; and ρ = the density of water. Considering 7, Eq. 5 can be rewritten as

$$\frac{\partial u'}{\partial t} + \frac{u_o}{g}\frac{\partial u'}{\partial x} + \frac{\partial d'}{\partial x} + S_o\left(2\frac{u'}{u_o} - \frac{d'}{d_o}\right) = 0 \quad (9)$$

or most practical applications, the Manning equation is preferred over the zy equation. The er, however, has the advantage of nondimensionality,

and it is for this reason that it is used here. Furthermore, the constant C_f is consistent with the small perturbation assumption.

Wave Models

The propagation of shallow water waves is controlled by the balance of the various forces included in the equation of motion. In Eq. 2, the first term represents the local inertia term, the second term represents the convective inertia term, the third term represents the pressure differential term, and the fourth accounts for the friction and bed slopes. Various wave models can be construed, depending on which of these four terms is assumed negligible when compared with the remaining terms.

The following chart provides a ready reference to the various wave models that are recognized.

Term	I	II	III	IV	
Equation of motion	$\frac{1}{g}\frac{\partial u}{\partial t}$ +	$\frac{u}{g}\frac{\partial u}{\partial x}$ +	$\frac{\partial d}{\partial x}$ +	$(S_f - S_o) = 0$	(2)

Wave model and terms used to describe it are: (1) Kinematic wave IV; (2) diffusion wave III + IV; (3) steady dynamic wave II + III + IV; (4) dynamic wave I + II + III + IV; and (5) gravity wave I + II + III.

Small Perturbation Analysis

In order to provide for a convenient way to take explicit account of the various wave models, Eq. 9 is recast as

$$\frac{l}{g}\frac{\partial u'}{\partial t} + \frac{au_o}{g}\frac{\partial u'}{\partial x} + p\frac{\partial d'}{\partial x} + kS_o\left(2\frac{u'}{u_o} - \frac{d'}{d_o}\right) = 0 \quad (10)$$

in which l, a, p, and k are integers that can take values of 0 and 1 only, depending on which terms of Eq. 9 are used to describe the motion.

The solution for a small perturbation in the depth of flow is postulated in the following exponential form:

$$\frac{d'}{d_o} = \hat{d}\exp\left[i(\hat{\sigma}\hat{x} - \hat{\beta}\hat{t})\right] \quad (11)$$

in which d' is a small perturbation to d_o; $\hat{d}$ is a dimensionless depth amplitude function; $\hat{\sigma}$ is a dimensionless wave number; $\hat{\beta}$ is a dimensionless complex propagation factor; and $\hat{x}$ and $\hat{t}$ are dimensionless space and time coordinates such that

$$\hat{\sigma} = \left(\frac{2\pi}{L}\right)L_o \quad (12)$$

$$\hat{\beta}_R = \left(\frac{2\pi}{T}\right)\frac{L_o}{u_o} \quad (13)$$

$\hat{\beta}$ mplitude propagation factor (14

$$\hat{x} = \frac{x}{L_o} \quad (15)$$

$$\hat{t} = t\frac{u_o}{L_o} \quad (16)$$

L = the wavelength of the disturbance; and T = the period. The value L_o = the horizontal length in which the steady uniform flow drops a head equal to its depth, and it is defined as $L_o = d_o/S_o$. The dimensionless celerity of the disturbance is given by

$$\hat{c} = \frac{\frac{L}{T}}{u_o} = \frac{\hat{\beta}_R}{\hat{\sigma}} \quad (17)$$

The wave attenuation follows an exponential law in which the amplitude at a given time t = the initial amplitude at time t_o multiplied by $(e^{\hat{\beta}_I \hat{t}})$, in which $\hat{t} = (t - t_o)u_o/L_o$. When comparing wave amplitudes after one propagation period, the value of $\hat{t}$ is $\hat{t} = T u_o/L_o$, or likewise, $\hat{t} = \frac{2\pi}{|\hat{\beta}_R|}$. The logarithmic decrement (10) δ is defined as $\delta = \hat{\beta}_I T u_o/L_o$, or $\delta = 2\pi\frac{\hat{\beta}_I}{|\hat{\beta}_R|}$. The value of δ is a measure of the rate at which the unsteady component of the motion changes upon propagation. For δ positive, amplification sets in; for δ negative, the motion attenuates and dies away.

The depth disturbance is associated with a velocity disturbance of the form

$$\frac{u'}{u_o} = \hat{u}\exp\left[i(\hat{\sigma}\hat{x} - \hat{\beta}\hat{t})\right] \quad (18)$$

in which $\hat{u}$ is a dimensionless velocity amplitude function. The substitution of Eqs. 11 and 18 into Eqs. 4 and 10 yields, respectively:

$$\hat{\sigma}\hat{u} + (\hat{\sigma} - \hat{\beta})\hat{d} = 0 \quad (19)$$

$$[2k + iF_o^2(a\hat{\sigma} - l\hat{\beta})]\hat{u} + (ip\hat{\sigma} - k)\hat{d} = 0 \quad (20)$$

in which $F_o^2 = \frac{u_o^2}{gd_o}$ (21)

Eqs. 19 and 20 constitute a homogeneous system of linear equations in the unknowns $\hat{u}$ and $\hat{d}$. For the solution to be nontrivial, the determinant of the coefficient matrix must vanish. Accordingly,

$$il\hat{\beta}^2F_o^2 - i\hat{\sigma}^2(p - aF_o^2) + 3k\hat{\sigma} - 2k\hat{\beta} - i\hat{\sigma}\hat{\beta}(l + a)F_o^2 = 0 \quad (22)$$

Eq. 22 is the characteristic equation governing the propagation of small amplitude water waves. In the treatment that follows, successive simplifications will be made to conform to the various types of wave models considered in the previous section.

Kinematic Wave Model

In the kinematic wave model, the inertia and pressure terms are negligible as compared to the friction-bed slope term.

Accordingly, in Eq. 22, $l = a = p = 0$; and $k = 1$, resulting in

$$3\hat{\sigma} - 2\hat{\beta} = 0 \quad (23)$$

Since all the imaginary terms have dropped out in Eq. 23, $\hat{\beta}_I = 0$; and $\hat{\beta}_R = \hat{\beta}$. The logarithmic decrement δ_k is then

$$\delta_k = 2\pi\frac{\hat{\beta}_I}{\hat{\beta}_R} = 0 \quad (24)$$

and the dimensionless celerity of the kinematic wave is

$$\hat{c}_k = \frac{\hat{\beta}_R}{\hat{\sigma}} = \frac{3}{2} \quad (25)$$

Equations 23–25 warrant the following conclusions regarding kinematic wave propagation: (1) Since Eq. 23 is of the first order, kinematic waves propagate only in the downstream direction; (2) the celerity of a kinematic wave is independent of F_o and $\hat{\sigma}$, and equal to 1.5 times the mean flow velocity; and (3) the attenuation of a kinematic wave is zero, i.e., a kinematic wave propagates downstream without dissipation.

Diffusion Wave Model

In the diffusion wave model, the inertia terms are considered negligible, but the pressure term is taken into account in the calculations. Accordingly, in Eq. 22, $l = a = 0$; $p = k = 1$, resulting in

$$-i\hat{\sigma}^2 + 3\hat{\sigma} - 2\hat{\beta} = 0 \quad (26)$$

and $\hat{\beta} = \frac{3\hat{\sigma} - i\hat{\sigma}^2}{2}$ (27)

and the celerity of the diffusion wave is

$$\hat{c}_d = \frac{\hat{\beta}_R}{\hat{\sigma}} = \frac{3}{2} \quad (28)$$

The logarithmic decrement of the diffusion wave is

$$\delta_d = 2\pi\frac{\hat{\beta}_I}{\hat{\beta}_R} = -2\pi\left(\frac{\hat{\sigma}}{3}\right) \quad (29)$$

The following conclusions are derived for diffusion waves: (1) Because Eq. 26 is of first order in $\hat{\beta}$, diffusion waves propagate downstream only, and their celerity is independent of F_o and $\hat{\sigma}$ and equal to 1.5 the mean flow velocity; and (2) diffusion waves attenuate as they propagate downstream, and the rate of attenuation is controlled by the dimensionless wave number $\hat{\sigma}$. The larger the dimensionless wave number, the larger the attenuation.

Steady Dynamic Wave Model

In the steady dynamic wave model, the convective inertia term is brought into the problem, and the local inertia term is neglected. Accordingly, in Eq. 22, $l = 0$; and $a = p = k = 1$, resulting in

$$-i\hat{\sigma}^2(1 - F_o^2) + 3\hat{\sigma} - 2\hat{\beta} - i\hat{\sigma}\hat{\beta}F_o^2 = 0 \quad (30)$$

and
$$\hat{\beta} = \frac{3\hat{\sigma} - i\hat{\sigma}^2(1 - F_o^2)}{2 + i\hat{\sigma}F_o^2} \quad (31)$$

or
$$\hat{\beta} = \frac{\hat{\sigma}\,[6 - \hat{\sigma}^2F_o^2(1 - F_o^2)] - i\hat{\sigma}^2(2 + F_o^2)}{4 + \hat{\sigma}^2F_o^4} \quad (32)$$

From Eq. 32, the celerity of the steady dynamic model is

$$\hat{c}_s = 1 + \frac{2 - \hat{\sigma}^2F_o^2}{4 + \hat{\sigma}^2F_o^4} \quad (33)$$

The logarithmic decrement of the steady dynamic model is

$$\delta_s = -2\pi\frac{\hat{\sigma}(2 + F_o^2)}{6 - \hat{\sigma}^2F_o^2(1 - F_o^2)} \quad (34)$$

The following conclusions are derived regarding the steady dynamic model: (1) The propagation of the steady dynamic wave is in one direction, since Eq. 30 is of first order in $\hat{\beta}$; and (2) the celerity and attenuation characteristics are functions of the Froude number of the steady uniform flow F_o and the dimensionless wave number $\hat{\sigma}$.

Dynamic Wave Model

In the dynamic wave model, all terms in the equation of motion are considered. Thus, in Eq. 22, $l = a = p = k = 1$. It follows that

$$(F_o^2)\hat{\beta}^2 - 2(\hat{\sigma}F_o^2 - i)\hat{\beta} - [\hat{\sigma}^2(1 - F_o^2) + 3\hat{\sigma}i] = 0 \quad (35)$$

Equation 35 is of the second order, resulting in two roots. Physically speaking, dynamic waves propagate along two characteristic paths, which can face either: (1) One upstream and another downstream; or (2) both downstream. In the case of propagation in different directions, it is expedient to define as "primary wave" the wave that travels downstream, and identify its celerity and logarithmic decrement by $\hat{c}_1$ and δ_1, respectively. The "secondary wave" is defined as the wave traveling upstream with celerity $\hat{c}_2$ and logarithmic decrement δ_2. In the case of both waves traveling downstream, "primary wave" is the faster wave, and "secondary wave" is the slower wave.

The solution of Eq. 35 is

$$\hat{\beta} = \hat{\sigma}(1 - i\zeta) + \hat{\sigma}\left[\left(\frac{1}{F_o^2} - \zeta^2\right) + i\zeta\right]^{1/2} \quad (36)$$

in which
$$\zeta = \frac{1}{\hat{\sigma}F_o^2} \quad (37)$$

An expression of the same type as Eq. 37 is referred to in the literature as kinematic flow number (9).

The complex square root argument can be expressed in polar form as

$$A + iB = C(\cos\theta + i\sin\theta) \quad (38)$$

in which
$$A = \frac{1}{F_o^2} - \zeta^2 \quad (39)$$

$$B = \zeta \quad (40)$$

$$C = \left[\left(\frac{1}{F_o^2} - \zeta^2\right)^2 + \zeta^2\right]^{1/2} \quad (41)$$

$$\theta = \arctan\frac{B}{A} \quad (42)$$

and the root of the complex argument is

$$(A + iB)^{1/2} = C^{1/2}\left(\cos\frac{\theta + 2k\pi}{2} + i\sin\frac{\theta + 2k\pi}{2}\right); \quad \text{for } k = 0, 1 \quad (43)$$

and by use of the half-angle relations

$$(A + iB)^{1/2} = \pm C^{1/2}\left[\left(\frac{1 + \cos\theta}{2}\right)^{1/2} + i\left(\frac{1 - \cos\theta}{2}\right)^{1/2}\right] \quad (44)$$

in which use has been made of the fact that because $\zeta \geq 0$, $\theta/2$ falls in the first quadrant.

Since
$$\cos\theta = \frac{A}{C} \quad (45)$$

it follows that

$$(A + iB)^{1/2} = \pm\left[\left(\frac{C + A}{2}\right)^{1/2} + i\left(\frac{C - A}{2}\right)^{1/2}\right] \quad (46)$$

or
$$\hat{\beta} = \hat{\sigma}(1 - i\zeta) \pm \hat{\sigma}\left[\left(\frac{C + A}{2}\right)^{1/2} + i\left(\frac{C - A}{2}\right)^{1/2}\right] \quad (47)$$

From Eq. 47, the following two roots are obtained:

$$\hat{\beta}_1 = \hat{\sigma}\left[1 + \left(\frac{C + A}{2}\right)^{1/2}\right] - i\hat{\sigma}\left[\zeta - \left(\frac{C - A}{2}\right)^{1/2}\right] \quad (48)$$

$$\hat{\beta}_2 = \hat{\sigma}\left[1 - \left(\frac{C + A}{2}\right)^{1/2}\right] - i\hat{\sigma}\left[\zeta + \left(\frac{C - A}{2}\right)^{1/2}\right] \quad (49)$$

Now call
$$D = \left(\frac{C + A}{2}\right)^{1/2} \quad (50)$$

and
$$E = \left(\frac{C - A}{2}\right)^{1/2} \quad (51)$$

and the celerity and attenuation functions are given by

$$\text{primary wave} \quad \hat{c}_1 = 1 + \left(\frac{C + A}{2}\right)^{1/2} \qquad (52)$$

TABLE 1.—Propagation Characteristics of Shallow Water Waves in Open Channel Flow

Type of wave (1)	Relative celerity $\hat{c}_r$ (2)	Logarithmic decrement δ (3)
Kinematic	1/2	0
Diffusion	1/2	$-2\pi(\hat{\sigma}/3)$
Steady dynamic	$(2 - \hat{\sigma}^2 F_o^2)/(4 + \hat{\sigma}^2 F_o^4)$	$-2\pi\,\hat{\sigma}(2 + F_o^2)/[6 - \hat{\sigma}^2 F_o^2(1 - F_o^2)]$
(*a*) Dynamic		
Primary wave	$+[(C + A)/2]^{1/2}$	$-2\pi(\zeta - E)/\lvert 1 + D\rvert$
Secondary wave	$-[(C + A)/2]^{1/2}$	$-2\pi(\zeta + E)/\lvert 1 - D\rvert$
(*b*) Gravity		
Primary wave	$+1/F_o$	0
Secondary wave	$-1/F_o$	0

Note: $\zeta = 1/(\hat{\sigma}F_o^2)$; $A = (1/F_o^2) - \zeta^2$; $C = \{[(1/F_o^2) - \zeta^2]^2 + \zeta^2\}^{1/2}$; $D = [(C + A)/2]^{1/2}$; $E = [(C - A)/2]^{1/2}$.

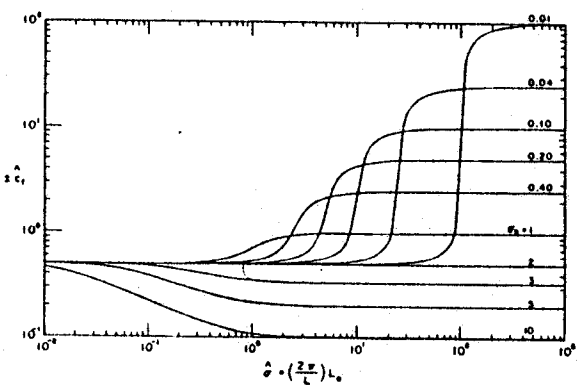

FIG. 1.—Dimensionless Relative Celerity $\hat{c}_r$ versus Dimensionless Wave Number $\hat{\sigma}$; Curve Parameter = Froude Number F_o ($0.01 \le F_o \le 10$)

$$\delta_1 = -2\pi \frac{\zeta - E}{|1 + D|} \qquad (53)$$

$$\text{and secondary wave} \quad \hat{c}_2 = 1 - \left(\frac{C + A}{2}\right)^{1/2} \qquad (54)$$

$$\delta_2 = -2\pi \frac{\zeta + E}{|1 - D|} \qquad (55)$$

Gravity Wave Model

In the gravity wave model, the friction and bed slope terms are excluded from the momentum equation. It follows that, in Eq. 22, $l = a = p = 1$ and $k = 0$, resulting in

$$\hat{\beta}^2 F_o^2 - 2\hat{\sigma}\hat{\beta}F_o^2 - \hat{\sigma}^2(1 - F_o^2) = 0 \qquad (56)$$

Since Eq. 56 is of the second order in $\hat{\beta}$ and contains no imaginary terms gravity waves have two characteristic directions and are not subject to attenuation.

Solving for $\hat{\beta}_R$ in Eq. 56

$$\hat{\beta}_R = \hat{\sigma}\left(\frac{F_o^2 \pm F_o}{F_o^2}\right) \qquad (57)$$

and the celerity of a gravity wave is given as

$$\hat{c}_g = \frac{\hat{\beta}_R}{\hat{\sigma}} = 1 \pm \frac{1}{F_o} \qquad (58)$$

or in the more usual way of expressing it (Lagrange formula)

$$c_g = u_o \pm \sqrt{gd_o} \qquad (59)$$

Gravity waves propagate along two characteristic directions. In subcritical flow, one direction is downstream, with celerity $c_1 = u_o + \sqrt{gd_o}$, and another is upstream, with celerity $c_2 = u_o - \sqrt{gd_o}$. In critical flow, $c_1 = 2u_o$; and $c_2 = 0$. In supercritical flow, both waves travel downstream, with celerities $c_1 = u_o + \sqrt{gd_o}$; and $c_2 = u_o - \sqrt{gd_o}$.

A summary of the propagation characteristics of the various waves described is given in Table 1. The celerity shown in Table 1 is the relative celerity $\hat{c}_r$ in which

$$\hat{c}_r = \hat{c} - 1 \qquad (60)$$

Analysis of Dynamic Model

Eqs. 52–55 enable the calculation of the propagation characteristics of the dynamic wave model, as a function of the Froude number F_o of the steady uniform flow and the dimensionless wave number $\hat{\sigma}$ of the sinusoidal perturbation superimposed on the steady uniform flow.

Fig. 1 shows the calculated values of the dimensionless relative celerity versus the dimensionless wave number $\hat{\sigma}$, for Froude numbers between 0.01–10. The following conclusions are derived from this figure:

1. There are three well-defined bands in the wave number spectrum: (a) a kinematic band corresponding to small values of the wave number $\hat{\sigma}$, in which the relative celerity $\hat{c}_r$ is independent of both $\hat{\sigma}$ and the Froude number F_o; (b) a gravity band corresponding to large values of $\hat{\sigma}$, in which $\hat{c}_r$ is independent

of $\hat{\sigma}$ and dependent only on F_o; and (c) a dynamic band, in which $\hat{c}_r$ is a function of both $\hat{\sigma}$ and F_o.

In the kinematic band, $\hat{c}_r$ approaches asymptotically a constant value of 0.5,

TABLE 2.—Celerity[a] and Attenuation[b] Characteristics of the Dynamic Wave

Froude number (1)	Primary Wave $\hat{c}_1$ (2)	Primary Wave δ_1 (3)	Secondary Wave $\hat{c}_2$ (4)	Secondary Wave δ_2 (5)
$F_o < 1$	+	−	−	−
			+	−
$F_o = 1$	+	−	0	−
			+	−
$1 < F_o < 2$	+	−	+	−
$F_o = 2$	+	0	+	−
$F_o > 2$	+	+	+	−

[a]Downstream celerity +; upstream celerity −.
[b]Attenuation −; amplification +.

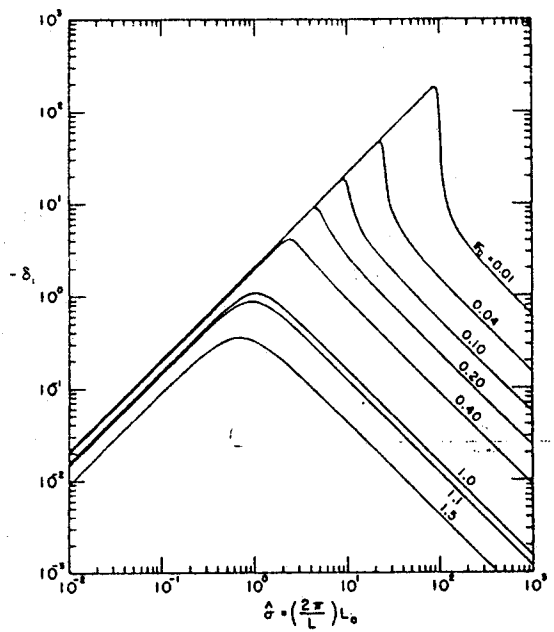

FIG. 2.—Primary Wave Logarithmic Decrement $-\delta_1$ versus Dimensionless Wave Number $\hat{\sigma}$; Curve Parameter = Froude Number F_o ($F_o < 2$)

which corresponds to that of a kinematic wave. In the gravity band, $\hat{c}_r$ approaches asymptotically the value $1/F_o$, which corresponds to that of a gravity wave. In the dynamic band, $\hat{c}_r$ lies between the kinematic and gravity wave celerity values.

2. The location of the dynamic band in the $\hat{\sigma}$ spectrum is a function of F_o.

A corollary resulting from Fig. 1 is that for $F_o = 2$, $\hat{c}_r = 0.5$ for all values of $\hat{\sigma}$. Thus, at $F_o = 2$, all waves, kinematic, dynamic, and gravity, have celerities equal to the kinematic value. The conclusions of Fig. 1 regarding the limiting value of $\hat{c}_r$ in the kinematic and gravity bands can be obtained analytically based on limit theory. It can be shown that as $\hat{\sigma} \to \infty$, $\hat{c}_r \to 1/F_o$, and as $\hat{\sigma} \to 0$, $\hat{c}_r \to 0.5$ (for F_o constant).

The calculation of the logarithmic decrements δ_1 and δ_2 as a function of $\hat{\sigma}$ and F_o, by means of Eqs. 53 and 55 enable the following general conclusions:

1. For $F_o < 2$, primary waves propagate downstream and attenuate; for $F_o = 2$, primary waves propagate downstream and neither amplify nor attenuate throughout the $\hat{\sigma}$ spectrum; for $F_o > 2$, primary waves propagate downstream and amplify.

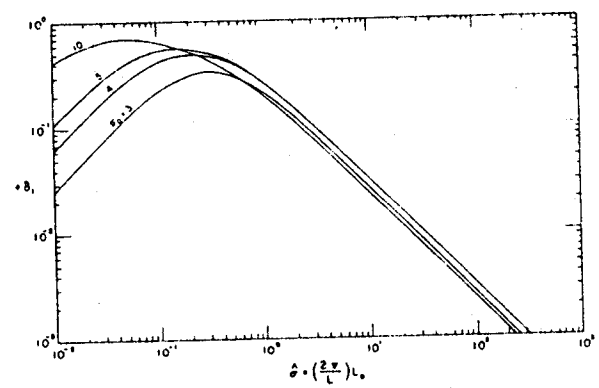

FIG. 3.—Primary Wave Logarithmic Decrement $+\delta_1$ versus Dimensionless Wave Number $\hat{\sigma}$; Curve Parameter = Froude Number F_o ($F_o > 2$)

2. For $F_o < 1$, secondary waves propagate upstream ($\hat{c}_r > 1$), or downstream ($\hat{c}_r < 1$). For $F = 1$, secondary waves remain stationary ($\hat{c}_r = 1$), or propagate downstream ($c_r < 1$). For $F_o > 1$, secondary waves propagate downstream. Secondary waves attenuate for all F_o and $\hat{\sigma}$.

Table 2 summarizes the conclusions of the foregoing paragraph.

Primary Wave Attenuation Analysis, $F_o < 2$.—Fig. 2 depicts the variation of the logarithmic decrement δ_1 for $F_o < 2$, as a function of $\hat{\sigma}$. The following conclusions are drawn: (1) The logarithmic decrement δ_1 is maximum (in absolute value) at a value of $\hat{\sigma}$ corresponding to the point of inflexion of the $\hat{c}_r$ versus $\hat{\sigma}$ curve (Fig. 1). The value of $\hat{\sigma}$ for which δ_1 is a maximum (in absolute value) decreases with increasing F_o; and (2) the logarithmic decrement δ_1 is minimized (in absolute value) at both ends of the $\hat{\sigma}$ spectrum. As $\hat{\sigma} \to 0$, $\delta_1 \to 0$, corresponding

to the kinematic wave case; as $\hat{\sigma} \to \infty$, $\delta_1 \to 0$, corresponding to the gravity wave case.

A general conclusion derived from Fig. 2 relates to the fact that for $F_o < 2$, primary waves will be subject to very strong attenuation in the dynamic band, and to very weak attenuation in the gravity and kinematic bands.

Primary Wave Amplification Analysis, $F_o > 2$.—Fig. 3 depicts the variation of the logarithmic decrement δ_1 for $F_o > 2$, as a function of $\hat{\sigma}$. The following conclusions are drawn: (1) The logarithmic decrement δ_1 has a maximum positive value at a value of $\hat{\sigma}$ corresponding to the point of inflexion of the $\hat{c}_r$ versus $\hat{\sigma}$ curve (Fig. 1). The value of $\hat{\sigma}$ for which δ_1 is a maximum decreases with increasing F_o; and (2) the logarithmic decrement δ_1 is minimized at both ends of the $\hat{\sigma}$ spectrum. As $\hat{\sigma} \to 0$, $\delta_1 \to 0$, corresponding to the kinematic wave case; as $\hat{\sigma} \to \infty$, $\delta_1 \to 0$, corresponding to the gravity wave case.

A general conclusion derived from Fig. 3 relates to the fact that for $F_o >$

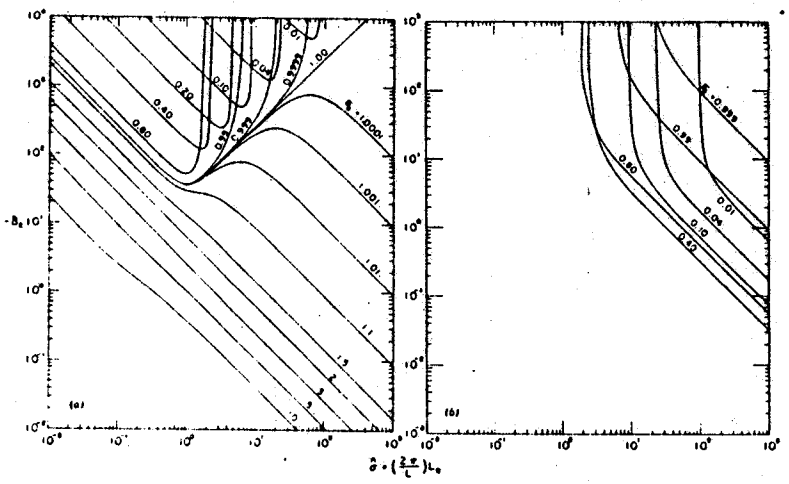

FIG. 4.—Secondary Wave Logarithmic Decrement $-\delta_2$ versus Dimensionless Wave Number $\hat{\sigma}$; Curve Parameter = Froude Number F_o: (*a*) $0.01 \le F_o \le 10$; (*b*) $0.01 \le F_o \le 0.999$

2, primary waves will be subject to very strong amplification in the dynamic band, and to very weak amplification in the gravity and kinematic bands.

Secondary Wave Attenuation Analysis.—Figs. 4(*a*) and 4(*b*) depict the variation of the logarithmic decrement δ_2 for $0.01 \le F_o \le 10$ as a function of $\hat{\sigma}$. The following conclusions are drawn: (1) In subcritical flow, $F_o < 1$, the attenuation of the secondary wave is very strong, and the strength decreases as $\hat{\sigma}$ increases in the gravity band (large $\hat{\sigma}$); (2) at critical flow, $F_o = 1$, the attenuation of the secondary wave is very strong, with a minimum around the center of the dynamic band (intermediate $\hat{\sigma}$); and (3) in supercritical flow, $F_o > 1$ the attenuation of the secondary wave has the pattern shown. For $F_o \ge 2$, δ_2 decreases as $\hat{\sigma}$ increases.

Dynamic Wave Propagation

The propagation of a dynamic wave has been shown to be a function of

two dimensionless parameters, the wave number $\hat{\sigma}$, and the Froude number F_o. The wave number $\hat{\sigma}$ can be interpreted as a ratio of two lengths L_e and L, in which L is the wavelength and L_e is the horizontal length in which the steady uniform flow drops a head equal to its depth. The square of the Froude number F_o is the ratio of twice the velocity head to the flow depth, where the velocity head h_{u_o} is given by

$$h_{u_o} = \frac{u_o^2}{2g} \qquad (61)$$

For $F_o < 2$, the celerity of a dynamic wave that propagates downstream is larger than the kinematic wave celerity, and smaller than the gravity wave celerity. In fact, the kinematic wave celerity constitutes a lower bound to which the dynamic value tends as the wave number $\hat{\sigma}$ decreases. Conversely, the gravity wave celerity is an upper bound to the dynamic wave celerity as the wave number $\hat{\sigma}$ increases. To place this conclusion in the proper perspective it is perhaps of interest to quote here from Stoker's work [(8), p. 486], regarding the celerities of small disturbances and progressive waves:

> . . . What seems to happen is the following: small forerunners of a disturbance travel with the speed $\sqrt{gd}$ relative to the flowing stream, but the resistance forces act in such a way as to decrease the speed of the main portion of the disturbance far below the values given by $\sqrt{gd}$; i.e., to a value corresponding closely to the speed of a steady progressive wave that travels unchanged in form . . .

In reviewing Stoker's work, it is apparent that his reference to a smal disturbance is to a wave with a large $\hat{\sigma}$ (gravity wave) and to progressive wave to that with a small $\hat{\sigma}$ (kinematic wave). He proceeds to further elaborate o the limitations of methods of water routing based solely on the kinematic approach for the cases in which the dynamic effects cannot be disregarded.

For $F_o \ge 2$, the celerity of a dynamic wave that propagates downstrear is smaller than the kinematic wave celerity and larger than the gravity wav celerity. In fact, the kinematic wave celerity is an upper bound to the dynami value, whereas the gravity wave celerity is a lower bound to the dynamic valu

A significant conclusion regarding dynamic wave propagation can be obtaine from the summary presented in Table 2. For primary waves, $F_o = 2$ is th threshold dividing the attenuation ($F_o < 2$) and amplification ($F_o > 2$) tendencie For secondary waves, however, $F_o = 1$ is the threshold dividing the propagatio upstream ($F_o < 1$) or downstream ($F_o > 1$) for gravity waves. Thus, F_o = 2 is verified to be as important a threshold value as $F_o = 1$ in describing th dynamics of open channel flow phenomena.

Summary and Conclusions

The propagation characteristics of various types of shallow water waves i open channel flow are calculated on the basis of linear stability theory. Th celerity and attenuation functions of kinematic, diffusion, steady dynami dynamic, and gravity waves are derived. For the most general case, i.e., th dynamic wave model, the propagation characteristics are expressed as a functic

of the steady uniform flow Froude number and the dimensionless wave number of the unsteady component of the motion.

For the dynamic model, the wave number spectrum is divided into three bands: (1) A gravity band corresponding to large wave number, in which the wave celerity is the gravity wave celerity; (2) a kinematic band corresponding to a small wave number in which the wave celerity is the kinematic wave celerity; and (3) a dynamic band corresponding to midspectrum values of the wave number, in which the wave celerity falls between the gravity and kinematic celerity values.

Primary dynamic waves propagate downstream, and they attenuate for $F_o < 2$ and amplify for $F_o > 2$. At the $F_o = 2$ threshold, primary dynamic waves neither attenuate nor amplify.

For $F_o \leq 1$, secondary dynamic waves either propagate upstream or downstream, depending on the wave number. At $F_o = 1$, secondary dynamic waves remain stationary or propagate downstream, depending on the wave number. For $F_o > 1$, secondary waves propagate downstream. Secondary waves attenuate throughout the entire wave number spectrum.

Applications

The analysis of the foregoing sections provides an appropriate framework for the systematic study of shallow water waves in open channel flow. Numerous applications are envisioned, among which some of the most important are:

1. The assessment of the accuracy of kinematic and diffusion wave models, and the determination of the criteria for their applicability.
2. The study of the formation of roll waves in open channel flow. The present theory validates the observed fact that roll waves are formed for $F_o > 2$, since there can be no wave amplification for $F_o \leq 2$ (using Chèzy friction).
3. The theory enables a comparison of the various approximate wave models, and an assessment of their capabilities and limitations.
4. Lastly, the theory provides a coherent treatment of the subject of wave propagation in open channel flow. The conclusions may prove of interest to engineers dealing with unsteady open channel flow phenomena.

Appendix I.—References

1. DeSaint-Venant, B., "Theorie du Mouvement Non-permanent des Eaux avec Application aux Crues des Rivierès et l' Introduction des Varées dans leur Lit," *Competes Rendus Hebdomadaires des Seances de l'Academie des Science*, Paris, France, Vol. 73, 1871, pp. 148–154.
2. Henderson, F. M., *Open Channel Flow*, The MacMillan Co., New York, N.Y., 1966.
3. Lagrange, I. L., "Mémoire sur la Théorie du Mouvement des Fluides," *Bulletin de la Classe des Sciences Academie Royal de Belique*, No. 1783, pp. 151–198.
4. Liggett, J. A., "Basic Equations of Unsteady Flow," *Unsteady Flow in Open Channels*, K. Mahmood and V. Yevjevich, ed., Vol. 1, Water Resources Publications, Fort Collins, Colo., 1975.
5. Lighthill, M. J., and Whitham, G. B., "On Kinematic Waves I, Flood Movement in Long Rivers," *Proceedings of the Royal Society of London*, Vol. A229, May, 1955, pp. 281–316.

6. Lin, C. C., *The Theory of Hydrodynamic Stability*, 1st ed., The Cambridge University Press, London, England, 1966.
7. Ponce, V. M., and Mahmood, K., "Meandering Thalwegs in Straight Alluvial Channels," *Proceedings of the 3rd Annual Symposium*, ASCE, Waterways, Harbors, and Coastal Engineering Division, Vol. 2, Aug., 1976, pp. 1418–1441.
8. Stoker, J. J., *Water Waves, the Mathematical Theory with Applications*, Wiley Interscience Publishers, Inc., New York, N.Y., 1957.
9. Woolhiser, D. A., and Liggett, J. A., "Unsteady One-Dimensional Flow over a Plane—The Rising Hydrograph," *Water Resources Research*, Vol. 3, No. 3, Third Quarter, pp. 753–771, 1967.
10. Wylie, C. R., *Advanced Engineering Mathematics*, 3rd ed., McGraw-Hill Book Co., New York, N.Y., 1966.

Appendix II.—Notation

The following symbols are used in this paper:

A = parameter, defined by Eq. 39;
a = integer;
B = parameter, defined by Eq. 40;
C = parameter, defined by Eq. 41;
C_f = Chezy coefficient;
D = parameter, defined by Eq. 50;
d = depth of flow;
E = parameter, defined by Eq. 51;
F_o = Froude number of steady uniform flow;
f = friction factor, defined by Eq. 7;
g = acceleration of gravity;
h_u = velocity head;
k = integer;
L = wavelength;
L_o = length in which the steady uniform flow drops a head equal to its depth;
l = integer;
p = integer;
S_f = friction slope;
S_o = bed slope;
T = wave period;
u = mean velocity;
$\hat{\beta}_I$ = amplitude propagation factor;
$\hat{\beta}_R$ = dimensionless frequency;
γ = unit weight of water;
δ = logarithmic decrement;
ζ = a type of kinematic flow number, as defined by Eq. 37;
θ = parameter, defined by Eq. 43;
$\hat{\sigma}$ = dimensionless wave number;
τ = bottom shear stress; and
∞ = infinity.

Subscripts

d = diffusive wave;

g = gravity wave;
I = imaginary;
k = kinematic wave;
o = steady uniform flow;
R = real;
r = relative to the main flow;
s = steady dynamic wave;
1 = primary dynamic wave; and
2 = secondary dynamic wave.

Superscripts

$'$ = perturbed variable; and
$\hat{}$ = dimensionless function.

JOURNAL OF THE
HYDRAULICS DIVISION

Applicability of Kinematic and Diffusion Models

By Victor Miguel Ponce,[1] Ruh-Ming Li,[2] Members, ASCE, and Daryl B. Simons,[3] F. ASCE

Introduction

The kinematic and diffusion wave models have found wide application in engineering practice. Both are approximations to the unsteady open channel flow phenomenon described by the complete Saint Venant equations. The diffusion model assumes that the inertia terms in the equation of motion are negligible as compared with the pressure, friction, and gravity terms. The kinematic model assumes that inertia and pressure terms are negligible as compared with the friction and gravity terms. Although approximate, both the kinematic and diffusion models have been shown to be fairly good descriptions of the physical phenomenon in a variety of cases. The kinematic model has been successfully applied to overland flow, as well as to the description of the travel of slow-rising flood waves. The subsidence of the flood wave, however, is better described by the diffusion model since the kinematic model, by definition, does not allow for subsidence. What do overland flow and slow-rising flood waves have in common that they lend themselves to description by these approximate models? The answer to this question is the subject of this paper.

Wave Propagation in Open Channel Flow

Recently, two of the writers (4) have developed an analytical solution for wave propagation in open channel flow, based on a linearized form of the Saint Venant equations as presented by Lighthill and Whitham (3). They took the linearized equations and sought a solution in sinusoidal form which led to a system of homogeneous linear equations. The nontrivial condition for the

Note.—Discussion open until August 1, 1978. To extend the closing date one month, a written request must be filed with the Editor of Technical Publications, ASCE. This paper is part of the copyrighted Journal of the Hydraulics Division, Proceedings of the American Society of Civil Engineers, Vol. 104, No. HY3, March, 1978. Manuscript was submitted for review for possible publication on August 18, 1977.

[1] Asst. Prof. of Civ. Engrg., Colorado State Univ., Fort Collins, Colo.
[2] Assoc. Prof. of Civ. Engrg., Colorado State Univ., Fort Collins, Colo.
[3] Assoc. Dean for Research and Prof. of Civ. Engrg., Colorado State Univ., Fort Collins, Colo.

eterminant of the coefficient matrix yielded the propagation celerity and ɔgarithmic decrement (5) of small sinusoidal perturbations to the equilibrium low, in terms of the steady equilibrium flow Froude number and a dimensionless vave number of the unsteady component of the motion. In addition, Ponce ınd Simons calculated the propagation celerity and logarithmic decrement corresponding to the kinematic and diffusion wave models. As it will be shown ıere, the findings of the theory can be used to determine limits for the applicability ɔf these approximate models, by comparing their propagation celerity and logarithmic decrement with those of the complete Saint Venant equations. At the outset, it is recognized that the validity of the theory is only as good as the assumptions used in its formulation. For instance, the linearized equations have been derived by neglecting second-order terms. Nevertheless, the findings of the theory provide a good insight into the underlying physical mechanism, and their validity as a first approximation appears beyond doubt.

Definitions

The following definitions are advanced: u_o = steady uniform flow mean velocity; d_o = steady uniform flow depth; S_0 = bed slope; L = wavelength of sinusoidal perturbation to steady equilibrium flow; T = wave period of sinusoidal perturbation to steady equilibrium flow; c = wave celerity; L_0 = reference channel length; F_0 = steady uniform flow Foude number; $\hat{\sigma}$ = dimensionless wave number of the unsteady component of the motion; and $\hat{\tau}$ = dimensionless wave period of the unsteady component of the motion, such that

$$c = \frac{L}{T} \quad (1)$$

$$L_0 = \frac{d_0}{S_0} \quad (2)$$

$$F_0 = \frac{u_0}{\sqrt{gd_0}} \quad (3)$$

$$\hat{\sigma} = \left(\frac{2\pi}{L}\right) L_0 \quad (4)$$

$$\hat{\tau} = T\left(\frac{u_0}{L_0}\right) \quad (5)$$

in which g = the acceleration of gravity.

The propagation celerity c can be expressed in dimensionless form by dividing it by u_0. The dimensionless propagation celerity $\hat{c}$ is

$$\hat{c} = \frac{c}{u_0} \quad (6)$$

The logarithmic decrement δ (5) is defined as

(7)

in which a_0 and a_1 = the wave amplitudes at the beginning and end of one wave period, respectively.

Two of the writers (4) have shown that for the dynamic model (that based on the complete Saint Venant equations), the dimensionless propagation celerity $\hat{c}$ and logarithmic decrement δ are functions of F_0 and $\hat{\sigma}$ (see Appendix I). In practice, however, it is desirable to express the space parameter $\hat{\sigma}$ as a function of the time parameter $\hat{\tau}$. Combining Eqs. 1, 4, 5, and 6

$$\hat{\tau} = \frac{2\pi}{\hat{c}\hat{\sigma}} \quad (8)$$

Thus, $\hat{c}$ and δ can be expressed as a function of F_0 and $\hat{\tau}$ by use of Eq. 8. Furthermore, the results of the theory suggest that for the comparison of diffusion and full dynamic models, a more appropriate parameter is $\hat{\tau}/F_0$. Making use of Eqs. 2, 3, and 5, $\hat{\tau}/F_0$ is expressed as

$$\frac{\hat{\tau}}{F_0} = T\left(\frac{S_0 u_0}{d_0 F_0}\right) \quad (9)$$

$$\text{or} \quad \frac{\hat{\tau}}{F_0} = TS_0\left(\frac{g}{d_0}\right)^{1/2} \quad (10)$$

Kinematic Wave Versus Diffusion Wave

The kinematic model breaks down when the neglect of the pressure term is not justified. Accordingly, it is of interest to compare the kinematic and diffusion models. Both models have a propagation celerity equal to 1.5 times the equilibrium flow velocity. They differ, however, in the attenuation. The logarithmic decrement of the kinematic model is 0, i.e., the kinematic model does not allow for physical attenuation. The attenuation often observed in numerical schemes based on the kinematic model is of an artificial nature (numerical damping due to truncation errors) (1). The logarithmic decrement of the diffusion model is (4)

$$\delta_d = -\frac{2\pi}{3}\hat{\sigma} \quad (11)$$

Substituting Eq. 8 into Eq. 11

$$\delta_d = -\frac{4}{3}\left(\frac{\pi^2}{\hat{c}\hat{\tau}}\right) \quad (12)$$

$$\text{Since} \quad \hat{c} = \hat{c}_d = \frac{3}{2} \quad (13)$$

$$\text{it follows that} \quad \delta_d = -\frac{8\pi^2}{9\hat{\tau}} \quad (14)$$

The kinematic model will be valid when the attenuation factor of the diffusion model, e^{δ_d}, is close to 1. Table 1 shows the values of e^{δ_d} for varic $\hat{\tau}$. Thus, for at least 95% accuracy of the kinematic wave solution after one p..pagation

period, the dimensionless period $\hat{\tau}$ has to be greater than 171.

For example, for a channel with $S_0 = 0.0001$, $d_0 = 10$ ft (3.05 m) and $u_0 = 3$ fps (0.91 m/s), an accuracy of at least 95% in the wave amplitude after one propagation period, requires that the period T be:

$$T \geq \frac{\hat{\tau}\, d_0}{S_0 u_0} = \frac{171 \times 10}{0.0001 \times 3} \cong 66 \text{ days} \quad (15)$$

If water discharge and channel friction are given, u_0 and d_0 can be calculated by the use of the appropriate uniform flow formula (Manning or Chezy).

As another example, assume a value of slope S_0 corresponding to overland flow. If $S_0 = 0.01$, $d_0 = 1$ ft (0.305 m) and $u_0 = 4$ fps (1.22 m/s), for this case

$$T \geq 1.2 \text{ hr} \quad (16)$$

Thus, for mild channel slopes, the period has to be very long for the kinematic model to apply (periods such as those of slow-rising flood waves). For steep slopes such as those prevalent in overland flow, the period does not need to be long. The steeper the slope, the shorter the period required to satisfy the kinematic flow assumption. The conclusion is that most overland flow problems

TABLE 1.—Dimensionless Period $\hat{\tau}$ Versus Attenuation Factor e^{δ_d}

e^{δ_d} (1)	$\hat{\tau}$ (2)
0.99	873
0.95	171
0.90	83

can be modeled as kinematic flow. Likewise, slow-rising flood waves that travel unchanged in form can also be modeled as kinematic flow.

An explanatory note is necessary here. The criteria of Table 1 are based on a comparison of the attenuation (described by the logarithmic decrement δ) of the analytical solutions for the kinematic and diffusion models. In a numerical solution, however, often the truncation errors may mask the nondiffusive character of the analytical solution of the kinematic wave, with the result that the numerical solution of the kinematic wave may resemble the analytical solution of the diffusion wave (1), further complicating the modeling.

Diffusion Wave Versus Dynamic Wave

The next step in the analysis is to compare the propagation celerity $\hat{c}_d$ and logarithmic decrement δ_d of the diffusion model with those of the full dynamic model. For $F_0 < 2$, the propagation celerity of the diffusion wave, $\hat{c}_d = 1.5$, is a lower bound for the dynamic celerity. Since only the primary dynamic wave (that which travels downstream) is of interest here, the dynamic wave celerity will be referred to as $\hat{c}_1$.

Fig. 1 shows the variation of $\hat{c}_1$ as a function of $\hat{\tau}/F_0$. It can be seen from this figure that $\hat{c}_1$ tends to $\hat{c}_d$ as $\hat{\tau}/F_0$ increases, for all F_0. Fig. 2 is an arithmetic

plot of $\hat{c}_1/\hat{c}_d$ versus $\hat{\tau}/F_0$ for $5 \leq \hat{\tau}/F_0 \leq 30$. From this figure, for $\hat{\tau}/F$ 8, the celerity error of the diffusion model is within 5%. The curve sh for $F_0 = 0.01$ is an error bound.

Keeping the celerity error to within 5% does not guarantee that the ampl error will remain within the same tolerance. Fig. 3 is a plot of $e^{\delta_1 - \delta_d}$ v $\hat{\tau}/F_0$, in which δ_1 and δ_d = the logarithmic decrements of the dynamic diffusion models, respectively. Fig. 3 shows that for $0.1 \leq F_0 \leq 0.4$, > 16, for the attenuation error of the diffusion model to be within 5%. a wider range of F_0, say, $0.01 \leq F_0 \leq 1.0$, $\hat{\tau}/F_0 \geq 45$. An exact valu

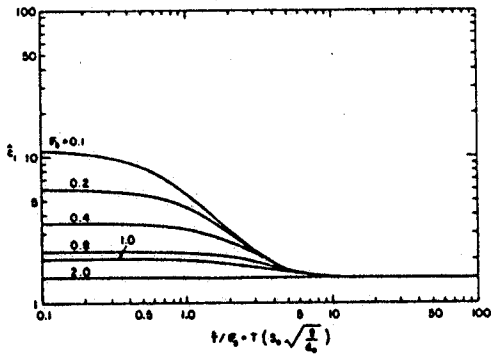

FIG. 1.—Dimensionless Celerity of Dynamic Model $\hat{c}_1$ Versus $\hat{\tau}/F_0$

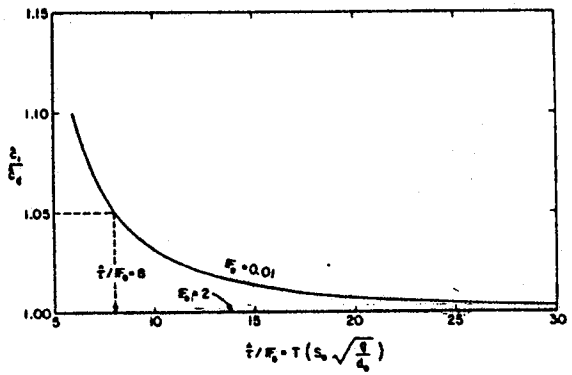

FIG. 2.—Ratio of Celerities $\hat{c}_1/\hat{c}_d$ Versus $\hat{\tau}/F_0$

the parameter $\hat{\tau}/F_0$ for a given error defies generalization, being as it is a fur of F_0. Nevertheless, from a practical standpoint, a value of $\hat{\tau}/F_0 > 30$ is postu (specific values of $\hat{\tau}/F_0$ for a given F_0 can be taken directly from Fig. 3).

Applying this criterion to the same example used before, for S_0 = (and d_0 = 10 ft (3.05 m)

$$TS_0\left(\frac{g}{d_0}\right)^{1/2} \geq 30$$

from which $T \geq 1.9$ days . . . . . (18)

In the second example shown, for $S_0 = 0.01$ and $d_0 = 1$ ft (0.305 m)

$T \geq 8.8$ min . . . . . (19)

On the basis of the examples shown, it is concluded that the diffusion model applies for a wider range of slopes and periods than the kinematic model, with the added advantage that the diffusion model does allow for physical attenuation. However, if inequality (Eq. 17) is not satisfied, the diffusion model breaks

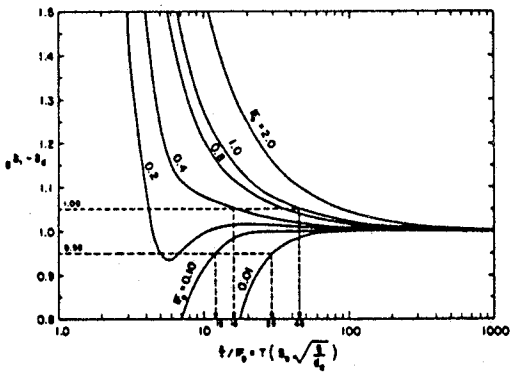

FIG. 3.—Ratio of Attenuation Factors $e^{\delta_1 - \delta_d}$ Versus $\hat{\tau}/F_0$

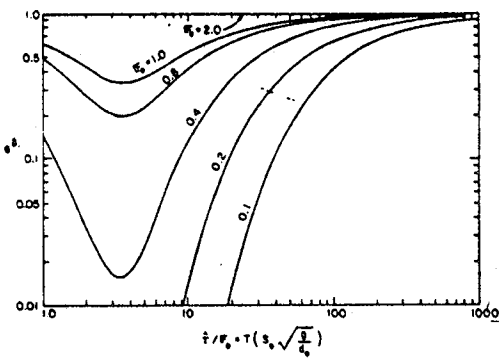

FIG. 4.—Attenuation Factor of Dynamic Model e^{δ_1} Versus $\hat{\tau}/F_0$

down and only the full dynamic model can properly account for the rate of travel and amount of attenuation of the wave.

Full Dynamic Model

Fig. 1 and 4 show $\hat{c}_1$ and e^{δ_1} as a function of F_0 and $\hat{\tau}/F_0$. For $\hat{\tau}/F_0 \leq 30$, i.e., the range where only the full dynamic model would apply, very strong attenuation is shown. For instance, for $\hat{\tau}/F_0 = 30$, and $F_0 = 0.2$, $e^{\delta_1} = 0.23$. This explains the nonpermanent characteristics of the dynamic wave: once formed, it will attenuate quickly. In this regard, it is of interest to point

out here the observations of Hayami (2) regarding the nonpermanent nature of dynamic disturbances in open channel flow. He reasoned that given all the irregularities present in natural river channels, it is striking that the general pattern of the flow closely resembles that of uniform flow. The reason for this lies in the strong dissipative tendencies of dynamic disturbances, its nonpermanency being manifested in the appearance of uniform flow. Kinematic and diffusion waves, however, do not share the strong dissipative tendencies of dynamic waves due precisely to their long duration, or relatively large bed slopes, or both.

Conclusions

The applicability of the kinematic and diffusion models is assessed by comparing the propagation characteristics of sinusoidal perturbations to the steady uniform flow for the kinematic, diffusion, and dynamic models (the dynamic model is that based on the complete Saint Venant equations). The comparison allows the determination of inequality criteria that need to be satisfied if the kinematic or diffusion models are to simulate the physical phenomena within a prescribed accuracy.

It is shown that bed slope and wave period (akin to wave duration in waves of shape other than sinusoidal) are the important physical characteristics in determining the applicability of the approximate models. Larger bed slopes or long wave periods will satisfy the inequality criteria. In practice, larger bed slopes are those of overland flow, and long wave periods are those corresponding to slow-rising flood waves.

The diffusion model is shown to be applicable for a wider range of bed slopes and wave periods than the kinematic model. Where the two models break down, only the dynamic model will simulate the physical phenomena. The dynamic model, however, is shown to have markedly strong dissipative tendencies. This conclusion has had ample corroboration in the literature.

Acknowledgments

The writers wish to acknowledge the United States Environmental Protection Agency, Environmental Research Laboratory, Athens, Ga., and the United States Department of Agriculture Forest Service, Rocky Mountain Forest and Range Experiment Station, Flagstaff, Ariz., for sponsoring this study.

Appendix I.—Equations for Propagation Celerity $\hat{c}$ and Logarithmic Decrement δ

The equations for $\hat{c}$ and δ of the complete dynamic model are $\hat{c}_{1,2} = 1 \pm D$

$$\delta_{1,2} = -2\pi \frac{B \mp E}{|1 \pm D|}$$

in which $A = (1/F_0^2) - B^2$; $B = 1/(\hat{\sigma} F_0^2)$; $C = (A^2 + B^2)^{1/2}$; $D = [(C + \ )/2]^{1/2}$; and $E = [(C - A)/2]^{1/2}$.

Appendix II.—References

1. Cunge, J., "On the Subject of a Flood Propagation Computation Method (Musl Method)," *Journal of Hydraulic Research*, Vol. 7, No. 2, 1969, pp. 205–230.
2. Hayami, S., "On the Propagation of Flood Waves," *Bulletin of the Disaster Pre Research Institute*, Kyoto, Japan, Vol. 1, No. 1, Dec., 1951.
3. Lighthill, M. J., and Whitham, G. B., "On Kinematic Waves I Flood Moven Long Rivers," *Proceedings*, Royal Society of London, London, England, Se Vol. 229, 1955, pp. 281–316.
4. Ponce, V. M., and Simons, D. B., "Shallow Wave Propagation in Open C Flow," *Journal of the Hydraulics Division*, ASCE, Vol. 103, HY12, Proc. Paper Dec., 1977, pp. 1461–1476.
5. Wylie, C. R., *Advanced Engineerings Mathematics*, 3rd ed., McGraw-Hill Boc Inc., New York, N.Y., 1966.

Appendix III.—Notation

The following symbols are used in this paper:

a_0 = wave amplitude at beginning of period;
a_1 = wave amplitude at end of period;
c = wave celerity, Eq. 1;
$\hat{c}$ = dimensionless wave celerity, Eq. 6;
d_0 = steady uniform flow depth;
F_0 = steady uniform flow Froude number;
g = acceleration of gravity;
L = wavelength;
L_0 = reference channel length, Eq. 2;
S_0 = bed slope;
u_0 = steady uniform flow mean velocity;
T = wave period;
δ = logarithmic decrement, Eq. 7;
$\hat{\tau}$ = dimensionless period, Eq. 5; and
$\hat{\sigma}$ = dimensionless wave number, Eq. 4.

Subscripts

1 = pertaining to primary dynamic wave (traveling downstream);
d = pertaining to diffusion model; and
k = pertaining to kinematic model.

FINAL REPORT

MAGNITUDE AND TIMING OF DAM RELEASES FROM EL VADO RESERVOIR FOR WHITE WATER RAFTING

prepared for

New Mexico State Park and
Recreation Division
Department of Natural Resources
Santa Fe, New Mexico

prepared by

Timothy J. Ward
Associate Professor of
Civil & Geological Engineering
New Mexico State University
Las Cruces, New Mexico

November 1982

TABLE OF CONTENTS

LIST OF TABLES..... ii

LIST OF FIGURES..... iii

EXECUTIVE SUMMARY..... iv

ACKNOWLEGEMENTS..... v

INTRODUCTION..... 1

PURPOSE..... 1

OBJECTIVES AND SCOPE..... 2

PHYSICAL CHARACTERISTICS OF THE SYSTEM..... 3

LOCATION AND HYDROLOGIC FEATURES..... 3

HYDROLOGY AND SYSTEM COMPONENTS..... 5

DATA ANALYSIS..... 9

DEVELOPMENT OF THE MANAGEMENTAL MODEL.....14

APPROACH.....14

CHANNEL MODEL.....14

Muskingum Method.....14

Muskingum-Cunge with Variable Parameters.....16

RESERVOIR MODEL.....20

MODEL APPLICATION.....21

SUMMARY AND CONCLUSIONS.....25

REFERENCES.....26

LIST OF TABLES

Table	Title	
1	Average Daily Flow for the Summer Period 1974-1980. Based on Average Dailies for the Month	10
2	Average Daily Pan Evaporations at El Vado and Abiquiu Reservoirs, Weekends of August 1 through October 15, 1974 through 1980	12
3	Muskingum Method Parameters K and X, El Vado to Abiquiu Reservoirs - Rio Chama. Discharges in cubic feet per second	16
4	Parameters for Rio Chama Cross Sections Used in Equations 13 and 14	18

LIST OF FIGURES

Figure	Title	
1	Sketch Map of the Study Area. Flow is from El Vado to Abiquiu	3
2	Schematic of the Rio Chama System in the Study Area	6

EXECUTIVE SUMMARY

Multiple uses of our scarce water resources is necessary to maintain and improve the quality of life in New Mexico. This study has investigated one such multiple use wherein downstream transfers of water between reservoirs can be scheduled to improve white water recreation. The section of river studied was a 29 mile reach of the Rio Chama between El Vado and Abiquiu reservoirs. A framework for decision making was developed via an interactive computer model. Given the system variables of inflows, outflows, desired flows, evaporation, and precipitation, the model computes hourly hydrographs at five river sections, and changes in reservoir volumes and elevations over the duration of the hydrograph. The model was verified against measured values and, with certain limitations discussed in the report, simulates the system fairly well. The model is intended as a management aid to study the consequences of scheduled water releases.

ACKNOWLEDGEMENTS

Numerous individuals have assisted in this project. Thanks go to my programmer, Jerry Duggan, for his aid in "crunching some numbers". Lynnette and Arlette Barboa spent long hours compiling and analyzing the data. Bill Dein and Terry Perkins of the U. S. Geological Survey provided unpublished materials invaluable to this project. They were always willing to help. Rick Lukens, graduate assistant in Agricultural Economics, shared his preliminary data from a river user survey taken this last summer. Finally, a special thanks goes to Bob Findling of State Parks Planning for recognizing the need for this study and giving of his time and energy.

Conserve New Mexico's Land and Water

INTRODUCTION

PURPOSE

In arid New Mexico, water based recreation is held at a premium. Much of the water related activity is associated with the major reservoirs. However, there are some important exceptions to this generalization. One of these is the use of certain rivers or river reaches for white water recreation, primarily rafting, canoeing, and kayaking. In New Mexico, the premier white water area is the upper Rio Grande, above Cochiti Reservoir. The other important area is the Rio Chama between El Vado and Abiquiu Reservoirs. On a good weekend over 100 people are attracted to rafting on the river.

Rafting is dependent on water, as is most everything else in the state. Therefore, when low flow season comes each year, rafting stops. Exceptions occur when water is released from El Vado Reservoir to meet the needs of users in the Middle Rio Grande Conservancy District or other legal constraints. If these releases occur on a weekend, and they are of sufficient magnitude and duration to provide a quality rafting experience, then the water enjoys a multiple use. Unfortunately, trying to guess when the releases will occur is often just a game of chance.

There are options, though, for use of water associated with the San Juan-Chama (SJC) Project. With the SJC, approximately 100,000 acre-feet (AF) per year are diverted from the San Juan River basin into the Rio Chama drainage above El Vado Reservoir. Of that amount, approximately 48,000 AF per year are for use by the City of Albuquerque. That water is not needed at this time and can be disposed of by the city through sales or trades, or it can be stored in Abiquiu Reservoir or "banked" in Elephant Butte Reservoir. With such flexibility, the city is in a good position to use its water to enhance white water recreation potential on the Rio Chama during the low flow period.

The purpose of this project was to study the historic and current conditons related to the hydrology and hydraulics of the two reservoir-one channel system, and to develop a framework for determining the magnitude, timing and consequences of releases on the system. This was done through data compilation, field studies, data analyses, and mathematical modeling.

OBJECTIVES AND SCOPE

Specific objectives of this project were:

1) Definition of the hydrology of the reach,
2) Determination of reservoir operating conditions,
3) Development of a water routing model for the reach, and
4) Application of the model.

The scope of work was limited to examining and analyzing available data on the hydrology of the system and the reservoir operation, and to field data collection where possible. A mathematical model based on storage routing, considering the available data base, was modified and applied to the river reach.

PHYSICAL CHARACTERISTICS OF THE SYSTEM

LOCATION AND HYDROLOGIC FEATURES

The river reach studied in this project is located between El Vado Reservoir, upstream, and Abiquiu Reservoir downstream on the Rio Chama (Figure 1) in northwestern New Mexico. Access to the river is poor, one reason for its appeal and also its lack of use for other purposes. The river winds its way between beautiful mesas and ampitheaters over most of its course. During spring runnoff or summer rainfalls, the river is fed by three major tributaries in this reach. These are the Rio Nutrias, Rio Cebolla, and Rio Gallina, respectively from upstream to downstream. These tributaries can and do provide large inflows of water and sediment at times.

Two gaging stations define the hydrology of the reach, Rio Chama below El Vado Dam (hereafter below El Vado) and Rio Chama above Abiquiu. These gages demark the beginning and ending points of the routing model, but also (roughly) the launch and take out points for the whitewater rafters.

The river can be classified as an armoured, fixed bed cobble and boulder stream. Because of high sediment loads from the streams draining the surrounding mesas, there are often large sand and gravel deposits overlying the bed at different points. Measured sediment discharges at the above Abiquiu site ranged from about 10 to 10,000 tons per day during water year (WY) 1980. Typical river widths during high flows are in the range of 100 to 150 feet. Width to depth ratios are on the order of 25 to 35 for high flows, and computed average velocities range between 4 and 9 feet per second. The river has an average slope between the gage sites of about 0.003, dropping approximately 421 feet in elevation from 6696' to 6275' msl. Relief of over 1,000 feet from stream bed to adjacent mesa tops is common, producing the beautiful scenery that abounds along the Rio Chama.

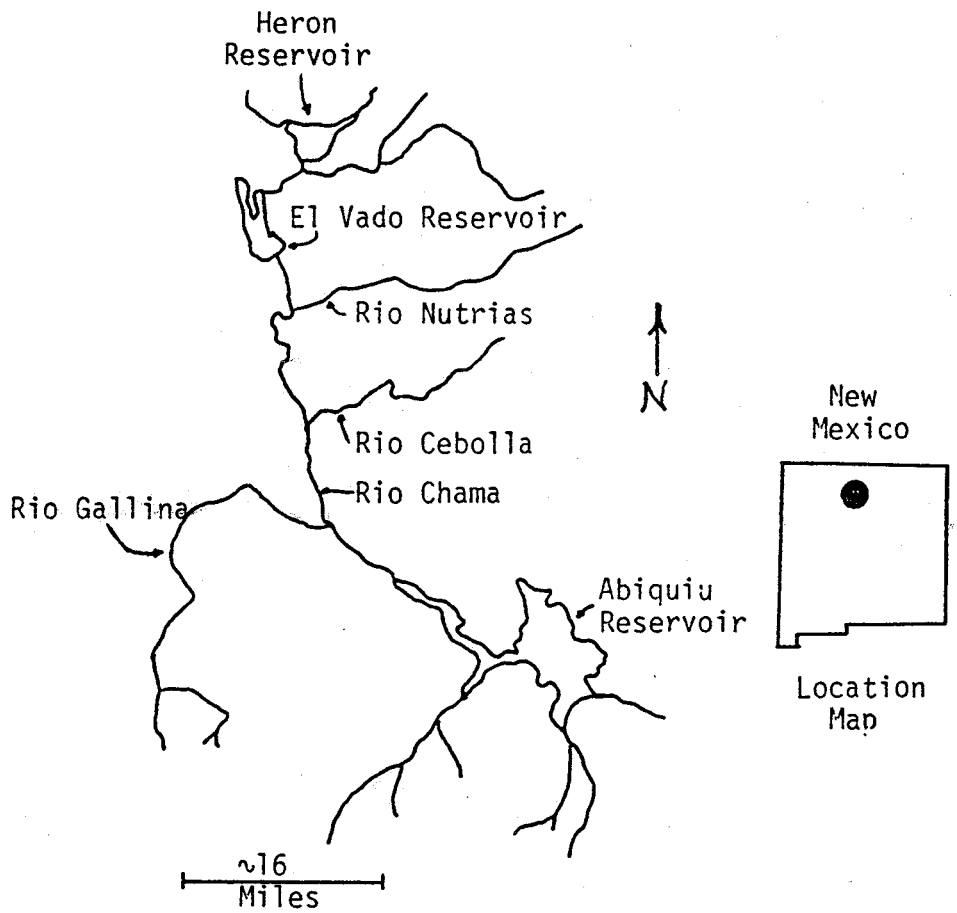

FIGURE 1 - Sketch Map of the Study Area. Flow is from El Vado to Abiquiu.

HYDROLOGY AND SYSTEM COMPONENTS

The hydrology of the system can be defined in terms of the existing hydrologic stations (Figure 2). In addition to the two mentioned earlier, there are Willow Creek below Heron Dam, Rio Chama near La Puente, (both inflows to El Vado Reservoir), El Vado Reservoir, Abiquiu Reservoir, and Rio Chama below Abiquiu Dam.

Heron Reservoir on Willow Creek stores water diverted through the Azotea Tunnel from the San Juan River basin. Average discharge from the Azotea Tunnel for ten years through WY 80 was 135 cubic feet per second (cfs) ∿ 98,000 AF per year. Diversions are almost exclusively during the period April through September. Under the laws controlling the diversions, diversions shall not exceed 1.35 million AF for any ten consecutive years or 270,000 AF in any one year (USBR, 1963). The projected average diversion is 110,000 AF per year. Heron Reservoir is operated primarily in response to its two major users, the Middle Rio Grande Conservancy District (MRGCD) with a contract for 20,900 AF and the City of Albuquerque with a contract for 48,200 AF. Albuquerque probably will not need all of its water to offset groundwater depletions until after the year 2000. The MRGCD purchased Albuquerque water in 1977 because of low flows in the Rio Grande. The U.S. Department of the Interior, Bureau of Reclamation (USBR) owns Heron Reservoir and MRGCD owns El Vado Reservoir, which is operated by the USBR to meet the needs of the water owners.

The Willow Creek below Heron Dam gage depicts reservoir operation. Average yearly water yield for nine years up to WY 1980 were 75,350 AF. The difference between Azotea Tunnel outflow and this value is approximately what is being stored in the reservoir (storage ranged from about 240,000 to 370,000 AF in 1980). Heron Reservoir which has a storage capabity of about 400,000 AF, was filled for the first time in 1982.

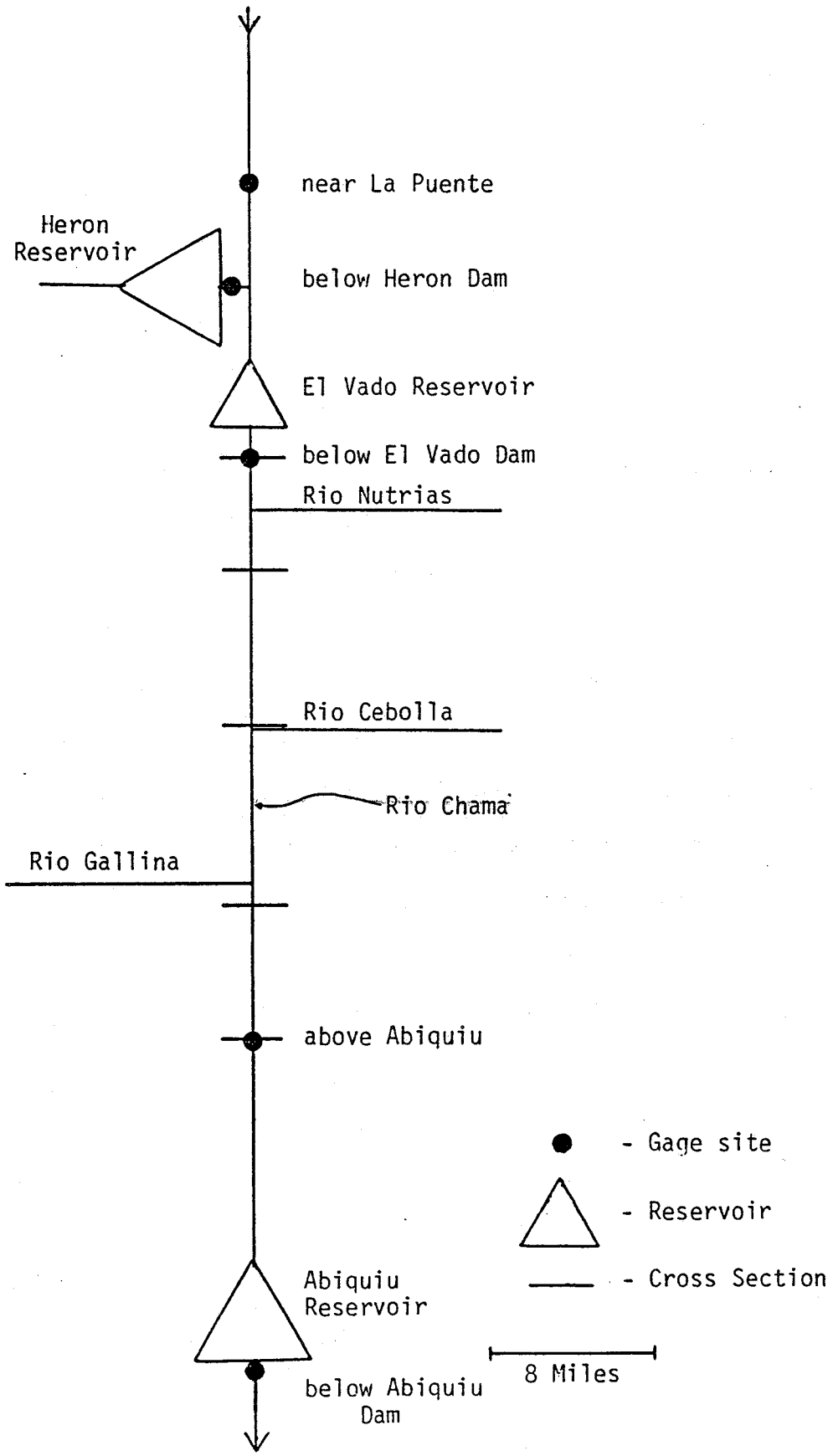

FIGURE 2 - Schematic of the Rio Chama System in the Study Area.

Flow records for below Heron show periods of releases for irrigation (April - September) and other downstream water transfers, such as to Cochiti and Elephant Butte Reservoirs since 1975. Therefore, the flow below Heron mimics the Azotea Tunnel inflow except for that inflow which is stored.

The other major inflow to El Vado Reservoir, the Rio Chama, is gaged near La Puente. Average water yield at that point is 231,000 AF for 25 years up through WY 1980. A large percentage of the yield comes during the spring runoff period of April through June. In WY 1980 this period accounted for over 90% of the total yield. Late summer and early fall flows are significant to the rest of the year. However, they are comparable to outflows from Heron Reservoir for the same period.

El Vado and Abiquiu reservoirs bound the river reach that was studied. El Vado is owned by MRGCD and operated by the USBR. Abiquiu is owned and operated by the U.S. Army Corps of Engineers (COE). Each has different purposes and functions. El Vado Dam was built by the Middle Rio Grande Conservancy District and completed in 1935, for the purpose of storing irrigation water. It was rehabilitated by the USBR with an improved emergency spillway and a new outlet works to handle releases of San Juan-Chama Project water. It has a capacity of about 195,000 AF.

El Vado Reservoir is filled, subject to the provisions of the Rio Grande Compact, by retaining all or part of the inflows in excess of downstream senior water rights on the Rio Chama. Filling is restricted to not exceed 2 feet per day (USBR, 1975). Storage is also limited to prevent use of the emergency spillway (Sabol and Gordon, 1980).

Releases are made to meet downstream water rights, to supply the Middle Rio Grande Conservancy District with releases from storage for irrigation purposes, and to bypass San Juan-Chama Project water releases from Heron

Reservoir. During April through October, whenever a low flow condition occurs on the Rio Chama, the release from El Vado Dam is to equal the natural inflow of the previous day. A low flow condition is defined as the period when the mean daily natural flow of the Rio Chama at Abiquiu Dam is equal to or less than 100 cfs. The outlet gates are normally set every day at about 1100 hours. All natural inflow must be bypassed; therefore, the reservoir storage will be reduced by the computed evaporation of the previous day (USBR, 1975). During November through March the natural inflow is bypassed. To avoid use of the erodible emergency spillway, reservoir operation required the reservoir surface be maintained below 6900.0 ft prior to June 1 and 6896.2 after June 1. The New Mexico State Park and Recreation Division has facilities on the lake and administers the recreational areas of El Vado Reservoir.

The Abiquiu Dam and Reservoir is located on the Rio Chama about 32 miles upstream from the confluence with the Rio Grande. The dam is a COE project originally built for flood and sediment control and is located about 30 miles northwest of Espanola. Late in 1981, Congress passed Public Law 97-140 which authorized the storage of up to 200,000 AF of the San Juan-Chama Project water in Abiquiu Reservoir. The total capacity of the reservoir is 1,383,000 AF of which 502,000 AF are for flood control and 66,400 AF are for sediment retention. Under a new operating plan, storages of that San Juan-Chama Project water owned by Albuquerque may increase the conservation pool to 200,000 AF. A 450,000 AF conservation pool is being studied by the COE. Maximum contents, up to 1980, were 205,300 AF in 1973. If higher permanent pools are maintained, a challenging section of the river will be inundated. This will occur at about 300,000 AF based on current area-elevation-capacity data, corresponding to an elevation of about 6240 feet above mean sea level.

The Abiquiu Dam and Reservoir is operated primarily for flood and sediment control in accordance with conditions and limitations stipulated in the Flood Control Act of 1960. Reservoir regulation is coordinated with Cochiti, Jemez Canyon, and Galisteo Reservoirs and with the San Juan-Chama to about 2000 cfs, which is the channel capacity below Abiquiu Dam. Flood control releases are contingent upon flows in the Rio Grande and inflows to Rio Chama below Abiquiu Dam. In all cases, flood control storage is released as soon as practicable after a flood, within the restrictions imposed by the Flood Control Act of 1960.

The potential for additional storage in Abiquiu and its impacts not only concern white water enthusiasts but also the Ecological Services of the U.S. Fish and Wildlife Services (Hoppe, 1982). Ecological Services views the changes with its potential impacts on riverine, riparian, and upland habitats. All effects of transferring Albuquerque water to Abiquiu must be addressed in a broader analysis than is capable within the scope of the project.

The final key site is the gage below Abiquiu Dam. Records show that it too reflects the response to irrigation bypasses and flood control needs.

DATA ANALYSES

In order to best understand the entire system, a set of data were analyzed. Information on how the system operates and what parameters are needed for the management model were derived from the data. The three months of most interest are August, September and October, primarily up to about October 15. This period contains 11 weekends. Data were compiled for these three months (and part of July) for stream flow, precipitation, and evaporation. The period was narrowed to post SJC project and was selected as 1974 through 1980. The average daily flow for the three month period was about 300 cfs. The average values for each of the months are shown in Table 1.

TABLE 1 - Average Daily Flow for the Summer Period 1974 - 1980. Based on Average Dailies for the Month.

Component	Month	Mean Flow, Cfs	Standard Deviation, Cfs
Inflow to El Vado	Aug.	96	52
(Willow Creek plus	Sept.	76	49
Rio Chama)	Oct.	63	34
Outflow from	Aug.	370	176
El Vado	Sept.	320	218
	Oct.	204	127
Inflow to	Aug.	379	171
Abiquiu	Sept.	328	224
	Oct.	192	147
Outflow from	Aug.	467	217
Abiquiu	Sept.	341	228
	Oct.	239	172

In comparison, the previous 14 years, WY 1960-1973, had a mean of about 180 cfs. This is a significant difference at the 10% level from a t - test. Such a difference is expected as the values in the post project period should be higher caused by project operation.

Daily flow values were studied using auto and cross correlation lagged up to seven days. This was done to examine how flows were interrelated and how the reservoirs were operated. Over 500 correlations were investigated. Auto correlations showed a strong value at lag 1, i.e. the second day was related to the first. Higher lags had decreasing correlations as expected. Cross correlations indicated differences. For the reservoirs operating to bypass inflows the lag 0 (same day) or lag 1 correlation should be significant, as it is at Abiquiu. The El Vado data, on the other hand, indicated poor cross correlations between inflow and outflow for five of the seven years. These poor correlations are caused by flow augmented transfer or storage.

River flows for the eleven-three day weekends per year were studied. Of the 225 days (six missing from October 1980), 31% had flows greater than or equal to about 500 cfs. Approximately 16% had average daily flows greater than or equal to about 750 cfs. There is a wide variation between years with some years having only three flows in the 500-600 cfs range.

Precipitation and pan evaporation data were also analyzed for the same period and only the weekends (261 days in this case). The chance of having rain on any weekend day was found to be 21%. The average daily rainfall, when it rained, was about 0.2 inches. Rainfall depths have an exponential distribution. It also appears that any weekend, 1 to 11, is just as likely to have rainfall as any other. The maximum daily precipitation for the period was 1.75 inches. Pan evaporation was also variable, but it was continuous. Table 2 lists the average rates for each reservoir for each of the 11 weekends.

TABLE 2 - Average Daily Pan Evaporations at El Vado and Abiquiu Reservoirs, Weekends of August 1 through October 15, 1974 through 1980.

	Evaporation in Inches Per Day	
Weekend	El Vado	Abiquiu
1	0.27	0.32
2	0.25	0.28
3	0.23	0.31
4	0.22	0.20
5	0.22	0.29
6	0.21	0.27
7	0.17	0.23
8	0.19	0.24
9	0.18	0.25
10	0.20	0.23
11	0.15	0.22

Results of the data analyses discussed above were used in model development. In addition, the average flows can be used by a manager to help set scenarios for the model.

One important piece of information that has recently become available in a preliminary form is what flows are desired by the white water recreationists. Rick Lukens (personal communication) has provided information from a field survey administered this summer. His data indicate that the ideal flow for all boaters (kayak, raft, canoe) has a median value of approximately 2300 cfs. Only 20% of the respondants felt that flows below 1000 cfs were acceptable. In comparison, fisherman desired flows with a median of 500 cfs, 73% wanted flows below 1000 cfs, and 94% wanted flows less than 2300 cfs. It has been suggested that 750 cfs be used as the standard for boating during the low flow period. Another set of data provided by Lukens yielded the fact that

during the period of April 8 through August 14, 1982, over 650 people used the Rio Chama for boating. About 50% of these people were on the river during the spring runoff period of May 22 to June 6, 1982. Flows at that time ranged between about 1600 and 3400 cfs. Therefore, it might be advantageous to investigate scenarios based upon higher flows than 750 cfs.

With the above data, some preliminary comparisons can be made. Given a desired flow level, a worse case augmentation can be determined. If a continuous flow of 2300 cfs for eleven-three day weekends is desired, simple computations indicate that over 150,000 AF is needed, far in excess of the available supply. Similarily, if 48,000 AF is available, the average flow for the same period could be augmented by 733 cfs. So there appears to be enough water for the 750 cfs level, but not for the median level indicated by boaters. The management model is designed to help investigate the tradeoffs.

DEVELOPMENT OF THE MANAGEMENT MODEL

APPROACH

What was needed for the study is a framework for analyzing different flow scenarios for the river reach between El Vado and Abiquiu. To fulfill this goal, an interactive computer model, which includes components for the two reservoirs and the river segment, was developed. The model is structured so that the user can rapidly modify systems variables that can be managed including magnitude of reservoir outflows, duration of outflows, and contents in the reservoirs. Some system variables, such as channel geometry, routing parameters, and natural inflow at La Puente are not subject to management decisions. Some are fixed in the model and others can be varied to study different scenarios. An application of the model is presented in a later section.

CHANNEL MODEL

Two types of models were studied, two versions of the Muskingum method and a finite difference diffusion wave model. After reviewing the available data base, the finite difference model was dropped from consideration as being more sophisticated than was warranted. Instead, two versions of the Muskingum method were studied, the generalized basic Muskingum method and the Muskingum-Cunge with variable parameters (MCVP).

Muskingum Method

The Muskingum method is well known to hydrologists and hydraulic engineers, and is well established in the literature (Chow, 1959). It was the first model studied for possible adoption.

Unpublished streamflow data in the form of hourly gage heights were obtained from the U. S. Geological Survey in Santa Fe. Stages for selected

releases were converted to discharges using stage rating tables supplied by the USGS. Seven releases from the period WY 1977 through 1979 were initially selected for further study. Two of these were eliminated on further inspection. The Muskingum model was applied to the data to determine the pertinent parameters. In the Muskingum model

$$S = K\,(XI + (1 - X))\,O \qquad (1)$$

where
- S = storage in reach
- I = inflow to reach (El Vado releases)
- O = outflow from reach (above Abiquiu gage)
- K = a time of travel parameter
- X = weighting parameter, i.e. if X=1 inflow controls storage, if X=0 outflow controls.

The above can be manipulated to give

$$O_2 = C_1 I_1 + C_2 I_2 + C_3 O_1 \qquad (2)$$

where
- O_2 = outflow from reach at time 2 (next time step)
- I_1 = inflow to reach at time 1 (current time step)
- I_2 = inflow to reach at time 2
- O_1 = outflow from reach at time 1

The coefficients are found from

$$C_1 = \frac{\Delta t + 2KX}{\Delta t + 2K(1-X)} \qquad (3)$$

$$C_2 = \frac{\Delta t - 2KX}{\Delta t + 2K(1-X)} \qquad (4)$$

and

$$C_3 = \frac{-(\Delta t + 2KX) + 2K}{\Delta t + 2K(1-X)} \qquad (5)$$

where

$$C_1 + C_2 + C_3 = 1.0 \qquad (6)$$

This model will work for a well behaved channel system, i.e. geometry and no inflows. Unfortunately, but as expected, the system changes geometry with discharge and inflows become a problem. This is evidenced by Table 3 which

shows the parameters as determined for each event.

Table 3 - Muskingum Method Parameters K and X, El Vado to Abiquiu Reservoirs - Rio Chama. Discharges in cubic feet per second.

Date	Average Q in	Average Q out	Best fit K (hours)	X	Q out	Peak Q in	Peak Q out
July 11-20, 77	815.4	785.1	12.88	0.0	787.2	1024	1088
Aug 24-Sept 3, 77	224.8	241.0	10.92	0.60	236.9	756	1095
Apr 4-6, 78	129.3	116.3	1.70	0.0	124.1	329.4	237.5
Sept 10-27, 78	349.6	351.9	4.99	0.1	351.4	522.1	508.3
Aug 6-9, 79	100.7	110.4	18.27	0.60	108.0	168.0	157.4

As the table indicates, there is no consistency between events using this model even though individual fits looked very good. Coefficient values of about 0.05, 0.05, and 0.90 for C_1, C_2, and C_3, respectively, are suggested to be used in the basic model.

Muskingum-Cunge with Variable Parameters

After mixed success with the basic Muskingum model, the next step was to apply a more sophisticated approach that accounted for variability in the channel geometry. This was the Muskingum-Cunge with variable parameters (Ponce and Yevjevich, 1978). The model is formulated as above in equations 1 through 6, except now the K and X parameters are allowed to vary depending on cross sectional hydraulic characteristics. In the revised scheme,

$$K = \frac{\Delta x}{c} \tag{7}$$

and

$$X = \tfrac{1}{2}\left(1 - \frac{q}{S_o c \Delta x}\right) \tag{8}$$

where

Δx = distance between cross sections or node points

c = flood wave celerity

q = unit width discharge

and So = channel bed slope

The celerity is found from

$$C_{i,j} = \left.\frac{dQ}{dA}\right|_{i,j} \tag{9}$$

and

$$q_{i,j} = \left.\frac{Q}{B}\right|_{i,j} \tag{10}$$

where Q = discharge at section j for time period i

A = cross sectional flow area for the above Q

and B = channel top width for the above Q

From Mannings equation or stream discharge measurements, relationships can be developed for Q, A, and B of the form

$$A = a_1 Q^{b_1} \tag{11}$$

and

$$B = A_2 Q^{b_2} \tag{12}$$

Substitution and manipulation with equations (9), (10), (11), and (12) gives

$$c = \frac{Q^{1-b_1}}{a_1 b_1} = a_1' \, Q^{b_1'} \tag{13}$$

$$q = \frac{Q^{1-b_2}}{a_2} = a_2' \, Q^{b_2'} \tag{14}$$

where a_1, a_2, b_1, b_2, a_1', b_1', a_2', b_2' are derived or measured parameters.

A four point implicit scheme is used in the model. In this scheme, the average c and q for the three known flows I_1, I_2, and O_1 are used to estimate O_2. Discharge O_2 is then used to solve for a fourth set of c and q values. All four c and q values from I_1, I_2, O_1, and O_2 are then used to estimate O_2 again until the error between estimates is less than 1%. This was usually

accomplished in less than five iterations.

One appealing characteristic of the MCVP method is that is allows one to subdivide the river segment for routing through measurement and use of channel cross sectional data. Sufficient information was provided for the below El Vado and above Abiquiu gages so that a and b paramenter could be derived (Bill Dein and Terry Perkins, USGS, Santa Fe, Personal Communication). On August 17 and 18 of 1982, channel surveys were conducted by the author, Bob Findling of State Parks Planning, and Andy Missey of NMSU. Channel slopes were measured at the below El Vado and above Abiquiu sites. Three intermediate cross sections were also measured--below the inflow of the Rio Gallina, above the inflow of the Rio Cebolla, and downstream of the Rio Nutrias. Cross sectional parameters and slopes were very similar at all five sections except the section downstream of the Rio Nutrias. This was not too surprising as the channel in the section was affected by tributary inflow and it was substantially wider than at other sections. From the supplied data and field measurements parameters were determined for each section as listed in Table 4.

Table 4 - Parameters for Rio Chama Cross Sections Used in Equations 13 and 14.

Section Number	Name	a_1'	b_1'	a_2'	b_2'	To next section. Slope, So	Distance, Δx, miles
1	below El Vado	0.11	0.60	0.021	0.87	0.003	5.48
2	below Nutrias	0.25	0.50	0.013	0.87	0.003	7.71
3	above Cebolla	0.09	0.63	0.023	0.90	0.002	8.71
4	below Gallina	0.26	0.48	0.029	0.84	0.003	6.90
5	above Abiquiu	0.22	0.51	0.030	0.85		

These parameters were derived by noting similarities with the two end stations and the results of channel surveys. The results they produce are realistic and within the bounds of measured values.

The MCVP model was tested with the same data base as listed in Table 3 and compared with the simplified version using only the two end sections. In the method the model predicts all flows at the first downstream section before proceeding to the next section. Another approach would be to move from one section to the next until all sections were completed before going to the next period. Based on the correlations between measured and computed outflows the basic method was a bit better in two cases, the MCVP was better in one case, and the two were about the same in the other cases. As discussed previously, there were some lag problems in the measured hydrographs that could not be reconciled but were used as a basis for testing anyway. Hydrographs at the intervening sections were produced by MCVP, a feature not available for the basic method. A cross spectral lagged correlation coefficients between measured inflow and measured the computed outflows were calculated. By way of comparison, the highest correlation was in the 4 to 8 hour range for the MCVP and a constant 6 hours for the basic. The MCVP should vary because lower flows should take longer (8 hours) to traverse the section then do higher flows (4 hours). In contrast, the structure of the basic method fixes the lag as a constant. A weighting scheme was attempted to help improve the MCVP estimates, but was abandoned with inconclusive results. Based on all the analyses, the MCVP was accepted for use because of its relatively good comparisons with measured values and the fact it provides information for intermediate sections. One limitation of the method, however, has been discussed by Ponce and Theurer (1982). In a numerical study of hypothetical channels they found that with a fixed time increment (one hour in this model) the space increment should be held below a

certain value. This constraint is violated for the Rio Chama primarily because, unlike hypothetical channels and time increments, real channels and flow data contain physical constraints as to where and how many sections can be practically accessed and measured. The three intermediate cross sections were chosen because of their relationship to other physical features. Because the space constraint is slightly violated, it is believed that it will not have a recognizable affect on the model performance. Ponce and Theurer also suggest that C_2 be constrained to $C_2 \geq 0.33$. This did not seem to affect the accuracy of the basic model where $C_2 = 0.05$ and the correlations were quite high in most cases. How important these constraints are for natural channels with variable geometry is yet to be demonstrated by a numerical study.

RESERVOIR MODEL

The channel model is linked to a simply mass balance reservoir model. The reservoir model is generic in that both El Vado and Abiquiu can be considered with only changes in input variables. The reservoir model is based upon

$$V_{i+1} = V_i + I - O - E + P$$

where V = reservoir contents at time period i or i+1

I = inflow to reservoir

O = outflow from the reservoir

E = evaporation from the reservoir

and P = precipitation into the reservoir

In the model, inflows and outflows are either defined by the user or computed by the routing model. Volumes are initially defined by the user then updated during each scenario; evaporation and precipitation are estimated from measured values taken at the dam sites or estimated by the user for each model run.

Evaporation is adjusted from pan values and precipitation is adjusted for reservoir surface area. Read in area-elevation-capacity tables are used to convert from any value to the other important parameters. The basic time period in the reservoir model is one day while in the routing model it is one hour. For consistency, all information is transformed into daily values before being displayed. The reservoir model was developed and tested using data from the period WY 1974 to WY 1980. Because the low flow months of August through October were of interest, only these times were used in model testing. River inflows and outflows are easily measured during this time. However, some of the ungaged tributaries to Abiquiu can provide inflows which can cause the Abiquiu model to generate negative volumes. This must be monitored as there is no easy method for accounting for these inflows at this time. Numerous regressions were attempted to relate the error in volume to other measured inputs, with only limited success. However, when the reservoir is high ($\sim$ 100,000 AF) and the major inflow is the Rio Chama, then the model predicts fairly close to measured. In contrast, the El Vado comparison was extremely close with the predicted and measured values being related almost one to one. After the reservoir and channel models were linked with appropriate interactive language, the management model was used to study different scenarios. An application of the model to a selected scenario is presented in the following section.

MODEL APPLICATION

The management model is in an interactive format. Questions are asked by the program and are answered from the keyboard. The data that are required include:

1) Current outflow from El Vado, in cfs

2) Current inflow to Abiquiu, in cfs

3) Required discharge(s) in the river, in cfs

4) Length of time(s) discharge(s) is to be sustained, in hours

5) Rate of river rise, in cfs per hour

6) Inflow to El Vado, in cfs

7) Outflow from Abiquiu, in cfs

8) Initial contents of El Vado and of Abiquiu

9) Evaporation and precipitation, both in inches, for El Vado and Abiquiu. These can be entered by the user. If not, the program estimates the values based on the weekend, 1 to 11, and the statistics of these variables for the two reservoirs.

The program then initializes the different variables, sets the inflow hydrograph, and, if needed, estimates evaporation and precipitation. The data set is printed upon request.

The program computes

1) Hydrographs at the next four downstream sections and prints them if requested,

2) inflow and outflow statistics and prints them if requested,

3) new reservoir volumes and elevations, and prints them if requested, and

4) updates the reservoir information for the next time period, if requested.

The user may then run again using updated information, change the information, or quit.

For an example, the following data was taken from USGS Water Resources Data of New Mexico, WY 1980, for September 20, 1980 - a Saturday.

1) El Vado outflow = 96 cfs
2) Abiquiu inflow = 101 cfs
3) Required discharge = 1000 cfs
4) Duration of discharge = 12 hours
5) Rate of rise = 250 cfs per hour
6) Inflow to El Vado = 96 cfs
7) Outflow from Abiquiu = 82 cfs
8) i) Contents of El Vado = 100700 AF
   ii) Contents of Abiquiu - 133600 AF
9) i) Evaporation from El Vado = 0.20 in/day
   ii) Precipitation on El Vado = 0.0 inches
   iii) Evaporation from Abiquiu = 0.23 in/day
   iv) Precipitation at Abiquiu = 0.10 inches

This situation requires a drawdown of El Vado to meet the required flow. The results are:

1) Arrival times of required flow:

Section	Time Since Release, hours
2 - Nutrias	1
3 - Cebolla	3
4 - Gallina	5
5 - above Abiquiu	6

2) Total duration of hydrograph from start at El Vado to return to initial conditions above Abiquiu site = 39 hours
3) Change in contents, El Vado = - 1249 AF
   Change in contents, Abiquiu = + 1197 AF

4) Change in elevation, El Vado = - 0.6 feet

Change in elevation, Abiquiu = + 0.4 feet

As can be seen from this example, the change in inflow and outflow has a fairly significant effect on the two reservoirs. One reason is that holding the flow at 1000 cfs for 12 hours transfers a lot of water. With the routing portion of the model, however, the effects of different schemes can be assessed to find the best combination of rise rate and duration.

SUMMARY AND CONCLUSIONS

This study had the goal of providing managers with a framework for evaluating the consequences of reservoir releases for white water recreationists. This framework is provided by a interactive model based on physical and stochastic processes. With the model a manager can estimate travel times of the release, reservoir drawdown, and reservoir filling, for different scenarios or in a real time operational manner.

The model does have some limitations. The data base on which it was calibrated has some weak points. A controlled release from El Vado and accurate measurements of travel times would aid model refinement. More field work to define each section, complete with detailed flow measurements would be beneficial. And finally, a better accounting of Abiquiu inflows is necessary for the mass balance approach.

In conclusion, the framework developed for this study is just a beginning. It will be linked into a larger overall project aimed at developing a Rio Grande system management model. When put in context with the entire system, the Rio Chama model developed here will be of great benefit in yet another application.

REFERENCES

Chow, V. T., 1959. Open Channel Hydraulics. McGraw-Hill Book Co., New York, N.Y., 679 p.

Hoppe, R. A., 1982. Letter to District Engineer, U.S. Army COE, Albuquerque District.

Ponce, V. M., and Yevjevich, V., 1978. The Muskingum-Cunge Method with Variable Parameters. Journal of the Hydraulics Division, ASCE, Vol. 104, No. HY12, December, pp. 1663-1667.

Ponce, V. M., and Theurer, F. D., 1982. Accuracy Criteria in Diffusion Routing. Journal of the Hydraulics Division, ASCE, Vol. 108, No. HY6, June. pp. 747-757.

Sabol, G. V., and Gordon, N., 1980. Model Development for Optimization of Sport Fisheries in the Rio Grande of New Mexico - Part A Volume II: Hydrology and Hydraulics of the Rio Grande in New Mexico, prepared for New Mexico Department of Game and Fish, Santa Fe. 88 pages.

U. S. Bureau of Reclamation (USBR), 1963. Accounting of water, San Juan-Chama Project. 27 p.

U. S. Bureau of Reclamation (USBR), 1975. Standing Operating Procedures for El Vado Dam. 44 p.